



UNIVERSITAT DE
BARCELONA

The role of the microenvironment in cancer progression and metastasis: an immunogenomics approach

Sandra Garcia Mulero

ADVERTIMENT. La consulta d'aquesta tesi queda condicionada a l'acceptació de les següents condicions d'ús: La difusió d'aquesta tesi per mitjà del servei TDX (www.tdx.cat) i a través del Dipòsit Digital de la UB (diposit.ub.edu) ha estat autoritzada pels titulars dels drets de propietat intel·lectual únicament per a usos privats emmarcats en activitats d'investigació i docència. No s'autoritza la seva reproducció amb finalitats de lucre ni la seva difusió i posada a disposició des d'un lloc aliè al servei TDX ni al Dipòsit Digital de la UB. No s'autoritza la presentació del seu contingut en una finestra o marc aliè a TDX o al Dipòsit Digital de la UB (framing). Aquesta reserva de drets afecta tant al resum de presentació de la tesi com als seus continguts. En la utilització o cita de parts de la tesi és obligat indicar el nom de la persona autora.

ADVERTENCIA. La consulta de esta tesis queda condicionada a la aceptación de las siguientes condiciones de uso: La difusión de esta tesis por medio del servicio TDR (www.tdx.cat) y a través del Repositorio Digital de la UB (diposit.ub.edu) ha sido autorizada por los titulares de los derechos de propiedad intelectual únicamente para usos privados enmarcados en actividades de investigación y docencia. No se autoriza su reproducción con finalidades de lucro ni su difusión y puesta a disposición desde un sitio ajeno al servicio TDR o al Repositorio Digital de la UB. No se autoriza la presentación de su contenido en una ventana o marco ajeno a TDR o al Repositorio Digital de la UB (framing). Esta reserva de derechos afecta tanto al resumen de presentación de la tesis como a sus contenidos. En la utilización o cita de partes de la tesis es obligado indicar el nombre de la persona autora.

WARNING. On having consulted this thesis you're accepting the following use conditions: Spreading this thesis by the TDX (www.tdx.cat) service and by the UB Digital Repository (diposit.ub.edu) has been authorized by the titular of the intellectual property rights only for private uses placed in investigation and teaching activities. Reproduction with lucrative aims is not authorized nor its spreading and availability from a site foreign to the TDX service or to the UB Digital Repository. Introducing its content in a window or frame foreign to the TDX service or to the UB Digital Repository is not authorized (framing). Those rights affect to the presentation summary of the thesis as well as to its contents. In the using or citation of parts of the thesis it's obliged to indicate the name of the author.



UNIVERSITAT DE
BARCELONA

THE ROLE OF THE MICROENVIRONMENT IN CANCER PROGRESSION AND METASTASIS: AN IMMUNOGENOMICS APPROACH

Thesis presented by

Sandra Garcia Mulero

To opt for a doctoral degree by the

University of Barcelona

Under the supervision of

Dra. Rebeca Sanz Pamplona
(co-director)

Dr. Víctor Raúl Moreno Aguado
(co-director and tutor)

Department of Clinical Sciences

Program of Medicine and Translational Research

Faculty of Medicine and Health Sciences. University of Barcelona

Barcelona, 28 September 2022



El Dr. **Victor Raúl Moreno Aguado**, de la Facultat de Medicina i Ciències de la Salut de la Universitat de Barcelona, i la Dra. **Rebeca Sanz Pamplona**, ambdós del Programa d'Analítica de dades en Oncologia de l'Institut Català d'Oncologia (ICO), el Programa Oncobell de l'Institut d'Investigació Biomèdica de Bellvitge (IDIBELL) i el Centre d'Investigació Biomèdica en Red d'Epidemiologia i Salut Pública (CIBERESP)

certifiquen

que la estudiant Sandra Garcia Mulero ha realitzat la tesi doctoral "The role of the microenvironment in cancer progression and metastasis: an immunogenomics approach" sota la seva direcció,

considerant

que la memòria resultant és apta per ser defensada públicament i per optar al grau de Doctorat per la Universitat de Barcelona,

i perquè quedi constància, signen aquest document a

Barcelona, VW de Setembre de VVVV.

"What you do makes a difference,
and you have to decide what kind of difference you want to make."

- Jane Goodall

Agradecimientos

Es una suerte poder trabajar en algo que aporte un beneficio a la sociedad, y me siento orgullosa de poner mi granito de arena en los avances sobre esta difícil enfermedad. Puedo decir que soy privilegiada por haber dado mis primeros pasos en el mundo profesional en este lugar, rodeada de tanto conocimiento, talento, y buenas personas.

Primero quiero agradecer a Rebeca Sanz, por la confianza en mí desde el principio, por la ayuda constante, todo lo que me has enseñado de biología y también por tu filosofía de vida, que me has transmitido en todo momento. Eres auténtica, una gran profesional, y no podría haber tenido mejor mentora. ¡Te deseo muchísima suerte en esta nueva etapa por tierras aragonesas!

Agradecer a Víctor Moreno, por ofrecerme la oportunidad de disfrutar de esta beca, que me ha permitido vivir unos años de gran aprendizaje, y con la que también he podido descubrir otra vertiente de la investigación dando clases a futuros médicos, que me ha encantado y a la que espero volver algún día.

A Josep Maria Piulats, por tu entusiasmo en la investigación y por abrirme las puertas a colaboraciones que he disfrutado muchísimo. Gracias por tu ímpetu en llevar la investigación a todos tus pacientes, y hacer que nuestro trabajo se vea reflejado, por modesta que sea nuestra contribución, en el día a día de un hospital.

Me gustaría agradecer también a todos los colaboradores con los que hemos trabajado durante estos años. A las chicas de cáncer hereditario, Laura Valle y Pilar Mur, por los súper proyectos en los que habéis contado con nosotras, y lo divertido que hacéis ir de congreso con vosotras. A los compañeros del CIT, en especial a Ramón Alemany, porque me habéis ayudado a entender un poquito mejor este complejo mundo de la inmunología vivida desde dentro de un laboratorio. ¡Mucha suerte en todos los nuevos proyectos!

Un agradecimiento especial a Henar, por hacerme perder el miedo a la estadística y ayudarme en todos los análisis de mis proyectos, te convertiste en una buena amiga durante estos años, ¡y una gran compi de conciertos! A Ferran, por estar siempre dispuesto a ayudarnos con pipelines, métodos y lo que hiciera falta. ¡Eres un coco andante! No puedo olvidarme de todos los compañeros de sala predoc y de escapadas

de la época pre-covid: Virginia, Joan, Ania, Jon, Sara,... A Olga, que siempre estás ahí para todos con una sonrisa permanente.

En definitiva, a todos los compañeros de la UBS y el PADO que he conocido durante estos años, los que habéis pasado por aquí y los que acabáis de llegar. Sois muchos y es imposible nombraros a todos, pero cada uno es especial y hace de este programa una gran familia. Lo más importante de esta experiencia han sido las personas que me han rodeado, y el recuerdo que dejáis de esta gran etapa que voy a recordar siempre con mucho cariño.

Finalmente, quiero dar las gracias a mi familia. A Jordi, por tu paciencia en mis días malos, por apuntarte siempre a todas mis locuras, y por todas nuestras tonterías que hacen la vida mucho más divertida. A mis padres, por el trabajo constante para que mi hermana y yo pudiéramos desarrollar nuestros proyectos de vida con la libertad que vosotros no tuvisteis. Gracias por los valores y la humildad que me habéis transmitido.

¡Gracias a todos!

Funding

This thesis has been financially supported by the grant “Ajuts de Personal Investigador predoctoral en Formació” (APIF) VXjk from the University of Barcelona.

The work carried out in this thesis has been funded by the Instituto de Salud Carlos III (FIS PIVX/XXmnm); the Agency for Management of University and Research Grants (AGAUR) of the Catalan Government (VXjmSGRmVp); the Centro de investigación biomédica en red Epidemiología y salud pública (CIBERESP) (CBXm/XV/VXXq); and the Grupo Español de Melanoma (GEM) (jkPSJXXn).

Table of contents

List of figures	III
List of tables	IV
Glossary of abbreviations	V
List of articles	VII
Abstract	IX
Resumen	X
I. INTRODUCTION	H
j. IMMUNOBIOLOGY OF CANCER	V
<i>!! The tumor microenvironment: a complex network</i>	7
j.j.j. Immune components of the TME	r
j.j.V. Stromal components of the TME	k
j.j.p. The dual role of the TME: a context-dependent function	jX
<i>!8. Tumor immunity and immune evasion</i>	!8
j.V.j. The cancer-immunity cycle	jp
j.V.V. Neoantigen presentation and T cell activation	jr
j.V.p. The cancer immunoediting process	jm
j.V.r. Mechanisms of immune evasion	jW
<i>!7. Tumor immune microenvironment heterogeneity</i>	8=
j.p.j. Uveal melanoma as a divergent tumor type	VV
j.p.V. The metastatic microenvironment	Vq
V. IMMUNO-ONCOLOGY FOR CANCER MANAGEMENT	Vk
<i>8.1. Cancer immunotherapy</i>	8?
V.j.j. Immune checkpoint inhibitors (ICIs)	Vk
V.j.V. Other immunotherapy-based treatments	pj
V.j.p. Current challenges of immunotherapy	pV
<i>8.8. Immune biomarkers for cancer management</i>	77
V.V.j. Current setting of immune biomarkers in oncology	pp
V.V.V. Immune signatures as response biomarkers	pn
p. IMMUNOGENOMICS FOR THE STUDY OF TUMOR IMMUNITY	pW
<i>7.1. Cancer omics databases as a source of biological data</i>	7?
<i>7.8. Computational tools for immune characterization</i>	D=

p.V.j. Quantification of immune infiltrates.....	rX
p.V.V. HLA typing and neoantigen prediction.....	rV
7.7. <i>New approaches in immunogenomics</i>	DF
II. HYPOTHESIS AND OBJECTIVES	NO
j. HYPOTHESIS.....	rW
j.j. Rationale of the project	rW
j.V. General hypothesis	rW
j.p. Specific hypothesis.....	rk
V. OBJECTIVES	qX
III. RESULTS	PH
STUDY j DISSECTING THE IMMUNITY OF UVEAL MELANOMA.....	qV
j.j. Additive role of immune system infiltration and angiogenesis in uveal melanoma progression.....	qV
j.V. Driver mutations in GNAQ and GNAj genes are likely to be antigenic in uveal melanoma patients	mj
STUDY V ROLE OF THE IMMUNE MICROENVIRONMENT IN METASTATIC HOMING	kp
IV. DISCUSSION	HQO
j. DISSECTING THE IMMUNITY OF UVEAL MELANOMA	jjj
j.j. Additive role of immune system infiltration and angiogenesis in uveal melanoma progression.....	jjj
j.V. Driver mutations in GNAQ and GNAj genes are likely to be antigenic in uveal melanoma patients	jjp
V. ROLE OF THE IMMUNE MICROENVIRONMENT IN METASTATIC HOMING.....	jjm
V.j. Lung metastases share common immune features regardless of primary tumor origin	jjm
V.V. Distinctive immune microenvironment across metastatic locations	jVX
p. FUTURE PERSPECTIVES OF PERSONALIZED ONCOLOGY	jVj
V. CONCLUSIONS	HRP
VI. BIBLIOGRAPHY	HRS

List of figures

Figure H. The hallmarks of cancer.....	V
Figure R. The tumor microenvironment.....	P
Figure U. TME dichotomous function in the primary tumor niche	jj
Figure N. The cancer-immunity cycle	jp
Figure P. Representation of median number of mutations across cancer types from the TCGA. Red lines represent the median mutations/mb per tumor type.....	jr
Figure V. Neoantigen processing and presentation.....	jq
Figure O. Immunoediting process.....	jm
Figure W. The immune landscape of solid tumors.....	Vj
Figure S. Main locations of uveal melanoma within the eye.....	VV
Figure HQ. G-protein pathway alterations.....	Vp
Figure HH. Different cancer types show divergent patterns of metastatic spread.....	Vn
Figure HR. Immunosuppressive cells promote tumor metastasis through multiple mechanisms in primary tumor and in the pre-metastatic niche	Vm
Figure HU. A) Mechanisms of action of anti-CTLA-r. B) Mechanism of action of anti-PD-j/Lj.....	pX
Figure HN. PD-Lj IHC staining in NSCLC tumor samples.....	pr
Figure HP. Immunoscore biomarker methodology.	pr
Figure HV. Correlation plot between OOR to anti-PD-j/Lj and TMB in somatic mutation per mega base in Vm different tumor types.....	pq
Figure HO. T-Cell inflammatory signature.....	pm
Figure HW. Overview of the main data types and the bioinformatics analysis for interrogating tumor immunity.....	pW
Figure HS. Omics data bases for omics integration analysis gives the possibility to tailor treatments in a personalized way.....	pk
Figure RQ. Overview of immune deconvolution algorithms (example is based on deconvolution-based approach).....	rj
Figure RH. Overview of the pipeline for neoantigen prediction.....	rp
Figure RR. NetMHCcons web resource for HLA binding affinity prediction from neoantigens	rr
Figure RU. Graphical overview of the different factors influencing the advances in precision oncology	jVV

List of tables

Table H. Summary of immune innate and adaptive cell subtypes in the TME and their anti- or pro-tumorigenic functions. Adapted from Quail DF & Joyce JA, Nat Med, VXjp; and Hinshaw DC et al., Cancer Res, 2019	P
Table R. Stromal cells in the TME	S
Table U. Summary of current immunotherapy-based agents approved.	UH
Table N. Biomarkers of response to immunotherapy	UU
Table P. Description of some of the most used quantification methods from transcriptomic profiles. Adapted from Sturm G et al., Bioinformatics, VXjk.....	NH

Glossary of abbreviations

AP-H	activator protein-j
APC	antigen presenting cell
ATC	adoptive T cell transfer
BAPH	BRCAj associated protein j
BCR	B cell receptor
BMDC	bone marrow-derived cell
CAR	chimeric antigen receptor
CTLs	cytotoxic T-lymphocytes
CTLA-N	cytotoxic T lymphocyte-associated protein r
CRC	colorectal cancer
DC	dendritic cell
ECM	extracellular matrix
EMT	epithelial mesenchymal transition
FDA	food and drug administration
GM-CSF	granulocyte-macrophage colony-stimulating factor
gpHQQ	premelanosome protein
HLA	human leukocyte antigen
ICB	immune checkpoint blockade
IHC	immunohistochemistry
IL	interleukin
INDELs	insertions and deletions
KIR	killer immunoglobulin-like receptor
LAGU	lymphocyte-activation gene p
LDH	lactate dehydrogenase
LOH	loss of heterozygosity
MIF	macrophage migration inhibitory factor
MARTH	melanoma antigen recognized by T cells
MDSC	myeloid-derived suppressor cell
MHC	major histocompatibility complex
MMP	matrix metalloproteinase
MMRd	mismatch repair deficiency
MSI	microsatellite instability

NETs	neutrophil extracellular traps
NF-κB	nuclear factor κ -light chain enhancer of activated B cells
NGS	next generation sequencing
ORR	objective response rate
PDCDH	programmed cell death j
TCR	T cell receptor
TLS	tertiary lymphoid structure
TIMU	T cell immunoglobulin and mucin-domain containing-p
TMB	tumor mutational burden
TNF-α	tumor necrosis factor- α
TRPH	tyrosinase-related protein j
RCC	renal cell carcinoma
ROS	reactive oxygen species
RT-PCR	reverse transcription polymerase chain reaction
SCLC	small cell lung cancer
SNV	single nucleotide variant
TAM	tumor associated macrophage
TF	transcription factor
TCR	T cell receptor
TGF-β	transforming growth factor- β
TILs	tumor infiltrating lymphocytes
TIME	tumor immune microenvironment
TME	tumor microenvironment
TNF-α	tumor necrosis factor alpha
TSA	tumor specific antigen
VEGF	vascular endothelial growth factor

List of articles

The thesis will be presented in the format of a compendium of three scientific articles corresponding to the two main objectives. Two of the articles have already been published in international scientific journals; the third one has been deposited as a preprint in BioRxiv and will be sent for publication shortly.

The works presented are the result of two studies that recapitulate the work carried out during at the Unit of Biomarkers and Susceptibility (UBS), from the Oncology Data Analytics Program (ODAP), of the 'Institut Català d'Oncologia' (ICO) and the 'Institut d'Investigació Biomèdica de Bellvitge' (IDIBELL). Part of this work is also in collaboration with the Cancer Immunotherapy Unit (CIT) of the Oncobell program (IDIBELL).

Objective H | To decipher the role of the immune system in uveal melanoma

H.H. Sandra García-Mulero, María Henar Alonso, Luis P. Del Carpio, Rebeca Sanz-Pamplona, Josep María Piulats. *Additive Role of Immune System Infiltration and Angiogenesis in Uveal Melanoma Progression*. International Journal of Molecular Sciences. VV; Vnn (VXVj). <https://doi.org/jX.ppkX/ijmsVXqVnnk>. Impact Factor: q.k (VXVV), Quartile: Qj, Category: Biochemistry & Molecular biology.

H.R. Sandra García-Mulero, Marco Punta, Roberto Fornelino Stefano Lise, Mar Varela, Rafael Moreno, Marcel Costa-Garcia, Ramón Alemany, Josep María Piulats, Rebeca Sanz-Pamplona. Driver mutations in GNAQ and GNAJ1 genes as potential targets for precision immunotherapy in uveal melanoma patients

Objective R | To identify immune factors that modulate metastatic spread to specific organs

R.H. Sandra García-Mulero, María Henar Alonso, Julián Pardo, Cristina Santos, Xavier Sanjuan, Ramón Salazar, Víctor Moreno, Josep María Piulats, Rebeca Sanz-Pamplona. *Lung Metastases Share Common Immune Features Regardless of Primary Tumor Origin*. Journal for Immunotherapy of Cancer. W, EXXXrkj (VXVX) <https://doi.org/jX.jjpn/jitc-VXjk-XXXrkj>. Impact Factor: jp.mq (VXVV), Quartile: Qj, Category: Immunology and oncology.

Related articles by the author

The author has also participated in the following articles, as result of the collaborative work with researchers from ICO and other institutions. All them are related to immuno-oncology studies in various solid tumors.

- Juan A. Marín-Jiménez, **Sandra García-Mulero**, Xavier Matías-Guiu, and Josep M. Piulats. *Facts and Hopes in Immunotherapy of Endometrial Cancer*. Clinical Cancer Research: An Official Journal of the American Association for Cancer Research, July q, VVVV, clincanres.jqnr.VVVV. <https://doi.org/jX.jjqW/jXmW-XrpV.CCR-Vj-jqnr>.
- Pilar M Lanuza, M. Henar Alonso, Sandra Hidalgo, Iratxe Uranga-Murillo, **Sandra García-Mulero**, Raquel Arnau, Cristina Santos, et al. *Adoptive NK Cell Transfer as a Treatment in Colorectal Cancer Patients: Analyses of Tumour Cell Determinants Correlating With Efficacy In Vitro and In Vivo*. Frontiers in Immunology jp (VVVV): WkXWpn. <https://doi.org/jX.ppWk/fimmu.VVVV.WkXWpn>.
- Kayleigh Slater, Aisling B. Heeran, **Sandra Garcia-Mulero**, Helen Kalirai, Rebeca Sanz-Pamplona, Arman Rahman, Nebras Al-Attar, et al. *High Cysteinyl Leukotriene Receptor ! Expression Correlates with Poor Survival of Uveal Melanoma Patients and Cognate Antagonist Drugs Modulate the Growth, Cancer Secretome, and Metabolism of Uveal Melanoma Cells*. Cancers jV, no. jX (October jp, VVVX): EVkqX. <https://doi.org/jX.ppkX/cancersjVjXVqkX>.
- Lidia Franco-Luzón, **Sandra García-Mulero**, Rebeca Sanz-Pamplona, Gustavo Melen, David Ruano, Álvaro Lassaletta, Luís Madero, África González-Murillo, and Manuel Ramírez. *Genetic and Immune Changes Associated with Disease Progression under the Pressure of Oncolytic Therapy in A Neuroblastoma Outlier Patient*. Cancers jV, no. q (April VW, VVVX): EjjXr. <https://doi.org/jX.ppkX/cancersjVXqjjXr>.
- Florian Castet, **Sandra Garcia-Mulero**, Rebeca Sanz-Pamplona, Andres Cuellar, Oriol Casanovas, Josep Maria Caminal, and Josep Maria Piulats. *Uveal Melanoma, Angiogenesis and Immunotherapy, Is There Any Hope?*. Cancers jj, no. n (June jm, VVjk). <https://doi.org/jX.ppkX/cancersjjXnXWpr>.

Abstract

Cancer is a heterogeneous disease, in which many cell types interact with cancer cells, forming a complex network. The crosstalk between the cancer cells and the immune microenvironment is determinant in tumor growth and dissemination. The study of tumor immunity has improved during the last years thank to the emergence of omics technologies and immunogenomics approaches. On the other side, tumor microenvironment varies significantly depending on tumor type, molecular subgroups and stage of the disease, among others. Understanding the singularities of the tumor microenvironment in these different contextures will help to improve patients' management towards a personalized selection of immune treatments. In this thesis, we have exploited omics data by bioinformatic means for deciphering the molecular mechanisms underlying tumor progression and metastasis, as well as for the identification of new immune biomarkers for patients' stratification that correlates with clinical outcomes. This thesis provides threeThree comprehensive immunogenomics studies covering the crosstalk between tumor-immune system and its association with clinical outcomesare presented. First, we studied the role of the immune microenvironment in uveal melanoma primary tumors. We performed a meta-analysis that associates immune infiltration with poor prognosis, and we proved the additive role of immune activation and angiogenesis in uveal melanoma progression. Second, we gave new insights in the immunogenic potential of driver mutations in GNAQ and GNAJ1 genes in uveal melanoma patients, and proposed a candidate target for neoantigen vaccine therapy in uveal melanoma patients. Third, we performed a pan-cancer immune characterization of metastatic samples, and demonstrated that metastatic samples in the same location share immune phenotypes regardless of their primary tumor origin. A novel clustering found a subset of metastases that could be susceptible to respond to immunotherapy, and identified CD8 expression as a candidate biomarker of high immunogenic metastases. This thesis provides three comprehensive immunogenomics studies covering the crosstalk between tumor-immune system and its association with clinical outcomes. The work presented here can pave the way for future immunogenomics studies towards precision oncology in solid tumors.

Resumen

El cáncer es una enfermedad heterogénea, en la que distintos tipos celulares interactúan con las células tumorales formando una compleja red de comunicación. Esta comunicación entre el microambiente y las células cancerígenas juega un papel determinante en el crecimiento tumoral. El estudio de la inmunidad tumoral ha mejorado en los últimos años, gracias a los avances en las tecnologías ómicas y los métodos de inmunogenómica. Por otro lado, el microambiente tumoral puede variar significativamente en distintos contextos, dependiendo del tipo tumoral, estadio y subgrupo molecular, entre otros. Una correcta comprensión de estas singularidades es clave para mejorar el manejo de los pacientes, así como para el avance hacia inmunoterapias más dirigidas y efectivas. En esta tesis, se han usado distintas herramientas bioinformáticas con el objetivo de descifrar los mecanismos moleculares asociados con la progresión metastásica, y de identificar nuevos biomarcadores inmunes que correlacionan con respuesta clínica. Esta tesis contribuye al avance hacia la oncología de precisión en dos contextos tumorales. En primer lugar, se ha estudiado el papel del microambiente tumoral en melanoma uveal primario. Mediante un estudio de meta-análisis, se ha descrito que la infiltración de células inmunes está asociada con un peor pronóstico, confirmando el papel divergente del sistema inmune en esta enfermedad. Asimismo, se ha encontrado que mutaciones recurrentes en los genes *GNAQ* y *GNAJ1* pueden generar inmunogenicidad y podrían ser posibles candidatos para terapias personalizadas en pacientes con melanoma uveal. En segundo lugar, hemos realizado un estudio pan-cancer en muestras metastásicas que demuestra que las metástasis en pulmón tienen un perfil inmune característico independientemente del tumor primario. Se ha identificado un subgrupo de metástasis con alta activación inmune que podrían responder a inmunoterapia, y se ha identificado la expresión del gen *CDmr* como candidato a biomarcador de este subgrupo. Los resultados presentados pueden servir como punto de partida para futuros estudios en inmunogenómica hacia la personalización de la inmunoterapia en tumores sólidos.

I. INTRODUCTION

1. Immunobiology of cancer

Carcinogenesis is a complex process in which numerous molecular and cellular elements are involved (j). The hallmarks of cancer comprise the essential characteristics of a tumor. Hanahan et al. first defined six capabilities that gives cells the ability to become malignant. Later on, they were broadening to eight and finally to a total of 14 that were published in 2011 (Figure H) (V). According to the increasing knowledge about the importance of immune system in cancer disease, two new hallmarks are related to tumor immunity of the tumor: avoiding immune destruction and tumor-promoting inflammation.

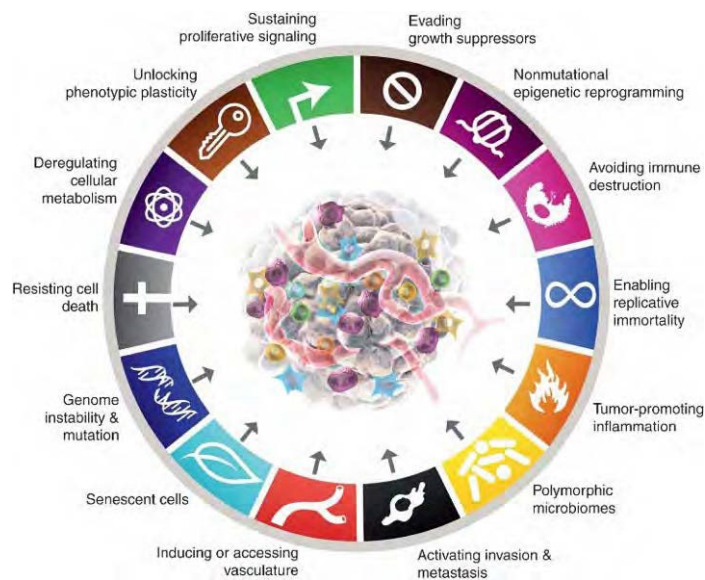


Figure . The hallmarks of cancer. Hanahan D, Weinberg RA. Cell, ;:::

Indeed, the role of the immune system in carcinogenesis was largely demonstrated during the past century, when its primary function of recognizing and eradicating malignant cells was described (p). However, it has been over the last decades when an explosion of knowledge about tumor immunology has emerged, with focus in the study of the immune contexture and the translation into immunotherapies. Recent discoveries in cancer immunology have re-defined the basis of tumor growth, and have provided new insights about the interactions between malignant cells and the immune system (r).

1.1. The tumor microenvironment: a complex network

The tumor microenvironment (TME) is a heterogeneous network comprised by multiple molecules and cell-types that surround and infiltrate the tumor (**Figure R**) (q). The TME is composed by three principal components, including cells (stromal and immune cell-types), soluble factors and extracellular matrix.

Soluble factors comprise cytokines, chemokines, interleukins and growth factors. These factors can be expressed either by the cancer cells or stromal cells within the microenvironment, and can have pro-tumoral or anti-tumoral effects. Main soluble factors are cytokines and chemokines, which are secreted proteins that control immune cells trafficking and determine the nature of the immune responses (n). On the other side, the **extracellular matrix** is a dense matrix containing different fibrous proteins (collagen, elastin and laminin), with the principal functions of structural scaffold for cells. During carcinogenesis, the components of the ECM are altered and can play a role promoting tumor growth (n).

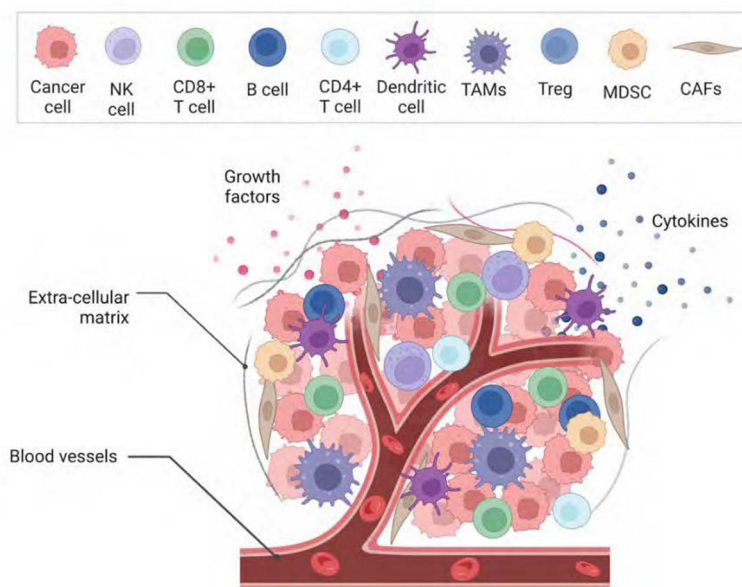


Figure 5. The tumor microenvironment. TME is a complex mass formed by different components including cancer cells, immune and stromal cell-types. Original figure by BioRender.

1.1.1. Immune components of the TME

The immune system is the network of biological processes that protect all organisms from disease by distinguishing the “non-self” from the host own tissue. It has pivotal functions for maintenance of the body’s homeostatic conditions (m). The immune system is a highly plastic and dynamic system, with a wide variety of cell subtypes and different maturation states. The immune response can be divided into two main levels: the innate immune response and the adaptive immune response.

The **innate immune response**, which is the first line of defense of our body against external pathogens, recognizes conserved molecular patterns in a non-specific and antigen independent manner. The innate immune cell-types (originated from myeloid precursors) includes macrophages, mast cells, granulocytes (neutrophils, eosinophils and basophils), dendritic cells (DCs), natural killers (NK) and myeloid-derived suppressor cells (MDSCs). The innate immunity uses pattern-recognition receptors (PRRs) to detect foreign pathogen from damaged tissues that trigger non-specific killing of infected cells (W).

The **adaptive immune response** is the second defense line, it is an adaptation to infection that provides specific response in an antigen-specific and cell-mediated manner, generating immunological memory and long-lasting protection. Immune cells that constitute the adaptive immune system (originated from the lymphoid lineage) comprises T and B lymphocytes, and their subtypes. Adaptive immunity needs from the activation by antigen presenting cells (APCs) and the recognition of antigens by specific cell receptors to take place (k).

All immune cell-types can be found within the TME, although the distribution and abundance can vary between different tumor types and between primary and metastatic locations (jX). Usually, they are located either in the core of the tumor, in the invasive margin, or in tertiary lymphoid structures (TLS). The most abundant immune cell-types within the TME are T cells and B cells, representing up to two thirds of the total of the immune infiltrating cells, followed by NK cells which are the third most abundant cell type (jj).

The characteristics and function of the main immune cell-types will be described through this section, with the focus on their role in cancer development (**Table H**). Nevertheless, immune cell-types are highly heterogeneous, and different pro- and

anti- tumoral effects have been recently described for the same cell-types depending on the contexture.

Table (. Summary of immune innate and adaptive cell subtypes in the TME and their anti- or pro-tumorigenic functions. Adapted from Quail DF & Joyce JA, Nat Med, ; and Hinshaw DC et al., Cancer Res, 2019.

Cell type	Function	Cytokine/chemokine secretion	Gene markers	Effect
T cells				
CD8+ cytotoxic T cells (CTLs)	Detection of abnormal antigens, killing of cells	IFN- γ , TNF- α , granzymes, perforin	CD3, CD8	Anti-tumorigenic
CD4+ Th1	Support CD8+ cells	IL-2, IFN- γ , TNF- α	CD3, CD4	Anti-tumorigenic
CD4+ Th2	Recruitment of eosinophils, mast cells, DCs, etc	IL-4, IL-5, IL-6, IL-10, IL-13	CD3, CD4	tumorigenic
T regulatory cells (Tregs)	Control autoimmunity, secretion of cancer growth factors	IL-6, IL-10, CCL28, TGF- β	CD4, CD25, FOXP3	Pro-tumorigenic
B cells				
B cells	AP to T cells, secretion of cytokines	IFN- γ	CD19, CD20	Depends on tumor type
B regulatory cells (Bregs)	Promote immunosuppressive phenotypes of macrophages, neutrophils and T cells	IL-10, TGF- β	CD19, CD20	Pro-tumorigenic
NK cells				
NK1	Killing tumor cells, produce inflammatory cytokines	IFN- γ , TNF- α , CCL5, IL-6, GM-CSF	NKp46, CD16, CD56	Anti-tumorigenic
NK2	Anergic phenotype	IL-5, IL-13	NKp46, CD16	Pro-tumorigenic
Dendritic cells				
Conventional DCs (cDCs)	Recognize, capture and present antigens to CD4+ and CD8+ T cells	IL-6, IL-12, IL-23, TNF- α , IFN- γ	CD11c, CD103	Anti-tumorigenic
Plasmacytoid DCs (pDCs)	Secretion of type 1 IFN, respond to viral infection	Type 1 IFN, TNF, IL-6	CD11c	Depends on tumor type
Macrophages				
M1	Activate Th1 responses, phagocytosis, and AP	IL-1, IL-6, IL-12, IFN- γ , TNF- α	CD80, CD86, IDO1, CXCL10	Anti-tumorigenic
M2	Immunosuppressive phenotype, inhibit CTLs, promote angiogenesis and ECM remodeling	IL-10, IL-18, CCL17, CCL22, TGF- β , VEGF	CD163, VEGF	Pro-tumorigenic
Neutrophils				
Early stages	Phagocytosis, release of ROS and NETs	TNF- α , IL-1, IFNs, MMP-8, ROS	TNF- α , I-CAM1, FAS, ROS	Depends on tumor type
Late stages	ECM remodeling, and promote local invasion and angiogenesis	IL-4, MMP-9, CXCL1, CXCL8, CCL3, TGF- β	Arginase, CCL2, CCL5	Pro-tumorigenic
MDSCs	Promotes angiogenesis, suppression of CTLs and NK cells activation	IL-10, IL-18, VEGF, IDO1	CD11b	Pro-tumorigenic

Tumor infiltrating lymphocytes (TILs)

Tumor infiltrating lymphocytes (TILs) refers to the T cells that infiltrate into the tumor, and are associated with better outcome in many cancer types (jV). There are two main subtypes of T lymphocytes: **CDW+ T cells**, also called cytotoxic lymphocytes (CTLs) and **CDN+ T helper cells**. All T lymphocytes express CDp and T-cell receptors (TCRs) that recognize specific antigens. They are mainly differentiated by carrying CDW or CDr surface protein, respectively. Specifically, CDW+ T cells detect the antigens that are presented by major histocompatibility complex class I (MHC class I), whereas CDr+ T cells detect antigens presented by MHC class II (jp).

CTLs are the primary effectors of anti-tumor immunity, and their principal function is the recognition and killing of tumor cells. CTLs are activated following recognition of tumor antigens presented on tumor cell surface by MHC class I. Once CTLs are activated, they kill target cells by the secretion of granzyme, perforin, and through the FasL-mediated apoptosis induction. They can also secrete some cytokines, such as IFN- ψ and TNF- α , that are inducers of cytotoxicity in cancer cells (q).

CDr+ T cells are mainly composed by Thj, ThV, and T regulatory cells (Tregs). The principal function of CDr+ T helper cells is the activation of other immune cells through different mechanisms. Thj secrete stimulatory cytokines like IL-V, IFN- ψ and CDrX ligand that activates CTLs, NKs and macrophages. ThV produce IL-r, IL-q and IL-jp that favors humoral immunity by B cells. Tregs function in normal conditions is to control excessive immune responses. In cancer, their principal role is to suppress cytotoxic T cells, B cells and dendritic cells through the expression of immunosuppressive and pro-inflammatory cytokines (jr).

Natural killers (NKs)

NK cells belong to the innate immune system, although they have a similar role to CTLs. High infiltration of NK cells is associated with improved prognosis in several cancer types. NK cells can effectively kill cancer cells through the release of perforin and granzymes, and induction of apoptosis through the FasL mechanism. NK cells can also produce pro-inflammatory cytokines such as IFN- γ , TNF, IL-n, GM-CSF and CCLq, that extend anti-tumor activity (jq).

NKs activation is independent of antigen recognition and is modulated by the repertoire of activating receptors (NKG2D, NCR1) and inhibitory receptors “killer immunoglobulin-like receptor” (KIRs). KIRs are receptors of HLA class I, and are the main repressors of activation against self-tissues. Under normal conditions, healthy cells express high levels of HLA class I, that ligates the KIR receptor, in order to evade NK cell attack. NK cells in the TME are activated through the activating receptors that bind to tumor cells under stress conditions. Through the activation of these receptors, NK cells have the ability to detect and attack cells with loss of HLA class I expression (jn).

B cells

B cells have an anti-tumoral function by antibody production and secretion of cytokines that promote cytotoxicity. They can also prompt T cell activation by antigen presentation. B cells are usually located at the margins of the tumor and can also be found in the tertiary lymphoid structures (TLSs). These are micro-lymphoid organs formed within the TME, composed predominantly by B cells and dendritic cells, that later become germinal center areas. TLS are associated with increased cytotoxicity and improved prognosis in many solid tumors (jm). A subtype of B cell, Bregs, are pro-tumor cells that express immunosuppressive cytokines like IL-10 and TGF- β , and promote the infiltration of pro-tumoral immune cells (jp).

Dendritic cells (DCs)

DCs are myeloid-derived cell-types that play a central role as APCs through the process of antigen capture and presentation to T cells at secondary lymph nodes. DCs are the bridge between the innate and the adaptive immunity. Once they are mature, DCs can infiltrate into the TME and activate the recruitment of immune effector cells. DCs can directly interact with B cells, T cells and NK cells for cross-activation. On the other side, DCs can be modulated by the cancer cells to a tolerogenic phenotype that rest non functional (jp).

Dendritic cells are a highly heterogeneous population composed by two main populations: conventional DCs (cDCs) and plasmacytoid DCs (pDCs), with further diversity and distinct subtypes. cDCs are subdivided in cDC1 and cDC2; cDC1 are considered the cross-presenting DCs, with key function in mediating T cell

inflammation and secretion of cytotoxic cytokines. The roles of the other DCs are less established, but cDCV are known to play a critical factor as enhancers of CD⁺ T cell response, while pDCs are mainly producers of type-I-IFNs (jX).

Macrophages

Macrophages are monocyte-derived cells and can be categorized as Mj or MV. Mj macrophages have an essential role of phagocytosis and killing cancer cells, also in production of pro-inflammatory cytokines and ROS species. Conversely, MV macrophages are immunosuppressive cell-types that promote tumor growth and participate in wound healing. They can promote angiogenesis and extracellular remodeling by expression of TGF- β and other secreted factors. Cancer cells can promote MV phenotype through the expression of cytokines like IL-r (jW).

Neutrophils

Neutrophils are granulocytes that in normal conditions become the first line of defense against infections. They are very abundant in the circulation, accounting for up to mX% of leukocytes in humans. The main mechanism of defense by neutrophils is degranulation, phagocytosis and release of extracellular traps. Primarily during tumor evolution, neutrophils act as anti-tumorigenic element, by secreting inflammatory cytokines and ROS. Later on, they shift to NV phenotype with pro-tumorigenic functions, such as the ECM modification and stimulation of angiogenesis (jk).

Myeloid-derived suppressor cells (MDSCs)

MDSCs consist of granulocytic and monocytic myeloid derived cells, morphologically similar to NV neutrophils and macrophages. MV macrophages are the major source of MDSCs. These cells have been strongly associated to a pro-tumorigenic microenvironment and bad prognosis. Their main functions are promotion of angiogenesis, induction of cell migration and inhibition of T cell function (VX).

1.1.2. Stromal components of the TME

Stromal cells are endogenous cells from the tissue stroma that cancer cells recruit to support their growth and propagation through secretion of growth factors and cytokines. Stromal cells composition can vary significantly between different tumor types, although main components include vascular endothelial cells and fibroblasts (Vj). Astrocytes, pericytes and adipocytes can also participate in the TME with key functions in some tumor types, although they are not in the scope of this thesis and will not be described.

Table R. Stromal cells in the TME.

Cell type	Function	Cytokine/ chemokine secretion	Gene markers	Effect
Endothelial cells	Formation of new blood vessels, promote cancer cells migration	VEGF	CD31, D34, VEGF	Pro-tumorigenic
Cancer-associated fibroblasts (CAFs)	Stimulates migration and invasion, ECM remodeling, promotes EMT and angiogenesis	Cytokines, growth factors, TGF- β	PDGF, FAP, FGFR, VDR	Pro-tumorigenic

Vascular endothelial cells

The vascular endothelium is the inner layer that surrounds blood vessels (veins, arteries, capillaries and lymphatic vessels), formed by a single layer of endothelial cells. Endothelial cells have a pro-tumoral effect through the formation of new blood vessels and promotion of cancer cells migration (Vj). The process of generation of new vessels in the TME is called **angiogenesis**, and it is modulated by tumor cells to bring in nutrients, oxygen and other metabolites into the tumor. Angiogenesis is mostly regulated by vascular endothelial growth factor (VEGF), which is upregulated under hypoxia conditions as well as by oncogenic signaling (like *Ras* and *Myc* pathways) (VV).

Cancer-associated fibroblasts (CAFs)

CAFs are activated fibroblasts that account for the principal component of the tumor stroma and play a critical role in tumorigenesis. They can have different origin, like tissue resident fibroblasts, or other cell-types like endothelial cells, adipocytes,

pericytes, stellate cells, and mesenchymal stem cells. Under injury, fibroblasts activate to myofibroblasts, which participate in wound healing, produce growth factors and trigger proliferation and extracellular matrix formation (Vp).

In the tumor microenvironment, cancer cells secrete factors that convert myofibroblasts into CAFs, which are a heterogeneous population of pro-tumorigenic cell-types. They dampen anti-tumor immune response through the expression of pro-inflammatory factors. CAFs also contributes to tumor growth by the expression of TGF- β , that drives epithelial mesenchymal transition (EMT) (Vr). EMT consists in the process where epithelial cells lose their cell-cell adhesions and are able to migrate and invade new stroma.

1.1.3. The dual role of the TME: a context-dependent function

The different elements comprising the TME are constantly evolving, establishing a dynamic crosstalk between tumor cells and its surrounding stroma. The TME has a dual role in tumor progression and metastasis: it can act as a friend or foe for tumor development (**Figure U**). In one way, the TME can modulate cancer cells to restrain tumor proliferation (Vq,Vn). Oppositely, cancer cells are able re-educate its TME as a means to convert it towards a favorable niche for tumor proliferation (Vm).

Overall, several evidences are giving new insights to the importance of immune components of the TME in tumor growth, dissemination and therapeutic resistance (VW,Vk). Cancer cells can hijack the immune system to facilitate tumor growth and progression. There is also a high contribution of stromal and vascular factors in the modulation of the TME. Specifically, angiogenic components plays an important role in tumorigenesis, directly contributing to immune evasion and tumor growth (pX).

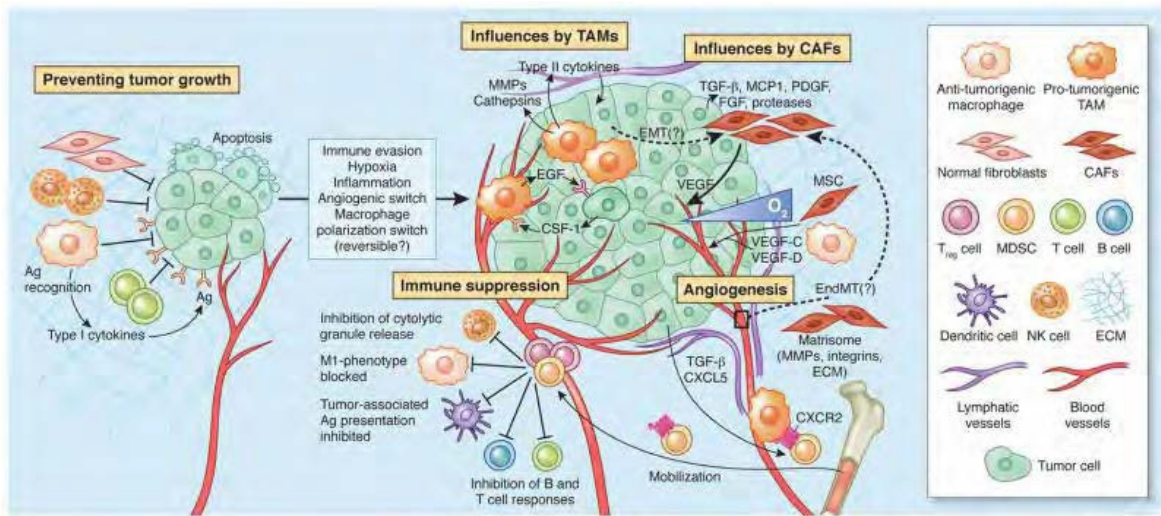


Figure @. TME dichotomous function in the primary tumor niche. High number of CD0+ T cells, CDQ+ ThL and NK cells characterize the anti-tumorigenic niche. Besides, macrophages ML and fibroblasts can also contribute to cancer cells destruction. Oppositely, a pro-tumorigenic niche is characterized by high presence of M: polarized macrophages, MDSCs and Tregs recruited from the circulation into the TME in response to chemokines secreted by cancer cells. These immunosuppressive cell-types suppress the activity of anti-tumoral cell-types like CTLs, NKs, DCs and B cells. In this context, TAMs and CAFS can trigger tumor growth by secretion of extracellular cytokines, growth factors (e.g., EGF, cathepsins), ECM remodeling factors, and induction of angiogenesis. Quail DF & Joyce JA, Nat Med, : ;LM.

1.2. Tumor immunity and immune evasion

The immunogenicity of a tumor is defined as the ability of the tumors to generate an immune response (pj). Two main interactions are required for effective immune response, both involving the antigen presentation process: (i) cancer neoantigens are presented to naïve T cells by activated APCs at the draining lymph nodes to prime tumor-reactive T cells, and (ii) neoantigens are presented by cancer cells and recognized by CDW+ T cells that triggers tumor destruction.

A high immunogenicity has been linked with good prognosis in numerous tumor types, being an essential feature for recognition and attack by the immune system. The immune surveillance mechanism selects low immunogenic clones, allowing cancer to evade the immune system and proliferate, in an evolutionary process called immunoediting (pV). Furthermore, cancer cells can escape the immune system by triggering different immune evasion mechanisms (pp).

1.2.1. The cancer-immunity cycle

The cancer-immunity cycle, defined by Chen & Mellman in VXjp (pr), represents the cyclic process that is required to generate an effective anti-tumor response. It is a simplified overview of the antitumor immunity, and divides the immune response in seven steps, from the release of antigens to the destruction of cancer cells (**Figure N**).

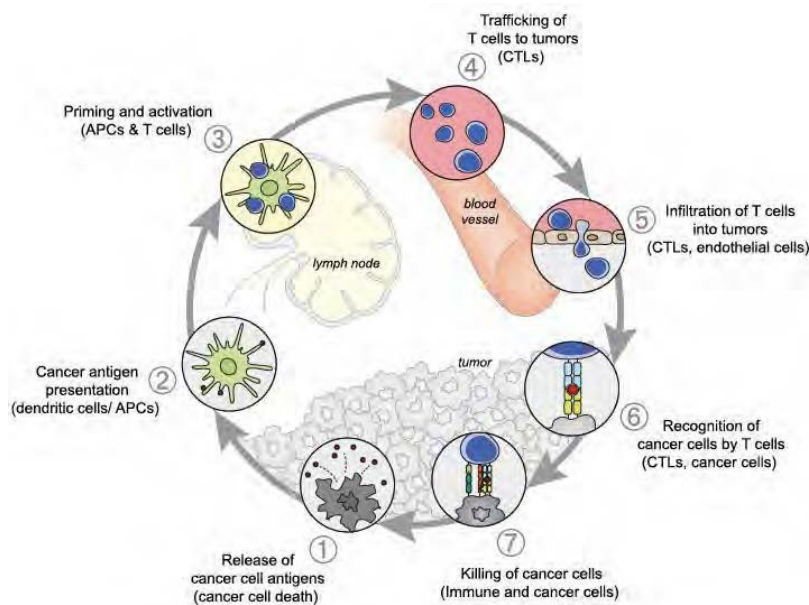


Figure A. The cancer-immunity cycle. (L) Neoantigens are generated by cancer cells, which are detected and processed by dendritic cells (DCs), that migrate to secondary lymph nodes and evolve to antigen presenting cells (APCs). (:) APCs present the neoantigens on MHC class I and II to T cell, (M) which triggers T cell priming and activation of effector T cells at the lymph nodes. (Q) Effector T cells traffic then to the blood vessels and (I) infiltrate into the tumor. (^) TCRs recognize specific neoantigens bound to MHC class I and (_), finally killing the cancer cells. Chen DS & Mellman I, *Immunity*, ;LM.

Different co-stimulatory signals are required for proper function of the cancer-immunity cycle. Interaction of CDVW, which is expressed on T cells, with its ligands CDWX (Bm-j) and CDWn (Bm-V) on APCs is the main co-stimulatory signal. CDVW activation triggers pathways that upregulate the expression of IL-V, that in turn upregulates the expression of cytokines like type-I-IFN, amplifies glucose intake and promote T cell survival and T cell response to stimulation. On the other hand, tumors express negative feedback regulatory mechanisms, also called co-inhibitory signals, aimed to evade the immune system. The principal co-inhibitory signals of T cell priming and activation are immune checkpoints CTLA-r and PD-Lj, respectively (pq).

1.2.2. Neoantigen presentation and T cell activation

Somatic mutations accumulate during tumorigenesis, mostly as a consequence of defects in the DNA replication and repair machinery, due to endogenous or exogenous mutagens. Tumor-specific antigens (TSAs) arise from somatic mutations, and consist in aberrant amino acid sequences patient-specific and not present in normal cells. TSAs arise from genomic alterations, including single nucleotide variants (SNV), insertions and deletions (INDELs), gene fusions, aberrant splicing events and integration of oncogenic viruses, among others. Point mutations result in single amino acid changes in the protein, whereas INDELs and other alterations produce frameshift peptides that can generate even greater antigenicity (pn).

The emergence of NGS technologies, along with the advances in bioinformatics algorithms, have allowed scientists to explore the mutational landscape of large omics datasets. In VXjp, Alexandrov et al. analyzed a total of mXrV cancer genomes and described the number of somatic mutations by tumor type (**Figure P**) (pm). Tumor mutational burden (TMB) is defined as the number of mutations per mega base.

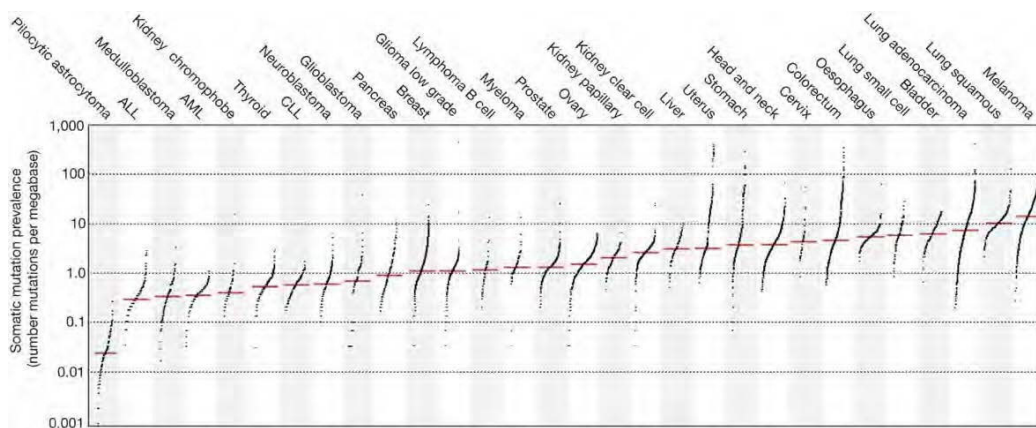


Figure B. Representation of median number of mutations across cancer types from the TCGA. Red lines represent the median mutations/mb per tumor type. This study revealed the high genetic heterogeneity between the different tumor tissues, as well as within tumor types. ALL, acute lymphoblastic leukemia; AML, acute myeloid leukemia; CLL, chronic lymphocytic leukemia. Alexandrov LB et al., *Nature*, ; ;

Tumors carrying >10 mutations/mb are usually categorized as ‘hypermutated’. Hypermutant tumors are usually those that are mostly caused by environmental factors, such as skin melanoma, caused by UV light, and lung cancers, caused by

carcinogens in tobacco (pW). In addition, a subset of colorectal, stomach and uterus cancer samples show extremely high TMB. These patients are catalogued as MSI and POLE tumors, both characterized by a high number of mutations, due to DNA mismatch repair deficiency and mutations in the polymerase ϵ , respectively (pm).

Tumor neoantigens result from the processing of these genetic alterations through the **antigen processing and presentation** machinery (**Figure V**), that present these small neoantigens on cancer cell surface and are recognized as foreign by specific CD8⁺ T cells, triggering the killing of the tumor cell (pk). MHC class I molecules bind to small peptides of 9-10 amino-acids length, which are presented in the peptide-binding groove, delimited at both ends by the flanking regions. On the other side, MHC class II molecules can also present peptides that are recognized by CD4⁺ T cells, although they can present peptides up to 25 amino-acids long, due to the conformation of the MHC-II, which is open at both ends allowing binding to extent out of the groove (rX).

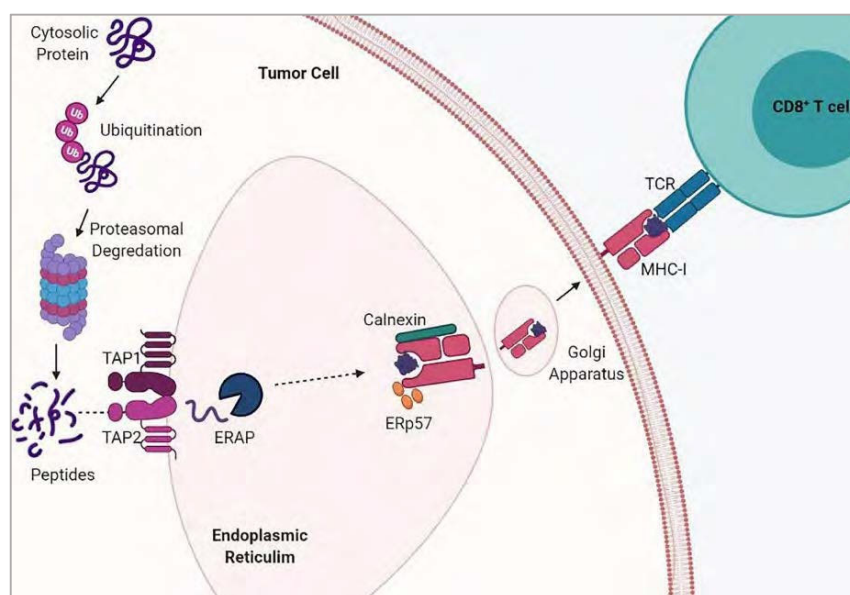


Figure H. Neoantigen processing and presentation. Somatic mutations are transcribed into mutant mRNA and translated into proteins which carry the mutated amino acid. By proteasome degradation, these proteins are degraded into 9-10 amino-acids length mutated peptides, transported into the endoplasmic reticulum (ER) through the transporter associated with antigen processing (TAP). Peptides are loaded on MHC class I molecules and B2M complex. MHC-peptide complex is transported to the cell surface and presents the neoantigen. CD8⁺ T cells recognize the MHC-peptide complex via specific TCR, triggering the activation of T cells against specific cancer cell. Taylor BC & Balko JM, Front Immunol, 2014;5:1000.

Major histocompatibility complex (MHC) molecules are cell-surface presenters of antigens to T cells, and allow T cells to differentiate healthy cells from infected or tumoral cells. **Human leukocyte antigen (HLA)** genes encode for the proteins that form the MHC. MHC class I genes include mainly HLA-A, HLA-B and HLA-C and are expressed by most cells of the body, while MHC class II genes include HLA-DP, HLA-DQ and HLA-DR and are expressed only by antigen presenting cells (rX). HLA genes are the most polymorphic region in the human genome, with more than pr,XXX known alleles, that can be grouped in HLA supertypes (rj). These polymorphisms cause variations in the peptide-binding specificities, generating a high diversity of MHC molecules for the recognition of large repertoire of peptides.

Antigen presentation is upregulated under inflammatory conditions, in response to inflammatory cytokine IFN- ψ , which triggers the activation of the JAK-STAT signaling pathway, leading to induction of the expression of the HLA-I heavy chain and beta-2-microglobulin (B2M), the two main components of the MHC complex (rV). High expression of HLA-I and HLA-II on tumors and APCs have been associated with better outcome in several cancer types, and has been used as a surrogate of immune activation in many studies (rp). Furthermore, higher HLA heterozygosity has been related to response to immunotherapy in melanoma patients (rr).

Nevertheless, the antigenicity extent of neoantigens remains unclear, since the ability of the MHC to bind the peptides is an essential part of the peptide presentation. The complexity of this binding involves several factors: the expression of the neoantigen in the cell, the percentage of tumor cells that express the neoantigen of interest, the proteasomal cleavage potential, the potential of transport in the ER, the stability of the MHC-peptide interaction and the binding potential of the interaction (rq). Furthermore, not only the expression of the neoantigen by MHC molecules is important, but also the infiltration of antigen-specific T cells is required for the immune response to be generated. Thus, even for tumor types with high TMB, T cell reactivity can be detected only for a small fraction of the somatic mutations (rn).

1.2.3. The cancer immunoediting process

As described in previous sections, the immune system plays a dual role in cancer, evolving from inhibiting carcinogenesis towards promoting tumor progression (rm). Cancer immunoediting is the process by which the immune system shapes tumor immunogenicity, and consists in three phases: elimination, equilibrium and escape (**Figure O**) The process of immunoediting triggers the emergence of tumor sub-clones with lower immunogenicity. These evasive characteristics can be due to either immune-adapted phenotype (selection of low antigenic mutations) or immune escape mechanisms (rW).

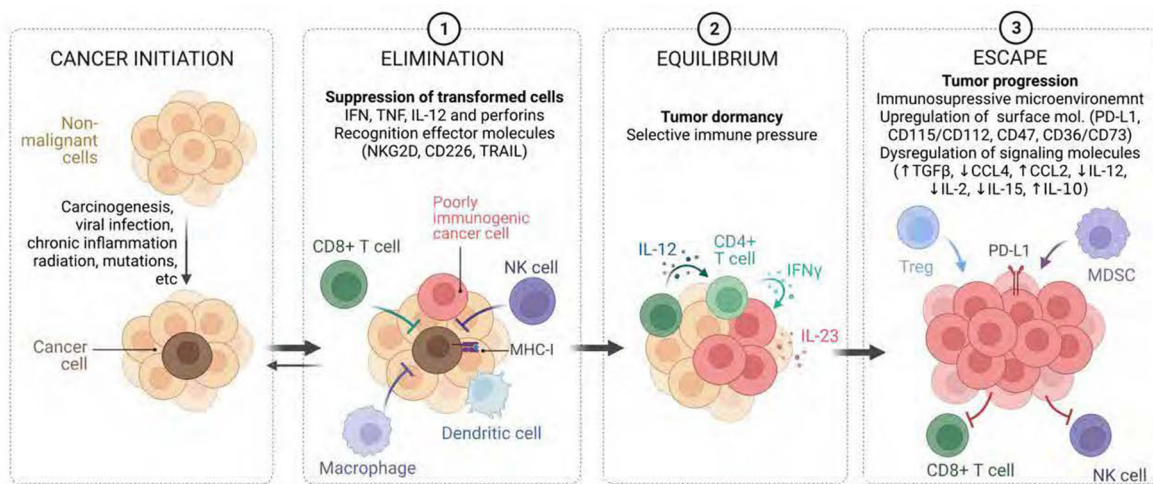


Figure J. Immunoediting process. In the first phase, **elimination**, the immune system is correctly recognizing and killing malignant cells. If this phase succeeds, all transformed cells would be eliminated and the tumor would not progress. However, if a few tumor clones are able to survive the elimination phase, they will progress into the **equilibrium** phase. In this phase, there is a constant pressure of the adaptive immune system over the tumor, and it is when low immunogenic sub-clones are selected for its advantage for evading the immune recognition. These immunoedited sub-clones can enter in the **escape** phase, in which the tumors progress and growth without immune pressure Adapted from O'Donnell JS, et al., Nat Rev Clin Oncol, ;;La.

1.2.4. Mechanisms of immune evasion

Cancer cells can escape the immune system by triggering different immune evasion mechanisms. Resistance mechanisms can be primary or acquired during therapy, and are mostly based in lack of antigen presentation and the modulation of the microenvironment through different molecules like oncogenic pathways or the expression of checkpoints (pp).

Impaired antigen presentation

Given the paramount importance of neoantigen presentation and recognition for an effective immune response, the main mechanisms of immune evasion are devoted to avoid immune recognition through defects in the antigen presentation machinery (rk). Different mechanisms can lead HLA class I downregulation; mutations in HLA and B2M genes, HLA class I loss of heterozygosity, and transcriptional repression of HLA-coding loci have been observed as innate and acquired mechanisms of resistance to immunotherapy (qX). Additionally, deleterious mutations or loss of β -2-Microglobulin (B2M), the invariant chain of the MHC, has been shown to generate defects in the antigen presentation pathway (qj). Other mutations can occur in other genes such as TAP1, TAP2, CALR and PDIA1 (qV).

HLA loss of heterozygosity (LOH) is an important mechanism of immune escape in immune hot tumor types. The loss of the HLA repertoire has been associated with different sub-clonal neoantigen burden, upregulated mutagenesis and higher PD-L1 expression in non-small cell lung cancer (qV). In a similar way, in lung cancer patients it was seen that relapsed tumors lost m to jW putative neoantigens, and those that were lost were the ones with higher affinity to be presented by MHC that could elicit a T cell response (qp).

Disruption of IFN- γ signaling

Another principal feature of immune evasion is the impairment of IFN- γ signaling pathway. An important function of IFN- γ is the upregulation the antigen presentation machinery upon the recognition by IFN- γ receptors (IFNGR1/2) on tumor cells, which triggers upregulation of MHC molecules through the JAK1 and JAK2 signal transducers. Functional mutations in the JAK1 and JAK2 of the IFN- γ pathway have

been described as a mechanisms of resistance in melanoma, making tumor cells less susceptible to the attack by T cells and resistance to the antiproliferative effects (qr,qq).

Nevertheless, defects in the IFN- γ signaling and loss of HLA triggers NK cells infiltration and attack, as a safeguard of T cell inhibition. Using CRISP-R screening methods, a recent study uncovered how cells that undergo these mechanisms are highly sensitive to destruction by NK cells (qn). In stage II CRC patients, our group has recently demonstrated the positive correlation between HLA-A downregulation and increase of NK cells infiltration. This phenotype was associated with better survival, evidencing the role of NK cells against resistant cancer cells (qm).

Oncogenic signaling

Oncogenic pathways can also influence the immune evasion by limiting the infiltration of cytotoxic lymphocytes into the tumor core and therefore generating an immune-excluded microenvironment. Some oncogenic pathways, like WNT- β -catenin, PTEN and MYC have been associated with lower T cell infiltration through the production of immunosuppressive cytokines, higher PD-Lj expression and failed infiltration of antigen presenting cells (APCs) (qW).

Expression of immunosuppressive molecules

Finally, the expression of mechanisms of immunosuppression includes the immune checkpoints (PD-Lj and CTLA-r) and other markers of T cell exhaustion, such as the expression of co-inhibitory receptors (T cell immunoglobulin and mucin-domain containing-p; TIM-p), lymphocyte-activation gene; LAG-p), and immunoregulatory molecules (indoleamine-V,p-dioxygenase; IDO). These molecules trigger loss of effector functions (\downarrow IFN- γ , IL-V and TNF- α) and loss of proliferative capacity of T and B cells (qk).

1.3. Tumor immune microenvironment heterogeneity

Cancer is a highly heterogeneous disease, with great variability across tumor types, stages of the disease, anatomical location and even among patients sharing location and histopathological features. The role and proportion of the immune components in the tumor niche is an important source of heterogeneity between cancers with implications in prognosis and therapy response (nX).

The classification of cancers based on their immune contexture has gained importance during last years (nj). Different immune profiles in solid tumors were first described in VXXk by Camus et al. in a cohort of primary colorectal cancer (CRC) (nV). They were able to discriminate between *hot*, altered (excluded) and *cold* immune phenotypes. The principal difference between these three groups is the presence and location of cytotoxic T cells infiltration (np). These distinct groups have differences in the risk of relapse and response to ICIs, and must be tackled through different treatment strategies (**Figure W**) (nr).

Inflamed tumors (so-called *hot* tumors) have high presence of TILs, functional CDW+ cells, high expression of immune checkpoints (PD-Lj, CTLA-r, LAGp, TIMp, etc), high levels of pro-inflammatory cytokines and high TMB. Advanced stage melanoma, renal cell carcinomas, and non-small-cell lung cancer (NSCLC) are examples of *hot* tumor types, where the administration of immunotherapies have been approved successfully. *Hot* tumors are more prone to benefit from immunotherapies, with durable responses in many cases.

Altered tumors (also named immunosuppressed or excluded) show high TMB, but increased immunosuppressive factors (angiogenesis, Tregs, TAMs and MDSCs), which prevents T cells from infiltrating the tumor. They also show high levels of hypoxia, expression of inhibitory cytokines, and ECM remodeling factors that creates a physical barrier. Some tumor types are being studied for its exclusion characteristics, like stable colorectal cancer, prostate cancer, bladder cancer, breast cancer, or head and neck squamous carcinoma. Altered tumors usually do not benefit from immunotherapies, and need treatment strategies to make them more susceptible to respond.

Finally, **non-inflamed** tumors (*cold* tumors) are characterized by low TMB, low TILs infiltrate, incorrect antigen presentation and lack of T cell priming and activation. These are the most challenging tumor type for immunotherapy, since they lack pre-existing immunity and they are not responders. Examples of cold tumors are ovarian cancer, pancreatic cancer, glioblastomas and uveal melanoma.

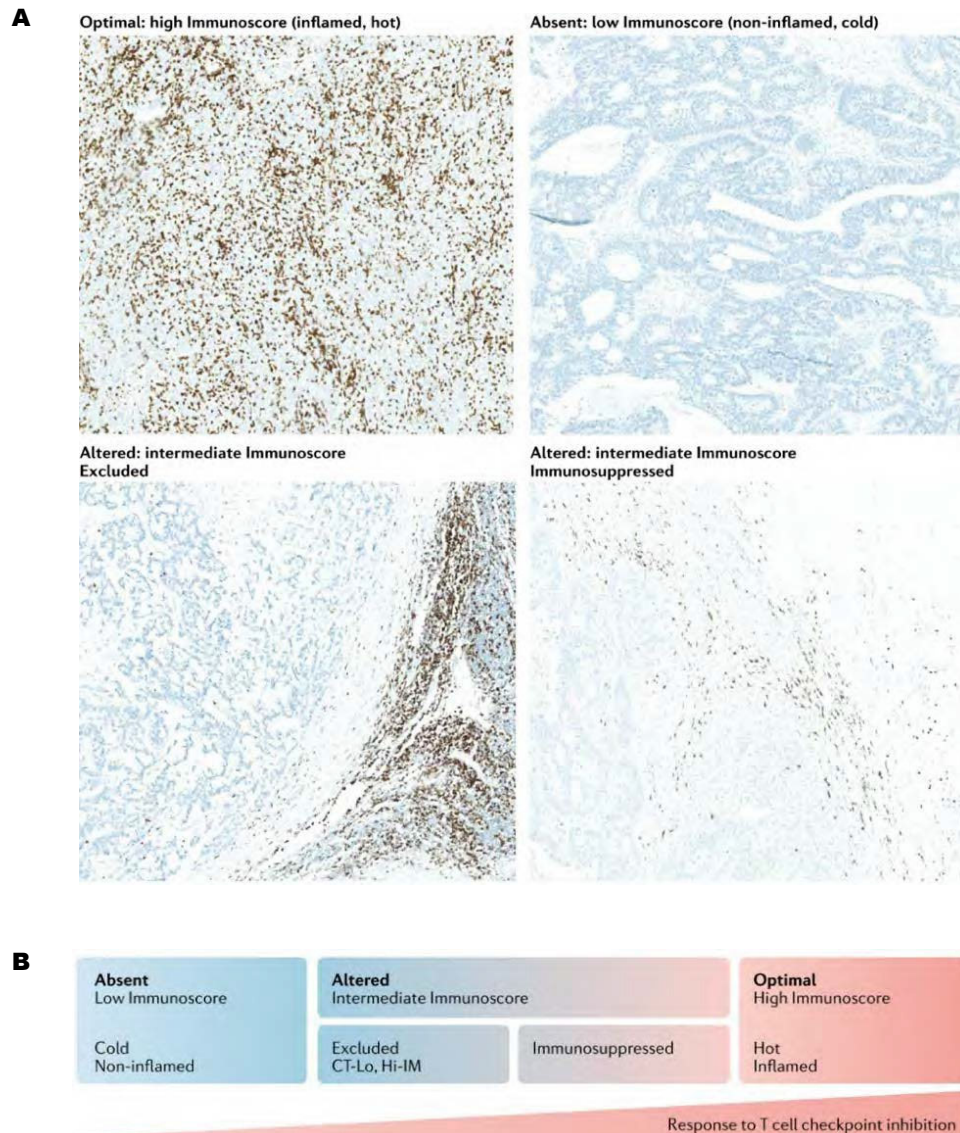


Figure M. The immune landscape of solid tumors. A) DAB staining (brown) on tumor slides represents CD8⁺ T cells, and alkaline phosphatase (blue) stains for homogenous tissue. **B)** The different immune phenotypes correlate with the gradual increase in response rate to ICIs. Figure from Galon J et al, Nat Rev Drug Discov, 2018.

1.3.1. Uveal melanoma as a divergent tumor type

Uveal melanoma (UM) is the most common ocular malignancy in adults, with an annual incidence of q cases per million in Europe (nq). It is considered a rare tumor due to its low incidence. Current treatments of primary UM are mainly based on radiotherapy and enucleation. Despite the success in the management of primary tumors, UM prognosis is bad, with up to $qX\%$ of patients developing metastasis, mostly to the liver ($Wk\%$) (nn). In these cases, median survival time is approximately jV months. The main reason for this low survival rates is the lack of therapeutic options for advanced disease since targeted therapies or immunotherapies have slightly improved results compared to chemotherapy (nm).

Clinical prognostic factors (sex and age), tumor thickness, location, cell morphology, vascularity, and molecular factors (chromosome p monosomy, chromosome W polysomy, and $BAPj$ loss) are usually used as prognosis factors of metastatic relapse (nW). UM originates in the melanocytes of the uveal tract (**Figure S**). Iris and ciliary body UM grow in the acellular corpus vitreous, protected by the blood-retinal barrier, which provides an immune privileged niche. In the case of UM growing in the choroid, it is separated from the retina by a membrane, so the immune privilege in this location is under revision (nk).

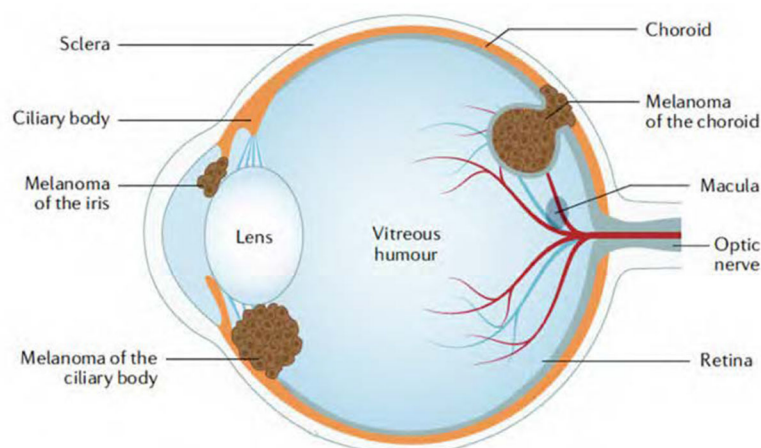


Figure P. Main locations of uveal melanoma within the eye. UM arises from melanocytes from the choroid ($O\%$), ciliary body ($]O\%$) and iris ($M-]%$). Jager MJ, Nat Rev is Primers, ;;;.

Up to 70% UM patients carry driver mutations at GNAQ/jj genes and 15% carry recurrent alterations in BAPj. GNAQ and GNAHH encode the α subunit of the heterotrimeric G proteins located in the inner surface of the cell membrane, which activate intracellular signaling (Figure HQ) (mX). GNAQ and GNAjj mutations are mutually-exclusive and are most frequently mutated at codon QVXk (70%), followed by codon RjWp (10%) and exceptionally codon GrW. CYSLTRV gene, a cell-surface leukotriene receptor of the G proteins is also mutated in about 15% of UM patients (nn).

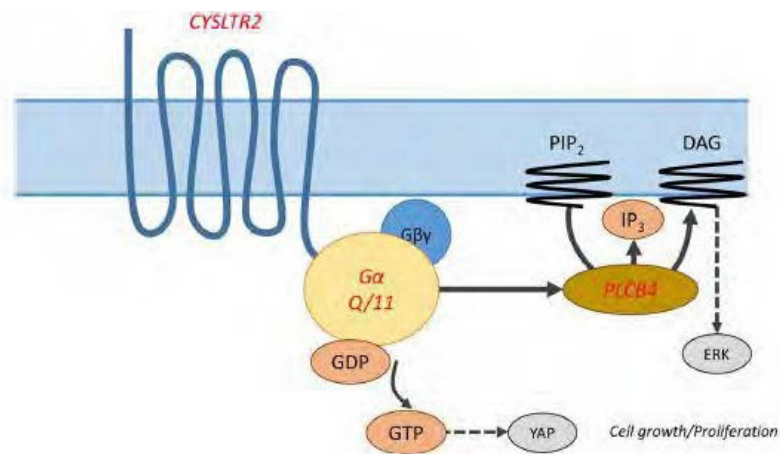


Figure (R. G-protein pathway alterations. Mutations at Q11, a hotspot of genes GNAQ or GNALL activates the G α_q pathway, leading to a constitutive signaling that activates different pathways like YAP, MAPK and APL pathways, stimulating cell proliferation. De Lange MJ, Mol Biomed, 2015;1:1.

Although it shares the cellular origin with cutaneous melanoma (CM), the biology and molecular mechanisms of UM are significantly different to those of CM. The principal differential characteristic of UM is the low antigenicity. In a study by H. Bailey et al. where they performed a pan-cancer analysis across 10,000 samples from 15 different cancer types from the TCGA, UM was the third lowest cancer type in TMB, only after rare tumor pheochromocytoma and paraganglioma, and thyroid carcinoma (mj). Other aspects where UM differs from CM is the dissemination via hematogenous spread. UM grows in one of the most capillary-rich tissues in the body and expression of angiogenic factors is considerably higher than in CM (mV). The expression of high levels of VEGF and fibroblasts growth factors facilitate tumor growth and blood dissemination, and is associated with worse prognosis and recurrence (mp).

Since the eye must maintain a low immunogenicity for protecting the ocular tissue and evading overreactions of the immune system, it develops special mechanisms for immune protection (mr). This ocular immune privilege is mainly conferred by low HLA class I levels and inhibition of NK cells via expression of pro-inflammatory macrophage migration inhibitory factor (MIF) cytokine. Also, recent studies have found infiltration of Tregs in healthy aqueous humor, which triggers expression of TGF- β and an immunosuppressive microenvironment (mq).

UM hijacks this immunosuppressive milieu of the eye in order to evade the immune system and promote tumor growth. UM cells can also generate evasion mechanisms by the expression of pro-oncogenic molecules such as indoleamine dioxygenase-j (IDO-j) and immune checkpoints (PD-Lj, LAG-p, TIMp, etc). UM protects from apoptosis by production of soluble FasL, which blocks the FasL-induced apoptosis by lymphocytes. Finally, it shows loss of allele specific HLA, which is a known mechanism of immune evasion (mn).

All these distinguishing features of uveal melanoma make it a distinctive tumor type. Therefore, it must be studied with a different perspective than most solid tumors, included skin melanoma (mm). The reasons underlying this negative prognostic role of immune infiltration remains unsolved so far.

1.3.2. The metastatic microenvironment

Metastasis is a complex process, which involves several changes that allow the migration of cancer cells from primary tumors to distant secondary organs (mW,mk). To propagate, malignant cells must undergo the 'metastatic cascade', which consists in a series of steps: invasion, systemic circulation, evade immune attack in the circulation, extravasation, and finally seeding to secondary organ (mW).

This cascade includes the immunoediting process, already described, which allows low immunogenic cells to evade the attack by the immune system and disseminate. Metastasis is a very inefficient process; the vast majority of cancer cells that migrate from the primary tumor are unable to colonize secondary organs and are eliminated by the immune system in the blood circulation. A small proportion, otherwise, survive in a latent state in blood or host tissues. This evolutionary pressure selects clones with best fitness to metastasize in distant organs (mk).

1.3.2.1. Organ-specific patterns of metastatic colonization

Metastatic organ-specific colonization (also called **organotropism**) is a process regulated by multiple factors like molecular features of cancer cells, circulation patterns and the secondary host tissue (WX). The concept of organotropism was classically explained by the 'seed and soil' hypothesis, first described by Stephan Paget in jWWk, which hypothesized that metastatic organ-specificity is a result of favorable interactions between cancer cells (the 'seed') and the microenvironment of the host organ (the 'soil') (Wj).

The patterns of metastatic colonization are characteristic for each cancer type (WV,Wp) (**Figure HH**). Some cancer types have one principal metastatic site (e.g., uveal melanoma to liver and prostate cancer to bone), while others metastasize to two or more metastatic sites in different frequency. For example, CRC metastasize predominantly to the liver, comprising about WX% of CRC metastasis, being lung the second organ in frequency with about jX to jq% of metastasis. Another case would be breast cancer, which metastasizes preferentially to bone (qX%), followed by liver, lungs, bone and brain in lower frequency (WV).

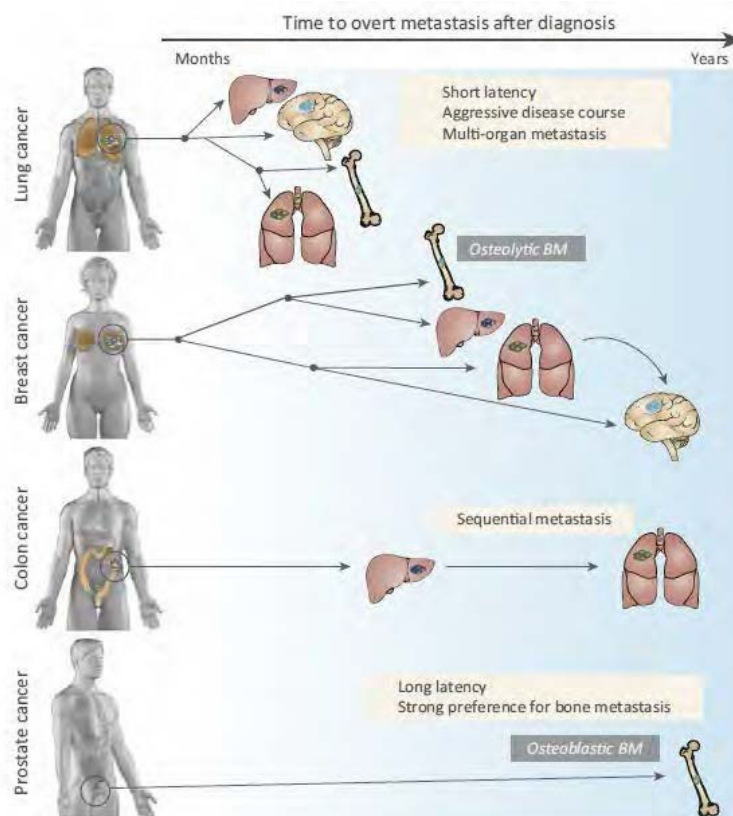


Figure 1. Different cancer types show divergent patterns of metastatic spread. The length of the arrows corresponds to the latency time. The first organ of each cancer type is the most frequent. Most cancer types have a specific metastatic pattern, which diverge in latency period, organotropism and the type of metastasis. Most frequent sites of metastasis are bone, brain, liver and lung. Obenauf AC & Massagué J, Trends Cancer, 2015; 4: 1-11.

Anatomical location of the primary tumor can partially explain the patterns of metastasis, as in the case of liver metastasis from colorectal cancer. Liver processes the blood from the gut through the portal venous, so it is the first organ where cancer cells arrive when they enter the blood circulation in the gut (Wr). However, organotropism cannot be explained by anatomical characteristics in other patterns. For example, brain metastases from breast and skin would not be their primary site. Therefore, there are other components that act as key players in this metastatic organotropism, which are still not completely understood.

1.3.2.2. The microenvironment of metastatic niches

Primary tumors are able to engage the formation of **pre-metastatic niches** in secondary organs by different mechanisms, such as primary tumor-derived factors (exosomes, vesicles and cytokines), bone marrow-derived cells (BMDCs), and stromal components (**Figure HR**) (Wq). Pre-metastatic niches promote a chronic inflammatory and immunosuppressive state on distant organs that facilitates future metastatic colonization (Wn).

Metastatic cells need an immune tolerant microenvironment in order to succeed in the seeding process. Metastatic-associated macrophages (MAMs) derive from circulating monocytes, and are the main supporters of cancer extravasation and cell growth in metastatic sites. Tregs in the metastatic niche can also promote metastatic homing by overexpression of cytokines and growth factors (Wm) (**Figure HR**).

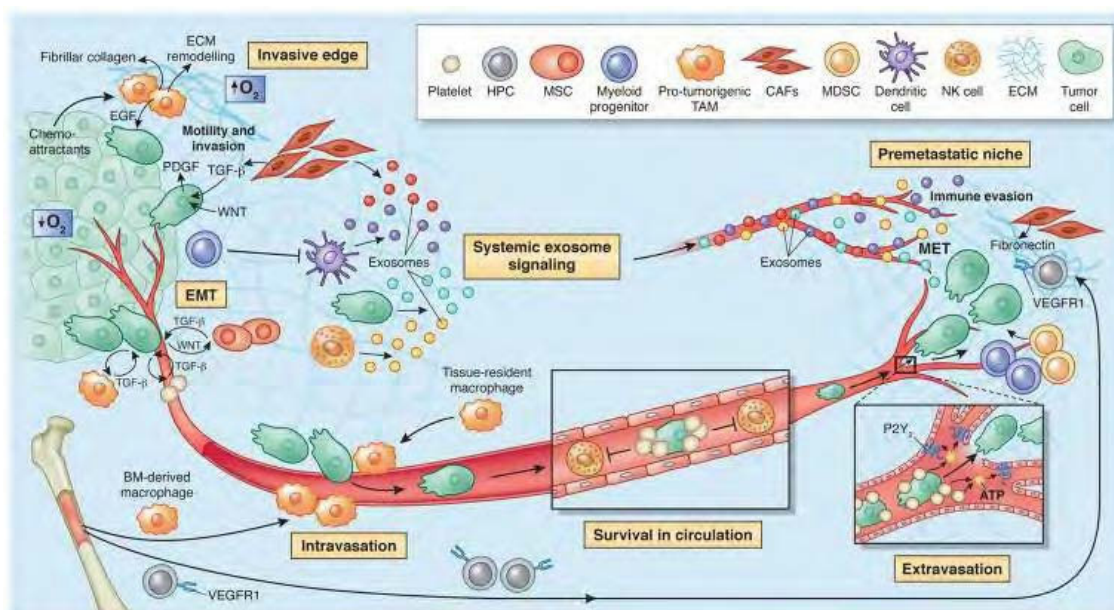


Figure (5. Immunosuppressive cells promote tumor metastasis through multiple mechanisms in primary tumor and in the pre-metastatic niche. In the primary tumor, TAMs, MDSCs and CAFs accumulate at the invasive margin of the tumor, and promote EMT and cell-cell contact loss on cancer cells, allowing the acquisition of an invasive phenotype. At the intravasation step, macrophages help tumor cells to cross the vessel barriers. In circulation, tumor cells evade the attack of the immune system by attaching to platelets and coagulation components. Primary tumors can modulate the secondary niche towards an immune tolerant environment to succeed in the seeding process through different mechanisms such as exosomes that modulate the stromal components of the pre-metastatic niche. Quail DF & Joyce JA. Nat Med, :;||.

The pre-metastatic niche composition differs between different host organs (WW). In liver, the formation of pre-metastatic niches includes tumor-secreted factors, BMDCs recruitment and ECM remodeling factors. In **lung**, the oxygen-rich environment dampens T cells response and promotes an immunotolerant environment that makes it favorable to metastatic formation. **Brain** metastasis is the most challenging metastatic organ because it is located in an immune-privileged organ. One of the mechanisms that has been observed in the pre-metastatic niches in the brain is the glucose metabolism. In the **bone**, by contrast, the pre-metastatic niche can be different depending on the type of colonization. In osteolytic bone metastasis, ECM regulators, IL-1 and MMPs are the regulators of the pre-metastatic niche. In osteoblastic, the mechanisms are not well defined, but could be influenced by tumor-derived factors like VEGF-A and fibroblast growth factor (Wq)

2. Immuno-oncology for cancer management

In the last years, massive knowledge has been reported about the role of immune system in cancer progression. In turns, immuno-oncology has emerged offering potential therapeutics and new biomarkers for cancer management.

2.1. Cancer immunotherapy

Immunotherapies are aimed to stimulate and restore the patients' immune system to attack malignant cells (Vk). In the last decades, the development of immunotherapies has represented a shifting point in patients' management. The most successful immunotherapies are immune checkpoint inhibitors (ICIs), although the rapid evolution on the field in the last years has yielded to the emergence of next-generation immunotherapies with comparable results (Wk).

2.1.1. Immune checkpoint inhibitors (ICIs)

ICIs are based on antibodies that block the interactions of immune checkpoints CTLA-r and PD-j/Lj in order to re-activate T cell responses. The discovery of ICIs was one of the major advances in cancer care in the last decades (kX). Indeed, James P. Allison and Tasuku Honjo were recognized with the Nobel Prize of physiology and medicine of VXjW for their contributions in the discovery of ICIs.

Ipilimumab (anti-CTLA-r) was the first checkpoint inhibitor to demonstrate good response rates in a Phase II clinical trial in patients with metastatic melanoma in VXjX and it was approved in VXjj by the American Food and Drug Administration (FDA) (kj). Few years after, pembrolizumab (anti-PDj) demonstrated better progression-free survival compared to ipilimumab, being approved by the FDA in VXjq as first-line agent in advanced metastatic melanoma (kV) (**Figure HU**).

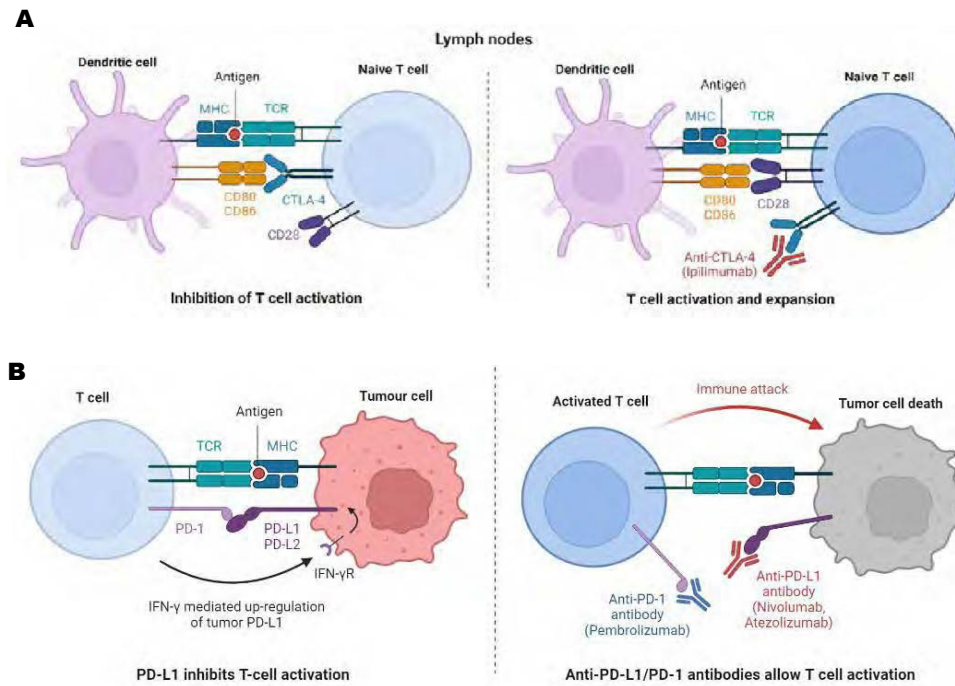


Figure (@. A) Mechanisms of action of anti-CTLA-4. In the lymph nodes, CTLA-4 binds to the co-stimulatory molecule CD80/CD86, leading to CD80/CD86 inhibition and decrease of T cell expansion. The anti-CTLA-4 antibody blockades this interaction, allowing the co-stimulatory binding, which increases the activation and expansion of naïve T cells. **B) Mechanism of action of anti-PD-1/PD-L1.** The binding of PD-L1 to its ligand PD-1 happens when peripheral T cells become quiescent because of prolonged antigen exposure. Monoclonal antibodies targeting PD-L1 and PD-1 block the interaction between these molecules. Once the interaction between PD-L1 and PD-1 is blocked, exhausted TILs can restore their function of cancer cells killing.

Over the last decade, a plethora of clinical trials on ICIs have been carried out in numerous tumor types, with heterogeneous responses (kp). In VXjm, the FDA approved immunotherapy as first-line treatment in hypermutated tumors harboring microsatellite instability (MSI-high) irrespective of tissue of origin, including some subtypes of colorectal, endometrial and gastric cancer.

In VXVV, a successful study was published in MSI-high locally advanced rectal cancer, in which they were able to generate overall response in all patients enrolled in a clinical trial with immunotherapy, evidencing the achievements of these treatments (kr). In the same line, results on a clinical trial in dMMR colon cancer were presented at this year's ESMO congress, where preoperative combinatory ICI treatment achieved pathologic response in kq% and disease-survival rate of jXX% (kq). Altogether, these impressive results are a proof-of-concept of the efficacy of immunotherapies.

2.1.2. Other immunotherapy-based treatments

Other immunotherapies, such as adoptive cellular therapies (ACTs), oncolytic viruses and neoantigens-based vaccine products are a growing field of research and have already reported promising results and improved responses in clinical trials (Table U) (kp).

Table @. Summary of current immunotherapy-based agents approved.

Class	Mechanism	Example	Tumor indication
Immune checkpoint inhibitors (ICIs)	Monoclonal antibodies against checkpoints	Ipilimumab (α CTLA-4), Pembrolizumab (α PD-1), Nivolumab (α PD-L1), Atezolizumab (α PD-L1)	Melanoma, lung, kidney, urothelial carcinoma, bladder, renal, stomach, squamous cell carcinoma, MSI-high tumors
Adoptive cell transfer (ACTs): CAR-T cells	Genetically engineered T cells targeting CD19	Tisagenlecleucel	Leukemias and B-cell lymphoma
Personalized vaccines	Vaccines loaded with patients' tumor neoantigens	NeoVax	Melanoma, glioblastoma, endometrial
Oncolytic virus	Genetically modified virus infection and lyse of T cells	T-VEC (attenuated HSV-1), ICOVIR (Adenovirus)	Melanoma, Neuroblastoma

ACTs consists in the transfusion of immune cells to the patients. There are different types: TILs transfusion (where immune-reactive T cells are expanded and infused back to the patients), chimeric antigen receptor (CAR)-T cells (T cells are engineered to express specific costimulatory molecules), and TCR-modified T cells, among others. Approved treatments with CAR-T cells have shown impressive results in the treatment of hematologic malignancies like leukemia and lymphoma, although it is still a challenge for solid tumors (kn).

Adoptive NK cell transfer has recently emerged as an alternative with therapeutic potential. NK cells can suppress tumor immune evasion mechanisms against T cells, thus targeting NK cells could be a proper strategy to overcome the resistance mechanisms to ICIs (qn). In solid cancers, pre-clinical models have demonstrated efficacy in ovarian cancer, glioblastoma and metastatic CRC. Current clinical trials with CAR-NK cells and allogenic NK cell transplantation in different tumors types are currently underway and results will be soon available (km).

Vaccine-based immunotherapies is another novel strategy for targeting the immune system and consists in the use of vaccines with the goal of amplifying the response of tumor-specific T cell. There are different approaches of vaccine immunotherapies; based on personalized neoantigen, dendritic cells, autologous cells or oncolytic virus vaccines (kp). Personalized vaccines with patient-specific neoantigens were first used in clinical trials for melanoma and prostate, where they have demonstrated encouraging results. Neoantigen vaccines therapies have a principal advantage compared to other immunotherapies; since they are targeted to tumor-specific neoantigen, which are not expressed by non-malignant cells, they can trigger tumor-specific immune response and reduce toxicities (kW).

2.1.3. Current challenges of immunotherapy

Despite the outstanding results of immunotherapies in a variety of advanced malignancies, its clinical benefit is still very limited to a certain subset of patients, and response varies across tumor types as well as between individual patients. Currently, ICIs have become the standard of care for melanoma and lung cancers, and generate durable responses in many cases. Unfortunately, only approximately VX% to pX% of patients respond to treatment (kk). Furthermore, the failure of immunotherapy for some of the most frequent and deadliest tumor types like pancreatic cancer, breast cancer and stable colorectal cancer is a major challenge for clinicians in the field (kX).

Currently, one of the main challenges in immuno-oncology is how to enlarge the number of patients that can benefit from immunotherapies. Many efforts are devoted to transforming non-responder tumors (immune *cold*) into responders (immune *hot*), as well as to overcome resistance mechanisms to ICIs (jXX). Recent advances in combination therapies have become a new opportunity to overcome this issue and are improving clinical responses. Some examples are combination of ICIs with chemotherapy, radiotherapy, oncolytic adenoviruses, targeted therapies, or with other immunoregulatory antibodies (PD-Lj, PD-j, CTLA-r, LAGp, TIMp, TIGIT, IDO, etc.) (jXj,jXV).

Other challenges of immunotherapies include the need for standardized protocols for the optimal dose, the surrogate endpoints, schedule and duration of therapy, the appropriate use of immunotherapies as adjuvant therapy, and the proper use of biomarkers for patient selection (jXj).

2.2. Immune biomarkers for cancer management

Biomarkers are defined as measurable indicators of biological processes or disease states that can aid clinical decisions. Biomarkers are very useful in oncology for several application like diagnosis, prediction of response to treatment and monitoring disease progression, among others. Recent advance in prognosis and prediction biomarkers based on omics data are improving the clinical management of cancer patients, for example in the use of targeted therapies (jXp).

In immuno-oncology, the identification of predictive response biomarkers is more challenging due to the multifactorial modulation of the immune response. Finding robust biomarkers for immunotherapy is especially necessary due to the potential toxicities and the high costs of these treatments. The advances of biomarkers discovery from NGS technologies will improve the screening of patients for an accurate selection of the patients who are more likely to benefit from immunotherapies (jXr).

2.2.1. Current setting of immune biomarkers in oncology

To date, several response biomarkers for immunotherapy have been described (Table N). PD-L1 and MSI status are the only biomarkers approved by the FDA to guide clinical decisions, although none of them is well established in the clinical practice. New approaches are focused in the combination of multiple biomarkers, intending to generate more accurate predictions. These biomarkers will integrate the information from tumor intrinsic (PD-L1, MSI, TMB) and extrinsic (TILs, cytokines) factors (jXp).

Table A. Biomarkers of response to immunotherapy.

Biomarker	Biological component	Assay method	Cancer types
PD-L1	Tumor intrinsic	IHC	Multiple cancer types
TMB	Tumor intrinsic	DNA gene panels, WES	Multiple cancer types
MSI-H/ MMRd	Tumor intrinsic	PCR/IHC	Colorectal, endometrial, gastric, renal carcinoma, etc.
Immunoscore	Tumor microenvironment	Digital pathology	Colorectal cancer
GEP	Tumor intrinsic, microenvironment	PCR, expression panels, microarray, RNA-seq	Melanoma, NSCLC
Cytokines	Circulating factors	Blood assay and count	Melanoma
LDH	Circulating factors	Blod assay	Melanoma

PD-L1/PD-1 expression

The expression of PD-L1 is the most rational biomarker since it is the main target of immunotherapies. The expression level of PD-L1 on tumor cells is measured by immunohistochemistry (IHC), a technique that consists in the measure of protein expression levels using antibodies that bind to the protein of interest (**Figure HN**) (jXq).

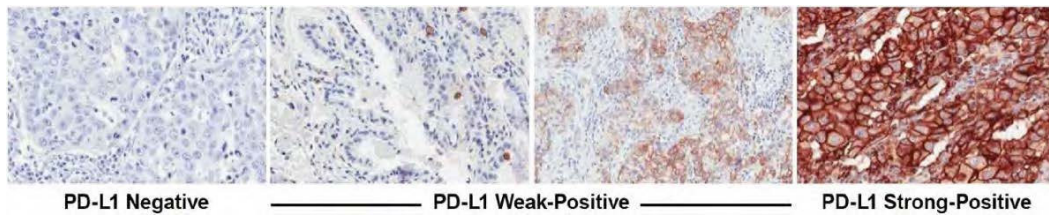


Figure (A. PD-L1(IHC staining in NSCLC tumor samples. This staining process is used for anti-PDL/LL treatment for patient selection. Sorensen SF, et al. Transl Oncol, ;L^.

Tumor infiltrating lymphocytes

The presence of T cells infiltration has clinical impact on prognosis (jXX). In VXjr, Galon et al. defined the “**Immunoscore**” assay as a prognostic marker in colorectal cancer based on the presence, density and localization of CDW+ and CDp+ T cells infiltrating in the tumor, measured by digital pathology (**Figure HP**) (jXm). The “Immunoscore” was validated in a big cohort with more than VnXX stage II-III CRC patients, with supporting evidence of its usefulness to include it for classifying CRC. A number of studies are trying to transfer this biomarker to other tumor types (jXW).

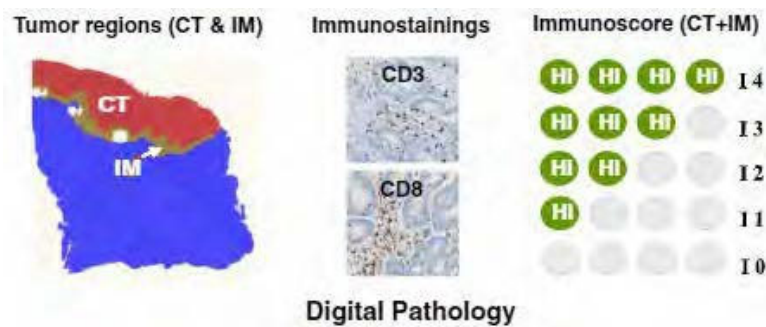


Figure (B. Immunoscore biomarker methodology. The immunoscore ranges from I; (cold) to IQ (hot) by combining the information from cell density of CDM and CDO in the core tumor (CT) and invasive margin (IM). Galon et al., J Pathol, ; ;lQ.

Tumor mutational burden

TMB is highly variable across the different tumor types, and a higher TMB has been associated with better response to ICIs in several studies (kW). In a review by Yarchoan et al. from VXjm, they showed the direct relationship between TMB and objective response rate (ORR) to anti-PD-j/Lj across Vm cancer types or subtypes (linear regression $p < X.XXj$, $r = X,mq$) (Figure HV) (jjX). This meta-analysis demonstrated the strong association between TMB and response to ICIs across many cancer types.

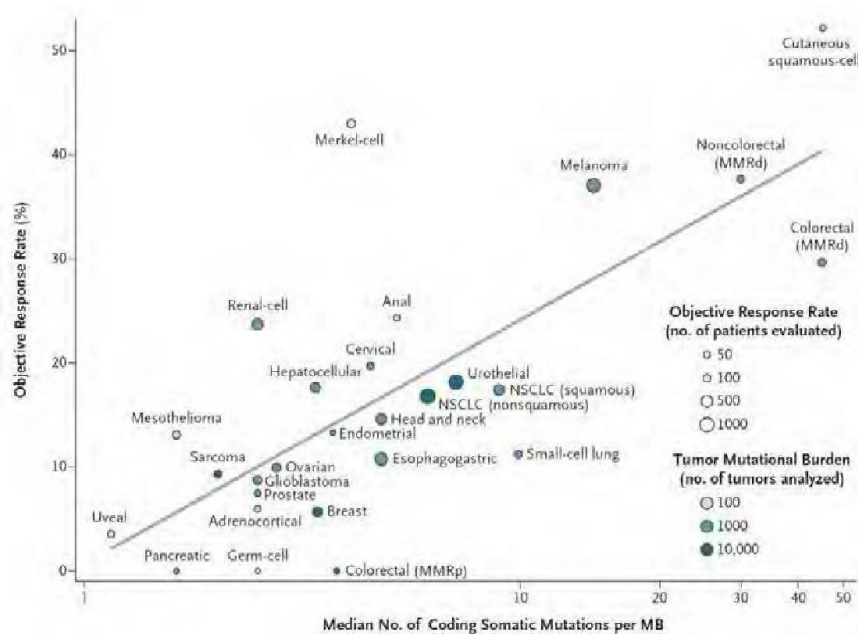


Figure (H. Correlation plot between OOR to anti-PD-/(/L(and TMB in somatic mutation per mega base in 5j different tumor types. Yarchoan et al., N Engl J Med, ;;L_.

Microsatellite instability (MSI)

Mismatch repair deficient (MMRd) status is defined by the lack of expression of different proteins from the DNA mismatch repair machinery. If those proteins are inactivated by mutational changes causing a large number of mutations, MSI-h status is defined. This molecular characteristic causes high mutational burden due to the lack of repair of the somatic mutations in the tumor. The use of MSI/MMRd status as biomarker of immunotherapy response has been demonstrated to have good prognosis power. MSI/MMRd status can be measured by different methods; PCR detection of MSI-H, IHC of dMMR and DNA sequencing. Detection by PCR and IHC are widely used in the clinics, for example for Lynch syndrome screening, while NGS methods are being used for research use only (jjj).

2.2.2. Immune signatures as response biomarkers

Transcriptomic technologies measure the expression levels of the mRNA of different genes at the cytoplasm of the cells. The main technologies for transcriptomics profiling are microarrays and RNA-seq. Transcriptomics profiling from bulk tumors have many applications in oncology, such as molecular subtyping, biomarkers discovery, gene expression signatures, and many more. Over the last years, numerous biomarkers from gene expression signatures have emerged as a result of the increase in the use of sequencing technologies, bioinformatics and improved statistical methods. These signatures are usually obtained by differential expression or other statistical methods and are markers of a specific phenotype (jjV).

Latest studies have demonstrated the efficacy of immune signatures from transcriptomics profiling as biomarkers for diagnosis, prognosis and response to immunotherapy across many cancer types (jjp). Immune signatures were first defined by Bindea et al., where they defined for the first time VW different immune cell-types, generating an “immune landscape” of solid tumors associated with clinical outcomes in a dataset of colorectal cancer (jjr). An example of immune response profile is the jW-genes **T-cell inflamed signature** (TIS). This transcriptomics profile was demonstrated to be highly associated to clinical response to anti-PD-Lj therapy across a wide variety of tumor types (jjq). TIS signature integrates genes of response to IFN- γ , from the functional status of the immune infiltrate (T cells, *HLA-E*, *CDZA* and *CD8*; NK cells, *NKH1*), antigen presentation (*PSMB1*, *HLA-DQA1*, *HLA-DRB1*, *CMKLR1*), chemokine expression (*CXCR1*, *CCLF*, *CXCL2*) and adaptive immune resistance (*PD-L1*, *PD-L8*, *TIGIT*, *LAG3*, *IDO1*, *CDVmn*, *STAT3*) (**Figure HO**).

Other groups have reported a variety of gene signatures related to the inflammatory process and T-cell response in different tumor types, such as the “tumor immune dysfunction and exclusion” (TIDE) signature (jjn) and the “immune-predictive score” (IPRES) signature (jjm). More recently, our group has also participated in a study on early-stage CRC, where immune profiles showed good prediction affinity of disease relapse (jjW).

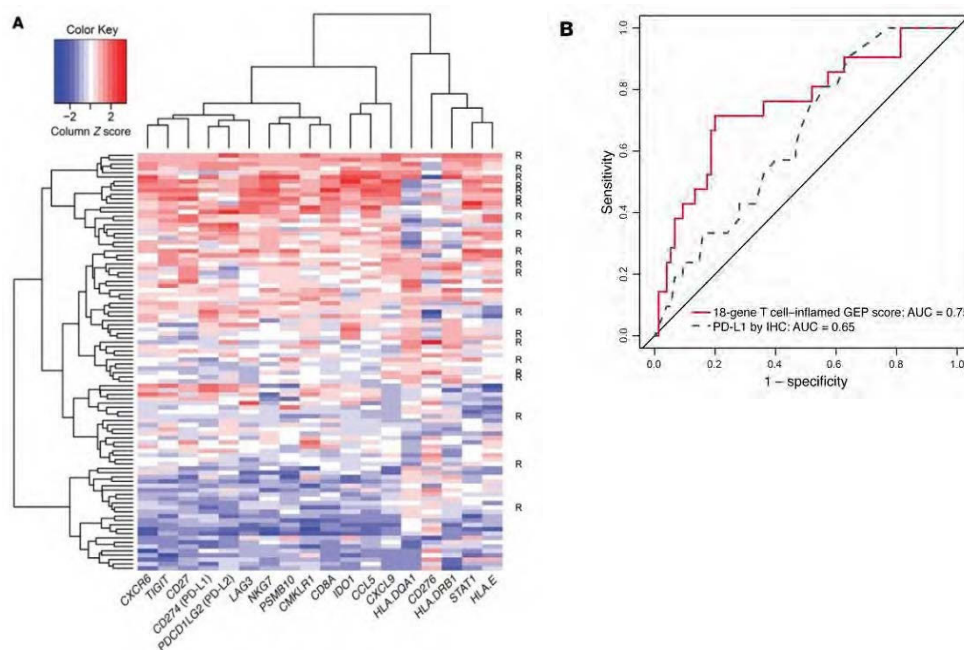


Figure J. T-Cell inflammatory signature. A) LO-genes TIS signature validation on a[^] samples from HNSCC treated with immunotherapy. B) AUC values from TIS score showed better prediction than AUC of PD-LL expression by IHC. Ayers M et al., J Clin Invest, ;;L_.

Machine learning techniques can be used to identify biomarkers from large-scale transcriptomics data and can improve the identification of gene signatures associated with response to ICIs with higher accuracy than current signatures. Litchfield et al. performed a meta-analysis of more than jXXX patients from seven different tumor types treated with ICIs, with available WES and transcriptomics data and machine learning methods. They found that a multivariate predictor combining TMB and CXCLk/CXCLjp expression to be a better prediction model of response to immunotherapy (AUC=X.Wn), outperforming the prediction power of TIS score (jjk).

Overall, immune signatures from transcriptomics have demonstrated to outperform classical biomarkers in the prediction of clinical responses (jVX). The principal limitation of these immune signatures is the translation into the clinical setting. Molecular assays of gene expression are still not included in the daily routine of most hospitals, thus making it difficult to do a screening for these high number of genes. Another limitation is that most of these signatures have been generated using datasets from *hot* tumors, mostly melanoma and lung, and the predictive values decrease when they are inferred to other cancer types or tumor stages (VW).

3. Immunogenomics for the study of tumor immunity

Bioinformatics consists in the use of computational methods to study biological data. The emergence of omics data, along with the advances in bioinformatics methods to analyze them, have transformed the study of tumor biology. Currently, bioinformatics is gaining applicability in the oncology clinical setting by its use in genetic diagnosis of hereditary cancer, molecular profiling for risk prediction, subgroups stratification and liquid biopsies, among other applications (jVj).

A new field is the study of the of the host-tumor interactions by bioinformatic tools. This approach is called **immunogenomics** and is revolutionizing the study of cancer immunity (kj, kp). Immune phenotyping enables the classification of tumors based on their TME and the identification of biomarkers of response to immunotherapy (**Figure HW**). Useful omics data for immunogenomics studies are genomics (WES), transcriptomics (microarrays, RNA-seq), single cell RNA-seq, peptidomics, and Immunoseq for the direct T-cell (TCR) and B-cell receptors (BCR) sequencing (kr, kq).

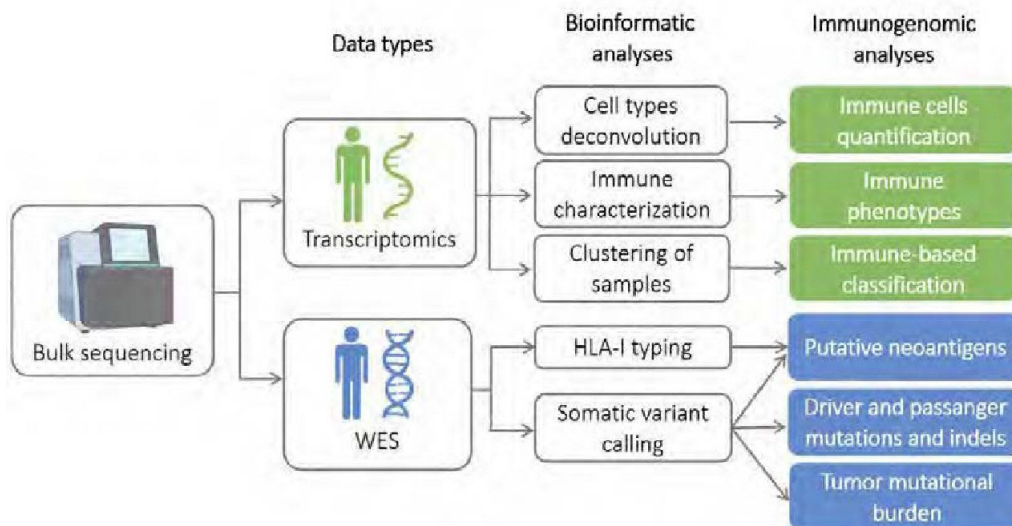


Figure (M. Overview of the main data types and the bioinformatics analysis for interrogating tumor immunity. Transcriptomics data allows to deconvolute cell fractions, characterize the gene expression of immune markers, and cluster samples based on immune features. Analysis of WES data is used to extract somatic mutations and indels, as well as to predict the class I HLA, for prediction of putative neoantigens.

3.1. Cancer omics databases as a source of biological data

Human cancer databases have become an extraordinary source of biological data for researchers, allowing the use of these data for the generation of new hypotheses, validation of experimental results, the discovery of new biomarkers and many other analyses (**Figure HS**) (jVq). One of the biggest human cancer databases is **The Cancer Genome Atlas (TCGA)**, which includes data from more than jj,XXX primary tumors across pp tumor types (jVn). This database is of great interest because it includes several omics data types and clinical data for most cancer types, allowing multi-omics and data integration analyses (jVm).

Apart from TCGA, one of the largest databases of cancer omics is the **Gene Expression Omnibus (GEO)**. It is an open repository for gene expression profiles that includes thousands of experiments from different species and diseases submitted by the research community (jVW). Finally, metastasis databases have also been developed during the last years. The Human Cancer Metastasis Database (HCMDB) (jVk) is an integrated database of metastatic samples collected from TCGA and the GEO. Currently, it contains Vk different cancer types, more than pX metastatic sites and jVr datasets.

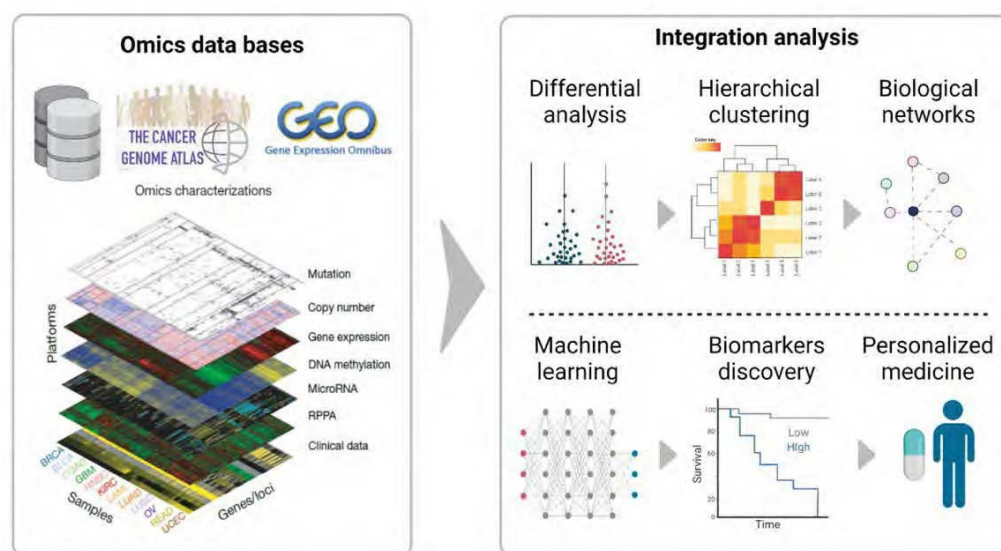


Figure (P. Omics data bases for omics integration analysis gives the possibility to tailor treatments in a personalized way. Adapted from Weinstein JN et al., Nat. Genet, ;LM.

3.2. Computational tools for immune characterization

A plethora of computational tools for dissecting the immune landscapes of tumors have been published in the recent times. Bioinformatics methods allows exploiting existing human omics databases for new discoveries in immunogenomics.

3.2.1. Quantification of immune infiltrates

The tumor microenvironment can be dissected into specific cell-types from transcriptomics data. This process of quantification is widely used in immunogenomics and many statistical methods have been developed for quantification of immune and stromal cell-types from bulk expression data (RNA-seq and microarrays) (jVr). Quantification tools can be divided in two categories based on the statistical method used for inferring cell-types: **marker gene-based** or **deconvolution-based** (Table P) (jpX).

Table B. Description of some of the most used quantification methods from transcriptomic profiles. Adapted from Sturm G et al., Bioinformatics, 2014.

Tool	Approach	Fraction	Cell-types	Good for	Technology
CIBERSORT	Deconvolution	Relative	22	Not specified	Microarray
CIBERSORT-abs	Deconvolution	Absolute	22	Not specified	Microarray
EPIC	Deconvolution	Absolute	6 immune + fibroblasts + endothelial	B cells, T CD4+, T CD8+, NK cells, macrophages / monocytes	RNA-seq
MCPcounter	Marker genes	Relative	8 immune + fibroblasts + endothelial	B cells, T CD8+, NK cells, macrophages / monocytes	RNA-seq, microarray
quanTIseq	Deconvolution	Absolute	10	T CD4+ non-reg, T regs, T CD8+	RNA-seq
TIMER	Deconvolution	Relative	6	Not specified	RNA-seq, microarray
xCell	Marker genes	Relative	64 immune and non-immune	T CD4+, T CD4+ non-reg, T regs,	RNA-seq, microarray

Marker gene-based methods are based on enrichment analysis of a list of genes. These methods are very useful for comparisons between phenotypes, but are not able to quantify inter-sample differences between cell-types abundance (jpj). Deconvolution tools require an *a priori* defined reference matrix consisting of the expected values of gene expression for each cell type, that are used to dissect the contribution of each signature profile to the aggregated bulk level of signals through linear regression methods (**Figure RQ**) (jpV). These methods are more specific and allow comparison between cell-types within samples, but are more susceptible to the background fraction (jpp).

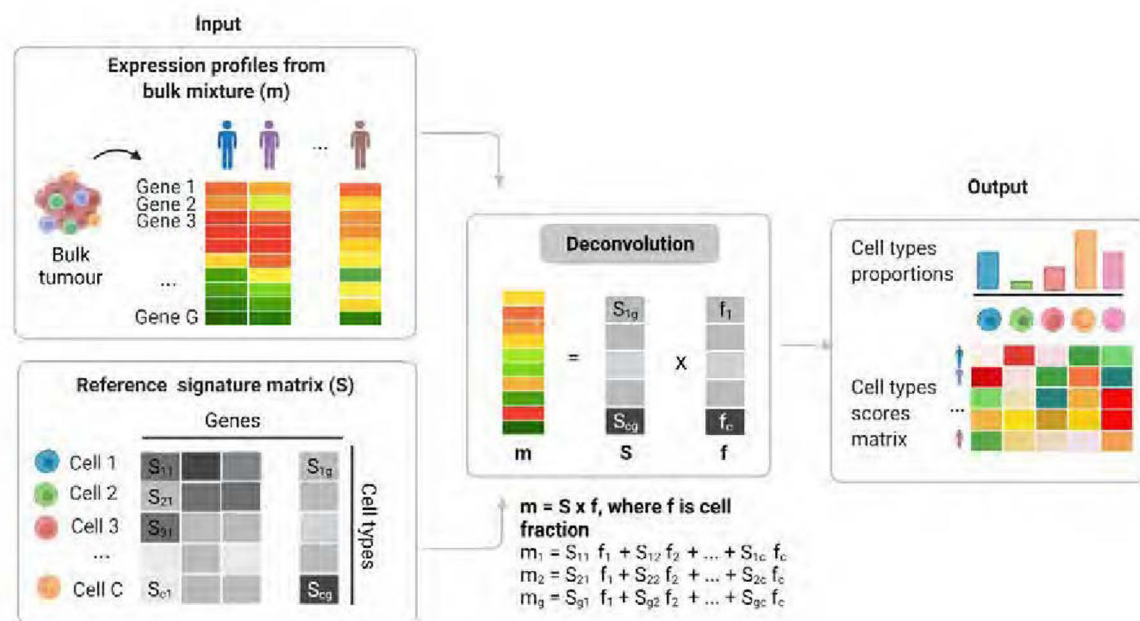


Figure 5R. Overview of immune deconvolution algorithms (example is based on deconvolution-based approach). All methods require the gene expression matrix (m). Reference-based methods use an *a priori* defined reference matrix of expected values (S). The contribution of each cell type (f) is estimated as the result of the linear regression model to dissect the contribution of each cell type to the bulk signal.

Additionally, quantification methods can also be divided into two groups based on the abundance level: **relative** fraction or **absolute** fraction. Relative scores only recaps the immune fraction of the samples, while absolute scores account for the total fractions in the sample (jpV). Absolute scores can be compared between samples and between cell-types, although they are not always necessary and might not be the optimal choice depending on the objective of the study.

The principal limitation of quantification tools is that the performance of these methods depends directly on the quality of the reference signatures, which can be highly divergent between tools. For instance, reference signatures can be generated using different platforms (single cell RNA-seq, immunohistochemistry, flow cytometry, etc). Moreover, cell-types profiles are generated using different tissues (blood or tumor tissue), as well as different tumor models. Another limitation is the possible multicollinearity caused by the fact that different immune cells can express the same genes under different conditions (jVp).

In addition to deconvolution methods, gene signatures that infer the immune contexture of the samples from transcriptomics data have been published during the last years. The **ESTIMATE** function (Estimation of STromal and Immune cells in MAlignant Tumor tissues using Expression data) (jpr) is an algorithm to infer the fraction of immune infiltration, stromal infiltration, and tumor purity in the tumor tissue. This algorithm was implemented for microarray and RNA-seq data, and the results of the resultant scores for all TCGA samples are freely available at their website.

Charoentong et al. generated a signature called **Immunophenoscore** (jqj), based on four gene signatures related to the immune activation and exclusion states (Antigen presentation, Suppressor cells, Effector cells and Checkpoints), and giving them different weights. This method is based on a machine learning algorithm (random forest) for selection of the best predictor genes in each cancer type. The function returns a z-score summarizing the global immune profile of the tumor sample, which was also described to be associated with response to ICI in melanoma.

3.2.2. HLA typing and neoantigen prediction

Advances in sequencing technologies and the improvements in cancer genomes analysis have provided a new procedure for targeting cancer-specific neoantigens generated from somatic mutations by *in silico* methods. This new strategy to target cancer cells can be exploited for personalized immunotherapy, including vaccines and adoptive cell transfer therapies (jpn). The identification of neoantigens from omics data (usually WES) is a multi-step analysis of high complexity that needs good quality data and specialized tools. The analysis can be divided in three main steps (**Figure RH**): (i) the mapping and variant calling, (ii) the generation of aberrant peptides from the mutated sequences, and (iii) the MHC-peptide binding prediction(jpm).

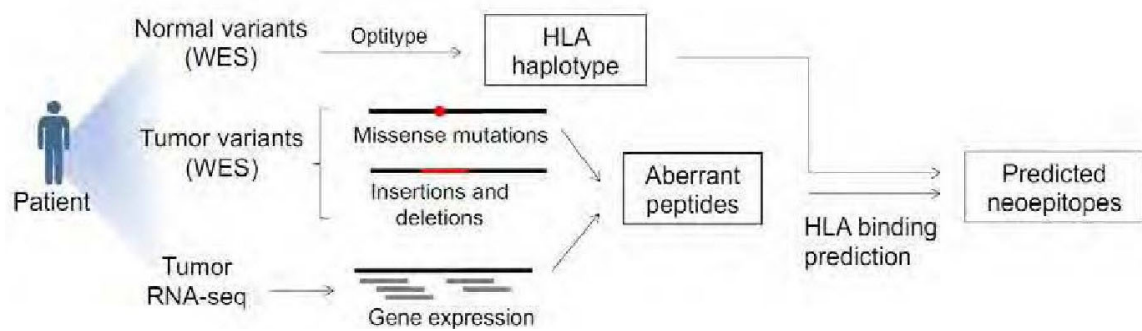


Figure 5. Overview of the pipeline for neoantigen prediction. In the optimal situation, available RNA-sequencing, blood WES and tumor WES from patient are sequenced and analyzed. WES from blood is used to remove germline variants and to perform HLA typing. Besides, somatic mutations (point mutations, insertions and deletions) are obtained from tumor WES. Germline mutations are filtered out from normal WES. RNA-seq is used for filtering out the neoepitopes that are located in genes that are not expressed in the sample.

The HLA genotype is the combination of HLA alleles of each individual. Every person carries V alleles of each of the p HLA class I genes, and it is unique for each individual (most people are heterozygous and express two different forms for each gene). The majority of HLA alleles are partially sequenced for the peptide-binding region (exons V and p) (jV k). HLA haplotypes nomenclature consists of a set of digits (e.g. HLA-A* XV : Xj) that are representative of these alleles (jp W). More levels of resolution can be added, but prediction tools only cover up to four-digit resolution. HLA haplotype can be inferred from omics data (RNA-seq and WES) with good accuracy, although the read length and coverage are key factors due to the high homology between different alleles. Multiple tools have been developed for this purpose, one of the most useful is Optitype, which works by alignment to an HLA reference sequence (jpk).

Somatic variant calling is the most critical step in neoantigen prediction, and can be further divided in several steps: (i) alignment to a reference genome, (ii) variant calling of SNVs and INDELS, and (iii) translation of mutated sequences into aberrant peptides. Many factors can influence the performance of this step as the type of genome, tumor purity, sequencing depth, and the software of use. Numerous algorithms have been developed for variant calling, and bioinformatics protocols have been generated to aid researchers through the pipeline. The neoepitopes can be manually generated from the list of mutations, or with the help of other tools for this purpose.

Finally, the binding affinity prediction of the MHC-peptide complex can be performed. Affinity prediction tools are based on artificial neural networks algorithms that generate accurate predictions, trained with data from mass spectrometry. The lower this binding affinity score, the stronger is the binding (jrX). One of the resources that shows better performance is NetMHCcons (jrj), which combines the three state-of-the-art prediction methods for high accurate predictions (Figure RU).

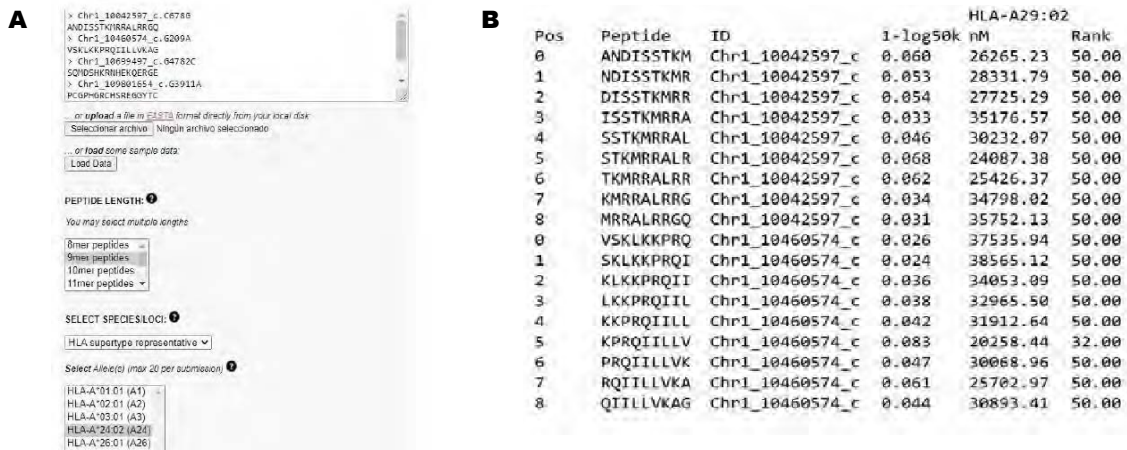


Figure 55. NetMHCcons web resource for HLA binding affinity prediction from neoantigens. A) The list of neoantigens is loaded, the length of the peptides is selected (usually amers), and the specific HLA haplotype of the sample is selected (or the super representative haplotype if it is not available). B) The output of the algorithm generates a table with all possible amers, the strength of the binding in nM IC], the prediction scores and the % rank. If the % rank is below :% it is considered weak binding and if it is below ;,]% is considered strong binding.

Current challenges in neoantigens prediction are focused in determining which neoantigens are eventually recognized by infiltrating T cells. Latest studies unveil that only q% of the *in silico* predicted neoantigens are eventually recognized by CDW+ T cells (jVn). Therefore, new tools need to improve the accuracy in the prediction of the binding and the stability of presentation of the HLA-peptide complex are needed. Another challenge is to improve HLA class II predictions (jrV).

3.3. New approaches in immunogenomics

Immunogenomics is a rapidly evolving field. The emergence of omics technologies and more powerful computational methods are allowing scientists to visualize the tumors in a way that was difficult to imagine only a few years ago. These technologies are opening new ways to study intra-tumor heterogeneity and can give deeper insights in the immunological components of the tumors for understanding tumor development and resistance to immunotherapies (jpm).

Single cell RNA-seq is a technology that allows the profiling of the transcriptomes of single cells within the tumor microenvironment and has revolutionized the field of cancer transcriptomics during the last years (jrr). Furthermore, spatial transcriptomics also incorporate the information of the spatial position of cells in the slide (jrj), allowing to establish spatial domains in the diverse anatomical regions of the sample, and to perform in-deep characterization of the biological processes within the tumor microenvironment (jrn). Another emerging technology for understanding intra-tumoral heterogeneity is multiplex imaging (jrm). This approach allows to cover several protein markers within their spatial context and visualize them in high resolution in a single image.

Another recent advance in immunogenomics is the TCR (and BCR) profiling consists in the sequencing of the genes encoding for the α and β chain that generate the diversity of antigen-specific receptors from TILs (jrW). TCR sequencing allows measuring and characterizing the lymphocyte's receptors to study the abundance and clonality of TCR and BCR repertoires. The clonality of receptors consists of an index that represents the number of distinct populations of T cells or B cells that carry identical receptors. Recently, our group led a study that revealed the association of T cell clonality with progression in colorectal cancer stage II patients (jrk). Single cell RNA-seq TCR profiling can give a better understanding of the interplay between the expression activity and the clonal evolution of different T cells in the tumor microenvironment (jrr).

On the other side, statistical methods to analyze cancer genomics are also rapidly evolving. Computational algorithms are shifting from classical statistics towards the use of methods based on artificial intelligence (AI) (jqX). These new approaches to

handle large omics datasets are paving the way to a more comprehensive view of the tumor biology and present improved solutions for effective patients' management and personalization of therapies.

In cancer transcriptomics, numerous AI models have emerged, most of them based on machine learning and deep learning methods. Supervised machine learning has many applications in oncology research, such as classification of cancer subtypes, biomarkers discovery, identification of novel targetable molecules and treatments design. Unsupervised algorithms based on AI are used to perform regression models, dimensionality reduction and for clustering tasks (jqj). Genomics studies based on machine learning algorithms are already improving the performance for prediction of response to therapies (jqV).

II. HYPOTHESIS AND OBJECTIVES

1. Hypothesis

1.1. Rationale of the project

Cancer is a heterogeneous disease, in which many different cell types are involved besides neoplastic cells. Tumor cells interact with the tumor microenvironment (TME), composed by stromal and immune cells, in a crosstalk implicated in key functions such as immune evasion, tumor progression and therapeutic resistance. The identification of biomarkers for precision oncology in solid tumors have improved during last years in parallel with the emergence of omics technologies and bioinformatics methods. However, there is still a need to better characterize the TME among different tumor niches, in order to discover new immune biomarkers that improve oncology patient's management.

1.2. General hypothesis

Immunogenomics studies are a useful approach for deciphering the molecular mechanisms underlying the complex crosstalk between patients' immune system and cancer cells, as well as for the identification of biomarkers that could be exploited for therapeutic purposes and patients' management.

1.3. Specific hypothesis

Study H | Dissecting the immunity of uveal melanoma

Since the eye is an immune-privileged organ, uveal melanoma is considered a *cold* tumor with low immunogenicity, that promotes an immunosuppressive microenvironment. In this study, two independent hypotheses have been proposed regarding the role of the immune system in prognosis and therapeutics, respectively.

An important distinctive characteristic of uveal melanoma is the hematogenous dissemination, with a crucial role of angiogenic factors. We hypothesize that **the crosstalk between the immune activation and angiogenesis is associated with disease progression** in uveal melanoma patients.

On the other side, the lack of immune infiltration in uveal melanoma explains the absence of the immunoediting process, which can be exploited for therapeutic purposes. Hence, we hypothesize that **driver mutations in GNAQ and GNAHH genes could be antigenic and elicit T cell response** in uveal melanoma patients.

Study R | Role of the immune microenvironment in metastatic homing

The metastatic spread patterns to distant organs are determined by molecular interactions between cancer cells and the target organ. Partially explained by the seed and soil hypothesis, the molecular factors that influence this organ-specific colonization are not completely understood yet, although it is well-known that the immune microenvironment of the host tissue plays a crucial role in this process.

Since the microenvironment of metastatic samples diverge from that of the primary tumors, we hypothesize that **metastatic tumors from the same secondary location share immune characteristics and immune evasion mechanisms regardless of primary tumor origin.**

2. Objectives

The main aim is to study the immune microenvironment of solid tumors, and to assess its association with tumor progression and metastatic homing. For this purpose, immunogenomics approaches will be used to exploit existing omics data.

Specific objectives:

Objective H | To decipher the role of the immune system in uveal melanoma

H.H. To assess the additive value of immune infiltration and angiogenesis in the prognosis of uveal melanoma patients, using gene expression data.

H.R. To evaluate the antigenicity of driver mutations in GNAQ and GNAJ1 genes in uveal melanoma patients.

Objective R | To identify immune factors that modulate metastatic spread to specific organs

R.H. To characterize the immune microenvironment and immune system activation of metastatic samples in bone, brain, liver and lung from six different primary sites based on transcriptomics data, and to describe differences and similarities across the different metastatic sites.

R.R. To generate a novel subgrouping of metastases based on their immune phenotypes and correlate them with clinical features.

III. RESULTS

Study 1 | Dissecting the immunity of uveal melanoma

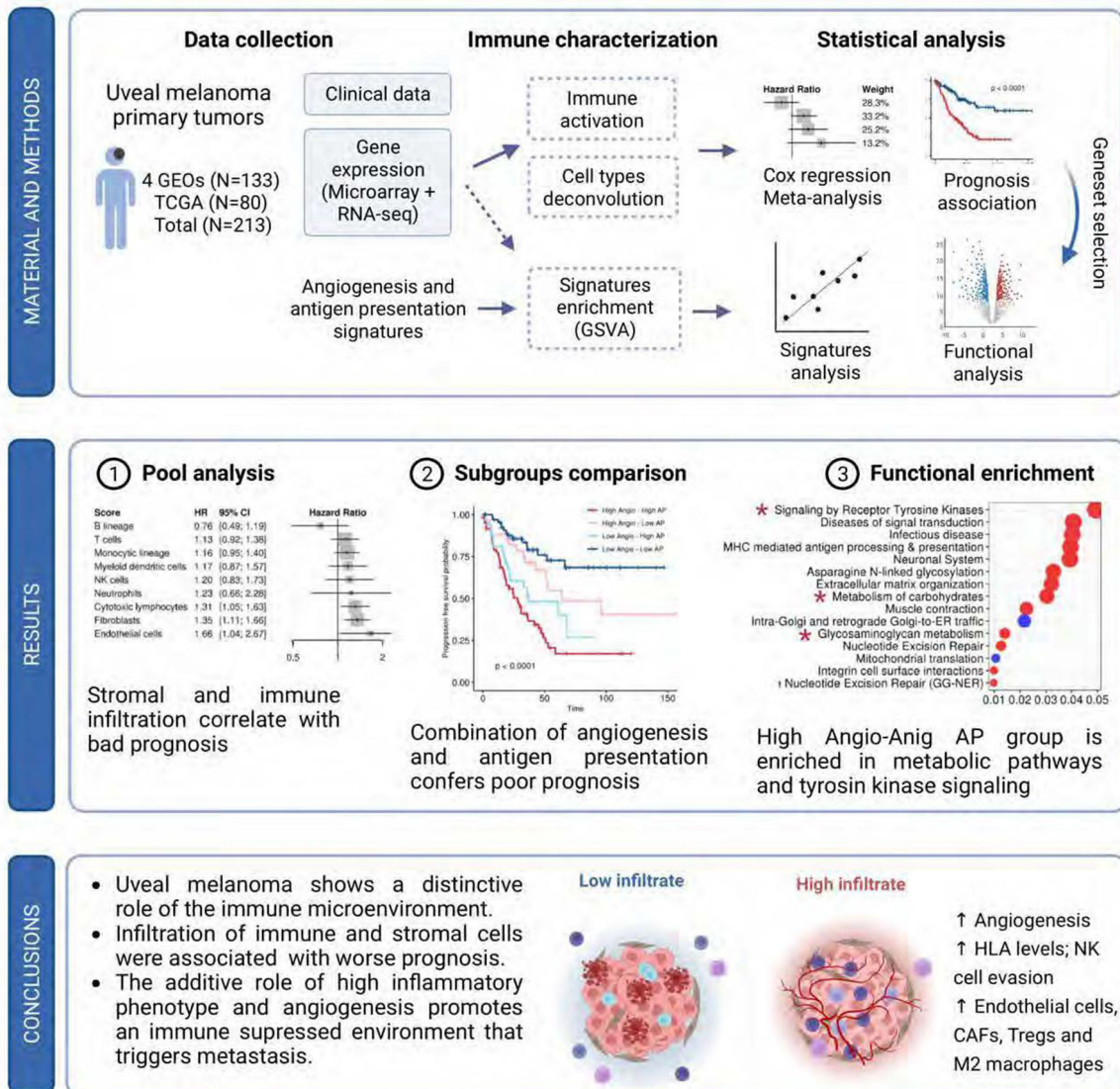
1.1. Additive role of immune system infiltration and angiogenesis in uveal melanoma progression

Article: Sandra García-Mulero, Maria Henar Alonso, Luis P. Del Carpio, Rebeca Sanz-Pamplona, Josep María Piulats. *Additive Role of Immune System Infiltration and Angiogenesis in Uveal Melanoma Progression*. International Journal of Molecular Sciences. VV; Vnn (VXVj). <https://doi.org/jX.ppkX/ijmsVVXqVnnk>

Objective and main results:

The objective of this publication was to decipher the role of immune system activation and the tumor microenvironment in uveal melanoma prognosis, and to understand the crosstalk between immune system activation and angiogenesis and its role in disease progression. For that, we performed a characterization of the immune microenvironment of Vjp UM samples from q different public datasets, and assessed the association of non-tumoral infiltration with prognosis by univariate Cox regression models independently for each dataset. We found association of immune infiltration with worse prognosis. Specially, robust association across different quantification methods was found for cytotoxic cell-types (CDW+ T cells and NK cells), and macrophages Mj and MV. On the other side, B cells infiltration was associated with good prognosis. Interestingly, low HLA levels were also associated with better prognosis, suggesting a possible role of NK cells attack. Additionally, we found a cluster of samples with additive inflammatory and angiogenic functions, conferring a phenotype associated with extremely bad prognosis. This cluster of patients was enriched in KRAS signaling, and metabolic pathways such as PIpK-AKT-MTOR signaling and glycolysis.

Graphical abstract:





Article

Additive Role of Immune System Infiltration and Angiogenesis in Uveal Melanoma Progression

Sandra García-Mulero ^{1,2}, Maria Henar Alonso ^{1,2}, Luis P. del Carpio ³, Rebeca Sanz-Pamplona ^{1,*} and Josep M. Piulats ^{3,4,*}

- ¹ Unit of Biomarkers and Susceptibility, Oncology Data Analytics Program (ODAP), Catalan Institute of Oncology (ICO), Oncobell Program, Bellvitge Biomedical Research Institute (IDIBELL) and CIBERESP, Hospitalet de Llobregat, 08908 Barcelona, Spain; s.garciam@idibell.cat (S.G.-M.); mhalonso@iconcologia.net (M.H.A.)
 - ² Department of Clinical Sciences, Faculty of Medicine and Health Sciences, University of Barcelona, 08036 Barcelona, Spain
 - ³ Medical Oncology Department, Catalan Institute of Cancer (ICO), IDIBELL-OncoBell, Hospitalet de Llobregat, 08908 Barcelona, Spain; lpdelcarpio@iconcologia.net
 - ⁴ Clinical Research in Solid Tumors Group (CREST), Oncobell Program, Bellvitge Biomedical Research Institute (IDIBELL) and CIBERONC, Hospitalet de Llobregat, 08908 Barcelona, Spain
- * Correspondence: rebecasanz@iconcologia.net (R.S.-P.); jmpiculats@iconcologia.net (J.M.P.)

Abstract: Uveal melanoma (UM) is a malignant tumor that arises in the melanocytes of the uveal tract. It is the most frequent eye cancer, and despite new therapeutic approaches, prognosis is still poor, with up to 50% of patients developing metastasis with no efficient treatment options available. In contrast to cutaneous melanoma, UM is considered an “immune-cold” tumor due to the low mutational burden and the unique immunosuppressive microenvironment. To gain insight into the role of the UM microenvironment in regard to prognosis and metastatic progression, we have performed a pool analysis characterizing the UM microenvironment by using a bioinformatic approach. A variety of scores based on gene expression measuring stromal infiltration were calculated and used to assess association with prognosis. As a result, the highest immune and stromal scores were associated with poor prognosis. Specifically, stromal cells (fibroblasts and endothelial cells), T cells CD8+, natural killer (NK) cells, and macrophages M1 and M2 infiltration were associated with poor prognosis. Contrary to other tumors, lymphocytic infiltration is related to poor prognosis. Only B cells were associated with more favorable prognosis. UM samples scoring high in both angiogenesis (Angio) and antigen presentation (AP) pathways showed a poor prognosis suggesting an additive role of both functions. Almost all these tumors exhibited a chromosome 3 monosomy. Finally, an enrichment analysis showed that tumors classified as high Angio-high AP also activated metabolic pathways such as glycolysis or PI3K-AKT-MTOR. In summary, our pool analysis identified a cluster of samples with angiogenic and inflammatory phenotypes exhibiting poor prognosis and metabolic activation. Our analysis showed robust results replicated in a pool analysis merging different datasets from different analytic platforms.

Keywords: uveal melanoma; angiogenesis; immune system; pool analysis; prognosis; gene expression



Citation: García-Mulero, S.; Alonso, M.H.; del Carpio, L.P.; Sanz-Pamplona, R.; Piulats, J.M. Additive Role of Immune System Infiltration and Angiogenesis in Uveal Melanoma Progression. *Int. J. Mol. Sci.* **2021**, *22*, 2669. <https://doi.org/10.3390/ijms22052669>

Academic Editor: Karen Sisley

Received: 31 December 2020

Accepted: 27 February 2021

Published: 6 March 2021

Publisher's Note: MDPI stays neutral with regard to jurisdictional claims in published maps and institutional affiliations.



Copyright: © 2021 by the authors. Licensee MDPI, Basel, Switzerland. This article is an open access article distributed under the terms and conditions of the Creative Commons Attribution (CC BY) license (<https://creativecommons.org/licenses/by/4.0/>).

1. Introduction

Uveal melanoma (UM) is a malignant tumor arising at the melanocytes of the uveal tract [1]. It is the most frequent cancer in the eye, and is considered a rare tumor (10 cases per million incidence in Europe) [2]. Prognosis in UM is poor, with median overall survival (OS) of less than one year in most cases, and up to 50% of patients developing metastasis (M1), mostly in the liver. Currently, metastatic UM (MUM) does not have an effective standard treatment available and survival rates have not improved in the last decades [1,3–5]. Recent meta-analysis reviews on progression-free survival (PFS) and overall survival (OS) from

different clinical trials have shown that none of the different novel treatments carried out in recent years has improved the prognosis of UM patients, reinforcing the need for further research.

Immunotherapy has shown extraordinary results on cutaneous melanoma (CM). Monoclonal and combined therapies with anti-programmed death ligand 1 (PDL1) and anti-cytotoxic T-lymphocyte antigen-4 (CTLA-4) checkpoint inhibitors are already a standard therapy for CM. However, these results have not been reproduced in UM [6,7], which differs from CM at the genetic and molecular level and should be treated with specific treatments [8]. One important difference is the tumor mutational burden (TMB), which is very high in CM, which generates a great amount of neoantigens that renders high immunogenicity and attracts T CD8+ lymphocytes. By contrast, UM has a low TMB, and therefore is considered a tumor with low antigenicity [9].

Tumors with microsatellite instability (MSI) phenotype or harboring mutations in mismatch repair (MMR) genes are highly mutated. A recent study analyzing the frequency of MMR genes in three independent cohorts of UM patients showed that mutations in these genes were extremely rare [10]. Also explaining the low TMB, a work by Cross et al. analyzing microsatellite instability in UM demonstrated that, in contrast to CM, MSI not occurring in UM [11]. A study by Johansson et al. analyzing 103 UM by whole-genome sequencing from different sites of the uveal tract demonstrated that only patients with tumors located in the iris showed high TMB. This phenotype is associated with ultraviolet radiation signature, common in CM. However, only 8 out of 103 analyzed tumors were located in the iris [12]. Furthermore, UM is located in an immune-privileged organ with an immunosuppressive microenvironment, protected by the blood–ocular barrier, and an absence of lymphatic vessels that prevent the traffic of immune cells to the eye [13].

Molecular profiling has provided a new perspective of the biology of UM. The Cancer Genome Atlas (TCGA) recently performed the analysis of 80 UM primary tumors and identified four different molecular subtypes [14]. Molecular subgroups 1 and 2 are associated with disomy of chromosome 3 (D3) and better prognosis, whereas subgroups 3 and 4 are associated with monosomy of chromosome 3 (M3) and have worse prognosis. The immune profiling of TCGA-UM analysis is scarce and limited to the association of M3 tumors with higher levels of CD8+ T cells, Interferon gamma signaling, and immune suppressor factors. Therefore, the immune microenvironment of UM seems to be related to the genomic alterations, mostly to mutations in BAP1 gene, rather than to response to immune signaling [15]. In this regard, it has been recently described that UM tumors harboring mutations in BAP1 gene showed upregulation of several genes associated with suppressive immune responses [16].

Dissemination in UM is hematogenous, suggesting an important role of tumor angiogenesis (the development of new blood vessels) in tumor growth and metastasis. Indeed, we have previously shown that enrichment in pro-angiogenic factors was related to worse prognosis in UM but not in CM [17]. Angiogenesis is directly associated with immune evasion and resistance to immunotherapy by suppressing dendritic cell maturation, inhibiting T-cell effector response and recruiting myeloid derived suppressor cells. Thus, therapeutic strategies combining immunotherapy with anti-angiogenic factors could modulate the tumor microenvironment to make it more susceptible to the immune checkpoint inhibitors.

In this study, we perform a bioinformatics analysis using public gene expression data in order to perform an in-depth characterization of the tumor microenvironment of UM primary tumors and assess its association with prognosis.

2. Results

2.1. Clinical Description

A total of 213 primary UM patients from 5 datasets were included in the meta-analysis, described in Table 1. The median age was 62.3, with 41.3% female and 58.7% males. Up to 56% of patients had recurred with a median disease-free survival (DFS) of 38.6 months. Differences between the different datasets were evaluated for continuous variables (Kruskal–

Wallis test) and categorical variables (Chi-squared test of proportions). No differences were found for age, sex and recurrence status, while strong differences between datasets were found on chromosome 3 status, cell type and DFS. Due to the differences between datasets for DFS, all survival analyses were performed stratified by dataset.

Table 1. Baseline characteristics of samples included in the analysis by dataset. *p*-values for categorical variables indicate results from Chi-Squared Tests. *p*-values for continuous variables indicate results from Kruskal tests. DFS: disease-free survival.

Variable	Entire Cohort <i>n</i> = 213	GSE22138 <i>n</i> = 63	GSE27831 <i>n</i> = 29	GSE73652 <i>n</i> = 13	GSE84976 <i>n</i> = 28	TCGA <i>n</i> = 80	<i>p</i> -Value
Age	62.3	61.0	66.0		61.6	62.2	0.411
Sex							0.801
Female	71 (41.3%)	24 (38.1%)	12 (41.4%)	0 (0.0%)	0 (0.0%)	35 (43.8%)	
Male	101 (58.7%)	39 (61.9%)	17 (58.6%)	0 (0.0%)	0 (0.0%)	45 (56.2%)	
NA	41	0 (0.0%)	0 (0.0%)	13 (100%)	28 (100%)	0 (0.0%)	
Chr 3 status							<0.001
Disomy	64 (32.2%)	18 (28.6%)	11 (37.9%)	0 (0.0%)	14 (50.0%)	21 (26.2%)	
Partial monosomy	5 (2.5%)	5 (7.94%)	0 (0.0%)	0 (0.0%)	0 (0.0%)	0 (0.0%)	
Monosomy	94 (47.2%)	32 (50.8%)	17 (58.6%)	0 (0.0%)	14 (50.0%)	31 (38.8%)	
NA	36 (18.1%)	8 (12.7%)	1 (3.5%)	13 (100%)	0 (0.0%)	28 (35.0%)	
Cell type							<0.001
Epithelioid	40 (18.7%)	21 (33.3%)	6 (20.7%)	0 (0.0%)	0 (0.0%)	13 (16.2%)	
Mixed	72 (33.8%)	23 (36.5%)	12 (41.4%)	0 (0.0%)	0 (0.0%)	37 (46.2%)	
Spindle	39 (18.3%)	0 (0.0%)	9 (31%)	0 (0.0%)	0 (0.0%)	30 (37.5%)	
NA	60 (28.2%)	19 (30.2%)	0 (0.0%)	13 (100%)	28 (100%)	0 (0.0%)	
Recurrence							0.245
Non-recurrent	119 (55.9%)	28 (44.4%)	18 (62.1%)	8 (61.5%)	15 (53.6%)	50 (62.5%)	
Recurrent	94 (44.1%)	35 (55.6%)	11 (37.9%)	5 (38.5%)	13 (46.4%)	30 (37.5%)	
DFS Months	38.6	41.1	37.2		77.8	23.2	<0.001

2.2. Stromal and Immune Cell Infiltration Is Associated with Poor Prognosis in Uveal Melanoma (UM)

A variety of scores based on gene expression measuring stromal and immune cell infiltration were calculated and used to assess association with prognosis. First, we used the ESTIMATE (Estimation of Stromal and Immune Cells in Malignant Tumor Tissues Using Expression Data) tool to measure tumor purity and immune cell/stromal infiltration. The four resulting scores were used as global indicators since the tool does not deconvolute between different cell lineages. The tumor purity score had a trend toward better prognosis, although it was not significant (HR = 0.99 [0.97–1.01]). On the contrary, The ESTIMATE score, which is a measure of non-tumoral cell infiltration was associated with worse prognosis (HR = 1.01 [1–1.03]). The ESTIMATE score was calculated based on both immune and stromal scores, both associated with bad prognosis (immune score HR = 1.02 [1–1.05]; stromal score HR = 1.04 [0.99–1.08]), Figure 1A. Thus, highly infiltrated tumors (with both stromal and immune cells) showed a poor prognosis. In other words, the more tumor purity the better the prognosis. Table S1 shows the ESTIMATE scores in each sample.

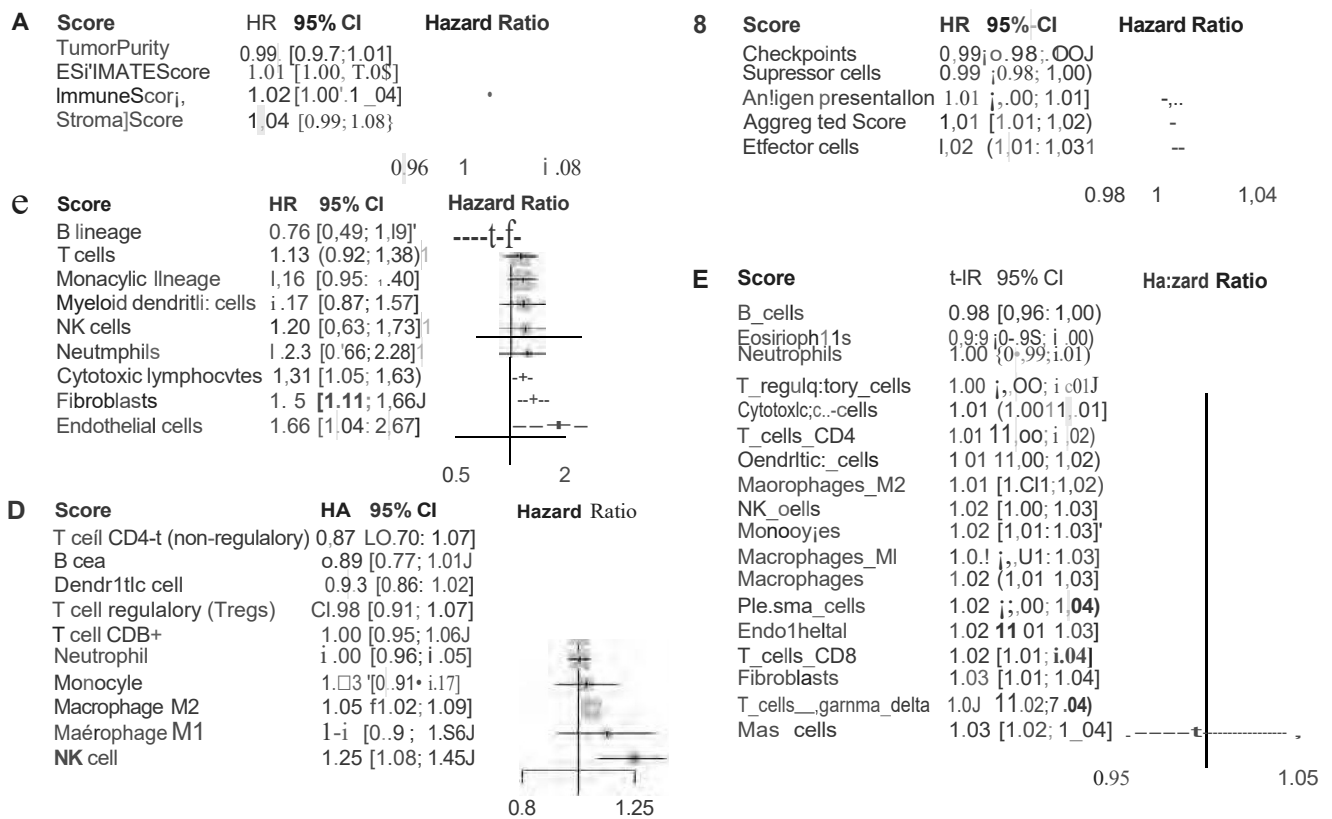


Figure 1. Forest plot showing survival analysis using immune and stroma infiltration scores. Horizontal bars indicate the 95% confidence intervals (CI) of the hazard ratio (HR). Each score was evaluated individually and ordered based on the summary effect. Univariate Cox HR analysis was performed using the disease-free survival time. (A) HR based on the ESTIMATE scores. (B) HR based on the immunophenoscore individual scores and Aggregated score. (C) HR based on immune cell infiltration scores from MCP-counter. (D) HR based on the immune infiltrates from Quantiscore analysis. (E) HR based on Quantiscore of immune infiltrates from CMSensuSME.

Next, immunophenoscore (IPS) scores were used as an indicator of immune system activation (Hugweil). The aggregated score, a composite score assuring the overall immunogenicity of a tumor, was associated with poor prognosis (HR = 1.01 [1.01-1.02]). Interestingly, when individual scores were investigated, effector cells (HR = 1.02 [1.01-1.03]) and antigen presentation (HR = 1.01 [1.00-1.01]) scores were associated with poor prognosis. On the contrary; checkpoints markers (HR = 0.99 [0.98-1]) and suppressor cell scores (HR = 0.99 [0.98-1]) were associated with better prognosis (Figure 1B). Forest plots showing separated ESTIMATE and IPS analysis for each dataset are available in Figure S1. In summary, immunogenic tumors (using high score in IPS) were associated with poor prognosis. Moreover, if samples were divided between high and low infiltrated according to the ESTIMATE score, those included in the high category scored higher in Antigen presentation and effector cells (figure S2A). Also, they show a trend toward poor prognosis (Log-rank-p-value = 0.07) (Figure S2B).

Finally, since ESTIMATE only performs a global estimation of tumor cell infiltration, a cell-type detailed analysis was possible using quantification methods based on gene expression. A general trend towards infiltration association with poor prognosis was observed. However, exceptions in several cell lineages emerged in the analysis (Figure 1C-E). The MCP-counter (Microenvironment Cell Populations-counter) method selected B cells as the only cells associated with better prognosis (HR = 0.76 [0.49-1.19]). By contrast, cytotoxic lymphocytes (HR = 1.31 [1.05-1.63]), fibroblasts (HR = 1.5 [1.11-1.66]), and endothelial cells (HR = 1.66 [1.04-2.67]), were significantly associated with poor prognosis (Figure 1C). The Quantiscore method, measuring additional cell lineages, showed CD4 T-cells (HR = 0.87 [0.70-1.07]), B-cell (HR = 0.89 [0.77-1.01]) and dendritic cell (HR = 0.93

[0.86-1.02,1), were associated with better prognosis. On the contrary, macrophages M1 (HR = 1.12 [0.93-1.36]), macrophages M2 (HR = 1.05 [1.02-1.09]), and NK cells (HR = 1.25 [1.08-1.45]) were associated with poor prognosis. Additionally the ConsensusTME (Consensus Tumor Microenvironment) method also selected B-cells (HR = 0.98 [0.96-1]), as good prognosis biomarkers along with eosinophils (HR = 0.99 [0.98-1]). Inconsistent results were found across different quantification methods when dendritic cells (DC) were interrogated. Since this is a heterogeneous group of cells, we use additional signatures to discriminate between immature DC (iDCs) and activated DC (aDCs). However, we did not observe an association between iDCs and/or aDCs with prognosis (Figure S3). The genes included in all signatures used in the analysis are listed in Table S2.

In summary, all methods indicated that B cells are associated with better prognosis. By contrast, stromal cells (fibroblasts and endothelial cells), T cells CD8+, NK cells, and macrophages M1 and M2 were associated with poor prognosis in at least two out of the three methods evaluated. Interestingly, B cells act as APCs through HLA class II whereas NK and CD8+ T cells destroy cells not expressing HLA class I or cells presenting antigens through HLA class I, respectively. Since the latter are inflammation-related pathways classically associated with better prognosis in other solid tumors, we speculated that UM is a divergent type of tumor in this regard.

Thus, to see whether antigen presentation genes were prognosis biomarkers in UMs, a survival analysis was done. Kaplan-Meier plots in Figure 2 showed that tumors showing high expression levels of genes related to the antigen presentation pathway were associated with poor prognosis. Tapasin 1 (TAP1) (Figure 2A), beta-2-microglobulin (B2M) (Figure 1C), human leukocyte antigen-B (HLA-B) (Figure 2F), HLA-E (Figure 2H) and HLA-F (Figure 2J) were the more significant genes with Log-rank p-values < 0.0001. Regarding cytotoxicity, tumors showing high expression of CD8A, GZMA and PRF1 were associated with poor prognosis (Figure 54).

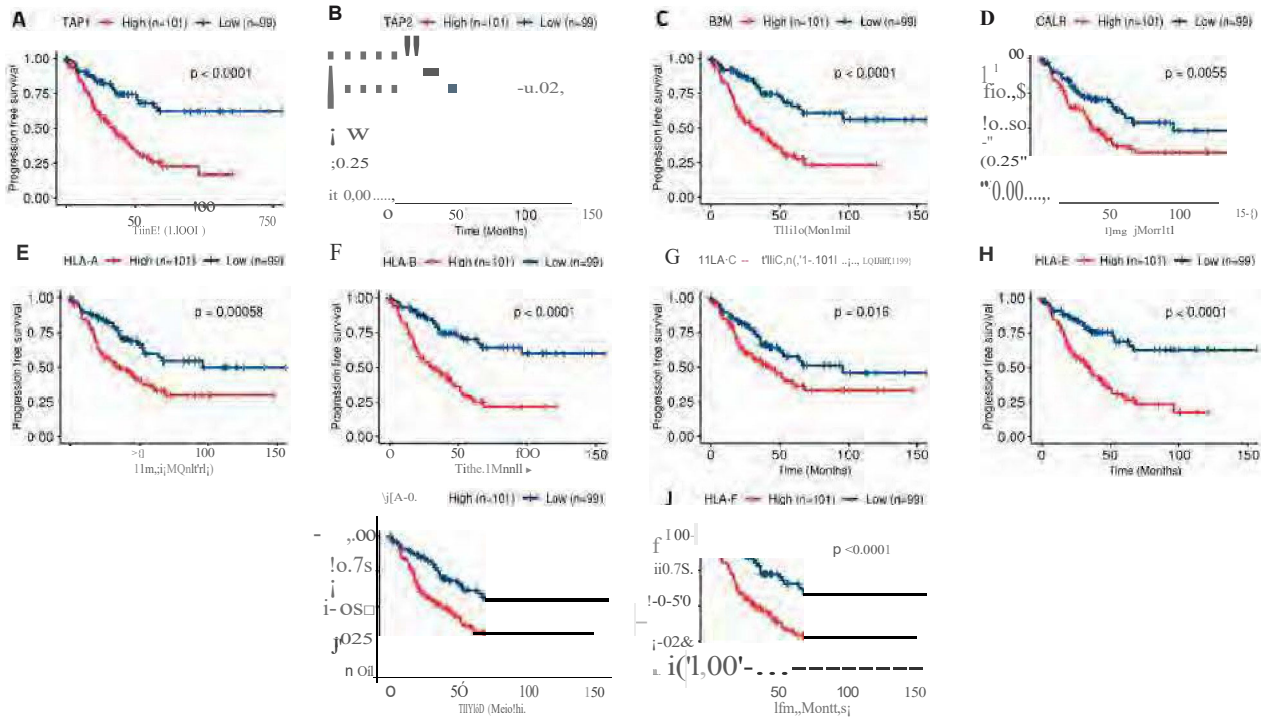


Figure 2. Kaplan-Meier survival curves with gene related to antigen processing and presentation machinery in uveal melanoma (UM) samples (n=200). Genes included are (A) tapasin-1 (TAP1), (B) TAP2, (C) beta-2-microglobulin (B2M), (D) calreticulin (CALR), (E) human leukocyte antigen-A (HLA-A), (F) HLA-B, (G) HLA-C, (H) HLA-E, (I) HLA-G, (J) HLA-F. Patients were divided into high and low groups by the median value within each dataset and joined afterwards. p-values of Log-rank tests are indicated. High expression is painted in red whereas low expression is painted in blue.

Mutational data was only available in the TCGA dataset. To see if the number of mutations was associated with prognosis, we calculated the tumor mutational burden (TMB). As expected in a cold tumor, only a median of 16 mutations per sample were found. TMB was not associated with prognosis.

2.3. Combination of Angiogenesis and Antigen Presentation Confers Poor Prognosis

Results showed that endothelial cells, fibroblasts (stromal cells) and immune cells (specifically cytotoxic ones) were associated with poor prognosis. Across these three microenvironmental factors, overlapping genes are scarce providing strength to the analysis.

Only one gene (HIF1A) has been found in common between fibroblasts and Angiogenesis signature. Consensus^{TME} signatures measuring immune cell infiltration overlap with angiogenesis signature in: B cells (PRKCB), monocytes (HIF1A and ARNT), Macrophages M2 (FLT1), T cells CD4+ (EIF2B5 and PLCG1), T cells CD8+ (FLT4 and PLCG1).

Apart from fibroblasts, endothelial cell infiltration was strongly associated with relapse; in agreement with previous results in the group. Thus, we wonder if these two features were additive and confers a particularly aggressive phenotype. To do this, we used angiogenesis (Angio) and antigen presentation pathways (AP) as reporter ones. Antigen presentation pathway was used as a surrogate of immune system activation. First, we assessed if a correlation between these two features existed. A statistically significant but moderate correlation was found when all samples were taken together ($R = 0.42$, $p = 2 \rightarrow 10^{-10}$, black line in the Figure 3A) and also when stratifying between relapsing ($R = 0.24$, $p = 0.021$, dark grey line in Figure 3A) and non-relapsing patients ($R = 0.44$, $p = 9.4 \rightarrow 10^{-7}$, light grey in Figure 3A). Next, we classified the samples based in the combination of the scores, obtaining four groups (High Angio-High AP, High Angio-Low AP, Low Angio-High AP, Low Angio-Low AP). As can also be seen in Figure 3A, the bar plot in Figure 3B showed that High Angio-High AP group includes the high number of recurrent samples, whereas Low Angio-Low AP group includes the higher number of non-recurrent. Phenotypes High Angio-Low AP and Low Angio-High AP exhibited an intermediate, similar numbers of recurrent samples (Chi-squared test, $p = 4.5 \rightarrow 10^{-6}$).

Indeed, a survival analysis shows strong differences in DFS probability between the four groups (Log-rank test, $p < 0.0001$), being the High Angio-High AP the group with worse prognosis in opposition to Low Angio-Low AP group (p -value = $4.4 \rightarrow 10^{-8}$) which is the group showing better survival (Figure 3C). Because intermediate phenotypes (High Angio-Low AP and Low Angio-High AP) have intermediate survival probability and those tumors classified as High Angio-High AP were more prone to metastasize, we think these two features had an additive role in prognosis. We tested the hypothesis that differences in recurrence time could exist between group of samples, being Low Angio-Low AP patients those relapsing later. Although no statistical differences were found, Figure S5 showed a trend towards High Angio-High AP tumors as the earlier relapsing ones.

Finally, we performed an unsupervised hierarchical clustering using Angio and AP scores that reflected the four groups previously described, as expected. The High Angio-Low AP and Low Angio-Low AP were separated clusters. A mixture in the dendrogram was observed between Low Angio-High AP and High Angio-High AP groups (Figure 3D). It is worth mentioning that there is an enrichment in samples harboring disomy in chromosome 3 in the Low Angio-Low AP cluster. On the contrary, almost all High Angio-High AP exhibited a chromosome 3 monosomy.

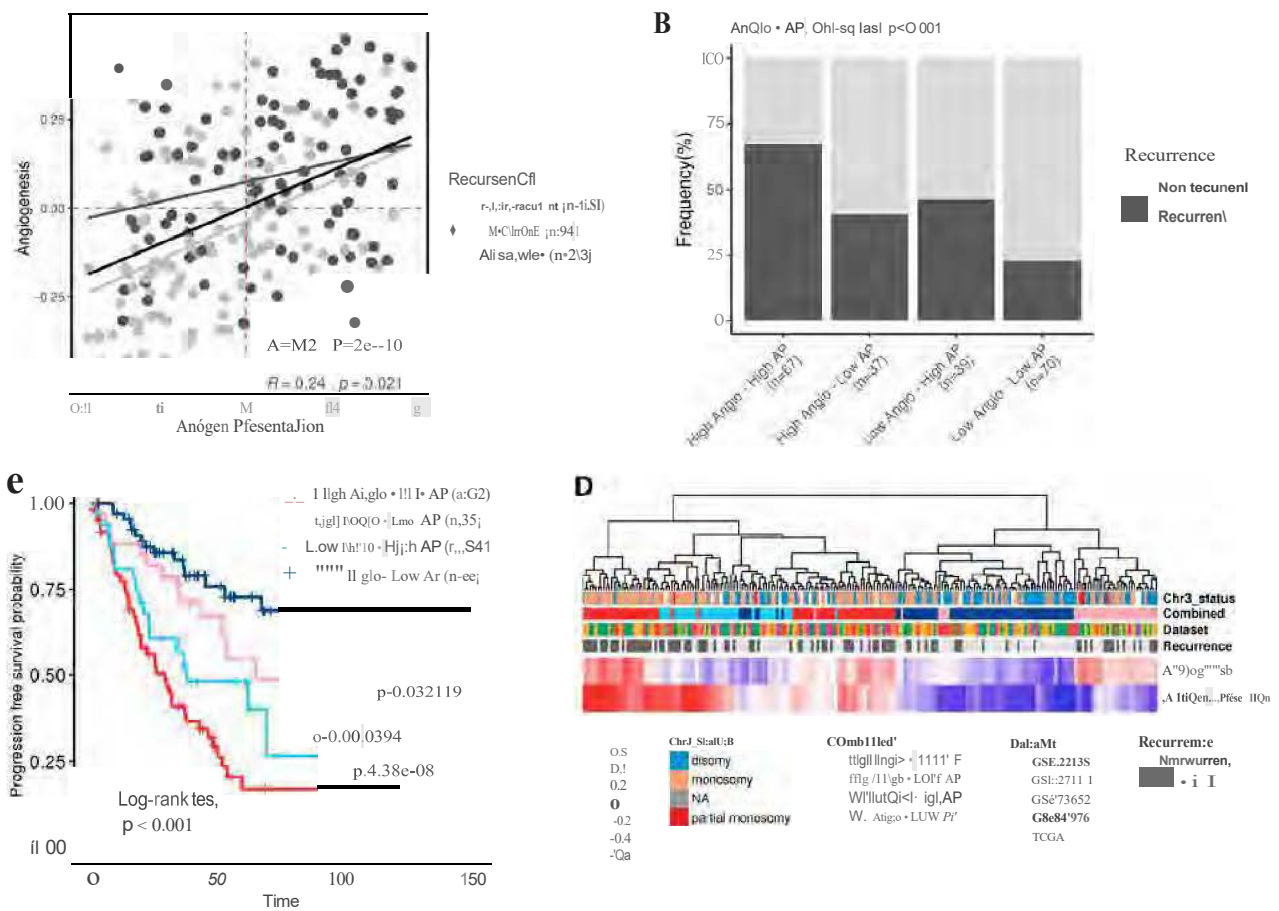


Figure 3. Combination of enrichment scores from angiogenesis (Angio) and antigen presentation (AP) signatures. (A) Correlation plot of Angio and AP signatures, colored by recurrent (light grey) and non-recurrent (dark grey) status. Black lines represent correlation for all samples, regardless of recurrence status. Spearman correlation was calculated and regression lines, correlation scores and p-values were added for each recurrence status and for all the samples. Dashed lines indicate the cut-off used for generating the four groups. (B) Bar plot showing the frequency of recurrent samples in the different groups of Angio-AP combinations. (C) Kaplan-Meier survival curves of the four groups from combination of Angio and AP scores. Log-rank p-value is indicated. Cox proportional hazard ratio test between the Low Angio-Low AP reference group and the other three groups was calculated, and p-values are also indicated. (D) Hierarchical clustering of all 213 samples using the Angio and AP scores. Bars on top represent chromosome-3 status, dataset, recurrence and combined score.

Next, we consider whether the poor prognosis group might be susceptible to treatment with immunotherapy. To answer this question, samples were scored using a genetic profile reported as a good predictor of clinical response to anti-PD1 pembrolizumab (T-cell inflammatory signature (TIS) score). As expected, tumors with inflammatory phenotype High Angio-High AP showed high TIS score values. Also, Low Angio-Low AP tumors showed very low values. However, it is interesting to note that there were High Angio-High AP samples with low TIS score. On the contrary, a group of Low Angio-High AP samples showed high TIS score thus was susceptible to be treated with immunotherapy (Figure 4).

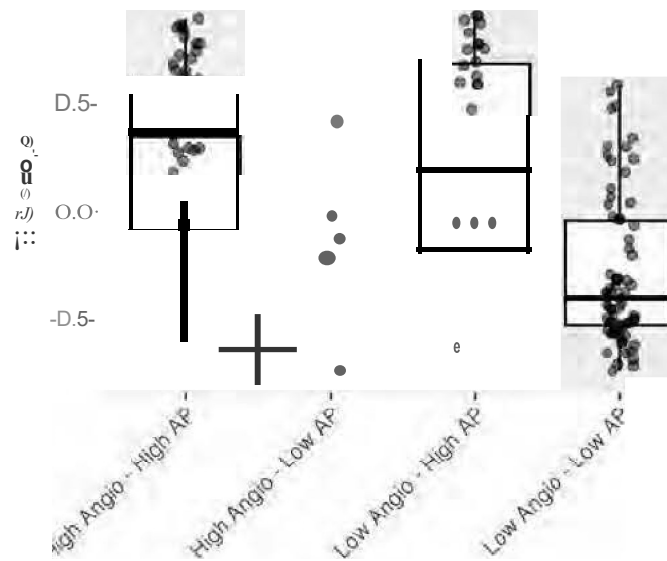


Figure 4. Boxplot showing T cell inflammatory signature (TIS) score across the four AngioAP combination groups.

Finally, we wonder if fibroblasts (Fibro) also have an additive effect on prognosis, along with AP. First, we assessed correlation between fibroblasts and endothelial cells infiltration finding a strong correlation ($R = 0.7$, Figure S6A). Therefore, we expected similar results with High AP/AP than with Fibro/AP. Indeed, the correlation between Fibro/AP is very similar to correlation between High AP/AP (statistically significant but moderate $R = 0.44$, Figure S6B). When tumors were stratified in four groups (High AP-High Fibro, High AP-Low Fibro, Low AP-High Fibro and Low AP-Low Fibro), tumors in Low AP-Low Fibro showed the better prognosis (Figure S6C).

2.4. Metabolic and Tyrosine Kinase Pathway Are Activated in Poor-Prognosis Tumors

In order to deepen our knowledge of the biological behavior of tumors with poor prognosis, a functional analysis comparing relapsing tumors between extreme phenotype was conducted. As expected, the enrichment analysis (Figure 5A) showed an angiogenesis and inflammatory response in High AP-High Angio tumors, along with immune-related pathways such as complement, tumor necrosis factor α -p11a (TNF- α) and interleukin-2 (IL2) signaling. However, other non-inflammation-related pathways emerged, such as glycolysis, epithelial-mesenchymal transition, KRAS signaling, mTORC1 signaling and PI3K-AKT-MTOR signaling. This suggested a crosstalk between immune infiltration, angiogenesis and metabolic pathway. Similar results were achieved when the permutation-labels method was used instead of the pre-ranked gene set enrichment analysis (GSEA). An alternative method, using the most differentially expressed genes reported signaling pathways and metabolism-related pathways as the most significant ones, as well as the antigen presentation pathway (Figure 5B).

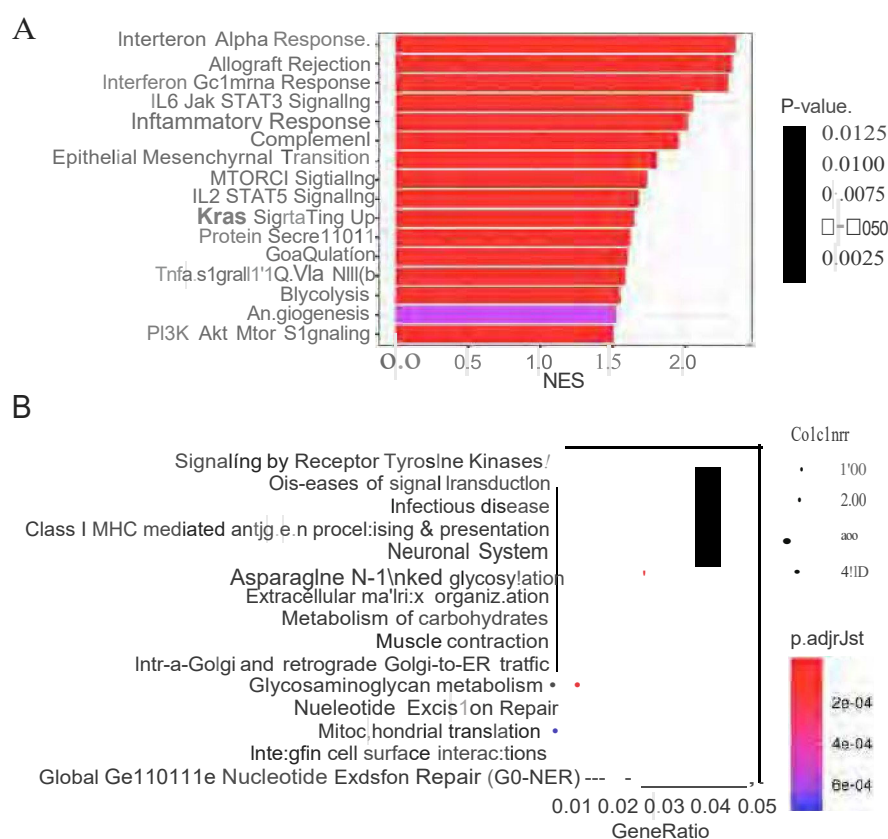


Figure 5. Functional analysis of recurrent tumors within phenotypes "High Anglo-High AP" ($n=45$) versus "Low Anglo-Low P" ($n=16$). (A) Bar plot of enriched Hallmarks from pre-ranked GSEA analysis, ordered by NES and colored by p-values. (B) Dot plot of enriched pathways [from DEGs in the "High Anglo-High AP" phenotype], colored by adjusted p-values. GeneRatio corresponds to the frequency of gene from the gene set in the list of DEGs. Count represents the total number of genes. GSEA: Gene Set Enrichment Analysis, NES: Normalized Enrichment Score, DEGs: Differentially Expressed Genes.

3. Discussion

To show the importance of inflammation and other stromal cells, we have performed a pool analysis of 5 datasets containing prognostic, and transcriptomic information from 213 primary Mesenchymal samples available in the literature [18–21]. We have identified a cluster of samples with angiogenic and inflammatory phenotypes exhibiting poor prognosis (Figure 6.). Contrary to what is found in other tumors, lymphocytic infiltration is related to poor prognosis. In a similar vein, a study by Luo and Ma [22] in UCEC also associated CD8 lymphocytic infiltration with poor prognosis (univariate analysis), and B-cell infiltration with better prognosis (multivariate analysis). This association between inflammation and poor prognosis in uveal melanoma has already been described in individual studies [14,23–25].

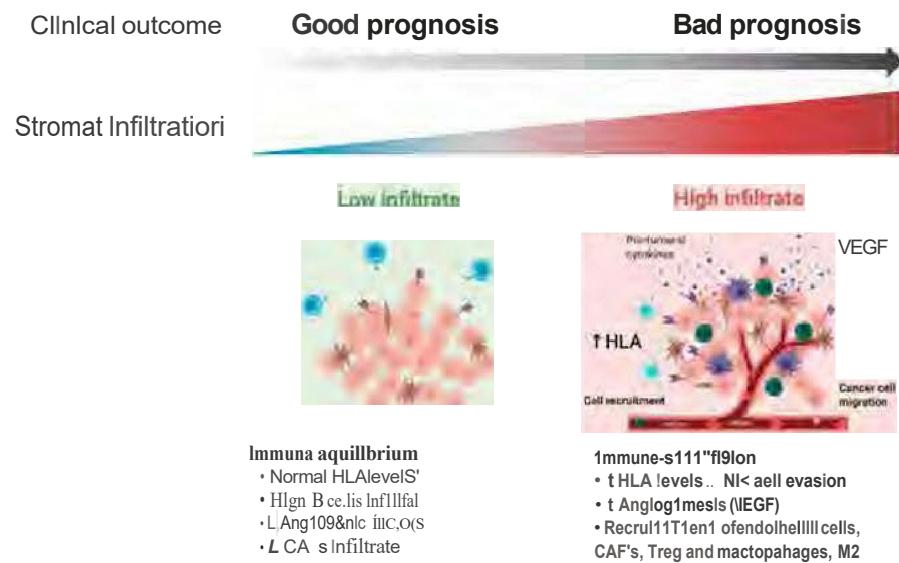


Figure 6. Hypothesis. Our results suggest a combinatory contribution of angiogenesis and inflammation in Uveal melanoma. Infiltration of macrophages, fibroblasts and natural killer (NK) cells associated with poor prognosis, whereas infiltration of B cells is associated with good prognosis. In an over-expression scenario, it might trigger a mechanism to evade the NK-cell-mediated attack. This immunosuppressive environment, together with the high levels of stromal activity and checkpoints blockade, allows Uveal melanoma cells to disseminate and metastasize. Few therapeutic strategies such as, combining immune checkpoint inhibitors (anti-programmed death ligand 1 (PD1) or anti-cytotoxic T-lymphocyte antigen-4 (CTLA4)) with anti-angiogenic targeted therapy (anti-vascular endothelial growth factor (VEGF)) could improve patients' response. Figure created with BioRender.com.

Tumor-infiltrating Lymphocytes (TILs) in primary UM are mainly CD8+ cytotoxic T cells and were present in all 43 cases analyzed by Funckhorrst et al. [2]. In addition, CD4+ -helper cells could also be found in 91% of the samples, and approximately half of these were FoxP3+ regulatory T cells. It is also noteworthy that a well-characterized prognostic factor in UM, such as: chromosome 3 monosomy, seems to be strongly correlated with larger lymphocytic infiltration. The key question here is why TILs lead to poor prognosis. One of the hypotheses is that metastatic dissemination is required to create an immune response due to the peculiar immune ocular characteristics [25]. If that hypothesis is true, only the UM that disseminates outside the eye should have TILs in the primary tumor. The immunosuppressive microenvironment of the primary site, along with inhibitory characteristics displayed by Uveal melanoma cells, would render this infiltration non-effective when it comes to immune-surveillance. Another, more intriguing possibility is that TILs not only fail to eliminate tumor cells but also help tumor growth [26]. Many examples demonstrate that inflammation can promote proliferation and survival of cancer cells [1, 27]. Activated TILs would produce inflammatory mediators, generating a cancer-related inflammatory microenvironment. The cell-type detailed analysis performed using quantification methods based on gene expression found cytotoxic lymphocytes, macrophages and NK cells associated with poor prognosis in at least two of the three methods evaluated. On the other hand, B cells were found to be correlated with better prognosis with all bioinformatic tools tested.

There are no previous reports associating B cells with better prognosis in uveal melanoma, but recently different studies have associated the presence of B cells with survival and immunotherapy response in different tumors [28-31].

The cell-type detailed analysis also revealed fibroblasts and endothelial cell signatures associated with poor prognosis. UM arises in one of the most capillary-rich tissues of the body and disseminates hematogenously. Highly vascularized Uveal melanoma tumors are more aggressive and indicate a worse prognosis. Recently, we have shown that primary Uveal melanoma included in the TCGA that relapses systemically shows a much higher angiogenesis enrichment score than

non-relapsed patients [17]. Differences in disease-free survival (DFS) when comparing high vs. low angiogenesis enrichment scores were statistically significant in UM patients but did not show significance when we compared signature high vs. low using primary tumors included in the CM dataset from the TCGA.

We next sought to study if there was association between T-cell activation and angiogenesis signatures. We identified a group of patients with extremely poor prognosis characterized by high levels of activation of both signatures and 82.9% 5-year relapse rate. On the other hand, tumors with low activation showed good prognosis with only 31.5% of patients relapsing at 5 years. VEGF, along with other angiogenic factors, plays a crucial role in modulating the immune system and fostering an immunosuppressive microenvironment by directly suppressing dendritic cell maturation, inhibiting T-cells by enhancing PD-1 and other inhibitory checkpoints, disrupting the normal differentiation of hematopoietic precursor cells, and recruiting immunosuppressive cells such as T-cells and myeloid derived suppressor cells [31,32]. Thus, a pro-angiogenic environment could be a reason why immunotherapy with checkpoint inhibitors has not been very effective in metastatic uveal melanoma compared to other tumors. Angiogenesis activation has been a hallmark of tumors resistant to checkpoint inhibitors and is associated with more immune-suppressed stroma in different cancers probably due to the close relationship between aberrant cancer angiogenesis and immunosuppression [33,34].

Several antiangiogenic drugs have been used to treat MUM [17]. It is difficult to reach a full conclusion because most of the trials are small and lack a comparator arm, but from the results we can assume that although no objective responses are seen, clinical trials with antiangiogenic drugs usually show slightly higher PFS and OS than clinical trials with conventional chemotherapy. Based on these observations, it would be of special interest to test the activity of antiangiogenic drugs combined with checkpoint inhibitors and see if we can reproduce results observed in other diseases where checkpoint inhibitors in monotherapy do not work such as endometrial cancer. Interestingly, hepatocellular carcinoma, another disease with liver involvement, has become a target for this combination strategy after the IMbrave150 (Atezolizumab plus Bevacizumab in Unresectable Hepatocellular Carcinoma) study showed the superiority of atezolizumab and bevacizumab vs. sorafenib in terms of OS [35].

In order to find other weaknesses that could arise due to therapeutic interventions, we compared primary UM tumors with high angiogenic and antigen presentation activation, with tumors with low activation of both pathways. Interestingly, glycolysis and the PI3K-AKT-MTOR pathways were among the non-infiltration-related pathways. These metabolic pathways have already been linked to immune-resistance to checkpoint inhibitors in different studies [34,36–38]. Interestingly, a recent study has shown that UM is among the tumors with the highest oxidative phosphorylation gene expression and correlates with prognosis in primary UM [39]. Our group has recently made the same observation in MUM patients [40]. We evaluated glucose metabolism in liver metastasis using positron emission tomography (PET-CT) with [18F]-fluorodeoxyglucose (FDG). Increased metabolic activity in liver metastases was found to be an independent predictor of overall survival even in patients with small lesions (M1a).

Our analysis showed robust results replicated in a pool analysis merging different datasets from different analytic platforms. However, this study has limitations. Because it is an in-silico analysis using public data, we have no control over initial stages of the analysis such as sample selection or RNA extraction. Transcriptomic data in each dataset has been analyzed and normalized separately. Also, clinical information is scarce. Specifically, anti-tumoral treatments could affect stromal and immune infiltration. Unfortunately, therapy information was not available and/or detailed. Thus, further experimental validation is needed in order to validate the hypothesis in Figure 6.

4. Materials and Methods

4.1. Patients and Samples

Gene expression, mutations, and clinical data from 80 UM primary tumor samples from the TCGA-UM dataset were collected from the cBioPortal. RNA-seq was downloaded in fragments per kilobase per million (FPKM), then converted to log₂ scale. Also, a total of 133 UM primary samples analyzed using microarrays were downloaded from the Gene Expression Omnibus (GEO) repository; accession numbers GSE27831 ($n = 29$) [18], GSE22168 ($n = 63$) [19], GSE73652 ($n = 13$) [20], GSE84976 ($n = 28$) [21]. Gene expression data from GEO was log₂ scaled. To control for the batch effect, an adjustment was performed using Combat function from R package “sva”. All datasets include information of progression-free survival (PFS), except GSE73652 which only includes the recurrence status. Table S3 includes a detailed description of the datasets.

4.2. Microenvironment Characterization

Gene expression data was used to characterize the immune microenvironment of samples, using a variety of bioinformatics tools. The immunophenoscore (IPS) function was used to measure the immune state of the samples [41]. IPS uses a number of markers of immune response or immune toleration to quantify four different immune phenotypes in a tumor sample (Antigen Presentation, Effector Cells, Suppressor Cells and Checkpoint markers). It also generates an aggregated z-score summarizing the global immune state of the samples. Then, the ESTIMATE R package was used to predict the purity from the samples. ESTIMATE is a tool that predicts the tumor purity and infiltrating stromal/immune cells from gene signatures [42]. ESTIMATE calculates four scores. The Stromal score and the Immune score were calculated using gene expression signatures. Then, a combination of both generates the ESTIMATE score, a measure of the global infiltration of non-tumoral cells in a sample. Finally, the ESTIMATE score is used to calculate the score called Tumor purity, a measure of the number of tumor cells in a sample that are inversely correlated with the ESTIMATE score. The higher the ESTIMATE score, the lower the Tumor purity score.

Three different methodologies of quantification were used; MCP-counter, Quantiseq, and Consensus^{TME}. We have followed the recommendations by Strum et al. [43] and used three different methods to obtain robust results. However, each methodology analyzes a different number of cell types and with different levels of detail that can generate ambiguity when comparing results. The Immunedeconv R package was used to infer cell infiltration using MCP-counter and Quantiseq methods [43]. MCP-counter is a method based on marker genes that quantifies the relative fraction of 10 cell types, including two stromal cell types. Quantiseq is a deconvolution method that infers the absolute fraction and shows a more detailed picture of the immune cell subtypes. Finally, a list of the total 18 gene markers from Consensus^{TME} was used to perform the enrichment analysis with gene set variation analysis (GSVA) [44]. All analyses were performed independently for the different datasets and resultant scores matrices were joined for further analysis.

In addition, we have searched for gene expression signatures discriminating between dendritic cells. Specifically, immature dendritic cells (iDC) and activated dendritic cells (aDC) were extracted from Tamborero et al. [34].

4.3. TMB (Tumor Mutational Burden)

Mutational data was only available in the TCGA data and were used to calculate tumor mutational burden (TMB) per sample.

4.4. Angiogenesis and Antigen Presentation Enrichment Analysis

Angiogenesis (Angio) and antigen presentation (AP) gene sets were manually selected from the curated gene set collection of the Molecular Signatures Database (MSigDB) (BIO-CARTA_VEGF_PATHWAY and REACTOME_ANTIGEN_PRESENTATION, respectively). The GSVA R packages were used to perform Gene Set Variation Analysis [45]. This function performs a non-parametric, unsupervised analysis for estimating variation of the given

gene sets through the samples in the expression matrix, returning an enrichment score for each sample. The GSVA function was performed with 1000 bootstraps and arguments as default. GSVA was performed independently on the different datasets and resultant matrices were joined for further analysis. The association between the two scores was evaluated with the Spearman correlation test for all samples, recurrent and non-recurrent. Samples were divided into “High” and “Low” groups for each score, with a zero value as cut-off. Next, samples were divided into four groups based on the combination of the two scores (High Angio-High AP; High Angio-Low AP; Low Angio-High AP; Low Angio-Low AP). The frequency of recurrence between the four groups was evaluated with a Chi-squared test.

4.5. Hierarchical Clustering

Samples were clustered by agglomerative hierarchical clustering on the basis of the GSVA enrichment scores on the two selected gene sets. Sample distances were computed via the R function “dist”, with Euclidean distance. Next, the “hclust” function generated a clustering from the distances, with the “average” linkage method. Finally, a heatmap was plotted and a dendrogram was drawn for distance-tree visualization purposes.

4.6. Functional Analysis

To identify enrichment in specific cellular functions and pathways, a GSEA was performed comparing the recurrent samples from extreme phenotypes (‘High Angio-High AP’ vs. ‘Low Angio-Low AP’) [46]. GSEA analysis was performed with the clusterProfiler R package. Gene sets Hallmarks and Canonical pathways from MSigDB were interrogated. Samples were scored with the GSVA method using the T-cell inflammatory (TIS) signature [47].

4.7. Statistical Methods

All statistical analyses were performed with R version 3.5.0 (R Foundation for Statistical Computing, Vienna, Austria). For homogenization of methods, all comparisons between continuous variables were analyzed using non-parametric tests (Wilcoxon test and Kruskal-Wallis test). For all tests applied, differences were considered statistically significant when p -value < 0.05. The Cox proportional hazard regression model was used to assess the prognostic effect of the different scores. Cox analysis was performed independently for the different cohorts. A random-effects model was used to summarize the effect for each of the different scores with the “metagen” function from R package meta. This function performs a meta-analysis based on hazard ratio estimates and their standard errors. The overall effect is calculated with the inverse variance method. The results were plotted in a forest plot. For the pool analysis, all samples were joined and a Cox regression model stratified by dataset was performed. Results were summarized and plotted with a forest plot. Survival probabilities were plotted with the Kaplan–Meier method, and the Log-rank test was used to compare the survival proportions among different groups. For categorical variables, samples were divided into “High” and “Low” groups based on the cut-off points (zero value for scores, median value for gene expression).

Supplementary Materials: The following are available online at <https://www.mdpi.com/1422-0067/22/5/2669/s1>. Figure S1: Meta-analysis of immune markers by dataset for the different scores of ESTIMATE (A) and Immunophenoscore (B). Figure S2: A. Boxplots of scores of antigen presentation, effector cells, suppressor cells and checkpoint markers for High ($n = 106$) and Low ($n = 107$) Immune groups. B. Kaplan-Meier survival curves for High and Low groups. Patients were divided into High and Low groups by the median value of the ESTIMATE score. Figure S3: Meta-analysis of dendritic cell markers by dataset for Activated dendritic cells (aDCs) (A) and Immature dendritic cells (iDCs) (B). Figure S4: Kaplan-Meier survival curves for cytotoxic markers CD8A (A), GZMA (B) and PRF1 (C). Patients were divided by the median expression value for each dataset and joined afterwards. Figure S5: Boxplots showing time to recurrence by Angio-AP groups. Figure S6: (A) Fibroblasts and endothelial cells correlation plot (Spearman correlation). (B) Correlation plot between Fibroblasts

and Antigen Presentation signatures colored by recurrent (light grey) and non-recurrent (dark grey) status. Black line represents correlation for all samples, regardless of recurrence status. Spearman correlation is indicated (C) Kaplan-Meier survival curves for the four groups combining Fibroblasts and AP scores. Table S1: Resultant scores of the ESTIMATE method and immune groups generated from the ESTIMATE score. Table S2: Gene signatures of the different methods used in the analysis. Table S3: Detailed clinical and molecular information for each dataset.

Author Contributions: Conceptualization, R.S.-P. and J.M.P.; methodology, S.G.-M., R.S.-P. and M.H.A.; formal analysis, S.G.-M. and R.S.-P.; data curation, S.G.-M.; statistical support, M.H.A.; writing – original draft preparation, S.G.-M., R.S.-P. and J.M.P.; writing – review and editing, J.M.P. and L.P.d.C.; supervision, R.S.-P. and J.M.P. All authors have read and agreed to the published version of the manuscript.

Funding: This research was funded by Grupo Español de Melanoma (GEM) grant number 19PSJ006.

Institutional Review Board Statement: Ethical review and approval were waived for this study, due to data was downloaded from open access repository and ethical approval was done by the authors of the individual studies cited.

Informed Consent Statement: Patient consent was waived due to data was downloaded from open access repository and informed consent was done by the authors of the individual studies cited.

Data Availability Statement: Publicly available datasets were analyzed in this study. All R code used for the analyses are openly available for reproducibility of the results in a GitHub repository at <https://github.com/odap-ubs/uveal-pool-analysis>.

Acknowledgments: We thank CERCA Program, Generalitat de Catalunya for institutional support. We also thank the Consortium for Biomedical Research in Epidemiology and Public Health (CIBERESP). Luis del Carpio is recipient of a Clinical Junior grant from Spanish Association Against Cancer (AECC) Foundation.

Conflicts of Interest: J.M.P. is consultant for Roche-Genentech, Bristol-Myers Squibb, Merck Sharp and Dohme, Merck Serono, Janssen, Astellas, VCN Biotech and BeiGene; J.M.P. has received research grants from Bristol-Myers Squibb, Merck Sharp and Dohme, Merck Serono, Janssen and AstraZeneca.

Abbreviations

aDC	activated dendritic cell
Angio	Angiogenesis
AP	Antigen Presentation
B2M	Beta-2-Microglobulin
BAP1	BRCA1 Associated Protein 1
CALR	Calreticulin
CI	Confidence Interval
CM	Cutaneous Melanoma
CTLA-4	Cytotoxic T-Lymphocyte Antigen-4
D3	Disomy of Chromosome 3
DC	dendritic cell
DEG	Differentially Expressed Genes
DFS	Disease Free Survival
FPKM	Fragments per Kilobase per Million
GEO	Gene Expression Omnibus
GSEA	Gene Set Enrichment Analysis
GSVA	Gene Set Variation Analysis
GZMA	Granzyme A
HLA	Human Leukocyte Antigen
HR	Hazard Ratio
iDC	immature dendritic cell

IL2	Interleukin-2
IPS	Immunophenoscore
KM	Kaplan-Meier
M1	liver metastasis
M1a	small lesion liver metastasis
M3	Monosomy of Chromosome 3
MSigDB	Molecular Signatures Database
mTORC1	Mammalian target of rapamycin complex 1
MUM	Metastatic Uveal Melanoma
NES	Normalized Enrichment Score
NK	Natural Killer
OS	Overall Survival
PD-1	Programmed Cell death protein 1
PDL1	Programmed Death Ligand 1
PET-TC	Positron emission tomography
PFS	Progression Free Survival
PI3K	Phosphoinositide 3-kinase
PRF	Perforin
TAP	Tapasin
TIL	Tumor Infiltrating Lymphocyte
TIS	T-cell Inflammatory Signature
TMB	Tumor Mutational Burden
TME	Tumor microenvironment
TNF- α	Tumor Necrosis Factor alpha
UM	Uveal Melanoma
VEGF	Vascular Endothelial Growth Factor

References

1. Carvajal, R.D.; Schwartz, G.K.; Tezel, T.; Marr, B.; Francis, J.H.; Nathan, P.D. Metastatic Disease from Uveal Melanoma: Treatment Options and Future Prospects. *Br. J. Ophthalmol.* **2017**, *101*, 38–44. [[CrossRef](#)] [[PubMed](#)]
2. Mallone, S.; De Vries, E.; Guzzo, M.; Midena, E.; Verne, J.; Coebergh, J.W.; Marcos-Gragera, R.; Ardanaz, E.; Martinez, R.; Chirlaque, M.D.; et al. Descriptive Epidemiology of Malignant Mucosal and Uveal Melanomas and Adnexal Skin Carcinomas in Europe. *Eur. J. Cancer* **2012**, *48*, 1167–1175. [[CrossRef](#)]
3. Yang, J.; Manson, D.K.; Marr, B.P.; Carvajal, R.D. Treatment of Uveal Melanoma: Where Are We Now? *Ther. Adv. Med. Oncol.* **2018**, *10*, 175883401875717. [[CrossRef](#)] [[PubMed](#)]
4. Caminal, J.M.; Ribes, J.; Clèries, R.; Ibáñez, N.; Arias, L.; Piulats, J.M.; Pera, J.; Gutierrez, C.; Arruga, J. Relative Survival of Patients with Uveal Melanoma Managed in a Single Center. *Melanoma Res.* **2012**, *22*, 271–277. [[CrossRef](#)] [[PubMed](#)]
5. Pons, F.; Plana, M.; Caminal, J.M.; Pera, J.; Fernandes, I.; Perez, J.; Garcia-Del-Muro, X.; Marcoval, J.; Penin, R.; Fabra, A.; et al. Metastatic Uveal Melanoma: Is There a Role for Conventional Chemotherapy?—A Single Center Study Based on 58 Patients. *Melanoma Res.* **2011**, *21*, 217–222. [[CrossRef](#)] [[PubMed](#)]
6. Piulats, J.M.; Espinosa, E.; de la Cruz Merino, L.; Varela, M.; Alonso Carrión, L.; Martín-Algarra, S.; López Castro, R.; Curiel, T.; Rodríguez-Abreu, D.; Redrado, M.; et al. Nivolumab Plus Ipilimumab for Treatment-Naïve Metastatic Uveal Melanoma: An Open-Label, Multicenter, Phase II Trial by the Spanish Multidisciplinary Melanoma Group (GEM-1402). *J. Clin. Oncol.* **2021**, JCO2000550. [[CrossRef](#)]
7. Algazi, A.P.; Tsai, K.K.; Shoushtari, A.N.; Munhoz, R.R.; Eroglu, Z.; Piulats, J.M.; Ott, P.A.; Johnson, D.B.; Hwang, J.; Daud, A.I.; et al. Clinical Outcomes in Metastatic Uveal Melanoma Treated with PD-1 and PD-L1 Antibodies: PD-1 Blockade in Uveal Melanoma. *Cancer* **2016**, *122*, 3344–3353. [[CrossRef](#)]
8. Rossi, E.; Schinzari, G.; Zizzari, I.G.; Maiorano, B.A.; Pagliara, M.M.; Sammarco, M.G.; Fiorentino, V.; Petrone, G.; Cassano, A.; Rindi, G.; et al. Immunological Backbone of Uveal Melanoma: Is There a Rationale for Immunotherapy? *Cancers* **2019**, *11*, 1055. [[CrossRef](#)]
9. Jager, M.J.; Shields, C.L.; Cebulla, C.M.; Abdel-Rahman, M.H.; Grossniklaus, H.E.; Stern, M.-H.; Carvajal, R.D.; Belfort, R.N.; Jia, R.; Shields, J.A.; et al. Uveal Melanoma. *Nat. Rev. Dis. Primers* **2020**, *6*, 24. [[CrossRef](#)]
10. Toomey, C.B.; Protopsaltis, N.J.; Phou, S.; Bakhoum, M.F.; Thorson, J.A.; Ediriwickrema, L.S.; Korn, B.S.; Kikkawa, D.O.; Goldbaum, M.H.; Lin, J.H. Prevalence of mismatch repair gene mutations in uveal melanoma. *Retina* **2020**, *40*, 2216–2220. [[CrossRef](#)]
11. Cross, N.A.; Murray, A.K.; Rennie, I.G.; Ganesh, A.; Sisley, K. Instability of Microsatellites Is an Infrequent Event in Uveal Melanoma. *Melanoma Res.* **2003**, *13*, 435–440. [[CrossRef](#)]

12. Johansson, P.A.; Brooks, K.; Newell, F.; Palmer, J.M.; Wilmott, J.S.; Pritchard, A.L.; Broit, N.; Wood, S.; Carlino, M.S.; Leonard, C.; et al. Whole Genome Landscapes of Uveal Melanoma Show an Ultraviolet Radiation Signature in Iris Tumours. *Nat. Commun.* **2020**, *11*, 2408. [[CrossRef](#)]
13. Niederkorn, J.Y. Immune Escape Mechanisms of Intraocular Tumors. *Prog. Retin. Eye Res.* **2009**, *28*, 329–347. [[CrossRef](#)]
14. Robertson, A.G.; Shih, J.; Yau, C.; Gibb, E.A.; Oba, J.; Hess, J.M.; Uzunangelov, V.; Walter, V.; Danilova, L.; Lichtenberg, M.; et al. Integrative Analysis Identifies Four Molecular and Clinical Subsets in Uveal Melanoma. *Cancer Cell* **2017**, *32*, 204–220. [[CrossRef](#)] [[PubMed](#)]
15. Oliva, M.; Rullan, A.J.; Piulats, J.M. Uveal Melanoma as a Target for Immune-Therapy. *Ann. Transl. Med.* **2016**, *4*, 172. [[CrossRef](#)]
16. Figueiredo, C.R.; Kalirai, H.; Sacco, J.J.; Azevedo, R.A.; Duckworth, A.; Slupsky, J.R.; Coulson, J.M.; Coupland, S.E. Loss of BAP1 Expression Is Associated with an Immunosuppressive Microenvironment in Uveal Melanoma, with Implications for Immunotherapy Development. *J. Pathol.* **2020**, *250*, 420–439. [[CrossRef](#)] [[PubMed](#)]
17. Castet, F.; Garcia-Mulero, S.; Sanz-Pamplona, R.; Cuellar, A.; Casanovas, O.; Caminal, J.; Piulats, J. Uveal Melanoma, Angiogenesis and Immunotherapy, Is There Any Hope? *Cancers* **2019**, *11*, 834. [[CrossRef](#)]
18. Gangemi, R.; Mirisola, V.; Barisione, G.; Fabbì, M.; Brizzolara, A.; Lanza, F.; Mosci, C.; Salvi, S.; Gualco, M.; Truini, M.; et al. Mda-9/Syntenin Is Expressed in Uveal Melanoma and Correlates with Metastatic Progression. *PLoS ONE* **2012**, *7*, e29989. [[CrossRef](#)] [[PubMed](#)]
19. Laurent, C.; Valet, F.; Planque, N.; Silveri, L.; Maacha, S.; Anezo, O.; Hupe, P.; Plancher, C.; Reyes, C.; Albaud, B.; et al. High PTP4A3 Phosphatase Expression Correlates with Metastatic Risk in Uveal Melanoma Patients. *Cancer Res.* **2011**, *71*, 666–674. [[CrossRef](#)]
20. Field, M.G.; Decatur, C.L.; Kurtenbach, S.; Gezgin, G.; van der Velden, P.A.; Jager, M.J.; Kozak, K.N.; Harbour, J.W. PRAME as an Independent Biomarker for Metastasis in Uveal Melanoma. *Clin. Cancer Res.* **2016**, *22*, 1234–1242. [[CrossRef](#)]
21. Fagone, P.; Caltabiano, R.; Russo, A.; Lupo, G.; Anfuso, C.D.; Basile, M.S.; Longo, A.; Nicoletti, F.; De Pasquale, R.; Libra, M.; et al. Identification of Novel Chemotherapeutic Strategies for Metastatic Uveal Melanoma. *Sci. Rep.* **2017**, *7*, 44564. [[CrossRef](#)] [[PubMed](#)]
22. Luo, H.; Ma, C. Identification of Prognostic Genes in Uveal Melanoma Microenvironment. *PLoS ONE* **2020**, *15*, e0242263. [[CrossRef](#)]
23. Bronkhorst, I.H.G.; Vu, T.H.K.; Jordanova, E.S.; Luyten, G.P.M.; van der Burg, S.H.; Jager, M.J. Different Subsets of Tumor-Infiltrating Lymphocytes Correlate with Macrophage Influx and Monosomy 3 in Uveal Melanoma. *Investig. Ophthalmol. Vis. Sci.* **2012**, *53*, 5370. [[CrossRef](#)] [[PubMed](#)]
24. de la Cruz, P.O.; Specht, C.S.; McLean, I.W. Lymphocytic Infiltration in Uveal Malignant Melanoma. *Cancer* **1990**, *65*, 112–115. [[CrossRef](#)]
25. Whelchel, J.C.; Farah, S.E.; McLean, I.W.; Burnier, M.N. Immunohistochemistry of Infiltrating Lymphocytes in Uveal Malignant Melanoma. *Investig. Ophthalmol. Vis. Sci.* **1993**, *34*, 2603–2606. [[PubMed](#)]
26. Buder, K.; Gesierich, A.; Gelbrich, G.; Goebeler, M. Systemic Treatment of Metastatic Uveal Melanoma: Review of Literature and Future Perspectives. *Cancer Med.* **2013**, *2*, 674–686. [[CrossRef](#)]
27. Ellerhorst, J.A.; Cooksley, C.D.; Grimm, E.A. Autoimmunity and Hypothyroidism in Patients with Uveal Melanoma. *Melanoma Res.* **2001**, *11*, 633–637. [[CrossRef](#)] [[PubMed](#)]
28. Petitprez, F.; de Reyniès, A.; Keung, E.Z.; Chen, T.W.-W.; Sun, C.-M.; Calderaro, J.; Jeng, Y.-M.; Hsiao, L.-P.; Lacroix, L.; Bougouin, A.; et al. B Cells Are Associated with Survival and Immunotherapy Response in Sarcoma. *Nature* **2020**, *577*, 556–560. [[CrossRef](#)]
29. Cabrita, R.; Lauss, M.; Sanna, A.; Donia, M.; Skaarup Larsen, M.; Mitra, S.; Johansson, I.; Phung, B.; Harbst, K.; Vallon-Christersson, J.; et al. Tertiary Lymphoid Structures Improve Immunotherapy and Survival in Melanoma. *Nature* **2020**, *577*, 561–565. [[CrossRef](#)]
30. Helmink, B.A.; Reddy, S.M.; Gao, J.; Zhang, S.; Basar, R.; Thakur, R.; Yizhak, K.; Sade-Feldman, M.; Blando, J.; Han, G.; et al. B Cells and Tertiary Lymphoid Structures Promote Immunotherapy Response. *Nature* **2020**, *577*, 549–555. [[CrossRef](#)]
31. Fukumura, D.; Kloepper, J.; Amoozgar, Z.; Duda, D.G.; Jain, R.K. Enhancing Cancer Immunotherapy Using Antiangiogenics: Opportunities and Challenges. *Nat. Rev. Clin. Oncol.* **2018**, *15*, 325–340. [[CrossRef](#)]
32. Khan, K.A.; Kerbel, R.S. Improving Immunotherapy Outcomes with Anti-Angiogenic Treatments and Vice Versa. *Nat. Rev. Clin. Oncol.* **2018**, *15*, 310–324. [[CrossRef](#)] [[PubMed](#)]
33. Hugo, W.; Zaretsky, J.M.; Sun, L.; Song, C.; Moreno, B.H.; Hu-Lieskovan, S.; Berent-Maoz, B.; Pang, J.; Chmielowski, B.; Cherry, G.; et al. Genomic and Transcriptomic Features of Response to Anti-PD-1 Therapy in Metastatic Melanoma. *Cell* **2016**, *165*, 35–44. [[CrossRef](#)] [[PubMed](#)]
34. Tamborero, D.; Rubio-Perez, C.; Muiños, F.; Sabarinathan, R.; Piulats, J.M.; Muntasell, A.; Dienstmann, R.; Lopez-Bigas, N.; Gonzalez-Perez, A. A Pan-Cancer Landscape of Interactions between Solid Tumors and Infiltrating Immune Cell Populations. *Clin. Cancer Res.* **2018**, *24*, 3717–3728. [[CrossRef](#)]
35. Finn, R.S.; Qin, S.; Ikeda, M.; Galle, P.R.; Ducreux, M.; Kim, T.-Y.; Kudo, M.; Breder, V.; Merle, P.; Kaseb, A.O.; et al. Atezolizumab plus Bevacizumab in Unresectable Hepatocellular Carcinoma. *N. Engl. J. Med.* **2020**, *382*, 1894–1905. [[CrossRef](#)] [[PubMed](#)]
36. Peng, W.; Chen, J.Q.; Liu, C.; Malu, S.; Creasy, C.; Tetzlaff, M.T.; Xu, C.; McKenzie, J.A.; Zhang, C.; Liang, X.; et al. Loss of PTEN Promotes Resistance to T Cell-Mediated Immunotherapy. *Cancer Discov.* **2016**, *6*, 202–216. [[CrossRef](#)] [[PubMed](#)]

37. Chang, C.-H.; Qiu, J.; O'Sullivan, D.; Buck, M.D.; Noguchi, T.; Curtis, J.D.; Chen, Q.; Gindin, M.; Gubin, M.M.; van der Windt, G.J.W.; et al. Metabolic Competition in the Tumor Microenvironment Is a Driver of Cancer Progression. *Cell* **2015**, *162*, 1229–1241. [[CrossRef](#)]
38. Ho, P.-C.; Bihuniak, J.D.; Macintyre, A.N.; Staron, M.; Liu, X.; Amezquita, R.; Tsui, Y.-C.; Cui, G.; Micevic, G.; Perales, J.C.; et al. Phosphoenolpyruvate Is a Metabolic Checkpoint of Anti-Tumor T Cell Responses. *Cell* **2015**, *162*, 1217–1228. [[CrossRef](#)]
39. Chattopadhyay, C.; Oba, J.; Roszik, J.; Marszalek, J.R.; Chen, K.; Qi, Y.; Eterovic, K.; Robertson, A.G.; Burks, J.K.; McCannel, T.A.; et al. Elevated Endogenous SDHA Drives Pathological Metabolism in Highly Metastatic Uveal Melanoma. *Investig. Ophthalmol. Vis. Sci.* **2019**, *60*, 4187–4195. [[CrossRef](#)]
40. Del Carpio Huerta, L.P.; Algarra, M.; Llobera, A.S.; Rodríguez-Vida, A.; Ruiz, S.; Leiva, D.; Lorenzo, D.; Navarro, V.; Gutiérrez, C.; Caminal, J.M.; et al. Metabolic Activity of Liver Metastases May Predict Survival in Patients with Metastatic Uveal Melanoma. *Ann. Oncol.* **2020**, *31*, S672–S710.
41. Charoentong, P.; Finotello, F.; Angelova, M.; Mayer, C.; Efremova, M.; Rieder, D.; Hackl, H.; Trajanoski, Z. Pan-Cancer Immunogenomic Analyses Reveal Genotype-Immunophenotype Relationships and Predictors of Response to Checkpoint Blockade. *Cell Rep.* **2017**, *18*, 248–262. [[CrossRef](#)] [[PubMed](#)]
42. Yoshihara, K.; Shahmoradgoli, M.; Martínez, E.; Vegesna, R.; Kim, H.; Torres-Garcia, W.; Treviño, V.; Shen, H.; Laird, P.W.; Levine, D.A.; et al. Inferring Tumour Purity and Stromal and Immune Cell Admixture from Expression Data. *Nat. Commun.* **2013**, *4*, 2612. [[CrossRef](#)] [[PubMed](#)]
43. Sturm, G.; Finotello, F.; List, M. Immunedeconv: An R Package for Unified Access to Computational Methods for Estimating Immune Cell Fractions from Bulk RNA-Sequencing Data. *Methods Mol. Biol.* **2020**, *2120*, 223–232. [[CrossRef](#)] [[PubMed](#)]
44. Jiménez-Sánchez, A.; Cast, O.; Miller, M.L. Comprehensive Benchmarking and Integration of Tumor Microenvironment Cell Estimation Methods. *Cancer Res.* **2019**, *79*, 6238–6246. [[CrossRef](#)]
45. Hänzelmann, S.; Castelo, R.; Guinney, J. GSEA: Gene Set Variation Analysis for Microarray and RNA-Seq Data. *BMC Bioinform.* **2013**, *14*, 7. [[CrossRef](#)]
46. Subramanian, A.; Tamayo, P.; Mootha, V.K.; Mukherjee, S.; Ebert, B.L.; Gillette, M.A.; Paulovich, A.; Pomeroy, S.L.; Golub, T.R.; Lander, E.S.; et al. Gene Set Enrichment Analysis: A Knowledge-Based Approach for Interpreting Genome-Wide Expression Profiles. *Proc. Natl. Acad. Sci. USA* **2005**, *102*, 15545–15550. [[CrossRef](#)] [[PubMed](#)]
47. Liu, D.; Schilling, B.; Liu, D.; Sucker, A.; Livingstone, E.; Jerby-Arnon, L.; Zimmer, L.; Gutzmer, R.; Satzger, I.; Loquai, C.; et al. Integrative Molecular and Clinical Modeling of Clinical Outcomes to PD1 Blockade in Patients with Metastatic Melanoma. *Nat. Med.* **2019**, *25*, 1916–1927. [[CrossRef](#)] [[PubMed](#)]

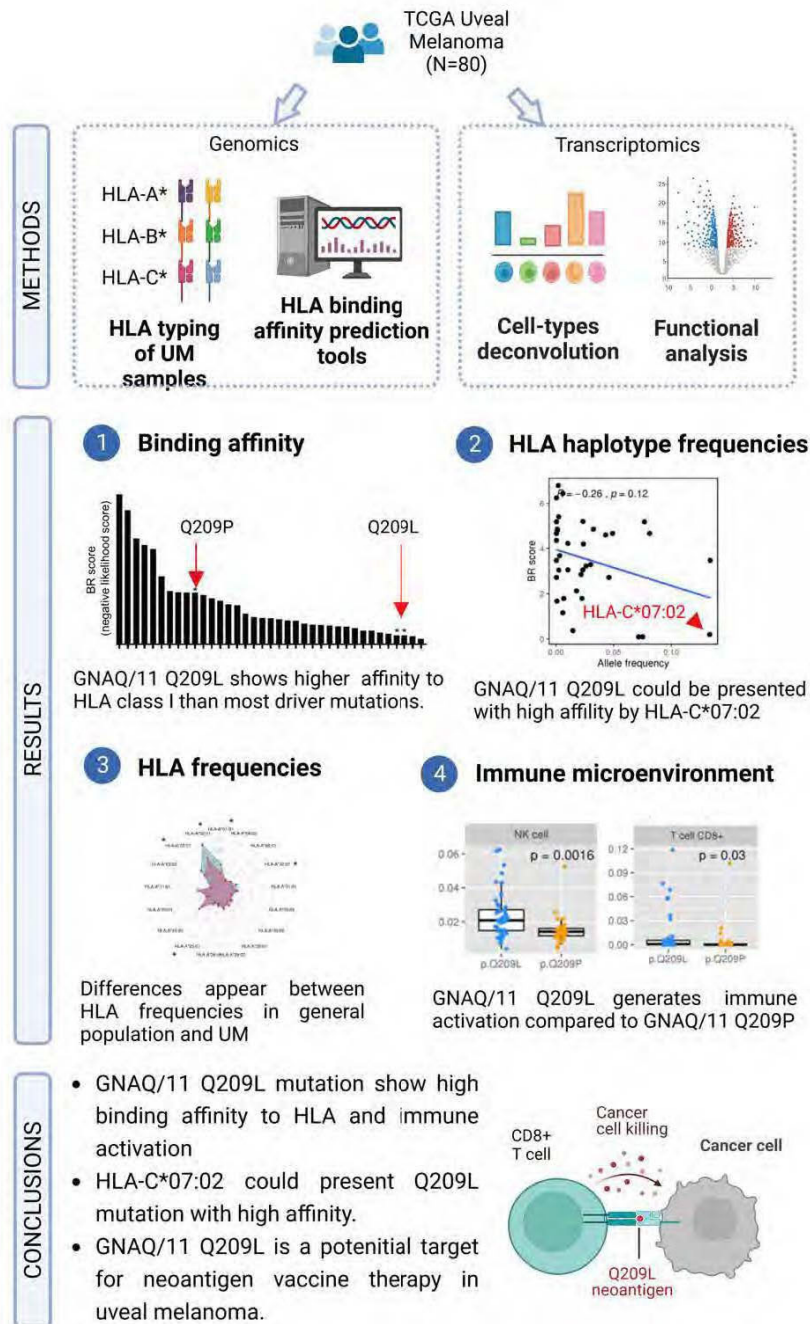
1.2. Driver mutations in GNAQ and GNA11 genes are likely to be antigenic in uveal melanoma patients

Article: [Sandra García-Mulero](#), Marco Punta, Roberto Fornelino Stefano Lise, Mar Varela, Rafael Moreno, Marcel Costa-Garcia, Ramón Alemany, Josep María Piulats, Rebeca Sanz-Pamplona. *Driver mutations in GNAQ and GNA11 genes as a tentative cancer vaccine in uveal melanoma patients.*

Objective and main results:

The second objective of the Study j on uveal melanoma was to evaluate the antigenicity of driver mutations in GNAQ and GNA11 genes taking into account HLA genotype, to describe differences in the immune profile between samples harboring QVXkP or QVXkL amino acid changes, and to assess their association with clinical phenotypes. In this study, we have evaluated the immunogenic potential of GNAQ/11 QVXkL and GNAQ QVXkP mutations through *in silico* methods, in order to find novel potential targets for immunotherapeutic approaches in uveal melanoma. The antigenicity of driver mutations GNAQ/11 QVXkL and QVXkP in uveal melanoma was assessed by bioinformatic tools. QVXkL peptide showed stronger binding affinity to HLA class I than QVXkP peptide, and was more likely to be presented by HLA class I than most driver mutations. The HLA haplotypes with higher binding affinity to QVXkL were defined. We found that HLA-C*04:01:01:01 was the best candidate for presenting QVXkL mutation, since it shows a strong binding affinity (BR<V) and high frequency (Vq%) in the general population. Results from gene expression analysis showed that samples harboring expressed higher HLA class I levels and high infiltration of CD4+ T cells and NK cells. The functional analysis showed enrichment of hypoxia, mTOR signaling, oxidative phosphorylation and fatty acid metabolism for QVXkP mutated patients.

Graphic abstract



Driver mutations in GNAQ and GNA11 genes as potential targets for precision immunotherapy in uveal melanoma patients

Sandra García-Mulero^{1,2}, Roberto Fornelino¹, Marco Punta³, Stefano Lise³, Mar Varela⁴, Rafael Moreno⁵, Marcel Costa-García⁵, Alena Gros⁶, Ramón Alemany⁵, Josep María Piulats⁷, Rebeca Sanz-Pamplona^{1,8}

¹Unit of Biomarkers and Susceptibility, Oncology Data Analytics Program (ODAP), Catalan Institute of Oncology (ICO), Oncobell Program, Bellvitge Biomedical Research Institute (IDIBELL) and CIBERESP, L'Hospitalet de Llobregat, Barcelona, Spain.

²Department of Clinical Sciences, Faculty of Medicine and Health Sciences, University of Barcelona, Barcelona, Spain.

³Bioinformatics Core, Centre for Evolution and Cancer, The Institute of Cancer Research, London, SM2 5NG, United Kingdom.

⁴Department of Pathology, Bellvitge University Hospital, L'Hospitalet, Barcelona, Spain.

⁵Translational Research Laboratory, ICO, Oncobell Program, IDIBELL.

⁶Tumor Immunology and Immunotherapy, Vall d'Hebron Institute of Oncology (VHIO), Vall d'Hebron Barcelona Hospital Campus, C/Natzaret, 115-117, 08035 Barcelona, Spain.

⁷Department of Medical Oncology, ICO, IDIBELL and CIBERONC, L'Hospitalet de Llobregat, Barcelona, Spain.

⁸ARAID Researcher, Aragon Health Research Institute (IISA), Zaragoza, Spain.

E-mail: rebecasanz@iconcologia.net

Abstract

Uveal melanoma (UM) is the most common ocular malignancy in adults. Nearly 95% of UM patients carry the mutually exclusive mutations in the homologous genes GNAQ (aminoacid change Q209L/Q209P) and GNA11 (aminoacid change Q209L). UM is located in an immunosuppressed organ and do not suffer immunoediting. Therefore, we hypothesize that driver mutations in GNAQ/11 genes could be recognized by the immune system. Genomic and transcriptomic data for primary uveal tumors was collected from TCGA-UM dataset (n=80). The immunogenic potential for GNAQ/GNA11 Q209L/Q209P mutations was assessed using a variety of tools and HLA types information. The immune microenvironment was characterized using gene expression data. All prediction tools showed stronger GNAQ/11 Q209L binding to HLA. The immunogenicity analysis revealed that Q209L is likely to be presented by more than 73% of individuals in 1000G database whereas Q209P is only predicted to be presented in 24% of individuals. GNAQ/11 Q209L showed higher likelihood to be presented by HLA-I molecules than almost all driver mutations analyzed. Samples carrying Q209L had a higher immune-reactive phenotype: (i) expression of antigen presenting genes HLA-A (p=0.009) and B2M (p=0.043); (ii) immunophenoscore (p=0.008); (iii) infiltration of immune system cells NK (p=0.002) and CD8+ T lymphocytes (p=0.02). Results suggest a high potential immunogenicity of the GNAQ/11 Q209L variant that could allow the generation of novel therapeutic tools to treat UM like neoantigen vaccinations.

Keywords: uveal meelanoma, driver mutations, antigenicity, immunotherapy.

1. Introduction

Despite being considered a rare tumor (10 cases per million incidence in Europe), uveal melanoma (UM) is the most common ocular malignancy in adults (1). Prognosis is still poor, with up to 50% of patients developing metastasis, mostly in the liver. Metastatic UM does not have an effective standard treatment available and survival rates have not improved in the last decades (2).

At the molecular level, UM is very different from cutaneous melanoma. Both arise from melanocytes, but they do not share somatic mutations driving carcinogenesis. UM shows exclusive mutations in the GNA gene family. Nearly 95% of UM patients carry the mutually exclusive mutations GNAQ/GNA11 in the hotspot Q209. These mutations change the conserved catalytic glutamine for a Proline, P, or Leucine, L, leading to the constitutive activation of the GTPase domain (3). These oncogenic mutations in G protein-coupled receptor

(GPCR) activates pathways including MPAK, PI3K/AKT or YAP/TAZ promoting tumor progression (4).

Unlike cutaneous melanoma, UM do not respond to immune checkpoint inhibitors (5,6). This could be due to several molecular and anatomical differences. UM is located in an immune-privileged organ, protected by the blood-ocular barrier and exhibits an immunosuppressive microenvironment. Because of that, it does not suffer immunoediting (7). Moreover, the tumor mutational burden (TMB) is very high in cutaneous melanoma but low in UM (8). Thus, UM generates low levels of neoantigens and is considered a tumor with low antigenicity (3). Also, we and others showed that immune cell infiltration is associated with poor prognosis in UM (9) (10,11).

Although driver mutations are normally catalogued as non-immunogenic, recent work support the possibility to develop immunotherapeutic drugs against neoantigens derived from recurrent mutations in cancer driver genes in some cases (12). We hypothesize that recurrent mutations in GNAQ and GNA11 genes could elicit T-cell responses. Given the predicted low immune selective pressure in UM, it could represent an attractive target for immunotherapeutic interventions. Also, we hypothesize that different mutations (Q209P or Q209L) could have different antigenicity and response from the immune system. Our objective is to computationally analyze the antigenicity of tumors harbouring GNAQ/11 mutations, to characterize their microenvironment, and to assess their association with clinical phenotypes. Our results suggest that Q209L mutation is more immunogenic than Q209P mutation, irrespectively of the mutated gene (GNAQ or GNA11).

2. Methods

2.1 Samples

Clinical and mutational data of paired primary uveal tumors and blood samples from patients was collected from TCGA-UM dataset (n=80 pairs). Annotated mutational data was downloaded from the cBioPortal (13). RNA-seq was downloaded in fragments per kilobase per million (FPKM), then converted to log₂ scale. Supplementary Table 1 includes a detailed description of patients included in the dataset. Comparison between groups were performed by Chi-squared test for categorical variables and Wilcoxon test for numerical variables. For survival analysis validation dataset, a series of a uveal melanoma from University Hospital of Bellvitge (n=73) with clinical and mutational status information was used.

2.2 Immunogenicity prediction of neoantigens GNAQ-L, GNAQ-P and GNA11-L

First, for each mutation, 19 mers amino acid sequences were extracted using an in-house script. Mutated amino acids were in the center of the sequence. Wild type sequences were also generated. The immunogenic potential for GNAQ-L, GNAQ-P and GNA11-L was assessed in a variety of binding prediction tools (NetMHC, NetMHCpan, NetMHCcons, NetMHCpanstab, MHCSeqNet and MHCflurry) using HLA supertypes and all 9mer combinations from the two mutated sequences as input (14-21).

Apart from solo binding prediction, NetCTL tool was used to predict proteasomal C terminal cleavage and TAP transport efficiency (22). The proteasome cleavage event is predicted using the version of the NetChop neural networks trained on C terminals of known CTL epitopes as described for the NetChop-3.0 server (23). The TAP transport efficiency is predicted using the weight matrix-based method described by Peters et al (22). NetCTL predicts MHC peptide binding using neural networks in NetMHC server and then calculates a combined score for the three measures. As an input, fasta files with GNAQ and GNA11 protein sequence was used.

2.3 HLA presentation scores

All HLA-presentation scores were defined starting from eluted ligand likelihood percentile ranks of peptides with respect to HLA allotypes obtained from the NetMHCpan-4.0 prediction method (15). NetMHCpanI were run (HLA type I only predictions) on all neopeptides of length 8 to 11 generated by each of the 3 mutations (GNAQ-L, GNAQ-P and GNA11-L) against a set of 195 HLA(-A/-B/-C) types found in the >1,000 individuals of the 1000Genomes project. For each individual there was information about 6 HLA types.

Each mutation was mapped to a protein sequence and associated to a set of 38 mutated peptides using an in-house Python script to generate all possible peptides of length 8 to 11 that spanned the mutation. A wild type peptide was associated to each specific mutant peptide that was identical to the mutant peptide except that the mutated amino acid is reverted to the wild type one. For each peptide in this set, the program NetMHCpan-4.0 (57) was used to calculate the eluted ligand likelihood percentile rank and predict the interaction core peptide (Icore) with respect to all HLA allotypes. The elution rank takes values in the range from 0 to 100, with lower values representing higher presentation likelihoods. We defined the presentation score of a mutation with respect to a specific HLA allotype as the minimum elution rank among all associated peptides but excluding those with a wild type Icore. We called this presentation BR score.

PHBR score (Patient Harmonic-Mean Best Rank) was calculated by combining the six best rank scores of the six HLA allotypes using a harmonic mean. Also, we calculated

Mutation	NetMHC	NetMHC-pan	NetMHC-cons	NetMHC-stabpan	MHC-SeqNet	MHC-flurry	MixMHCp red	Total
Q209P	1 (WB)	3 (WB)	0	1 (WB)	5	1	1	12
Q209L	5 (3 WB + 2 SB)	3 (2 WB + 1SB)	4 (2 WB + 2 SB)	3 (WB)	6	4	4	29

Table 1. Number of predicted bindings. WB: weak binding, SB: strong binding.

our Population-Wide Median Harmonic-Mean Best Rank (PMHBR) as the median of the PHBR scores of a mutation calculated over a set of individuals. Lower PMHBR scores correspond to higher likelihoods for the mutation to be presented across our 1000G or TCGA populations (24).

2.4 Immune microenvironment characterization

The immune microenvironment of the samples was characterised using gene expression data and a variety of bioinformatics tools. The immunophenoscore (IPS) function was used to measure the immune state of the samples by the quantification of four different immune phenotypes in a given tumor sample (Antigen Presentation, Effector Cells, Suppressor Cells and Checkpoint markers), using gene markers. Also, it computes an aggregated z-score summarizing the four immune phenotypes (26). Finally, samples were scored using the gene set variation analysis (GSVA) method with 18 gene markers lists from ConsensusTME (27) and the T-cell inflammatory (TIS) signature (28).

2.5 Survival analysis

A survival analysis was done with a cohort of patients from the Bellvitge University Hospital (n=73). Progression free survival (PFS) was assessed between patients harboring Q209P (n=25) and Q209L (n=48) mutation. Kaplan-Meier curves were plotted to represent the result and log-rank test was computed.

3. Results

3.1 GNAQ/GNA11 mutations in TCGA-UM dataset

GNAQ and GNA11 were the most frequent missense mutations in TCGA-UM dataset and were mutually exclusive (**Figure 1A**). Out of 80 TCGA-UM patients, 34 patients carried GNA11 p.Q209L (hereafter GNA11-L), 10 patients carried GNAQ p.Q209L (hereafter GNAQ-L), and 27 patients GNAQ p.Q209P (hereafter GNAQ-P). The other 9 samples were wild type at the position of interest; two patients carried GNAQ p.R183Q mutation, one more patient carried GNAQ p.G48V, one patient GNA11 p.R183C, and one patient GNA11 p.R166H. Two individuals were mutant at the same time for GNAQ and GNA11 but the second hit was not in position 209 (one case at positions GNAQ p.Q209L and

GNA11 p.R166H; second case at positions GNAQ p.R183Q and GNA11 p.R183C) (**Figure 1B**).

Despite being located in different chromosomes (Chr. 9 and Chr. 19, respectively), GNAQ and GNA11 genes are highly homologous and so are the resulting proteins. A BLAST alignment showed 90% identity between the two proteins (**Supplementary Figure 1**). GNAQ-L and GNA11-L suffered the same amino acid change in position 209 (from Q -Glutamine- to L -Leucine-), and given the high homology between these two proteins, the resulting 19-mer peptide in which the mutation is centred were identical. On the other hand, GNAQ-P changed from Q (Glutamine) to P (Proline). Because of this, and since we planned to study the potential immunogenicity of those mutations rather than protein function, we decided to compare patients harboring P mutated vs. patients harboring L mutated, irrespectively of the gene of origin (**Figure 1B**). In total, 71 (89%) patients carried the Q209P/L amino acid change, of which 44 (62%) carry amino acid change p.Q209L and 27 (38%) carry change p.Q209P.

To see whether there was any association between the different change Q209P or Q209L and the different clinical variables in the dataset, we performed a statistical test by mutation change (**Supplementary Table 2**). No association was found with age, sex, overall survival time and status, progression free survival status, recurrence, fraction of genome altered, SCNA subtype cluster, BAP1 mutation, Chromosome 3 status (disomy or monosomy), Chromosome 8 status (disomy or polysomy) or immune cluster. The only significant association was the mutation count (Wilcoxon test, p-val=0.028), indicating that patients with Q209L mutations have a slightly higher number of mutations (a mean of 13.3 vs. 11.1). However, this is not significant when multitesting correction was applied.

3.2 Binding affinity prediction of neoantigens GNAQ-L, GNAQ-P and GNA11-L

The 19 length peptides for GNAQ-L/GNA11-L (Q209L) (IFRMVDVGGGLRSERRKWIH) and GNAQ-P (Q209L) (IFRMVDVGGPRRSERRKWIH) were used to test the antigenicity of these mutations using a total of 7 different binding prediction tools, to avoid any bias related to similar Machine Learning algorithms or datasets used for the training. Most of these prediction tools focus on scoring the affinity of the inputted peptides for a specific HLA. However,

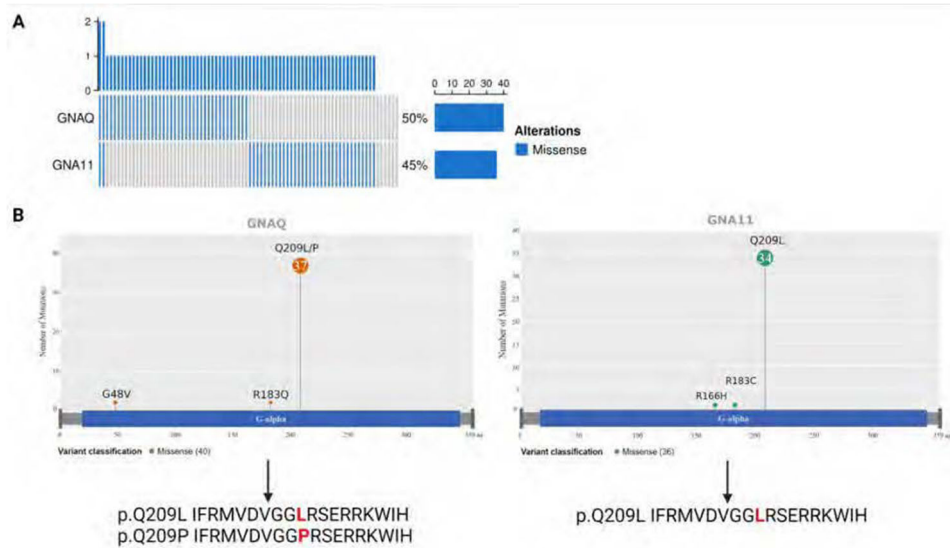


Figure 1. GNAQ and GNA11 mutations in TCGA UM samples **A)** Mutational status of GNAQ and GNA11 genes. Barplot shows mutated patients in blue and wild type in grey. Frequency of alterations are 50% for GNAQ and 45% for GNA11. **B)** Lollipop plot showing GNAQ and GNA11 mutations across the proteins and resulting peptides harbouring Q209P and Q209L mutations. Aminoacidic changes are marked in red.

NetMHCstabpan, which calculates a combined score for the affinity and stability of the binding was also used. As input, tools used all possible 9mer combinations from the two 19mer mutated sequences studied. Apart from the peptide sequences, we used all the HLA superfamilies for the predictions.

The outputs of the different tools were diverse. The NetMHC tools and MHCflurry calculate an affinity value measured in nM, which is used to filter the binders or no binders. These affinity values are also shown as a logarithmic transformations, called %Rank. Only the 9mers with a value of 500nM and below are considered binders. On the other hand, the output of MHCSeqNet is a probability value between 0.0 and 1.0, where 0.0 refers to a non-binder and 1.0 to a strong binder. Only those with more than 60% probability of binding were taken. Lastly, MixMHCpred does not provide affinity value, instead, it calculates a Score and a %Rank value for each HLA allele. For a single allele, scores larger than 0 correspond to %rank smaller than 1%. Therefore, in the case of this tool, we only choose the 9mers in which the best allele score is higher than 0 (**Supplementary Table 3**).

In summary, all methods predicted Q209L mutation as being more immunogenic (assuming the higher binding values the more immunogenic) than Q209P, except for NetMHCpan that predicted equal number of peptides with binding affinity (**Figure 2**). A total of 12 non-unique bindings with different HLA types were found for Q209P variant whereas a total of 29 bindings were found for Q209L. Although only 4 out of the 7 tested tools give information about the strength of the binding, no Q209P neoantigen was predicted as strong binder. However, 5 putative neoantigens were classified as strong binders in the case of Q209L (**Table 1**). The HLA haplotypes

giving rise to strong bindings with Q209L mutation were HLA-A*03:01, HLA-B*27:05 and HLA-B*39:01. For Q209P mutation, the HLA with strong bindings were HLA-A*03:01 and HLA-B*07:02 (**Supplementary Table 3**).

To know if these mutations would be likely to be presented by any individual from the 1000Genomes database, as a sample of healthy population, we calculated how many individuals have at least one mutant peptide (length 8 to 11) that has presentation likelihood below a given threshold for at least one of the HLA types of the individual. For threshold % rank <0.5 (Strong binding), up to 73% of individuals were predicted to present Q209L peptide, while only 24% of individuals were predicted to present Q209P peptide.

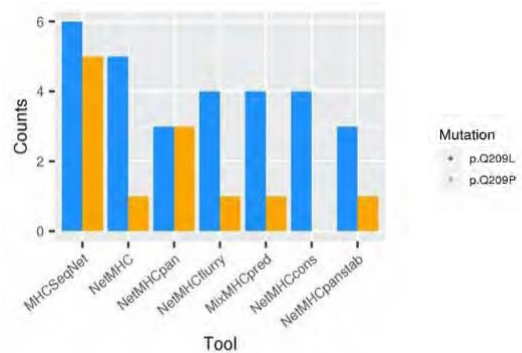


Figure 2. HLA-Q209L and HLA-Q209P binding prediction. Barplot showing the number of successful bindings predicted of Q209L change (in orange) and Q209P (in green) across seven prediction tools (in x axes), using HLA supertypes genotypes.

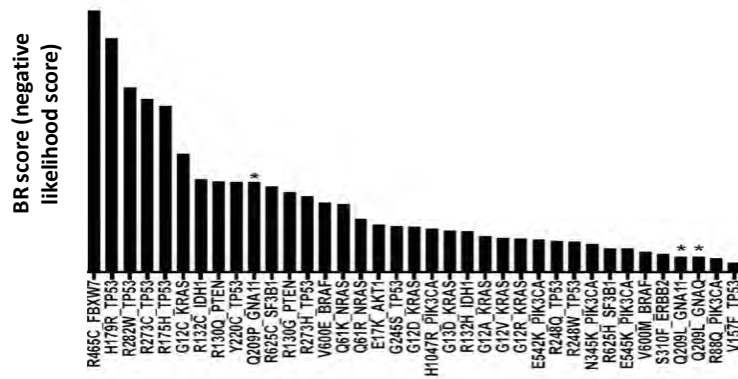


Figure 3. PMHBR score of a list of driver mutations across 1000 Genomes individuals. The lower PBHBR score the higher probability to be presented. Q209L shows higher likelihood to be presented by HLA molecules than Q209P and most driver mutations in cancer. Asterisks marks Q209P and Q209 L mutations.

Looking at threshold %rank <2 (Weak binding), 88% of individuals were presenting Q209L peptides and 74% of individuals present Q209P. Moreover, we generated a BR score for each sample carrying Q209L by taking the minimum BR score of all 6 BR per patient. The 69.7% of samples have at least one strong binding (BR<0.5), while 16.3% have a weak binding (0.5<BR<2) and 14% have no binding (BR>2).

Next, the percentage rank score of mutant peptides were compared to the percentage rank of their corresponding wild type (WT) peptides. This may be relevant because given the similarity between WT and mutants (a single aa difference) it is possible that if the WT is presented, the mutant (even if presented) may be subjected to tolerance mechanisms and thus not be immunogenic. For % rank < 0.5 threshold, in 59% of individuals the mutated peptide Q209L is predicted to be presented with strong binding while the Q209L WT is not. On the other side, only 8% of individuals are predicted to present the Q209P mutated peptides and not the Q209P WT peptide. So, mutation Q209L has the most encouraging differences with respect to WT.

Finally, the HLA binding affinity was predicted through a score of antigenicity for the two mutations Q209P and Q209L. This score is calculated based on the "Best rank" score of NetMHCpanI for the 100Genomes population. As explained, the BR score is the Best Rank for each individual, while the PMHBR is the median population BR score. The PMHBR score of Q209P is 3.66, while the PMHBR score of Q209L is 0.62. Then, we have compared these scores to other driver mutations, and we see that Q209L mutation has one of the lowest scores, meaning that it has higher likelihood to be presented across the population than most of the driver mutations of different cancer types (Figure 3).

Apart from binding to HLA, for a neoantigen to be presented it needs to be processed by the proteasome and transported by the TAP mechanism. We used NetCTL to predict proteasomal C terminal cleavage and TAP transport efficiency. As a result, for Q209L we got 3 putative

neoantigens whereas we got only 2 in the case of the Q209P. For Q209L, NetCTL selected 9 mer FRMVDVVGGL as a good candidate to be presented by HLA-B*27:05 and HLA-B*39:01 and RMVDVGGGLR to be presented by HLA-A*03:01. These two peptides were also predicted to be binders by all the other tools. The former as a strong binder and the later a weak binder.

Taking together, all these results points to Q209L mutation to be more immunogenic, being predicted to be properly processed and presented with good affinity and stability.

3.3 HLA haplotypes frequencies with uveal melanoma risk and survival

Next, we wanted to assess if having different HLA haplotypes (implying different binding affinity for Q209L) has an impact on uveal melanoma risk or survival. First, we wonder if there was a relationship between HLA haplotype frequency and the BR scores. In the general population, the BR score of Q209L mutation is not correlated with HLA frequency for HLA-A and HLA-B genes (Figure 4A), while BR score and HLA-C exhibited a non-significant trend towards negative correlation. For UM patients, the negative correlation between HLA-C haplotype frequency and the BR score is stronger (Spearman correlation, p=0.057, Figure 4B). Results from 1000G population pointed to HLA-C*07:02 as the allele with the more frequency and lower BR score. On the contrary, HLA-A*24:02 is an example of frequent allele with no predicted binding affinity for Q209L (Figure 4C).

HLA frequencies between uveal patients and general, healthy population (1000G) were compared by binomial test and resulting frequencies were plotted in a radar plot (Figure 5A, Supplementary Table 4). As a result, 10 haplotypes showed differences at FDR<0.05 between uveal and population frequency, of which 9 showed higher frequency in uveal melanoma patients; HLA-A*01:01, HLA-A*02:01, HLA-B*08:01, HLA-B*15:01, HLA-B*18:01, HLA-

B*44:02, HLA-C*01:02, HLA-C*05:01, HLA-C*07:01, HLA-C*12:03. Of those alleles, only HLA-C*07:01 and HLA-A*01:01 have BR score of high antigenicity ($BR < 2$), while the other seven with higher frequency in uveal melanoma have high BR value scores ($BR > 2$; low antigenicity scores), suggesting a genetic selection in uveal melanoma patients made neoantigen Q209L to be hidden.

The same analysis was performed for comparing the HLA frequencies between patients harbouring Q209L or Q209P mutations (**Supplementary Figure 2**). In this case, no statistical differences were found between the frequencies. Finally, to find out whether there could be selection towards lower antigenic binding in patients carrying the highly antigenic Q209L change and relapsing, we compared the HLA frequencies in patients carrying Q209L mutation, between recurrent and non-recurrent uveal melanoma samples. As in the previous comparison, none of the HLA haplotypes compared by binomial test showed statistically significant differences. On the contrary, there is a tendency towards higher frequency in HLA-B*44:02, HLA-B*07:02 and HLA-B*18:01 in non-recurrent samples, which are three haplotypes with low binding affinity to Q209L. (**Figure 5**). Also, we wonder if HLA haplotypes with higher chances of presenting Q209L were absent in uveal melanoma patients. However, there are not statistically significant differences in BR score between haplotypes present and missing in uveal melanoma patients (**Supplementary Figure 3**).

Finally, a survival analysis was done in a total of 73 human samples from the Bellvitge University Hospital ($n=73$) between Q209L and Q209P. As a result, Q209L patients showed slightly better progression free survival (PFS) than Q209P patients (Log-rank test $p=0.038$). (**Supplementary Figure 4**). However, in TCGA data, we have not found any relationship between P/L mutations and prognosis.

In summary, no clear associations have been found between HLA haplotypes and risk of suffering uveal melanoma neither between HLA frequency and survival. It is important to point

out that there is a possibility that we do not find statistical differences between recurrent ($n=17$) and non-recurrent ($n=26$) Q209L patients due to the low sample size.

3.4 Samples harboring GNAQ-P or GNA-L mutations showed differences in the tumor microenvironment

We used expression data to characterize the immune state of samples carrying Q209L mutation or Q209P mutation. First, we evaluated whether there were differences in the levels of antigen processing and presentation genes (**Figure 6A**). All genes related to MHC class I showed higher gene expression in patients carrying Q209L mutation (Wilcoxon test; HLA-A, $p=0.009$; HLA-B, $p=0.039$; HLA-C, $p=0.034$, B2M, $p=0.043$).

Next, we used a number of tools to characterize the immune system activation status of samples. The T-cell inflamed signature (TIS score) was estimated and showed no differences between Q209L and Q209P mutated patients (**Figure 6B**). The Immunophenoscore, that is used as global score of the immune state of the samples, was significantly higher in Q209L mutated patients ($p=0.0081$) (**Figure 6C**). This score is based on four sub-scores that represent the activation of Antigen presentation, Effector cells, suppressor cells and checkpoint markers (neither of those showed statistically significant differences, although there is a tendency to higher antigen presentation and effector cells activation in Q209L patients).

To explore the infiltrate in detail, we used Quantiseq method for estimating the infiltration of immune cells in the tumour microenvironment (**Figure 6D**). We found higher infiltration of T cells CD8+ ($p=0.03$) and NK cells ($p=0.0016$) in Q209L patients. To validate these results, we estimated the scores with a second method, called ConsensusTME (consensus tumor microenvironment) (**Supplementary Figure 5**). In agreement with the previous method, we found that patients carrying Q209L mutations tended to higher infiltration scores for CD8 T cells ($p=0.065$). In contrast, we

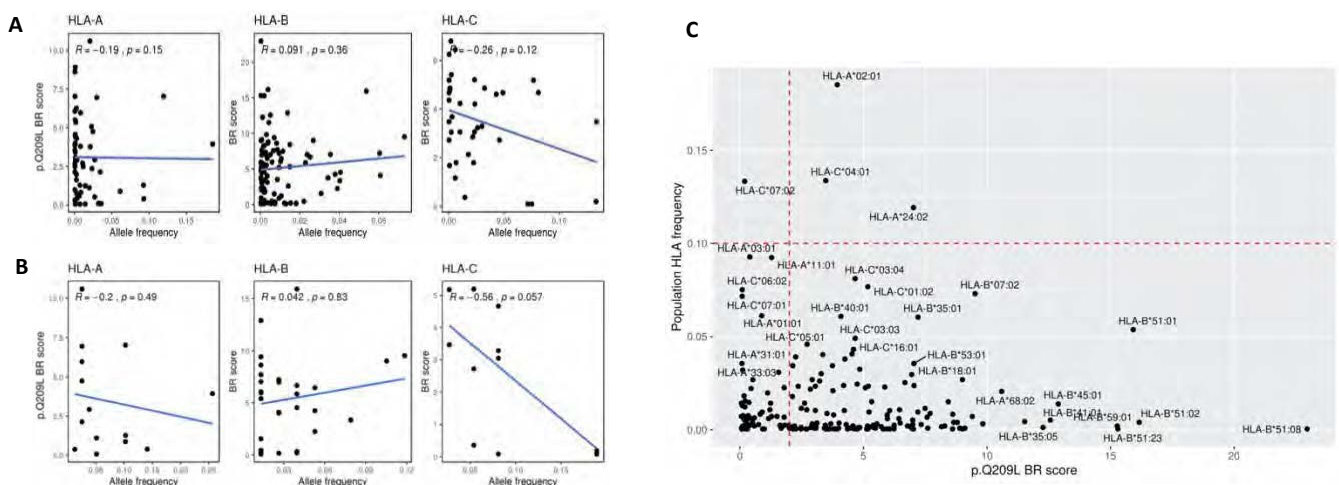


Figure 4. Correlation between presentation probability and HLA haplotypes. Plots showed correlation between BR score of Q209L and the HLA-A, HLA-B and HLA-C type frequency in (A) general population and (B) in UM patients. C) Plot showing BR score for Q209L in x axis and population HLA frequency in y axis with HLA haplotypes of high frequency annotated.



Figure 5. HLA frequency association with UM risk and survival. Radar plots comparing frequencies in HLA haplotype for HLA-A gene, HLA-B gene and HLA-C genes **A**) Between UM patients (green) and 1000 Genomes individuals (purple), and between recurrent (red) and non-recurrent (green) patients harbouring Q209L **B**). Asterisks correspond to haplotypes with statistical differences by Binomial test (FDR p-adjusted < 0.05). Only haplotypes which are present in uveal melanoma patients are depicted.

found no differences in NK cells. No differences were found for the other cell types with this method, although there was a trend towards higher scores of B cells in Q209P patients. Despite the variability between the methods, all results suggest a distinct immune microenvironment modulation, indicating a high immune reactive phenotype in tumours harbouring Q209L mutations.

Finally, to look at differences in activated biological pathways, a differential expression followed by gene-set enrichment analysis between Q209L carriers and Q209P carriers was performed. A total of 12 genes were found at p-value<0.05 and absolute values of logFC>1, of which 9 were overexpressed in Q209L patients and 3 were overexpressed in Q209P patients (Supplementary Table 5). In the functional analysis, as expected, most enriched gene sets for Q209L patients were related with immune system (IFN- γ , p-adj=1.38e-12; IFN- α , p-adj=3.06e-8, IL6/JAK/STAT3, p-adj=1.4e-3). Also, other pathways related with tumour growth and metabolism emerged (mTOR signalling, p-adj=5.16e-5; hypoxia, p-adj=0.011, oxidative phosphorylation, p-adj=0.03,

and fatty acid metabolism, p=0.04) (Supplementary Figure 6, Supplementary Table 6). Otherwise, there was not any pathways enriched in Q209P patients. This result suggests a crosstalk between immune infiltrate and other components of the tumour biology in Q209L carriers.

4. Discussion

Activating mutations in the G α q signaling pathway at the level of GNAQ and GNA11 genes are considered alterations driving proliferation in UM. Lot of research has been devoted to understanding molecular mechanisms behind these alterations, which transfer signaling from GPCRs to downstream effectors by activating the pathway constitutively. Also, to develop blocking drugs (29). Despite these efforts, no novel treatment targeting this pathway has improved the prognosis of UM patients. Due to the exclusive immune microenvironment of UM, here we propose to study these driver mutations from an immunogenic point of view.

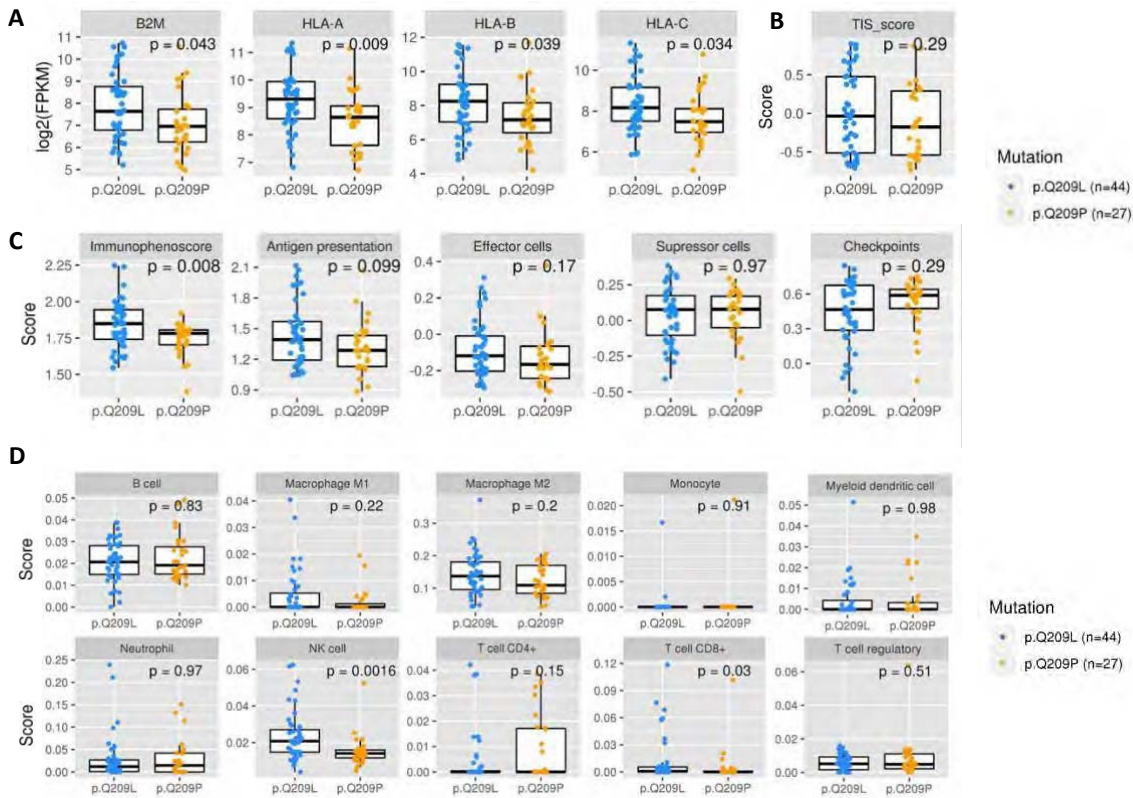


Figure 6. Characterization of immune state in patients carrying Q209L variant and Q209P variant. A) Levels of expression of antigen presenting genes B2M, HLA-A, HLA-B and HLA-C. B) T cell Inflammatory signalling (TIS) score. C) Immunophenoscore (IPS), antigen presentation, effector cells, suppressor cells, and checkpoints scores. D) Immune cell infiltration. Wilcoxon test were used to calculate statistically significant differences (p -value < 0.05).

Our hypothesis is that different amino acids in the same position (P or L) activates different immune response in the patient, rather than being GNAQ or GNA11 mutant. To the best of our knowledge, little is known about differences between tumors harboring Q209P or Q209L mutations. A study by Maziarz et al showed fundamental difference in the molecular properties of Gq Q209P compared with proteins harboring Q209L, due to different structural conformations of the aberrant proteins (30).

Contrary to other driver mutations such as those in p53 or BRAF, among others; GNAQ and GNA11 are UM-exclusive mutations. On one hand, these alterations could help cancer cells to acquire an eye-specific adaptation. On the other hand, it might be hypothesized that tumoral cells harboring these mutations in other organs are destroyed by immune system in early stages of the disease. In this regard, it has been reported that highly recurrent oncogenic mutations have poor HLA class I presentation (31). Punta et al reported that the median PMHBR of highly recurrent driver mutations in TCGA is 1.84 whereas the median PMHBR of passenger mutations in TCGA is 1.391. Thus, a driver mutation's frequency in cancer patients negatively correlates with the population ability to present it (24,31). Our results point to Q209L to be more

immunogenic than Q209P in 1000G population. Despite being a driver mutation, it was more likely to be presented in comparison with other recurrent ones. In agreement, all tested tools except NetMHCpan predicted Q209L derived peptide as high immunogenic.

Neoantigens shared among groups of patients have become increasingly popular therapeutic targets. Obviously, non-recurrent, passenger mutations generating neoantigens needs personalized logistics to be therapeutically exploited. On the contrary, public mutations simplifies all this process. In this regard, several public neoantigens from mutations in KRAS, BRAF and TP53 genes has been described so far (12). It is worth to mention a recent work by Samuels et al. describing the combination of HLA-A*01:01 and driver mutation RAS.Q61K as potentially immunogenic in 3% of melanoma patients (39).

We have found differences in immune system activation and infiltration between Q209L and Q209P tumors, being Q209L those scoring better in immunophenoscore. In agreement, Q209L tumors showed higher expression of genes related to antigen presentation. Interestingly, Q209L tumors showed higher infiltration of T-cells and NK cells. It has been reported that normal ocular cells express little or no MHC

class I molecules in order to avoid recognition by cytotoxic T-cells. Aqueous humor or eye contains immunosuppressive factors inhibiting NK cells such as TGF-beta or MIF. Paradoxically, metastasizing cells in UM upregulate HLA molecules. Probably, this is because uveal melanoma cells with lower HLA expression are susceptible to be detected and eliminated by NK cells (32). In agreement, in-vitro studies have demonstrated the ability of cytotoxic NK cells to detect and kill uveal melanoma cells (33,34).

Also, differences at functional level have been found. Interestingly, Q209L score better in pathways related to inflammation like interferon alpha and gamma response reinforcing those tumors to be more immunogenic. However, no changes in the inflammatory microenvironment neither in HLA expression has been found in a similar study comparing Q209L vs. Q209P primary uveal tumors (35).

Although a trend was observed towards more frequent HLA in UM showing low BR scores, no clear associations have been found between HLA haplotypes and risk of suffering uveal melanoma neither between HLA frequency and survival. These suggest that genetics of patients do not impact directly on disease initiation or progression through Q209L presentation, or at least there are other implicated factors. One could expect HLA alleles showing low BR score (meaning high likelihood of the neoantigen to be presented by HLA) in healthy population and HLA alleles showing high BR score in UM patients. The low number of UM samples prevented us to discard the hypothesis that people presenting Q209L neoantigen are at lower risk to develop UM. Interestingly, a negative correlation has been found between BR score and HLA-C frequency in both uveal patients and general population suggesting HLA-C as the best presenting allele for this specific neoantigen.

In terms of prognosis, mutations in GNA11 have been moderately associated with poor prognosis and found more frequently in metastatic UM; in comparison with GNAQ mutations (36,37). Other analysis, however, found not differences (35). Looking at amino acidic change, in TCGA-UM data, a marginal p-value of 0,06 pointed to Q209L to be associated with high risk of relapse. No differences in survival status were found. However, in controversy, our results in an independent dataset of primary UM samples showed Q209P patients to have poor prognosis (log-rank=0,04). Interestingly, Terai et al. identified that differences in mutation patterns (Q209P vs. Q209L) in GNAQ and GNA11, rather than GNAQ and GNA11 themselves, might predict the survival of metastatic UM patients. After development of metastasis, patients with GNAQ Q209P mutant tumors had a more favorable outcome than patients with GNA11 Q209L and GNAQ Q 209L mutant tumors (38). Also controversial, but in the primary tumor setting, a work by van Weeghel et al found not differences in prognosis based on Q209P or L mutation but in Chromosome 3 status (monosomy or disomy), as

previously reported. In our data, there is not association between Chromosome 3 status and Q209P or L mutation.

This study has several limitations. It has not been validated in independent datasets because of scarce data about amino acidic change in GNAQ, GNA11 mutations. Functional analysis comparing tumors harboring Q209P and Q209L could be biased by differences in number of samples between the two groups. Unfortunately, binding predictors do not perform well with HLA-II so the role of these genes deserves further study. Also, prediction binding algorithms could produce false positive results. The limited sample size is also a drawback. Finally, the study is primarily computational.

Despite the shortcomings, it is worth to mention that an existing patent (WO2019241666) validates our observations. It already defines a technology for the development of a vaccine to treat uveal melanoma based on GANQ/GNAL11 mutations. It shows how the binding of the mutated peptide FRMVDVGGGL, which was also found in our study, with the HLA is more immunogenic than the binding with wild type peptide. Also, they describe that the critical amino acids for the binding were R in position 2 and Q/L in position 9, located in MHC pocket acting as an anchor.

Treatment of UM continues to be a challenge, especially in metastatic patients. Although preliminary, our work paves the way for future therapeutic options such as NK cell therapy or neoantigen vaccines. In this study, we report that GANQ/GNAL11 mutations can generate immunogenicity and we have proposed a potential candidate for neoantigen vaccine targeting uveal melanoma.

Acknowledgements

We thank CERCA Program, Generalitat de Catalunya for institutional support. We also thank the Consortium for Biomedical Research in Epidemiology and Public Health (CIBERESP).

References

1. Mallone S, De Vries E, Guzzo M, Midena E, Verne J, Coebergh JW, et al. Descriptive epidemiology of malignant mucosal and uveal melanomas and adnexal skin carcinomas in Europe. *Eur J Cancer*. 2012 May;48(8):1167-75.
2. Yang J, Manson DK, Marr BP, Carvajal RD. Treatment of uveal melanoma: where are we now? *Ther Adv Med Oncol*. 2018;10:1758834018757175.
3. Jager MJ, Shields CL, Cebulla CM, Abdel-Rahman MH, Grossniklaus HE, Stern MH, et al. Uveal melanoma. *Nat Rev Dis Primers*. 2020 Apr 9;6(1):24.

4. Park JJ, Diefenbach RJ, Joshua AM, Kefford RF, Carlino MS, Rizos H. Oncogenic signaling in uveal melanoma. *Pigment Cell Melanoma Res.* 2018 Nov;31(6):661-72.
5. Piulats JM, Espinosa E, de la Cruz Merino L, Varela M, Alonso Carrión L, Martín-Algarra S, et al. Nivolumab Plus Ipilimumab for Treatment-Naïve Metastatic Uveal Melanoma: An Open-Label, Multicenter, Phase II Trial by the Spanish Multidisciplinary Melanoma Group (GEM-1402). *J Clin Oncol.* 2021 Feb 20;39(6):586-98.
6. Algazi AP, Tsai KK, Shoushtari AN, Munhoz RR, Eroglu Z, Piulats JM, et al. Clinical outcomes in metastatic uveal melanoma treated with PD-1 and PD-L1 antibodies. *Cancer.* 2016 Nov 15;122(21):3344-53.
7. Niederkorn JY. Immune escape mechanisms of intraocular tumors. *Prog Retin Eye Res.* 2009 Sep;28(5):329-47.
8. Cross NA, Murray AK, Rennie IG, Ganesh A, Sisley K. Instability of microsatellites is an infrequent event in uveal melanoma. *Melanoma Res.* 2003 Oct;13(5):435-40.
9. García-Mulero S, Alonso MH, Del Carpio LP, Sanz-Pamplona R, Piulats JM. Additive Role of Immune System Infiltration and Angiogenesis in Uveal Melanoma Progression. *Int J Mol Sci.* 2021 Mar 6;22(5):2669.
10. de la Cruz PO, Specht CS, McLean IW. Lymphocytic infiltration in uveal malignant melanoma. *Cancer.* 1990 Jan 1;65(1):112-5.
11. Whelchel JC, Farah SE, McLean IW, Burnier MN. Immunohistochemistry of infiltrating lymphocytes in uveal malignant melanoma. *Invest Ophthalmol Vis Sci.* 1993 Jul;34(8):2603-6.
12. Pearlman AH, Hwang MS, Konig MF, Hsiue EHC, Douglass J, DiNapoli SR, et al. Targeting public neoantigens for cancer immunotherapy. *Nat Cancer.* 2021 May;2(5):487-97.
13. Cerami E, Gao J, Dogrusoz U, Gross BE, Sumer SO, Aksoy BA, et al. The cBio cancer genomics portal: an open platform for exploring multidimensional cancer genomics data. *Cancer Discov.* 2012 May;2(5):401-4.
14. Nielsen M, Lundegaard C, Worning P, Lauemøller SL, Lamberth K, Buus S, et al. Reliable prediction of T-cell epitopes using neural networks with novel sequence representations. *Protein Sci.* 2003 May;12(5):1007-17.
15. Andreatta M, Nielsen M. Gapped sequence alignment using artificial neural networks: application to the MHC class I system. *Bioinformatics.* 2016 Feb 15;32(4):511-7.
16. Reynisson B, Alvarez B, Paul S, Peters B, Nielsen M. NetMHCpan-4.1 and NetMHCIIpan-4.0: improved predictions of MHC antigen presentation by concurrent motif deconvolution and integration of MS MHC eluted ligand data. *Nucleic Acids Res.* 2020 Jul 2;48(W1):W449-54.
17. Karosiene E, Lundegaard C, Lund O, Nielsen M. NetMHCcons: a consensus method for the major histocompatibility complex class I predictions. *Immunogenetics.* 2012 Mar;64(3):177-86.
18. Rasmussen M, Fenoy E, Harndahl M, Kristensen AB, Nielsen IK, Nielsen M, et al. Pan-Specific Prediction of Peptide-MHC Class I Complex Stability, a Correlate of T Cell Immunogenicity. *J Immunol.* 2016 Aug 15;197(4):1517-24.
19. O'Donnell TJ, Rubinsteyn A, Laserson U. MHCflurry 2.0: Improved Pan-Allele Prediction of MHC Class I-Presented Peptides by Incorporating Antigen Processing. *Cell Syst.* 2020 Oct 21;11(4):418-9.
20. Phloyphisut P, Pornputtpong N, Sriswasdi S, Chuangsuwanich E. MHCSeqNet: a deep neural network model for universal MHC binding prediction. *BMC Bioinformatics.* 2019 May 28;20(1):270.
21. Bassani-Sternberg M, Chong C, Guillaume P, Solleder M, Pak H, Gannon PO, et al. Deciphering HLA-I motifs across HLA peptidomes improves neo-antigen predictions and identifies allosteric regulating HLA specificity. *PLoS Comput Biol.* 2017 Aug;13(8):e1005725.
22. Peters B, Bulik S, Tampe R, Van Endert PM, Holzhütter HG. Identifying MHC class I epitopes by predicting the TAP transport efficiency of epitope precursors. *J Immunol.* 2003 Aug 15;171(4):1741-9.
23. Nielsen M, Lundegaard C, Lund O, Keimig C. The role of the proteasome in generating cytotoxic T-cell epitopes: insights obtained from improved predictions of proteasomal cleavage. *Immunogenetics.* 2005 Apr;57(1-2):33-41.
24. Punta M, Jennings VA, Melcher AA, Lise S. The Immunogenic Potential of Recurrent Cancer Drug

4. Park JJ, Diefenbach RJ, Joshua AM, Kefford RF, Carlino MS, Rizos H. Oncogenic signaling in uveal melanoma. *Pigment Cell Melanoma Res.* 2018 Nov;31(6):661-72.
5. Piulats JM, Espinosa E, de la Cruz Merino L, Varela M, Alonso Carrión L, Martín-Algarra S, et al. Nivolumab Plus Ipilimumab for Treatment-Naïve Metastatic Uveal Melanoma: An Open-Label, Multicenter, Phase II Trial by the Spanish Multidisciplinary Melanoma Group (GEM-1402). *J Clin Oncol.* 2021 Feb 20;39(6):586-98.
6. Algazi AP, Tsai KK, Shoushtari AN, Munhoz RR, Eroglu Z, Piulats JM, et al. Clinical outcomes in metastatic uveal melanoma treated with PD-1 and PD-L1 antibodies. *Cancer.* 2016 Nov 15;122(21):3344-53.
7. Niederkorn JY. Immune escape mechanisms of intraocular tumors. *Prog Retin Eye Res.* 2009 Sep;28(5):329-47.
8. Cross NA, Murray AK, Rennie IG, Ganesh A, Sisley K. Instability of microsatellites is an infrequent event in uveal melanoma. *Melanoma Res.* 2003 Oct;13(5):435-40.
9. García-Mulero S, Alonso MH, Del Carpio LP, Sanz-Pamplona R, Piulats JM. Additive Role of Immune System Infiltration and Angiogenesis in Uveal Melanoma Progression. *Int J Mol Sci.* 2021 Mar 6;22(5):2669.
10. de la Cruz PO, Specht CS, McLean IW. Lymphocytic infiltration in uveal malignant melanoma. *Cancer.* 1990 Jan 1;65(1):112-5.
11. Wheelchel JC, Farah SE, McLean IW, Burnier MN. Immunohistochemistry of infiltrating lymphocytes in uveal malignant melanoma. *Invest Ophthalmol Vis Sci.* 1993 Jul;34(8):2603-6.
12. Pearlman AH, Hwang MS, Konig MF, Hsiue EHC, Douglass J, DiNapoli SR, et al. Targeting public neoantigens for cancer immunotherapy. *Nat Cancer.* 2021 May;2(5):487-97.
13. Cerami E, Gao J, Dogrusoz U, Gross BE, Sumer SO, Aksoy BA, et al. The cBio cancer genomics portal: an open platform for exploring multidimensional cancer genomics data. *Cancer Discov.* 2012 May;2(5):401-4.
14. Nielsen M, Lundegaard C, Worning P, Lauemøller SL, Lamberth K, Buus S, et al. Reliable prediction of T-cell epitopes using neural networks with novel sequence representations. *Protein Sci.* 2003 May;12(5):1007-17.
15. Andreatta M, Nielsen M. Gapped sequence alignment using artificial neural networks: application to the MHC class I system. *Bioinformatics.* 2016 Feb 15;32(4):511-7.
16. Reynisson B, Alvarez B, Paul S, Peters B, Nielsen M. NetMHCpan-4.1 and NetMHCIIpan-4.0: improved predictions of MHC antigen presentation by concurrent motif deconvolution and integration of MS MHC eluted ligand data. *Nucleic Acids Res.* 2020 Jul 2;48(W1):W449-54.
17. Karosiene E, Lundegaard C, Lund O, Nielsen M. NetMHCcons: a consensus method for the major histocompatibility complex class I predictions. *Immunogenetics.* 2012 Mar;64(3):177-86.
18. Rasmussen M, Fenoy E, Harndahl M, Kristensen AB, Nielsen IK, Nielsen M, et al. Pan-Specific Prediction of Peptide-MHC Class I Complex Stability, a Correlate of T Cell Immunogenicity. *J Immunol.* 2016 Aug 15;197(4):1517-24.
19. O'Donnell TJ, Rubinsteyn A, Laserson U. MHCflurry 2.0: Improved Pan-Allele Prediction of MHC Class I-Presented Peptides by Incorporating Antigen Processing. *Cell Syst.* 2020 Oct 21;11(4):418-9.
20. Phloyphisut P, Pornputtpong N, Sriswasdi S, Chuangsuwanich E. MHCSeqNet: a deep neural network model for universal MHC binding prediction. *BMC Bioinformatics.* 2019 May 28;20(1):270.
21. Bassani-Sternberg M, Chong C, Guillaume P, Solleder M, Pak H, Gannon PO, et al. Deciphering HLA-I motifs across HLA peptidomes improves neo-antigen predictions and identifies allosteric regulating HLA specificity. *PLoS Comput Biol.* 2017 Aug;13(8):e1005725.
22. Peters B, Bulik S, Tampe R, Van Endert PM, Holzhütter HG. Identifying MHC class I epitopes by predicting the TAP transport efficiency of epitope precursors. *J Immunol.* 2003 Aug 15;171(4):1741-9.
23. Nielsen M, Lundegaard C, Lund O, Keimig C. The role of the proteasome in generating cytotoxic T-cell epitopes: insights obtained from improved predictions of proteasomal cleavage. *Immunogenetics.* 2005 Apr;57(1-2):33-41.
24. Punta M, Jennings VA, Melcher AA, Lise S. The Immunogenic Potential of Recurrent Cancer Drug

- Resistance Mutations: An In Silico Study. *Front Immunol.* 2020;11:524968.
25. Szolek A, Schubert B, Mohr C, Sturm M, Feldhahn M, Kohlbacher O. OptiType: precision HLA typing from next-generation sequencing data. *Bioinformatics.* 2014 Dec 1;30(23):3310-6.
 26. Charoentong P, Finotello F, Angelova M, Mayer C, Efremova M, Rieder D, et al. Pan-cancer Immunogenomic Analyses Reveal Genotype-Immunophenotype Relationships and Predictors of Response to Checkpoint Blockade. *Cell Rep.* 2017 03;18(1):248-62.
 27. Hänzelmann S, Castelo R, Guinney J. GSVA: gene set variation analysis for microarray and RNA-seq data. *BMC Bioinformatics.* 2013 Jan 16;14:7.
 28. Ayers M, Lunceford J, Nebozhyn M, Murphy E, Loboda A, Kaufman DR, et al. IFN- γ -related mRNA profile predicts clinical response to PD-1 blockade. *J Clin Invest.* 2017 Aug 1;127(8):2930-40.
 29. Ma J, Weng L, Bastian BC, Chen X. Functional characterization of uveal melanoma oncogenes. *Oncogene.* 2021 Jan;40(4):806-20.
 30. Maziarz M, Leyme A, Marivin A, Luebbbers A, Patel PP, Chen Z, et al. Atypical activation of the G protein G α q by the oncogenic mutation Q209P. *J Biol Chem.* 2018 Dec 21;293(51):19586-99.
 31. Marty R, Kaabinejadian S, Rossell D, Slifker MJ, van de Haar J, Engin HB, et al. MHC-I Genotype Restricts the Oncogenic Mutational Landscape. *Cell.* 2017 Nov 30;171(6):1272-1283.e15.
 32. Javed A, Milhem M. Role of Natural Killer Cells in Uveal Melanoma. *Cancers (Basel).* 2020 Dec 9;12(12):E3694.
 33. Maat W, van der Slik AR, Verhoeven DHJ, Alizadeh BZ, Ly LV, Verduijn W, et al. Evidence for natural killer cell-mediated protection from metastasis formation in uveal melanoma patients. *Invest Ophthalmol Vis Sci.* 2009 Jun;50(6):2888-95.
 34. Ma D, Luyten GP, Luijckx TM, Niederkorn JY. Relationship between natural killer cell susceptibility and metastasis of human uveal melanoma cells in a murine model. *Invest Ophthalmol Vis Sci.* 1995 Feb;36(2):435-41.
 35. van Weeghel C, Wierenga APA, Versluis M, van Hall T, van der Velden PA, Kroes WGM, et al. Do GNAQ and GNA11 Differentially Affect Inflammation and HLA Expression in Uveal Melanoma? *Cancers (Basel).* 2019 Aug 7;11(8):E1127.
 36. Griewank KG, van de Nes J, Schilling B, Moll I, Sucker A, Kakavand H, et al. Genetic and clinico-pathologic analysis of metastatic uveal melanoma. *Mod Pathol.* 2014 Feb;27(2):175-83.
 37. Bauer J, Kilic E, Vaarwater J, Bastian BC, Garbe C, de Klein A. Oncogenic GNAQ mutations are not correlated with disease-free survival in uveal melanoma. *Br J Cancer.* 2009 Sep 1;101(5):813-5.
 38. Terai M, Shimada A, Chervoneva I, Hulse L, Danielson M, Swensen J, et al. Prognostic Values of G-Protein Mutations in Metastatic Uveal Melanoma. *Cancers (Basel).* 2021 Nov 17;13(22):5749.
 39. Peri A, Greenstein E, Alon M, Pai JA, Dingjan T, Reich-Zeliger S, et al. Combined presentation and immunogenicity analysis reveals a recurrent RAS.Q61K neoantigen in melanoma. *J Clin Invest.* 2021 Oct 15;131(20):e129466.

Supplementary materials

Supplementary Figure 1. GNAQ and GNA11 protein alignment. Green square marks selected peptides for subsequent binding prediction analysis. Q Amino acid changing to L or P in mutated proteins are marked in red.

```

Query: sp|P50148|GNAQ_HUMAN Guanine nucleotide-binding protein G(q) subunit alpha 05-Homo sapiens OX=9606 GN=GNAQ PE=1 SV=4 Query ID: |c|query_55461 Length: 359

>sp|P29992|GNA11_HUMAN Guanine nucleotide-binding protein subunit alpha-11 05-Homo sapiens OX=9606 GN=GNA11 PE=1 SV=2
Sequence ID: Query_55463 Length: 359
Range 1: 1 to 359

Score:685 bits(1768), Expect:0.0,
Method:Compositional matrix adjust.,
Identities:324/359(90%), Positives:345/359(96%), Gaps:0/359(0%)

Query 1 MTLESIMACCLSEEAKEARRINDEIERQLRRKRDARRELKLLLLGTGESGKSTFIKQMR 60
Sbjct 1 MTLESMACCLS+FE++RRIN FIF+QLRRKRDARRELKLLLLGTGESGKSTFIKQMR 60

Query 61 IIHGSGYSDEDKRGFTKLVYQNIFFTAQAMIRAMDLLKIPYKYENKAHAQLVREVDVEK 120
IIHGIGYS+EDKRGFTKLVYQNIFFTAQAMIRAM+LLKI YKYE NKAIA LIREVDVEK 120
Sbjct 61 IIHGAGYSEEDKRGFTKLVYQNIFFTAQAMIRAMETLKILYKYEQNKANALLIREVDVEK 120

Query 121 VSAFENPYVDAIKSLMNDPGIQECYDRRREYQLSDSTKYYLNDLDRVADPAYLPTQQDVL 180
V+ FE+ YV AIK+LW DPGIQECYDRRREYQLSDS KYYL D+R+A YLPTQQDVL 180
Sbjct 121 VTFEHQYVSAIKTLNEDPGIQECYDRRREYQLSDSAKYYLTDVDRIATLGLYLTQQDVL 180

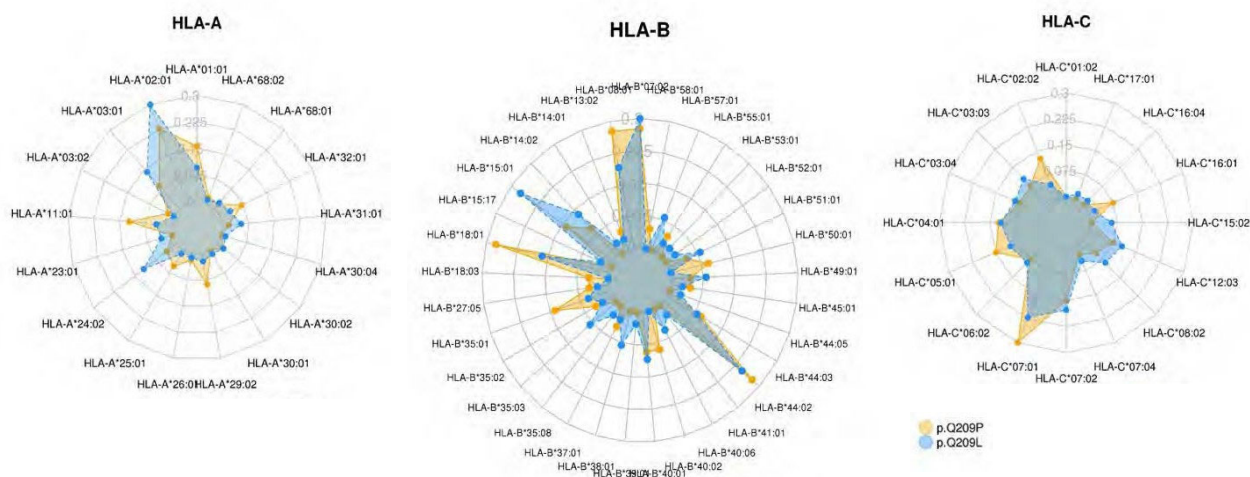
Query 181 RVRVPTTGIIIEYPFDLQSEFFRMVDVGGQSSERRKWIHCFENVTSINFLVALSEYDQVLV 240
RVRVPTTGIIIEYPFDL++FRMVDVGGQSSERRKWIHCFENVTSINFLVALSEYDQVLV 240
Sbjct 181 RVRVPTTGIIIEYPFDLENLFRMVDVGGQSSERRKWIHCFENVTSINFLVALSEYDQVLV 240

Query 241 ESDNENRMEESKALFRTIITYPWFQNSSVILFLNKDLLLEEKIMYSHLVDVYFPEYDGPQR 300
ESDNENRMEESKALFRTIITYPWFQNSSVILFLNKDLLLEKI+YSHLVDVYFPEYDGPQR 300
Sbjct 241 ESDNENRMEESKALFRTIITYPWFQNSSVILFLNKDLLLEOKILYSHLVDVYFPEYDGPQR 300

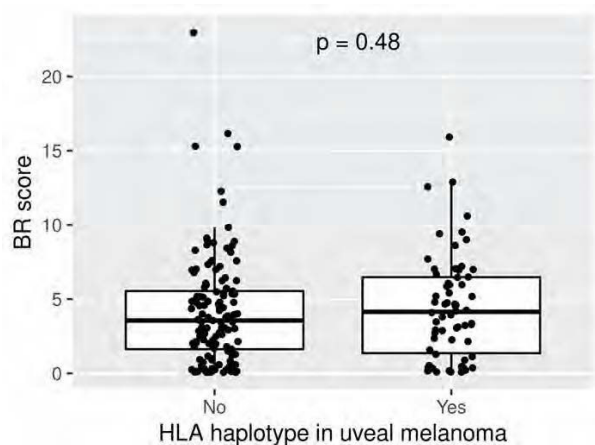
Query 301 DAQAAREFILKMFVDLNPDSDKIIYSHFTCATDTENIRFVAAVKDTILQLNLKEYNLV 359
DAQAAREFILKMFVDLNPDSDKIIYSHFTCATDTENIRFVAAVKDTILQLNLKEYNLV 359
Sbjct 301 DAQAAREFILKMFVDLNPDSDKIIYSHFTCATDTENIRFVAAVKDTILQLNLKEYNLV 359
  
```

<https://blast.ncbi.nlm.nih.gov/Blast.cgi>

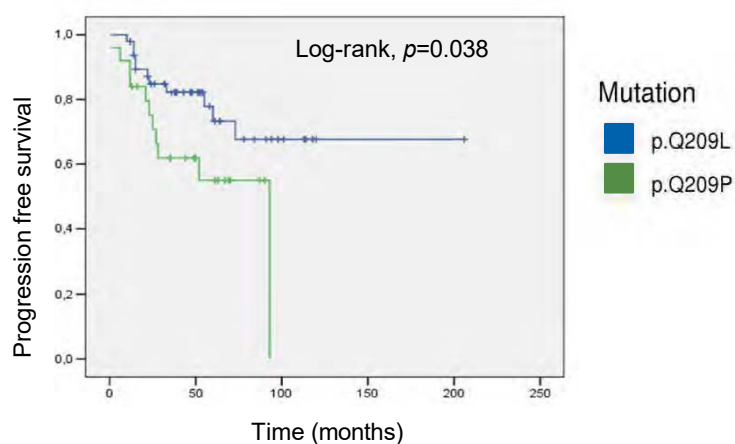
Supplementary Figure 2. Radar plots comparing frequencies in HLA haplotype for HLA-A gene, HLA-B gene and HLA-C genes between patients harbouring Q209L and Q209P. Asterisks correspond to haplotypes with statistical differences by Binomial test (FDR p-adjusted < 0.05).



Supplementary Figure 3. Comparison of BR scores between present and absent haplotypes in uveal melanoma patients. Not statistically significant differences were observed.

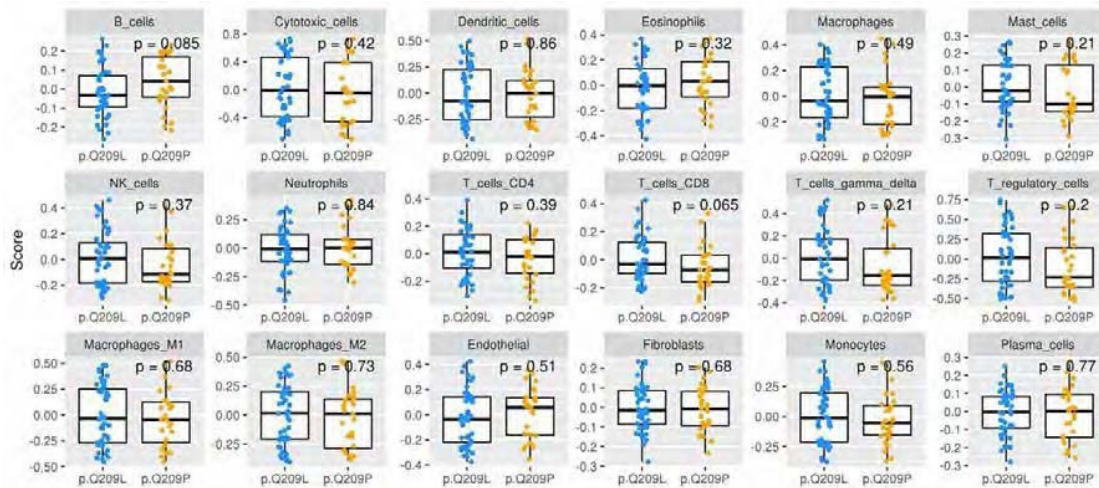


Supplementary Figure 4. Survival analysis. Kaplan-Meier curve showing Q209L carriers having better disease-free survival (DFS) than Q209P carriers.

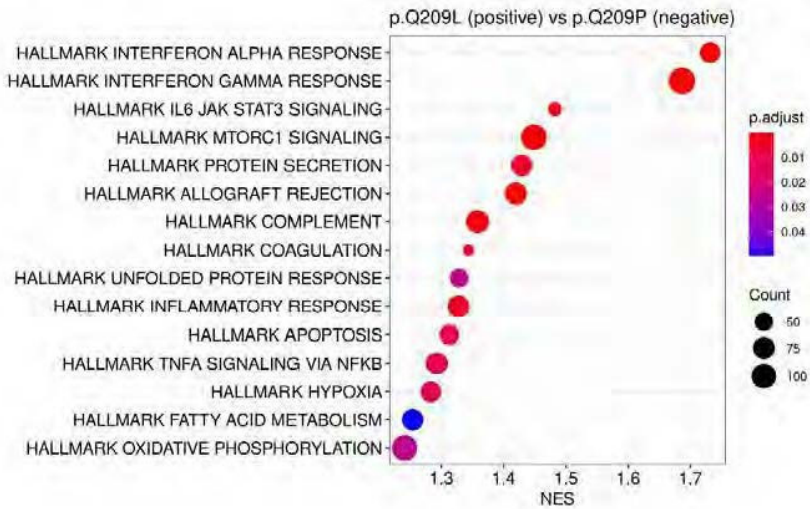


Mutation	N	N events	N censored	Median PFS	95% IC
Q209L	48	11	37(77.1%)	151.95	(123.85-180.06)
Q209P	25	11	14(56.0%)	61.47	(45.75-77.18)

Supplementary Figure 5. Cell infiltration using ConsensusTME tool.



Supplementary Figure 6. Functional enrichment analysis. Plot showing statistically significant functions over-expressed in in samples carrying Q209L variant. Gene Set Enrichment Analysis (GSEA) sere used.



Supplementary Table 1. Baseline characteristics of 80 TCGA-UM samples.

	<i>[ALL]</i> N=80	<i>N</i>
Age	62.2 (14.0)	80
Sex:		80
Female	35 (43.8%)	
Male	45 (56.2%)	
Overall Survival Months	26.7 (18.1)	80
Overall Survival Status:		80
Deceased	23 (28.7%)	
Living	57 (71.2%)	
Progress Free Survival Months	23.2 (17.5)	79
Progression Free Status:		80
Censored	50 (62.5%)	
Progression	30 (37.5%)	
Disease specific Survival status:		80
Alive or Dead Tumor Free	59 (73.8%)	
Dead with Tumor	21 (26.2%)	
Recurrence:		80
Non-recurrent	54 (67.5%)	
Recurrent	26 (32.5%)	
Fraction Genome Altered	0.16 (0.12)	80
Mutation Count	16.9 (42.3)	80
SCNA cluster:		80
1	15 (18.8%)	
2	23 (28.7%)	
3	22 (27.5%)	
4	20 (25.0%)	
BAP1 mutation	13 (16.2%)	80
Chromosome 3 status:		80
Disomy	21 (26.2%)	
Monosomy	31 (38.8%)	
'Missing'	28 (35.0%)	
Chromosome 8 status:		80
Disomy	19 (23.8%)	
Polysomy	33 (41.2%)	
'Missing'	28 (35.0%)	
Immune cluster:		80
High	24 (30.0%)	
Low	56 (70.0%)	
Mutation:		80
GNA11 p.Q209L	34 (42.5%)	
GNAQ p.Q209L	9 (11.2%)	
GNAQ p.Q209P	27 (33.8%)	
GNAQ,GNA11 p.Q209L,p.R166H	1 (1.25%)	
WT	9 (11.2%)	
prot:		80
p.G48V	1 (1.25%)	
p.Q209L	44 (55.0%)	
p.Q209P	27 (33.8%)	
p.R183Q	1 (1.25%)	
p.R183Q,p.R183C	1 (1.25%)	
WT	6 (7.50%)	

Supplementary Table 2. Baseline characteristics of 71 mutated samples from TCGA-UM by amino-acid change. P-values for categorical variables were calculated by Chi-Squared Tests. P-values for continuous variables were calculated by Wilcoxon tests.

	P.Q209L N=44	P.Q209P N=27	P-VALUE
Age	62.7 (14.7)	62.1 (13.2)	0.850
Sex:			0.399
Female	17 (38.6%)	14 (51.9%)	
Male	27 (61.4%)	13 (48.1%)	
Overall Survival Months	25.0 (16.7)	27.9 (21.3)	0.549
Overall Survival Status:			0.341
Deceased	14 (31.8%)	5 (18.5%)	
Living	30 (68.2%)	22 (81.5%)	
Progress Free Survival Months	21.1 (16.5)	25.0 (19.9)	0.405
Progression Free Status:			0.304
Censored	26 (59.1%)	20 (74.1%)	
Progression	18 (40.9%)	7 (25.9%)	
Disease specific Survival status:			0.260
Alive or Dead Tumor Free	31 (70.5%)	23 (85.2%)	
Dead with Tumor	13 (29.5%)	4 (14.8%)	
Recurrence:			0.062
Non-recurrent	27 (61.4%)	23 (85.2%)	
Recurrent	17 (38.6%)	4 (14.8%)	
Fraction Genome Altered	0.15 (0.10)	0.14 (0.11)	0.630
Mutation Count	11.1 (4.17)	13.3 (3.77)	0.028
SCNA cluster:			0.160
1	7 (15.9%)	8 (29.6%)	
2	11 (25.0%)	10 (37.0%)	
3	13 (29.5%)	3 (11.1%)	
4	13 (29.5%)	6 (22.2%)	
BAP1 mutation	7 (15.9%)	5 (18.5%)	0.757
Chromosome 3 status:			0.384
Disomy	11 (37.9%)	9 (56.2%)	
Monosomy	18 (62.1%)	7 (43.8%)	
Chromosome 8 status:			0.598
Disomy	9 (31.0%)	7 (43.8%)	
Polysomy	20 (69.0%)	9 (56.2%)	
Immune cluster:			1.000
High	13 (29.5%)	8 (29.6%)	
Low	31 (70.5%)	19 (70.4%)	

Supplementary Table 3. Peptides predicted to bind to HLA by MHCSeqNet, NetMHC, NetMHCpan, MHCflurry, MixMHCpred, NetMHCcons and NetMHCpanstab tools. Attached in excel format.

Supplementary Table 4. Results from binomial tests comparing HLA frequencies between general population and uveal melanoma population, ordered by BR score. HLA haplotypes with statistical differences and higher frequency in UM are coloured in yellow. Only HLA haplotypes present in UM patients were compared. BR; Q209L BR score, BR_peptide; 9 mer amino acid of best rank for the allele. Freq_uveal; frequency of haplotype in uveal melanoma samples, Freq_pop; frequency of haplotype in the 1000Genomes population, pval_adj; p-value adjusted by FDR, N; number of UM patients with the HLA allele, diff; frequency difference.

HLA allele	BR	BR_peptide	Freq_uveal	Freq_pop	pval	pval_adj	N	diff
HLA-A*31:01	0.08	RMVDVGGLR	0.04	0.04	0.52	0.71	7.00	-0.01
HLA-B*39:01	0.09	FRMVDVGGL	0.01	0.01	0.73	0.87	1.00	0.01
HLA-C*07:01	0.09	FRMVDVGGL	0.18	0.07	1.00	0.00	28.00	-0.11
HLA-C*06:02	0.09	FRMVDVGGL	0.05	0.08	0.65	0.81	10.00	0.02
HLA-B*14:01	0.17	FRMVDVGGL	0.01	0.01	0.59	0.77	1.00	0.00
HLA-B*14:02	0.17	FRMVDVGGL	0.04	0.02	0.03	0.13	7.00	-0.03
HLA-C*07:02	0.19	FRMVDVGGL	0.18	0.13	1.00	1.00	21.00	-0.04
HLA-B*27:05	0.21	FRMVDVGGL	0.02	0.02	0.74	0.87	3.00	0.00
HLA-B*38:01	0.33	FRMVDVGGL	0.03	0.01	0.03	0.15	4.00	-0.02
HLA-C*07:04	0.37	FRMVDVGGL	0.04	0.01	0.30	0.55	4.00	-0.02
HLA-A*03:02	0.39	RMVDVGGLR	0.01	0.00	0.32	0.55	1.00	0.00
HLA-A*03:01	0.40	RMVDVGGLR	0.13	0.09	0.10	0.28	21.00	-0.04
HLA-B*57:01	0.45	GLRSERRKW	0.02	0.02	1.00	1.00	3.00	0.00
HLA-A*68:01	0.52	DVGGLRSER	0.03	0.03	1.00	1.00	4.00	0.00
HLA-A*01:01	0.89	MVDVGGLRS	0.13	0.06	0.00	0.02	20.00	-0.06
HLA-A*32:01	1.12	GLRSERRKW	0.05	0.02	0.01	0.08	8.00	-0.03
HLA-A*11:01	1.28	RMVDVGGLR	0.09	0.09	1.00	1.00	14.00	0.00
HLA-B*58:01	1.57	GLRSERRKW	0.01	0.03	0.10	0.28	1.00	0.02
HLA-A*30:01	2.14	RMVDVGGLR	0.01	0.03	0.19	0.42	2.00	0.02
HLA-B*15:01	2.26	GLRSERRKW	0.09	0.04	0.01	0.04	14.00	-0.05
HLA-A*30:02	2.36	RMVDVGGLR	0.02	0.02	1.00	1.00	3.00	0.00
HLA-C*05:01	2.72	MVDVGGLRS	0.06	0.05	0.00	0.02	17.00	-0.02
HLA-A*30:04	2.87	RMVDVGGLR	0.01	0.00	0.17	0.41	1.00	-0.01
HLA-A*29:02	2.92	RMVDVGGLR	0.04	0.03	0.21	0.43	7.00	-0.02
HLA-C*02:02	3.05	FRMVDVGGL	0.05	0.02	0.01	0.08	9.00	-0.03
HLA-B*15:17	3.12	GLRSERRKW	0.01	0.00	0.43	0.65	1.00	0.00
HLA-C*08:02	3.22	MVDVGGLRS	0.03	0.03	0.07	0.26	8.00	0.00
HLA-C*12:03	3.29	FRMVDVGGL	0.08	0.03	0.00	0.03	12.00	-0.05
HLA-B*44:02	3.35	GLRSERRKW	0.12	0.04	0.20	0.00	19.00	-0.08
HLA-C*04:01	3.47	FRMVDVGGL	0.03	0.13	0.10	0.28	14.00	0.11
HLA-B*18:03	3.80	FRMVDVGGL	0.01	0.00	0.06	0.22	1.00	-0.01
HLA-A*02:01	3.94	RMVDVGGL	0.29	0.19	0.00	0.02	46.00	-0.10
HLA-B*40:01	4.09	FRMVDVGGL	0.04	0.06	0.51	0.71	7.00	0.02
HLA-C*17:01	4.20	RMVDVGGL	0.01	0.02	0.19	0.42	1.00	0.01
HLA-B*08:01	4.25	LRSEERRKI	0.09	0.04	0.00	0.03	14.00	-0.05
HLA-B*44:03	4.53	GLRSERRKW	0.04	0.04	1.00	1.00	6.00	0.00

HLA-C*16:01	4.60	RMVDVGGL	0.03	0.04	0.33	0.56	4.00	0.02
HLA-C*03:03	4.66	FRMVDVGGL	0.11	0.05	0.46	0.66	10.00	-0.06
HLA-C*03:04	4.66	FRMVDVGGL	0.11	0.08	0.66	0.81	11.00	-0.03
HLA-A*26:01	4.75	DVGGLRSER	0.01	0.02	0.45	0.66	2.00	0.01
HLA-C*16:04	4.79	FRMVDVGGL	0.01	0.00	0.17	0.41	1.00	-0.01
HLA-C*01:02	5.18	RMVDVGGL	0.01	0.08	0.70	0.00	1.00	0.06
HLA-C*15:02	5.19	RMVDVGGL	0.03	0.02	0.43	0.65	5.00	0.00
HLA-B*44:05	5.41	GLRSERRKW	0.01	0.00	0.17	0.41	1.00	-0.01
HLA-B*40:02	5.86	FRMVDVGGL	0.02	0.02	1.00	1.00	3.00	0.00
HLA-A*25:01	5.96	DVGGLRSER	0.03	0.01	0.04	0.16	4.00	-0.02
HLA-B*37:01	5.97	FRMVDVGGL	0.01	0.01	0.24	0.49	2.00	-0.01
HLA-B*35:03	6.06	MVDVGGLRS	0.03	0.01	0.08	0.28	4.00	-0.02
HLA-B*49:01	6.46	FRMVDVGGL	0.03	0.01	0.09	0.28	4.00	-0.01
HLA-B*35:08	6.49	MVDVGGLRS	0.01	0.00	0.43	0.65	1.00	0.00
HLA-B*13:02	6.68	RMVDVGGL	0.02	0.03	0.80	0.91	3.00	0.01
HLA-A*23:01	6.95	IFRMVDVGGL	0.02	0.03	0.64	0.81	3.00	0.01
HLA-B*35:02	6.99	MVDVGGLRS	0.01	0.01	0.20	0.42	2.00	-0.01
HLA-A*24:02	7.02	IFRMVDVGGL	0.09	0.12	0.27	0.53	14.00	0.03
HLA-B*53:01	7.04	GLRSERRKW	0.01	0.04	0.05	0.19	1.00	0.03
HLA-B*52:01	7.04	RMVDVGGL	0.01	0.02	0.60	0.77	2.00	0.01
HLA-B*35:01	7.21	MVDVGGLRS	0.03	0.06	0.14	0.36	5.00	0.03
HLA-B*40:06	7.70	FRMVDVGGL	0.01	0.01	0.41	0.65	2.00	0.00
HLA-B*55:01	8.61	FRMVDVGGL	0.01	0.01	0.38	0.63	2.00	0.00
HLA-B*18:01	9.00	FRMVDVGGL	0.08	0.03	0.00	0.02	12.00	-0.05
HLA-B*50:01	9.40	FRMVDVGGL	0.01	0.01	0.31	0.55	2.00	-0.01
HLA-B*07:02	9.52	GLRSERRKW	0.13	0.07	0.02	0.11	20.00	-0.05
HLA-A*68:02	10.59	MVDVGGLRS	0.01	0.02	0.78	0.90	2.00	0.01
HLA-B*41:01	12.56	FRMVDVGGL	0.01	0.01	0.56	0.76	1.00	0.00
HLA-B*45:01	12.89	VDVGGLRSE	0.01	0.01	1.00	1.00	2.00	0.00
HLA-B*51:01	15.92	FRMVDVGGL	0.03	0.05	0.29	0.55	5.00	0.02

Supplementary Table 5. Differentially expressed genes between GNAQ and GNA11 samples. Attached in excel.

Supplementary Table 6. Functional analysis results.

Description	setSize	Enrichment Score	NES	pvalue	p.adjust	qvalue	rank
HALLMARK_INTERFERON_ALPHA_RESPONSE	198	0.6380	1.6863	0.0000	0.0000	0.0000	4437
HALLMARK_MTORC1_SIG	96	0.6771	1.7315	0.0000	0.0000	0.0000	4437
HALLMARK_ALLOGRAFT_REJECTION	197	0.5482	1.4486	0.0000	0.0001	0.0000	4769
HALLMARK_COMPLEMENT	196	0.5373	1.4196	0.0000	0.0001	0.0001	4159
HALLMARK_IL6_JAK_STAT3_SIGNALING	200	0.5136	1.3583	0.0002	0.0015	0.0009	4711
HALLMARK_INFLAMMATION	87	0.5850	1.4823	0.0002	0.0015	0.0009	3108
HALLMARK_PROTEIN_SECRETION	200	0.5020	1.3278	0.0005	0.0036	0.0023	5102
HALLMARK_COAGULATION	96	0.5589	1.4292	0.0009	0.0053	0.0034	6435
HALLMARK_TNFA_SIGNALING_VIA_NFKB	138	0.5170	1.3438	0.0012	0.0069	0.0044	1783
HALLMARK_APOPTOSIS	199	0.4889	1.2927	0.0021	0.0103	0.0065	4152
HALLMARK_HYPOXIA	159	0.5016	1.3130	0.0023	0.0105	0.0066	3642
HALLMARK_UNFOLDED_PROTEIN_RESPONSE	197	0.4856	1.2832	0.0029	0.0120	0.0076	3143
HALLMARK_OXIDATIVE_PHOSPHORYLATION	110	0.5168	1.3288	0.0069	0.0266	0.0168	5050
HALLMARK_FATTY_ACID_METABOLISM	200	0.4693	1.2412	0.0079	0.0281	0.0177	6606
HALLMARK_FATTY_ACID	156	0.4796	1.2541	0.0149	0.0496	0.0313	6130

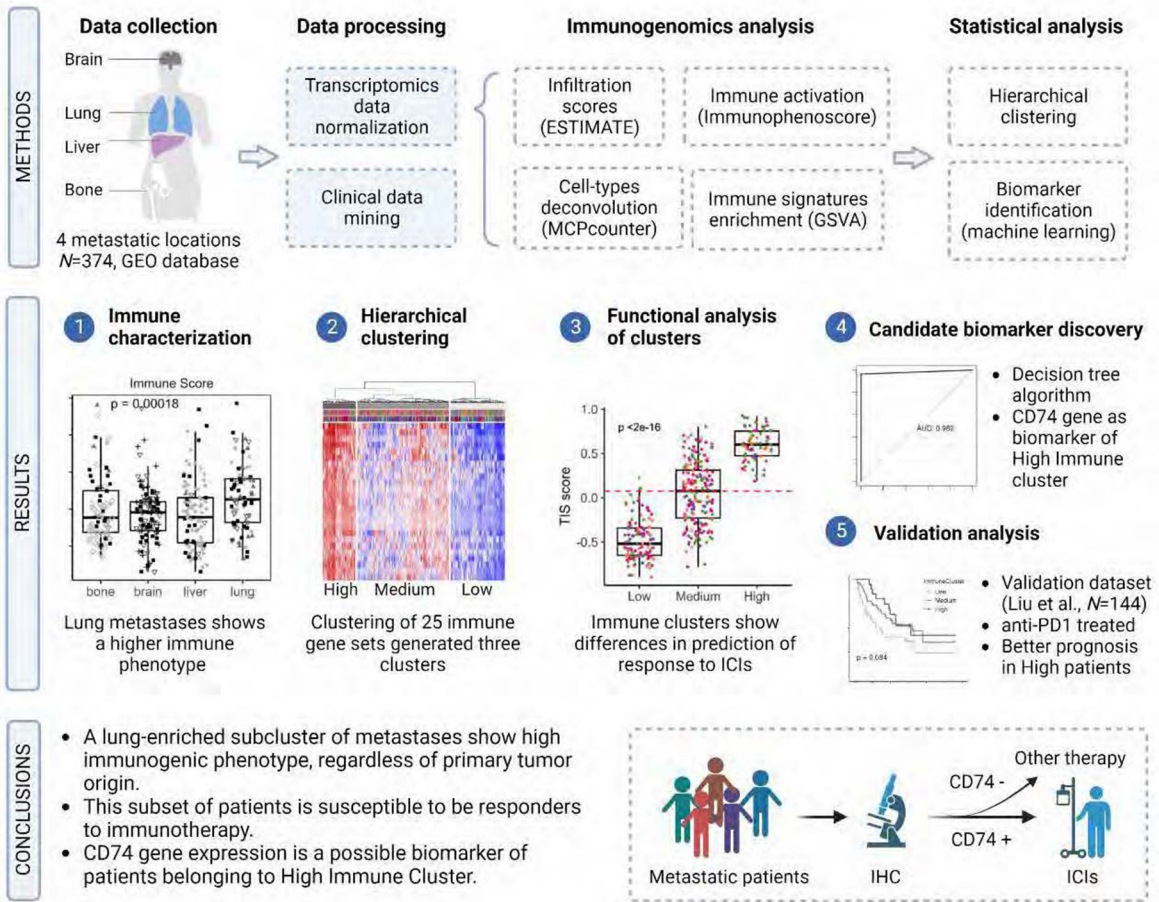
Study 2 | Role of the immune microenvironment in metastatic homing

Article: [Sandra García-Mulero](#), María Henar Alonso, Julián Pardo, Cristina Santos, Xavier Sanjuan, Ramón Salazar, Víctor Moreno, Josep María Piulats, Rebeca Sanz-Pamplona. *Lung Metastases Share Common Immune Features Regardless of Primary Tumor Origin*. *Journal for Immunotherapy of Cancer*. W, EXXXrkj (VXVX) <https://doi.org/jX.jipn/jitc-VXjk-XXXrkj>



Objective and main results:

The objectives of this publication were to characterize the immune microenvironment across different metastatic locations (bone, brain, liver and lung) from six different primary sites, and to generate a novel clustering of metastases based on their immune phenotypes. We used transcriptomics data to infer the immune state of pmr metastatic samples by quantification algorithms and statistical methods to generate a novel clustering of the samples based on their immune profiles. The different measures of immune activation showed strong differences between lung, and the other three sites of metastasis. The immune infiltration score was higher for lung, followed by bone, and lower values for liver and brain. Specifically, we found higher infiltration of adaptive immune components (T cells and B cells) and dendritic cells in lung metastases compared to bone, brain and liver metastasis. We identified three subgroups of metastases (High -HIC-, Medium -MIC- and Low -LIC- Immune Clusters) with differences at the inflammatory and infiltration levels. The High immune cluster (HIC) was enriched in lung metastasis and was characterized by high expression of PD-Lj, CTLA-r, HLA class II and high Immunoscore signature. We found a signature for HIC metastases, and a decision tree algorithm selected CDmr as the best predictor of HIC metastases.

Graphical abstract:



Lung metastases share common immune features regardless of primary tumor origin

Sandra García-Mulero,^{1,2} M Henar Alonso,^{1,2} Julián Pardo ,³ Cristina Santos,⁴ Xavier Sanjuan,⁵ Ramón Salazar,⁴ Victor Moreno,^{1,2} Josep María Piulats,⁴ Rebeca Sanz-Pamplona ¹

To cite: García-Mulero S, Alonso MH, Pardo J, et al. Lung metastases share common immune features regardless of primary tumor origin. *Journal for ImmunoTherapy of Cancer* 2020;**8**:e000491. doi:10.1136/jitc-2019-000491

► Additional material is published online only. To view please visit the journal online (<http://dx.doi.org/10.1136/jitc-2019-000491>).

JMP and RS-P are joint senior authors.

Accepted 12 May 2020

ABSTRACT

Background Only certain disseminated cells are able to grow in secondary organs to create a metastatic tumor. Under the hypothesis that the immune microenvironment of the host tissue may play an important role in this process, we have categorized metastatic samples based on their immune features.

Methods Gene expression data of metastatic samples (n=374) from four secondary sites (brain, bone, liver and lung) were used to characterize samples based on their immune and stromal infiltration using gene signatures and cell quantification tools. A clustering analysis was done that separated metastatic samples into three different immune categories: high, medium and low.

Results Significant differences were found between the immune profiles of samples metastasizing in distinct organs. Metastases in lung showed a higher immunogenic score than metastases in brain, liver or bone, regardless of their primary site of origin. Also, they preferentially clustered in the high immune group. Samples in this cluster exhibited a clear inflammatory phenotype, higher levels of immune infiltrate, overexpression of programmed death-ligand 1 (PD-L1) and cytotoxic T-lymphocyte-associated protein 4 (CTLA4) pathways and upregulation of genes predicting clinical response to programmed cell death protein 1 (PD-1) blockade (T-cell inflammatory signature). A decision tree algorithm was used to select CD74 as a biomarker that identify samples belonging to this high-immune subtype of metastases, having specificity of 0.96 and sensitivity of 1.

Conclusions We have found a group of lung-enriched metastases showing an inflammatory phenotype susceptible to be treated with immunotherapy.

BACKGROUND

Despite extraordinary advances in cancer research in the last decades, metastasis is the major cause of mortality in many cancer types and their complete understanding remains elusive.^{1–2} The metastatic process is very inefficient since only few of the many cells that migrate from the primary tumors successfully colonize distant sites. This is likely explained by the fact that circulating cancer cells in the bloodstream are exposed to the innate

immune system and probably the majority of them are destroyed.^{3,4}

Furthermore, once in the secondary organ, cancer cells are challenged by a hostile microenvironment with a particular immune composition so they might be vulnerable to immune surveillance.⁵ As example, the liver's lymphocyte population is selectively enriched in natural killer (NK) and T cells, which play critical roles in first-line immune defense against invading pathogens, modulation of liver injury and recruitment of circulating lymphocytes.⁶ In the brain, the blood–brain barrier and the brain-resident cell types (ie, microglia) make this organ an immune-suppressive environment.⁷ Indeed, only certain tumor cells within the primary tumor bulk are compatible with the cellular and molecular environment of specific secondary organs. This is likely to be the reason why although cancer cells are able to escape from the primary tumor and travel randomly around the body, their invasive fingerprint differs among cancer types.⁸ For instance, breast cancer metastasizes preferentially in bone (more than 50%) whereas around 65% of kidney tumors metastasize in lung and almost 85% of prostate cancer metastasizes in bone.⁹ The “seed and soil” hypothesis postulates that the organ-preference patterns of tumor metastasis are the product of favorable interactions between metastatic tumor cells (the “seed”) and their organ microenvironment (the “soil”). In this regard, the focus of research is currently moving to study the role of immune system cells in the metastatic process. The generation of an immunosuppressive microenvironment and the engaging of prometastatic inflammatory processes has been described to play an important role in metastatic homing.¹⁰ Also, studies have proved that systemic signals from primary tumors can influence the microenvironment



© Author(s) (or their employer(s)) 2020. Re-use permitted under CC BY-NC. No commercial re-use. See rights and permissions. Published by BMJ.

For numbered affiliations see end of article.

Correspondence to

Dr Rebeca Sanz-Pamplona; rebecasanz@iconcologia.net

Dr Josep María Piulats; jmpiulats@iconcologia.net

of distant organs by creating pre-metastatic niches that recruit supportive stromal cells before the arrival of circulating tumor cells. This pre-metastatic niche promotes metastasis by generation of inflammation and immunosuppression in the target organ.¹¹

Thus, the success of the metastatic growth is determined by a complex crosstalk between metastatic cells and target organ microenvironments.¹² In this work, we revisit the classic hypothesis of seed and soil through a pan-cancer study from an immune system perspective. Since metastatic cells must evade target organ immune surveillance to grow,¹³ we hypothesize that the immune microenvironment of the host tissue may play an important role in the process of metastatic cells selection and homing. Therefore, metastatic tumors in the same location might share mechanisms of immune evasion and subsequently could respond to the same immune treatment. By using bioinformatics techniques such as cell quantification algorithms or gene expression profiles, a molecular characterization of the immune microenvironment of metastatic samples in four different locations has been done. Then, a clustering analysis identified a subgroup of metastases sharing inflammation and immune infiltration features that might be targeted by immunotherapy drugs.

METHODS

Patients and samples

Gene expression and clinical data from 374 metastatic samples including brain, bone, liver and lung and 348 normal samples from the same locations were collected. A total of 16 datasets for metastases (GSE100534, GSE101607, GSE10961, GSE44660, GSE11078, GSE12630, GSE14017, GSE14018, GSE43837, GSE46141, GSE14108.1, GSE14108.2, GSE40367, GSE41258, GSE50496.1, GSE85258) were downloaded from open repository Gene Expression Omnibus (GEO). The clinical information and description of datasets is summarized in online supplementary table 1. Metastatic samples were originated from six different primary locations (breast, colon, non-small-cell lung cancer (NSCLC), kidney, prostate and skin melanoma). Frequencies of location of metastases are in general in agreement with those previously reported,⁹ although a slight enrichment in brain metastatic samples existed due to over-representation in some of the datasets (online supplementary figure 1). In addition, a total of 348 samples from normal healthy tissue were collected from five GEO datasets (GSE7307, GSE45878, GSE803, GSE3526, GSE1133; online supplementary table 2).

Normalized gene expression data from the 16 datasets comprising six different microarray platforms were joined and transformed to log₂ scale. An adjustment for reduction of the batch effect was performed with ComBat function from R package sva. Online supplementary figure 2 shows a principal component analysis of the samples based on gene expression data, showing the efficacy of this method to generate a homogenized dataset.

Data were analyzed separately for metastatic and normal samples.

Immune microenvironment characterization

Gene expression data were used to characterize the immune microenvironment of samples, using a variety of bioinformatics tools. The immunophenoscore (IPS) function was used to measure the immune state of the samples. IPS uses a number of markers of immune response or immune toleration to quantify and visualize four different immunophenotypes in a tumor sample (antigen presentation, effector cells, suppressor cells and checkpoint markers). It also generates a z-score summarizing these four categories. The higher the z-score of IPS, the more immunogenic the sample.¹⁴ To estimate the presence of immune cell populations in the metastatic tissues, two different tools were used. First, R package ESTIMATE was used.¹⁵ ESTIMATE (Estimation of STromal and Immune cells in MAlignant Tumor tissues using Expression data) is a tool that predicts the tumor purity from gene signatures and calculates three scores: (1) stromal score—predicts the presence of stromal cell types in tumor bulk, (2) immune score—infers the infiltration of immune cells in tumor tissue and (3) estimate score—estimation of the tumor purity. Then, to obtain a more detailed picture of immune cell type infiltration, R package MCPcounter was used.¹⁶ MCPcounter (Microenvironment Cell Populations-counter) is a method for quantification of immune cell's relative abundances in heterogeneous tissues using marker genes optimized for interrogating microarray data. Nine different cell types were interrogated (T cells, cytotoxic T cells, NK cells, B lineage, monocytic lineage, myeloid dendritic cells, neutrophils, endothelial cells and fibroblasts). Data were also interrogated with QuantiSeq (absolute method)¹⁷ and xCell (relative method)¹⁸ tools that also estimate immune cell infiltration.

For all the obtained scores, assumptions of normality and homoscedasticity were interrogated through statistical tests Levene and Shapiro, respectively. All comparisons between variables were analyzed using non-parametric tests (Kruskal-Wallis and Wilcoxon tests), for homogenization of methods, as variables were either not normally distributed, or variances were not equally distributed between groups. For all tests applied, differences were considered significant when $p < 0.05$. To probe the lack of correlation of the scores between each metastatic sample and its related primary site of origin, a comparison between the different primary sites of origin was performed, for each metastatic site.

Immune clustering

To make a cluster analysis separating samples on the basis of their immune status, a total of 25 immunity-related gene sets covering both innate and adaptive responses were manually selected from pathways' databases and publications (detailed in online supplementary table 3). Gene Set Variation Analysis from R package GSVA was

performed to obtain the immune profile of the metastatic samples. This function performs a non-parametric, unsupervised analysis for estimating variation of the given gene sets through the samples in the expression matrix, returning an enrichment score for each sample. GSVA function was performed with 1000 bootstraps and arguments as default.

The resulting GSVA enrichment scores were then used to cluster the samples by agglomerative hierarchical clustering. First, samples distances were computed via the R function `dist`, with Euclidean distance. Next, `hclust` function generated a clustering from the distances, with “Ward-D2” linkage method, where dissimilarities are squared for obtaining more accurate clustering. The same process was performed for gene set distances. Three categories, characterized by different immune and inflammatory enrichments, were defined and named as “Low ImmuneCluster (LIC),” “Medium ImmuneCluster (MIC)” and “High ImmuneCluster (HIC).” Function `cutree` (dendextend package) was used to divide the dendrogram tree in the three groups. Finally, for visualization purposes,

a heatmap was plotted with the representation of the 374 samples and 25 gene sets scores, previously scaled and centered. A dendrogram was drawn to visualize the distance tree for samples and gene sets. Proportions of the different tumor metastases among the three ImmuneClusters were tested by χ^2 test of proportions and plotted as barplot of percentages. Figure 1 shows a summary of the analysis performed from sample collection to immune microenvironment characterization.

Gene expression data from samples in Liu *et al*¹⁹ were downloaded for validation purposes. Metastatic samples (n=111) were classified into the three ImmuneClusters. Overall survival (OS) after immunotherapy treatment was plotted using a Kaplan-Meier curve stratifying by HIC, MIC and LIC.

Healthy tissue gene signatures

To calculate the Normal Tissue Signatures, normalized and ComBat-adjusted expression data for the 348 healthy samples were used. A differential expression analysis among the four healthy tissues was performed with R

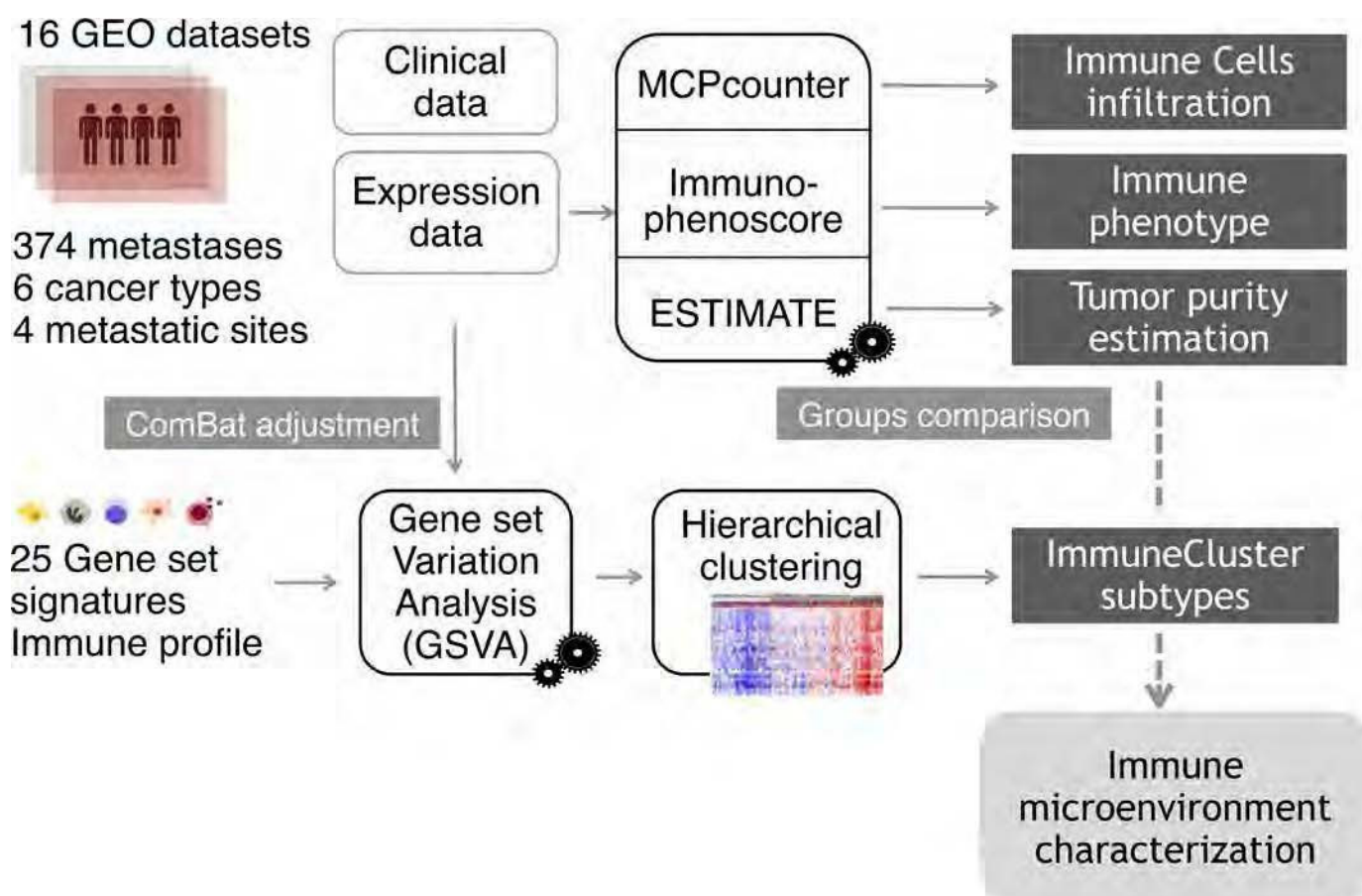


Figure 1 Analysis overview. Gene expression data from a cohort of 374 samples from four different metastatic locations were collected from Gene Expression Omnibus (GEO) database. To eliminate the batch effect, data were adjusted using the ComBat function. For each metastatic sample, tumor purity, proportion of immune cell infiltration and immune status were estimated using the R packages ESTIMATE (Estimation of STromal and Immune cells in MAlignant Tumor tissues using Expression data), MCPcounter (Microenvironment Cell Populations-counter) and the Immunophenoscore algorithm. Applying Gene Set Variation Analysis (GSVA) function, samples were scored according to the level of expression of a comprehensive set of gene signatures related to immune response. The resulting scores were used to cluster the metastatic samples on the basis of their immune profile.

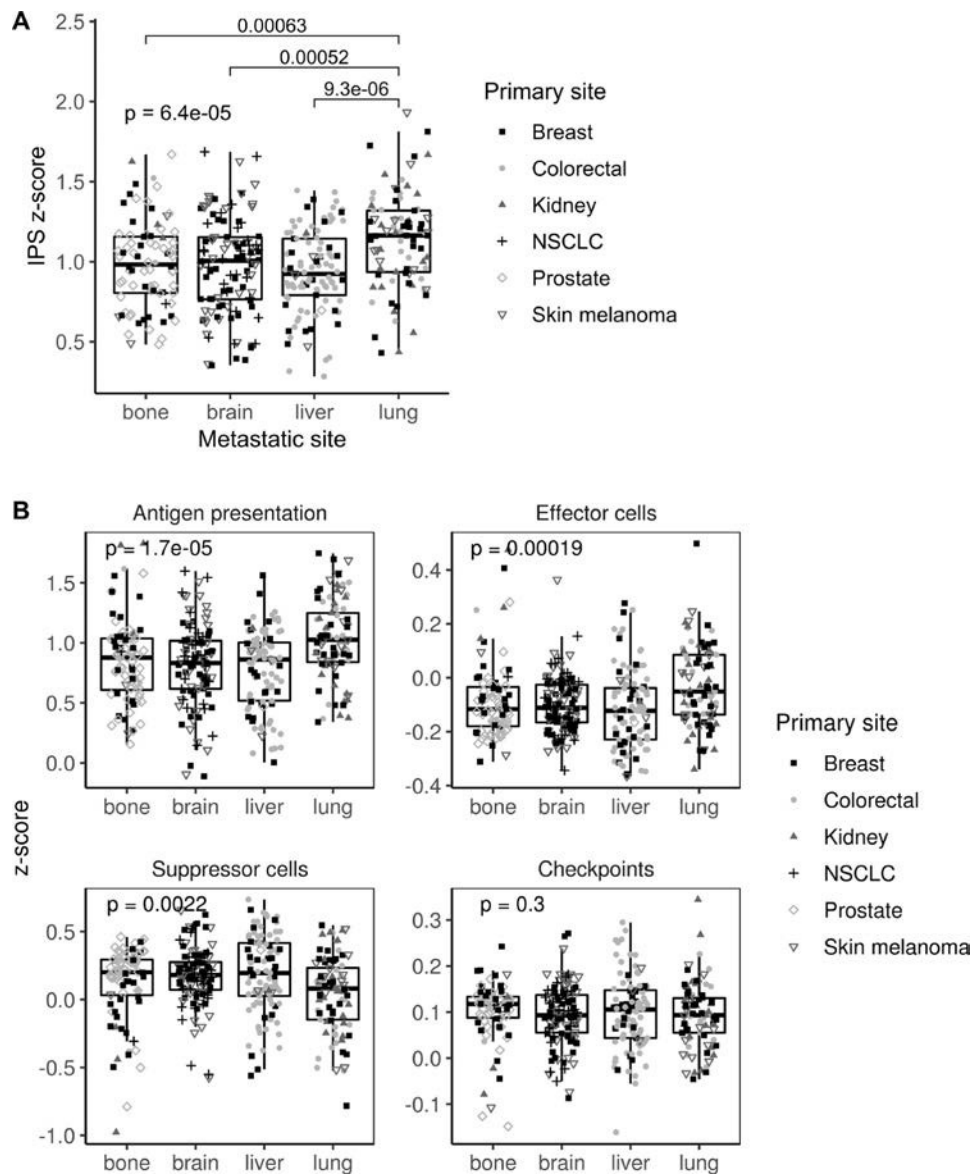


Figure 2 Immunophenoscore (IPS) scores across the four metastatic locations. (A) Boxplot showing the aggregated IPS z-score. (B) Boxplot showing the antigen presentation, effector cells, suppressor cells and checkpoint scores. Dot shapes represent the primary tumor origin of each metastatic sample. NSCLC, non-small-cell lung cancer.

package *Limma* to generate a gene profile exclusive for each tissue type (brain, bone, liver and lung). All metastatic samples were scored with these signatures and used to explore the presence of healthy tissue contamination. Also, Normal Tissue Signatures were added as a continuous covariate in the model matrix for the Combat function. The resulting adjusted expression matrix values were used to recalculate immune scores in all metastatic samples.

Functional analysis

To identify enrichment in specific cellular functions and pathways, a Gene Set Enrichment Analysis (GSEA) was performed comparing samples belonging to the extreme phenotypes HIC and LIC.²⁰ Gene sets from MsigDB were interrogated (Hallmarks, Gene Ontologies, Oncogenic

Pathways, Immunologic Pathways and Canonical Pathway that include the datasets KEGG, Reactome and Biocarta). Also, to predict their putative response to anti PD-L1 drug, metastatic samples were scored with the GSVA method using the T-cell inflammatory (TIS) signature. This is a genetic profile reported as a good predictor of clinical response to pembrolizumab across a wide variety of tumor types.²¹

Identification of genes to classify samples into ImmuneClusters

A classification algorithm was performed to find genes classifying samples into extreme phenotypes HIC and LIC. Data were divided into training (75% of samples, n=137) and test dataset (25% of samples, n=46). The Training dataset was used for predictor discovery and

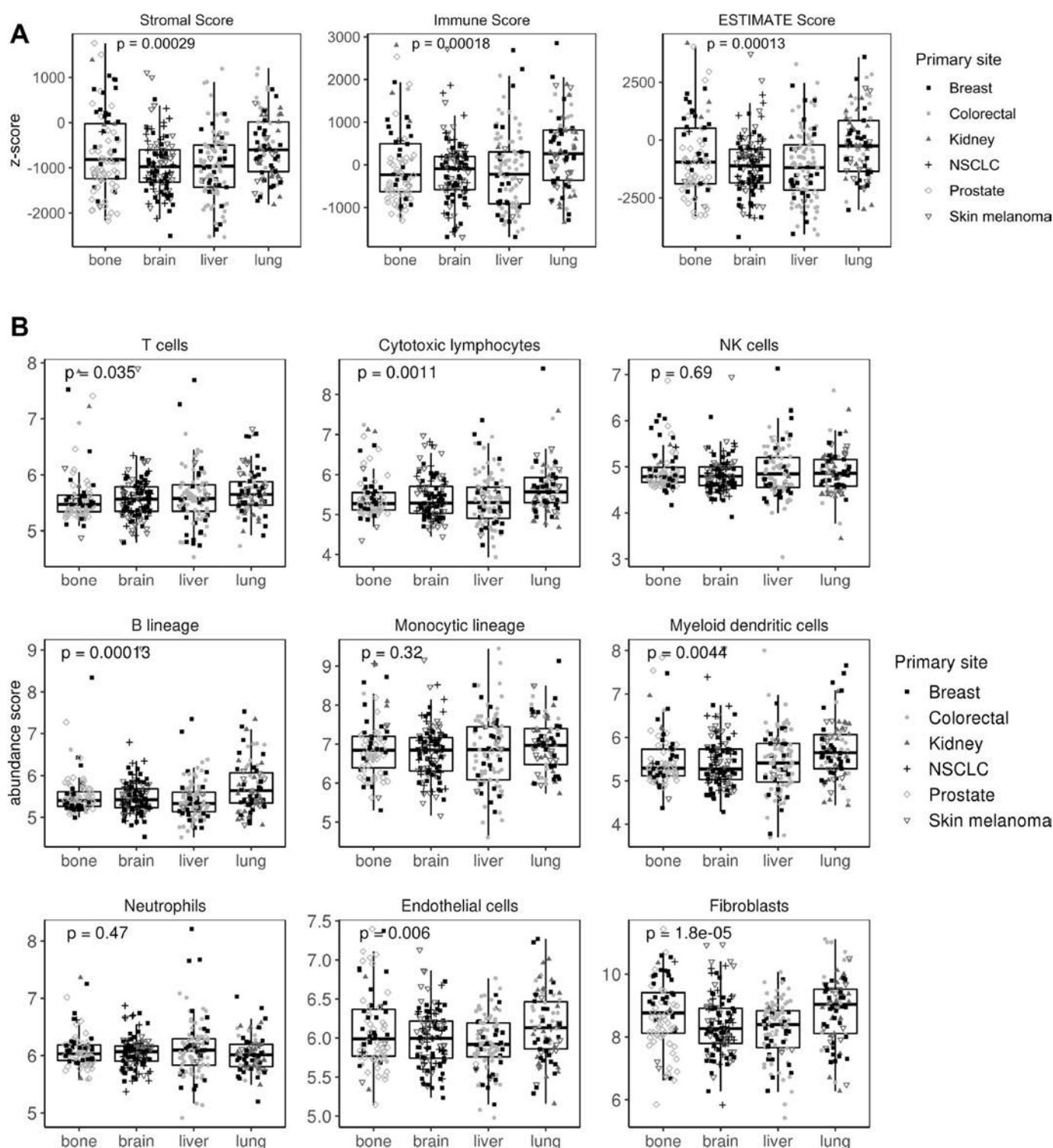


Figure 3 Stromal and immune infiltration across the four metastatic locations. (A) Boxplot showing stromal, immune and ESTIMATE (Estimation of STromal and Immune cells in MAlignant Tumor tissues using Expression data) scores for each sample. (B) Boxplot showing stromal and immune cell infiltration using MCPcounter (MicroenvironmentCell Populations-counter) tool. Shaped dots represent the primary tumor origin of each metastatic sample. NK, natural killer; NSCLC, non-small-cell lung cancer.

supervised classification to generate a plausible model. This division was carried out randomly and respecting the LIC/HIC proportions. The training datasets was used to identify differentially expressed genes (DEGs) between LIC and HIC groups. For this, an empirical Bayes analysis

with R package Limma was performed using Benjamini and Hochberg's method for false discovery rate correction. DEGs between these two extreme phenotypes were selected as those with \log_2 fold change (\log_2FC) $> \text{abs}(2)$ and adjusted p-value < 0.01 . The DEGs identified using

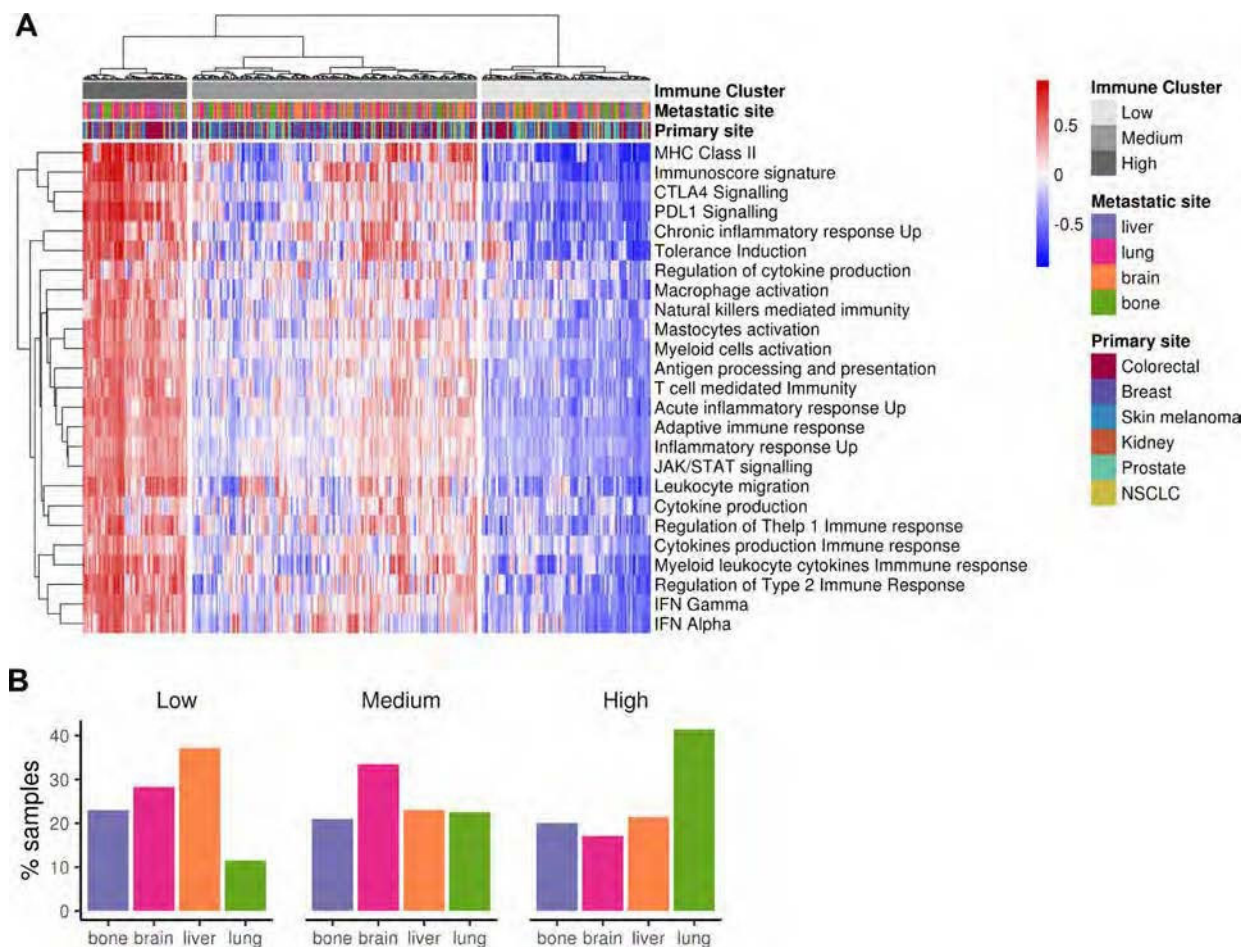


Figure 4 Clustering of metastatic samples using immune-related datasets. (A) Heatmap showing the metastatic samples grouped by hierarchical clustering using the GSVA enrichment scores for 25 innate and adaptive immunity-related gene sets. Samples are clustered in three major groups defined as Low ImmuneCluster (LIC), Medium ImmuneCluster (MIC) and High ImmuneCluster (HIC). Color bars at the top of the graph labels the samples by the metastatic site, their primary tumor of origin and the ImmuneCluster. (B) Barplot of metastatic location percentage in each ImmuneCluster. MHC, major histocompatibility complex; NSCLC, non-small-cell lung cancer.

the training set were used in a binary decision tree with cross-validation ($k=5$) to identify an optimal classification model for LIC/HIC. The classification was made with the R package caret. The classification accuracy was evaluated by calculating the sensitivity, specificity, likelihood ratio (LR) and area under the curve (AUC). Finally, the predictive power of the selected decision tree was validated in an independent dataset (GSE51244). This dataset is composed by 94 metastatic samples (lung and liver) from colorectal cancer (CRC). First, samples were classified into the three ImmuneClusters by our algorithm. Then, the samples were classified as CD74 high/CD74 low, by the median value of expression. Finally, the agreement between the CD74 high and HIC category was evaluated.

Availability of data and code

All data and R code used for the analysis are freely available at GitHub repository <https://github.com/odapubs/mets-immunecluster>.

RESULTS

Immune characterization of metastatic samples

Gene expression data were used to categorize metastatic samples according to their immune status. First, IPS scores were used as a general indicator of immune system activation across samples. Metastases in lung showed a higher IPS z-score than those in bone, brain or liver ($p=0.00006$), suggesting a different immune microenvironment modulation (figure 2A). Specifically, lung metastases showed higher scores for antigen presentation ($p=0.00002$) and effector cells ($p=0.0002$), whereas they showed the lower score for suppressor cells ($p=0.002$). Interestingly, no differences across metastatic locations were found in the immune checkpoint category (figure 2B).

Next, ESTIMATE software was used to interrogate samples about their stromal and immune cell infiltration. Metastasis in lung and bone showed more abundance of stromal cells. In agreement with the IPS results, lung metastases scored better in the immune category ($p=0.0002$; figure 3A). To explore this issue in detail,

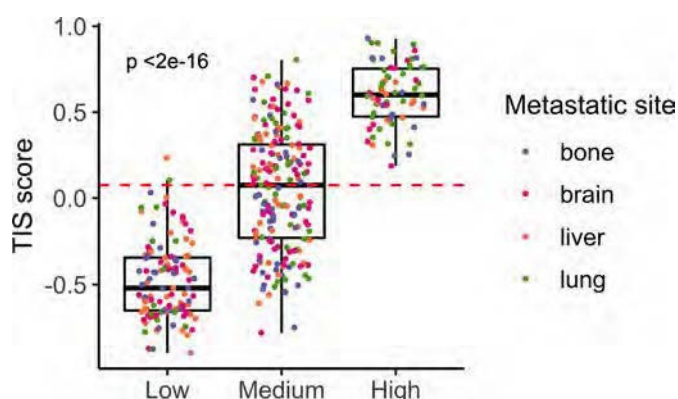


Figure 5 T-cell inflammatory signature (TIS) scores across ImmuneClusters. Barplot showing TIS measures for each metastatic sample. Red line indicates the median value. Color dots represent the metastatic site of the samples.

MCPcounter, a tool for the quantification of different immune cell populations was used. As a result, lung metastases scored high in B lineage ($p=0.0001$), cytotoxic lymphocytes ($p=0.001$), myeloid dendritic cells ($p=0.004$), endothelial cells ($p=0.006$) and T-cell categories ($p=0.03$). No differences were found in NK cells, monocytic lineage and neutrophil categories. Interestingly, both lung and bone metastases showed an enrichment in fibroblast in comparison with brain and liver samples ($p=0.00001$; [figure 3B](#)). To validate this results, other tools apart from MCPcounter were used. In agreement with our results, absolute method QuantiSeq validates B-cell and T-cell abundance (specifically CD8⁺ T cells) in lung metastases, whereas relative xCell algorithm validates lung metastases enrichment in dendritic and endothelial cells. Neither QuantiSeq nor xCell validates differences in cancer associated fibroblasts (CAF) infiltration. QuantiSeq detected monocytes as higher infiltrated in lung versus liver metastases (online supplementary table 4).

To exclude the possibility that normal tissue from surgical margins were biasing our results, profiles for healthy tissue gene expression in bone, brain, liver and lung using transcriptomic data were constructed. Strong differences were found when comparing metastatic and normal tissues suggesting that little contamination existed, if any (online supplementary figure 3). Only lung metastases showed some resemblance with lung normal tissue. However, no correlation was found between the IPS score and the normal tissue score in lung metastatic samples thus excluding the possibility that samples showing higher immune scores had more normal tissue contamination (online supplementary figure 4A). Moreover, immune characterization was repeated adjusting all samples' gene expression by their normal tissue score and almost the same results were obtained (online supplementary figure 4B and C).

Finally, we wondered if differences between the seeding organs existed. Within metastatic samples in brain and liver, no differences existed in IPS scores neither in infiltration composition regardless of their primary site or

origin (online supplementary figure 5A and B). This suggested that, to some extent, immune adaptation to the new environment is a mechanism shared across tumors metastasizing in brain and liver. However, differences existed in lung and bone metastases. In lung, only slight differences were found in B lineage infiltration score ($p=0.02$; online supplementary figure 5C). In bone metastases, significant and stronger differences existed since samples from colorectal and kidney primary tumors have higher levels of antigen presentation and effector cells score but lower suppressor cells score. Also, they have more lymphocytes and myeloid dendritic cell infiltration (online supplementary figure 5D). This result suggested that the primary origin of bone metastases is indeed affecting the immune phenotype of their subsequent metastases.

Clustering of metastatic samples based on their immune phenotype

To further explore the existence of metastases with a hot immune phenotype, manually curated gene sets related to both adaptive and innate immune responses were used to perform a hierarchical clustering for the 374 samples. Three groups emerged categorized as “HIC” (19%), “MIC” (51%) and “LIC” (30%) ([figure 4A](#)). Online supplementary figure 6A summarizes the GSVA scores for each metastatic site, lung being the most immunogenic one in agreement with previous results. Indeed, when proportion of metastases for each ImmuneCluster were represented, the HIC was enriched in lung metastases, whereas MIC was in brain and LIC in liver ([figure 4B](#)). When primary sites of origin were compared with the three clusters, kidney cancer type showed an enrichment of HIC samples (probably reflecting the enrichment of lung metastatic ones) whereas prostate was the one with the lower. Finally, normal tissues were also scored using this approach but pairs of normal-metastatic tissues did not cluster together (online supplementary figure 6B).

Functional characterization of metastases belonging to the HIC

One might expect metastases to be immune cold, as being very aggressive tumors. In agreement, the HIC was the one comprising the less number of samples. This was an interesting group of samples characterized by an elevated expression of the human leukocyte antigen class II (HLA-II) complex and genes involved in antigen presentation pathway. Also, they showed high levels of the therapeutic targets PD-L1 and CTLA4, thus suggesting a hypothetical treatment with immune checkpoint inhibitors. Supporting this hypothesis, all samples belonging to HIC scored very high in the TIS signature reporting to be correlated with response to anti PD-L1 checkpoint inhibitor pembrolizumab ($p<0.001$; [figure 5](#)). Moreover, independent dataset comprising metastatic samples from patients with melanoma treated with immune checkpoint inhibitors were classified into the ImmuneClusters and interrogated about survival. Interestingly, samples classified as HIC

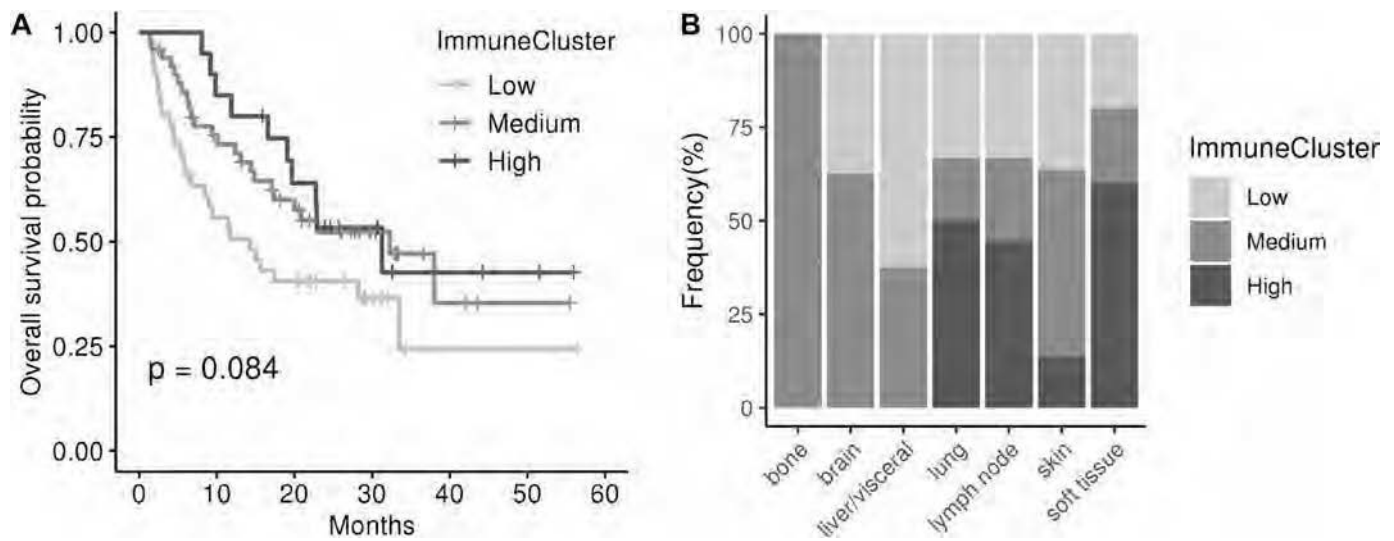


Figure 6 ImmuneCluster classification and response to immunotherapy. (A) Kaplan-Meier curve showing survival after immunotherapy treatment in metastatic melanoma. High ImmuneCluster and Medium ImmuneCluster samples exhibited a tendency toward better overall survival than Low ImmuneCluster samples (Log-rank test, $p=0.084$). (B) Frequency of metastases in each ImmuneCluster by location.

and MIC showed a tendency toward better OS than LIC samples (figure 6A). Half lung metastases were classified as HIC (figure 6B). Although number of samples was too small to reach a conclusion, it is worth that two out of the total four lung metastases experienced progressive disease, whereas one experienced stable disease and one achieved a complete response. On the contrary, six out of seven brain metastasis suffered progressive disease and only one exhibited a partial response. Although speculative, these results pave the way to a hypothetic treatment of the highly inflammatory metastatic tumors (figure 7).

Samples in the three clusters were interrogated about their level of immune infiltration. As expected, the HIC scored better in all categories being these tumors highly infiltrated in all categories both activating and inhibiting the immune system. It is interesting to note that all bone metastasis in the HIC scored very high in the T-cell category (online supplementary figure 7A). However, when markers of exhaustion were examined, samples belonging to HIC showed the higher levels of expression (online supplementary figure 7B). This result suggested that although highly infiltrated by T cells, these are not functional but exhausted.

Then, a functional analysis comparing samples belonging to the extreme phenotypes HIC and LIC was done using GSEA. As expected, HIC samples were highly enriched in immunity-related pathways and in inflammation ones such as interleukin (IL)-2-STAT5, IL-6-JAK-STAT3, interferon, tumor necrosis factor (TNF)- α , TNF- γ and nuclear factor kappa-light-chain-enhancer of activated B cells (NF- κ B), among others. Also, HIC samples were enriched in antigen presentation, Toll like receptor 4 (TLR4) signaling and CTLA4 pathways. Regarding cellular functions, inflammatory response and adaptive immune response emerged as the most significant ones (online supplementary table 5 and online supplementary

figure 8). Since those samples were initially clustered on the basis of their immune phenotypes, these results were not surprising at all. However, the functional analysis also reported interesting results not directly related to the immune system. For example, apoptosis and KRAS signaling pathways were upregulated pathways in HIC samples.

Identification of HIC biomarkers

The more differentially expressed genes (DEG) among ImmuneClusters were selected ($\log_2FC > \text{abs}(2)$, $n=43$; online supplementary table 6, online supplementary figure 9) and used to search for a biomarker or panel of biomarkers useful to identify samples belonging to the HIC. A decision tree algorithm with bootstrapping selected *CD74* as the gene that best categorizes between the two groups (online supplementary figure 10A). The model was first validated on the test samples within our dataset, with good prediction values (sensitivity=1, specificity=0.96, $LR(+)=9.8$, $LR(-)=0.2$, $AUC=0.98$, receiver operating characteristic curve in online supplementary figure 10B). When tested in an external dataset, *CD74* showed high accuracy classifying samples into LIC and HIC (classification error=0.1).

Interestingly, when samples belonging to MIC were reclassified, 76 out of 191 samples belonging to the MIC were classified as HIC, whereas 113 were classified as LIC in our dataset. In the validation dataset, 14 out of 18 samples belonging to this cluster were classified as HIC, whereas 4 were classified as LIC. This suggested that a percentage of metastasis showing and intermediate phenotype could resemble to the highly infiltrated ones. Indeed, when interrogated using the TIS score, about half of metastases classified as MIC scored very high suggesting a putative response to immunotherapy (figure 5). Thus, *CD74* might be marker of inflammatory metastases.

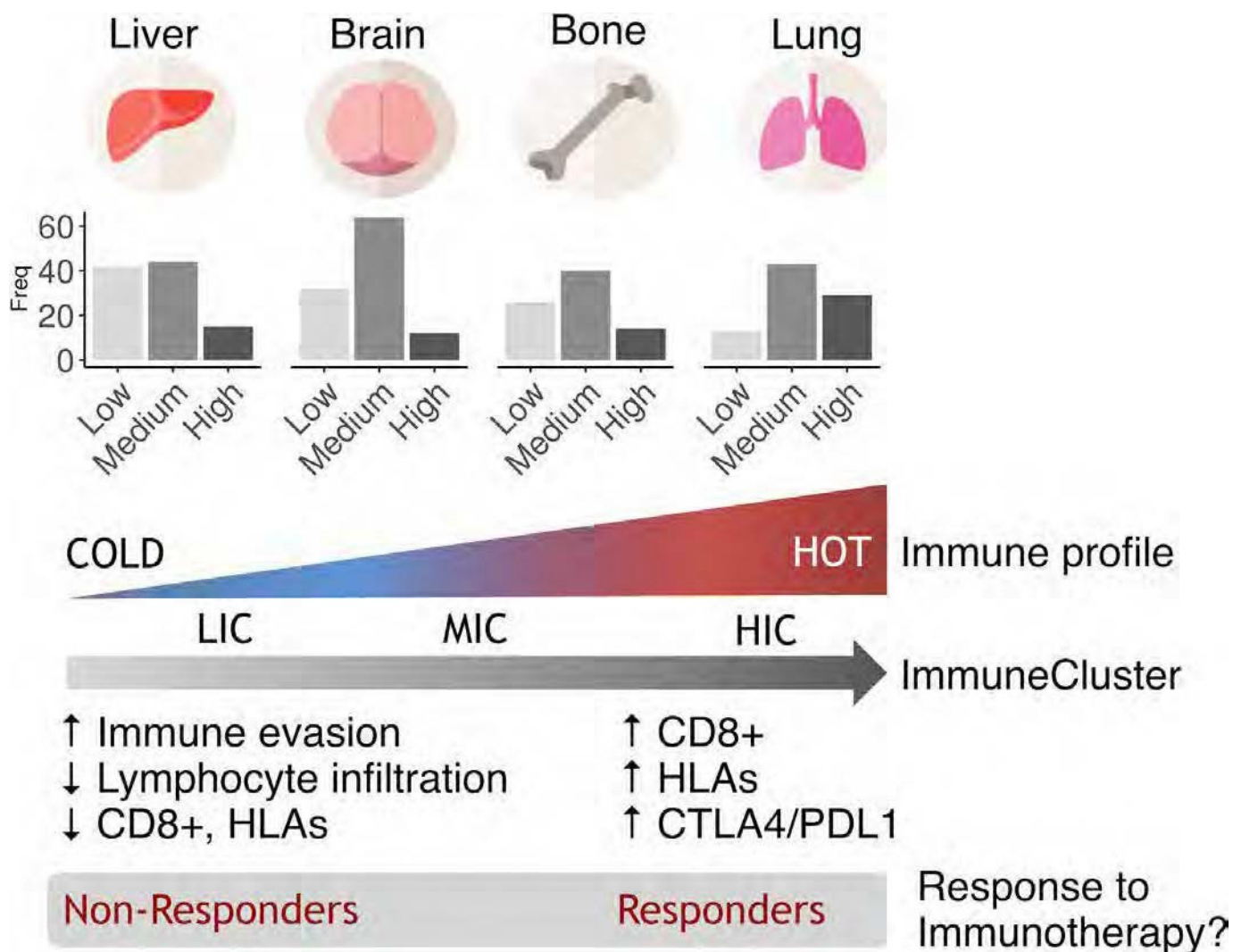


Figure 7 Hypothesis. Based on their immune status, metastatic samples could be clustered into three ImmuneClusters. Lung metastasis tend to be more immunogenic, while liver metastasis tends to be less immunogenic. Metastatic samples in the HIC cluster sharing an inflammatory phenotype might be immunotherapy responders, regardless of their primary site of origin.

DISCUSSION

Disseminated cells must evade immune system response to complete the metastatic invasion. Many examples exist in the literature demonstrating the contribution of immune system cells and molecules in several steps of the metastatic cascade, apart from other players. Inflammatory response and immune regulatory cells (both myeloid and lymphoid) have been reported to support spreading and metastasis.²²

Although pan-cancer analyses interrogating immune cell infiltration in primary tumors have been reported,²³ to our knowledge none has tackled this issue in metastatic samples. We hypothesized that metastatic tumors in the same organ from different primary tumors might share similar immune features and/or mechanisms to escape immune surveillance. Recently, corroborating our hypothesis, a study on bone metastases remarks the existence of tissue-specific checkpoint immunotherapy evasion.²⁴ Since brain, bone, liver and lungs are the secondary sites more prone to be invaded by disseminated cells, we

selected almost 400 metastatic samples in those organs to work with. By using transcriptomic data, we found significant differences in markers of immune microenvironment activation among the different metastatic locations. Lung metastases showed a tendency toward having a higher immunogenic environment compared with brain, bone and liver metastases. In agreement, cell lineage infiltration analysis revealed higher lymphocytic infiltration in lungs and also myeloid dendritic cells, whereas there are no differences for innate immunity components (NK, monocytic lineage, neutrophils). Interestingly, there is no association between the organ of origin of the lung metastases and these immune markers, indicating that differences found are independent of the cancer primary site. In agreement, a work by Remark *et al* showed no differences in T-cell infiltration in lung metastases coming from CRC or renal primary tumors, although they found differences in NK infiltration.²⁵

A cluster analysis identified a percentage of around 20% of metastatic samples classified as high immunogenic



(HIC). In line with our previous results, there was enrichment in lung metastatic samples in this subtype, mainly characterized by being highly inflammatory. It has been reported that immunosuppressive mechanisms that prevent massive immune reactions to pulmonary alveolar macrophages in the lungs are harnessed by tumors to facilitate metastasis. Therefore, the intrinsic properties of lung immune homeostasis could be, at least partially, responsible for the susceptibility of the lungs to metastasis.²⁶ Inquiringly, several reports suggested that in asthmatic people the use of anti-inflammatory inhaled corticosteroid is associated with a reduced risk of lung cancer but not of laryngeal cancer^{27–28} thus suggesting an inflammatory origin of tumors growing in this location. On the contrary, there is enrichment in liver metastases in the LIC pointing these metastases as the colder ones. An explanation could be that a high percentage of these secondary tumors show a vessel co-option pattern of metastatic growth. This is a replacement growth in which the tumor do not generate new vessels or an inflammatory reaction. As cancer cells grow, substitutes normal liver cells.²⁹ However, it is interesting to note that not all lung metastases were categorized in the HIC cluster. Furthermore, some metastases in bone, liver and brain also fell in this cluster thus sharing phenotypic and immune features. Although rare, 83% of bone metastases originating from CRC and kidney tumors belonged to HIC and showed an increase in immune markers. The osteolytic nature of these lesions (in contrast with other bone metastasis coming from other tumors like prostate) might explain, at least in part, the particular idiosyncrasy of these metastases. Supporting this hypothesis, one of the genes shown to be significantly increased in HICs, granzyme A, has emerged as a key proinflammatory molecule regulating osteoclast differentiation and bone erosion during rheumatoid arthritis.³⁰

It is worth to note that metastases belonging to HIC scored very high when interrogated with the TIS signature, whereas metastases in LIC scored very low. This is a gene expression level measuring the level of microenvironment inflammation. In a clinical trial encompassing 20 cohorts of patients with advanced solid tumors, TIS was able to predict pembrolizumab response (an anti-PD-L1 drug).³¹ Recently, the utility of such signature as an accurate and independent predictive biomarker has been validated in a pan-cancer study analyzing anti-PD-1 treatment benefit in primary tumors.³² Thus, we propose to treat HIC metastases with immune checkpoint inhibitors, irrespective of their primary site of origin. In agreement, and close to be statistically significant, melanoma metastatic samples classified into HIC and MIC showed better OS than LIC after treatment with anti-PD1 inhibitors pembrolizumab or nivolumab. Although promising, this hypothesis needs further study. In the same line, a study in melanoma and lung tumors reported poor response to pembrolizumab in liver metastases than in extrahepatic ones.³³ In agreement, most liver metastases belong to LIC cluster. In breast cancer, triple negative tumors have been

reported to be more susceptible to immune therapeutics.³⁴ We classified breast cancer metastatic samples into the intrinsic molecular subtypes and interestingly, almost 50% of lung metastases were classified as basal (mostly corresponding with triple negative tumors). However, no differences in the TIS score across molecular subtypes were observed (data not shown).

To classify metastatic samples into the inflammatory cluster HIC, a decision tree algorithm selected *CD74* as a good biomarker. *CD74* is a gene coding for a chaperone that associates with class II major histocompatibility complex (MHC-II) and regulates antigen presentation for immune response.³⁵ Interestingly, MHC-II has been proposed as a good predictor of response to immune checkpoint inhibitors in melanoma metastases.¹⁹ *CD74* also serves as cell surface receptor for the cytokine macrophage migration inhibitory factor (MIF) which, when bound to the encoded protein, initiates survival pathways and cell proliferation. MIF and *CD74* have been shown to regulate peripheral B-cell survival and were associated with tumor progression and metastasis.³⁵

It is worth to mention that among the different markers of cytotoxic T lymphocytes activation, *GZMA* was the only one that reached significance to be included in the HIC metastases group (online supplementary figure 9). A priori the appearance of markers of cytotoxic T lymphocytes activation in the inflammatory tumors susceptible to be treated with immunotherapy is not surprising and might pass unnoticed. However, several independent reports have recently identified *GZMA* as a key regulator of inflammation in different pathologies,³⁶ including carcinogenesis, which tempts us to speculate on the potential significance of this finding. Specifically, after our recent results indicating that inflammation induced by *GZMA* is key for the development of CRC in vivo and therapeutic inhibition of *GZMA* reduced gut inflammation and CRC development in mice (Santiago *et al* accepted for publication). Other interesting gene is C-C Motif Chemokine Ligand 5 (*CCL5*), a proinflammatory chemokine that has been reported to favor the formation of an immunosuppressive microenvironment in tumors like gastric or breast, among others.³⁷ *CCL5* shifts the balance between different leukocyte cell types by increasing the presence of deleterious TAMs and by inhibiting the antitumor T-cell activation.³⁸

Metastatic samples in HIC showed *KRAS* activation suggesting a crosstalk between this pathway in the tumorous cell and the immune microenvironment. Indeed, a relationship between *KRAS* pathway and inflammation has been described in a mouse lung model harboring *KRAS* G12D mutation.³⁹ Kitajima *et al* demonstrates that *KRAS* signaling activates carcinogenesis through upregulation of IL-6 and *CCL5* cytokines.⁴⁰ Also in agreement, patients with *KRAS*-mutant CRC develop lung metastases more frequently than *KRAS* wild-type (WT) counterpart.⁴¹ A recent study found *KRAS* WT tumors resistant to anti-epidermal growth factor receptor (EGFR) drugs having cytotoxic T-cell infiltration and overexpression of PD-L1

thus susceptible to be treated with immune checkpoint inhibitors.⁴²

This study has limitations mainly derived to the fact that results were inferred from public datasets. We had to normalize data generated by diverse laboratories and, though we used strategies to reduce batch effects, these methods may not be fully efficient and may also reduce biological variability. We have used gene expression signatures to try to control the contamination of tumor tissues with normal tissues. However, we cannot totally exclude this possibility and this issue would be considered in future studies. Also, clinical information was scarce. Association between samples in HIC cluster and prognosis and/or treatment response in other tumors apart from melanoma deserves further study.

In conclusion, our results suggest that tumor cells need to share similar molecular profiles to evade the immune surveillance and growth in a specific secondary niche, regardless of their origin. Furthermore, we have found a cluster of approximately 20% of metastatic tumors showing an inflammatory phenotype that mainly includes lung metastatic lesions. These tumors scored very high when interrogated with TIS signature suggesting a putative treatment with immune checkpoint inhibitors.

Author affiliations

¹Unit of Biomarkers and Susceptibility, Oncology Data Analytics Program (ODAP), Catalan Institute of Oncology (ICO), Oncobell Program, Bellvitge Biomedical Research Institute (IDIBELL) and CIBERESP, L'Hospitalet de Llobregat, Barcelona, Spain

²Department of Clinical Sciences, Faculty of Medicine and Health Sciences, University of Barcelona, Barcelona, Spain

³Immunotherapy, Inflammation and Cancer Group, Aragón Health Research Institute (IIS Aragón), Aragón i + D Foundation (ARAID), Zaragoza, Spain

⁴Department of Medical Oncology, Catalan Institute of Oncology (ICO), Oncobell Program, Bellvitge Biomedical Research Institute (IDIBELL)-CIBERONC, L'Hospitalet de Llobregat, Barcelona, Spain

⁵Department of Pathology, University Hospital Bellvitge (HUB-IDIBELL), L'Hospitalet de Llobregat, Barcelona, Spain

Acknowledgements We thank Spanish Association Against Cancer (AECC) Scientific Foundation. We also thank CERCA Program, Generalitat de Catalunya for institutional support and Josipa Bilic for critical reading of the manuscript.

Contributors RS-P and JMP conceived the presented idea. SG-M parsed data and performed the computations. MHA performed classification methods and helped with statistics. XS supervised biomarker identification. VM verified the analytical methods. JP investigated the role of inflammatory genes and supervised the findings of this work. CS and RS interpreted results from a clinical point of view. RS-P took the lead in writing the manuscript. All authors provided critical feedback and helped shape the research, analysis and manuscript.

Funding Agency for Management of University and Research Grants (AGAUR) of the Catalan Government (grant no 2017SGR723).

Competing interests VM is consultant to Bioiberica S.A.U. and Grupo Ferrer S.A., received research funds from Universal DX and is coinvestigator in grants with Aniling. JMP is consultant for Roche-Genentech, Bristol-Myers Squibb, Merck Sharp & Dohme, Merck Serono, Janssen, Astellas, VCN-Biotech and BeiGene; JMP has received research grants from Bristol-Myers Squibb, Merck Sharp & Dohme, Merck Serono, Janssen and AstraZeneca.

Patient consent for publication Not required.

Provenance and peer review Not commissioned; externally peer reviewed.

Data availability statement Data are available in a public, open access repository. All used data have been downloaded from GEO database.

Open access This is an open access article distributed in accordance with the Creative Commons Attribution Non Commercial (CC BY-NC 4.0) license, which permits others to distribute, remix, adapt, build upon this work non-commercially, and license their derivative works on different terms, provided the original work is properly cited, appropriate credit is given, any changes made indicated, and the use is non-commercial. See <http://creativecommons.org/licenses/by-nc/4.0/>.

ORCID iDs

Julián Pardo <http://orcid.org/0000-0003-0154-0730>

Rebeca Sanz-Pamplona <http://orcid.org/0000-0002-2187-3527>

REFERENCES

- 1 Arnold M, Sierra MS, Laversanne M, *et al*. Global patterns and trends in colorectal cancer incidence and mortality. *Gut* 2017;66:683–91.
- 2 Massagué J, Obenauf AC. Metastatic colonization by circulating tumour cells. *Nature* 2016;529:298–306.
- 3 Lambert AW, Pattabiraman DR, Weinberg RA. Emerging biological principles of metastasis. *Cell* 2017;168:670–91.
- 4 Valastyan S, Weinberg RA. Tumor metastasis: molecular insights and evolving paradigms. *Cell* 2011;147:275–92.
- 5 Mohme M, Rietdorf S, Pantel K. Circulating and disseminated tumour cells - mechanisms of immune surveillance and escape. *Nat Rev Clin Oncol* 2017;14:155–67.
- 6 Robinson MW, Harmon C, O'Farrelly C. Liver immunology and its role in inflammation and homeostasis. *Cell Mol Immunol* 2016;13:267–76.
- 7 Quail DF, Joyce JA. The microenvironmental landscape of brain tumors. *Cancer Cell* 2017;31:326–41.
- 8 Obenauf AC, Massagué J. Surviving at a distance: organ-specific metastasis. *Trends Cancer* 2015;1:76–91.
- 9 Budczies J, von Winterfeld M, Klauschen F, *et al*. The landscape of metastatic progression patterns across major human cancers. *Oncotarget* 2015;6:570–83.
- 10 Syn N, Wang L, Sethi G, *et al*. Exosome-Mediated metastasis: from epithelial-mesenchymal transition to escape from immunosurveillance. *Trends Pharmacol Sci* 2016;37:606–17.
- 11 Liu Y, Cao X. Characteristics and significance of the pre-metastatic niche. *Cancer Cell* 2016;30:668–81.
- 12 Stresing V, Baltziskueta E, Rubio N, *et al*. Peroxiredoxin 2 specifically regulates the oxidative and metabolic stress response of human metastatic breast cancer cells in lungs. *Oncogene* 2013;32:724–35.
- 13 Hanahan D, Weinberg RA. Hallmarks of cancer: the next generation. *Cell* 2011;144:646–74.
- 14 Charoentong P, Finotello F, Angelova M, *et al*. Pan-Cancer Immunogenomic analyses reveal Genotype-Immunophenotype relationships and predictors of response to checkpoint blockade. *Cell Rep* 2017;18:248–62.
- 15 Yoshihara K, Shahmoradgolji M, Martínez E, *et al*. Inferring tumour purity and stromal and immune cell admixture from expression data. *Nat Commun* 2013;4:2612.
- 16 Becht E, Giraldo NA, Lacroix L, *et al*. Estimating the population abundance of tissue-infiltrating immune and stromal cell populations using gene expression. *Genome Biol* 2016;17:218.
- 17 Plattner C, Finotello F, Rieder D. Deconvoluting tumor-infiltrating immune cells from RNA-Seq data using quanTIseq. *Methods Enzymol* 2020;636:261–85.
- 18 Aran D. Cell-Type enrichment analysis of bulk transcriptomes using xCell. *Methods Mol Biol* 2020;2120:263–76.
- 19 Liu D, Schilling B, Liu D, *et al*. Integrative molecular and clinical modeling of clinical outcomes to PD1 blockade in patients with metastatic melanoma. *Nat Med* 2019;25:1916–27.
- 20 Subramanian A, Tamayo P, Mootha VK, *et al*. Gene set enrichment analysis: a knowledge-based approach for interpreting genome-wide expression profiles. *Proc Natl Acad Sci U S A* 2005;102:15545–50.
- 21 Ayers M, Lunceford J, Nebozhyn M, *et al*. IFN- γ -related mRNA profile predicts clinical response to PD-1 blockade. *J Clin Invest* 2017;127:2930–40.
- 22 Keskinov AA, Shurin MR. Myeloid regulatory cells in tumor spreading and metastasis. *Immunobiology* 2015;220:236–42.
- 23 Tamborero D, Rubio-Perez C, Muiños F, *et al*. A pan-cancer landscape of interactions between solid tumors and infiltrating immune cell populations. *Clin Cancer Res* 2018;24:3717–28.
- 24 Jiao S, Subudhi SK, Aparicio A, *et al*. Differences in tumor microenvironment dictate T helper lineage polarization and response to immune checkpoint therapy. *Cell* 2019;179:e13:1177–90.
- 25 Remark R, Alifano M, Cremer I, *et al*. Characteristics and clinical impacts of the immune environments in colorectal and renal cell carcinoma lung metastases: influence of tumor origin. *Clin Cancer Res* 2013;19:4079–91.



- 26 Sharma SK, Chintala NK, Vadrevu SK, *et al.* Pulmonary alveolar macrophages contribute to the premetastatic niche by suppressing antitumor T cell responses in the lungs. *J Immunol* 2015;194:5529–38.
- 27 Lee C-H, Hyun MK, Jang EJ, *et al.* Inhaled corticosteroid use and risks of lung cancer and laryngeal cancer. *Respir Med* 2013;107:1222–33.
- 28 Lee YM, Kim SJ, Lee JH, *et al.* Inhaled corticosteroids in COPD and the risk of lung cancer. *Int J Cancer* 2018;143:2311–8.
- 29 Kuczynski EA, Vermeulen PB, Pezzella F, *et al.* Vessel co-option in cancer. *Nat Rev Clin Oncol* 2019;16:469–93.
- 30 Santiago L, Mena C, Arias M, *et al.* Granzyme a contributes to inflammatory arthritis in mice through stimulation of osteoclastogenesis. *Arthritis Rheumatol* 2017;69:320–34.
- 31 Ott PA, Bang Y-J, Piha-Paul SA, *et al.* T-Cell-Inflamed gene-expression profile, programmed death ligand 1 expression, and tumor mutational burden predict efficacy in patients treated with pembrolizumab across 20 cancers: KEYNOTE-028. *J Clin Oncol* 2019;37:318–27.
- 32 Damotte D, Warren S, Arrondeau J, *et al.* The tumor inflammation signature (TIS) is associated with anti-PD-1 treatment benefit in the CERTIM pan-cancer cohort. *J Transl Med* 2019;17:357.
- 33 Tumeh PC, Harview CL, Yearley JH, *et al.* PD-1 blockade induces responses by inhibiting adaptive immune resistance. *Nature* 2014;515:568–71.
- 34 Katz H, Alsharedi M. Immunotherapy in triple-negative breast cancer. *Med Oncol* 2018;35:13.
- 35 Shachar I, Haran M. The secret second life of an innocent chaperone: the story of CD74 and B cell/chronic lymphocytic leukemia cell survival. *Leuk Lymphoma* 2011;52:1446–54.
- 36 Arias M, Martínez-Lostao L, Santiago L, *et al.* The untold story of granzymes in oncoimmunology: novel opportunities with old acquaintances. *Trends Cancer* 2017;3:407–22.
- 37 Aldinucci D, Colombatti A. The inflammatory chemokine CCL5 and cancer progression. *Mediators Inflamm* 2014;2014:292376
- 38 Cook J, Hagemann T. Tumour-Associated macrophages and cancer. *Curr Opin Pharmacol* 2013;13:595–601.
- 39 Kortlever RM, Sodikin NM, Wilson CH, *et al.* Myc cooperates with Ras by programming inflammation and immune suppression. *Cell* 2017;171:e14:1301–15.
- 40 Kitajima S, Thummala R, Barbie DA. Inflammation as a driver and vulnerability of KRAS mediated oncogenesis. *Semin Cell Dev Biol* 2016;58:127–35.
- 41 Ghidini M, Personeni N, Bozzarelli S, *et al.* Kras mutation in lung metastases from colorectal cancer: prognostic implications. *Cancer Med* 2016;5:256–64.
- 42 Woolston A, Khan K, Spain G, *et al.* Genomic and transcriptomic determinants of therapy resistance and immune landscape evolution during anti-EGFR treatment in colorectal cancer. *Cancer Cell* 2019;36:35–50.

IV. DISCUSSION

Cancer remains a critical problem for public health and its incidence is increasing every year. There is an urgent need to improve survival rates. This is particularly important for the deadliest tumor types as well as for advanced stages of the disease. New therapeutic strategies, like immunotherapies, are contributing to the improvement of survival rates in oncology during the last years (Wk). However, due in part to the high heterogeneity of distinct tumor niches, a critical obstacle of immunotherapies is the lack of accurate biomarkers for clinical decision making. Moreover, molecular profiling of tumors has brought innovative perspectives in the understanding of tumor pathogenesis. Cancer management is progressively shifting from generalized treatment strategies towards a personalized selection of therapies based on the classification of patients into molecular subgroups. This new perspective for treating cancer patients is referred to as precision oncology (jqp).

Immunogenomics studies have contributed to the change of paradigm in our understanding of cancer biology. Indeed, several pan-cancer immunogenomics profiles from omics data have been reported during the last years (jqr,jqq). However, most studies are centered in immune *hot* (inflamed) tumor types, like cutaneous melanoma and lung carcinomas (jqn). Immunogenomics studies in *cold* tumors are still scarce, highlighting the need to deepen the knowledge of the tumor biology of these tumor contexts in order to find new strategies to make them more prone to respond to immunotherapies.

In uveal melanoma, one of the coldest tumor types, we performed an immunogenomics study of Vjp uveal melanoma primary samples from q different datasets. From all revised articles to date, our study includes the largest number of patients with available clinical and transcriptomics data.

On the other side, metastases known for being less immunogenic compared to primary tumors. This is due to the fact that metastatic cells have gone through the immunoediting process, must survive in blood stream and succeed to establish in secondary organs (Vm). Immunogenomics studies on metastatic samples are usually centered either on analyzing one metastatic location from different primary tumors (jqm) or on different metastatic locations from one cancer type (jqW). Here though, we were able to collect a total of pmr metastatic samples from the four most frequent sites of metastasis from jn different datasets. To our knowledge, this is the first pan-metastasis study of a large cohort of samples from different primary and metastatic locations coupled with clinical and transcriptomics public data.

Over the last years, a plethora of computational and biostatistical methods have been developed for suitable analysis of large volumes of omics data. The correct analysis workflow and appropriate application of bioinformatics tools is a crucial aspect in immunogenomics studies (jqk). A wide variety of bioinformatics tools for characterization of the immune phenotypes were used through the different studies, in order to generate a complete landscape of the immune profiles of the samples. Further, a high number of statistical methodologies were performed, such as Cox models and meta-analysis for association with prognosis, hierarchical clustering for the generation of novel clusters, and supervised machine learning for biomarkers discovery, among others.

From the methodological point of view, all analysis performed were selected carefully and with the support from expert statisticians to ensure an accurate use of the methods. We addressed this question by using a tool to remove batch effects and generate homogenized datasets (jnX). Another challenging analysis was the cell-types deconvolution, since results vary strongly between the different algorithms published. For this reason, we selected the methods based on a benchmark that provides a guideline for method selection based on the study design, type of data and the purpose of the study (jnj). We also performed various methods on the same data and matched between the different algorithms to achieve more robust results. A method that has been widely used through the different projects of this work for the functional analysis is the GSVA (Gene Set Variation Analysis) (jnV), which is a computational tool that performs unsupervised analysis for enrichment analysis. An advantage of this approach is that the enrichment scores can be generated in a sample by sample basis, meaning that scores are independent, which can be useful for clinical management (jVr).

A central aspect of this work has been the data mining of publicly available databases. Sequencing data from thousands of tumor samples are currently available for downloading from open databases, and these numbers are increasing exponentially. It is worth to mention how valuable it is to make data resources available to carry out biomedical research, being this work a suitable example (jnp). Accordingly, a Github repository has been generated where all code and data are freely available for the research community (<https://github.com/odap-ubs>).

We acknowledge the limitations of the project, the most relevant caused by the nature of transcriptomics data. Transcriptomics profiling offers a good perspective to

understand tumor biology, but it does not reflect the intrinsic heterogeneity of the different cell-types within the tumor bulk. Also, transcriptomics data can be highly variable depending on the platform used, the quality of the data, and the bioinformatics workflow performed. Since we used data that was already pre-processed and normalized separately, it is important to take into account this variability. Additionally, we could not avoid the technical challenges regarding the tissue sampling, since FFPE tissues can contain RNA that is degraded and fragmented, and this can generate lower quality RNA-seq (jnr).

Finally, proper data mining of the clinical information is critical when working with open repositories. Data is annotated in different formats in the different studies and it requires an effort for standardization. And the lack of clinical variables is a problematic aspect when working with open databases. For example, the information about the time of biopsy was not described for some of the datasets. This information is critical since previous treatments can have an effect on the immune biology of the tumor. Furthermore, the follow-up and survival data are not available for many studies.

Overall, bioinformatics methods have been applied to study the role of the immune microenvironment in different tumor tissues and its association with clinical outcomes and tentative immunotherapy options. In the next sections, the most relevant aspects of the two studies included in the thesis will be discussed, with particular focus on the translational potential of the results and recent discoveries in the field. Finally, last advances and future perspectives in personalized oncology will be shortly discussed.

1. Dissecting the immunity of uveal melanoma

To date, there is no effective treatment for metastatic patients and there is an urgent need to find biomarkers for prognosis prediction and therapeutic strategies (nW). In uveal melanoma the infiltration of inflammatory cell-types is associated with tumor progression and metastasis alike other tumor types, where a high immune activation is associated with better clinical outcomes (mn). This special immune modulation is partially explained by the low immunogenicity of this tumor and the immunosuppressive milieu of the eye (nn).

1.1. Additive role of immune system infiltration and angiogenesis in uveal melanoma progression

Molecular and immune profiling of UM are giving new insights in the immune modulation of this malignancy for improving treatment responses (mm,jnq). Over the last years, studies have been published aimed to deciphering the immune landscape of UM and generating signatures for response prediction. In a meta-analysis study comprising more than VXX UM patients, we have found association of immune infiltration with worse prognosis, especially for cytotoxic lymphocytes (CDW+ T cells, NK cells) and macrophages Mj and MV. These results are in the same line as previous studies based on transcriptomics data.

UM phenotype is characterized by low infiltration of stromal and immune components. In a pan-cancer study by Thorsson et al. (previously described), UM was shown as the lowest leukocyte infiltrated tumor type compared to other pV tumor types from the TCGA (jnn). Specifically, UM is characterized by a dominant infiltration of macrophages over T cells and NK cells. Paradoxically, a higher infiltration of inflammatory cell-types, like CDW+ T cells and NK cells, is associated with increased risk of metastasis (jnm). The molecular analysis of the TCGA dataset revealed further sub-classification into four molecular subgroups with differences at the genetic, transcriptomic and immune level (jnq).

We identified B cells to be highly associated with better prognosis. This result is in agreement with other studies that found high expression of B cells and humoral immune activation in responders (mn). Expression of B cells and the presence of tertiary lymphoid structures have been reported to be enriched in patients who respond to ICIs in various tumor types (melanoma, renal cell carcinoma) (jnW).

There are several reasons that could explain the peculiar context and modulation of UM microenvironment. Some studies have pointed to the pro-inflammatory cytokines, such as IFN- γ , to induce upregulation of HLA class I, which in turn promotes high expression of IDO-j, PD-Lj, and most importantly, triggers a mechanism of evasion from attack by NK cells (jnk). We also evaluated the levels of HLA class I and II expression as a marker of prognosis. High HLA class I levels are associated with poor prognosis, as seen in previous studies (jmX). NK cells have been reported to eliminate tumor cells lacking HLA class I expression but not cells that express HLA (jmj). Thus, upregulation of HLA expression is a pivotal mechanism of immune evasion and can lead to metastatic dissemination.

Another potential cause for the distinctive role of the immune microenvironment in UM is the high vascularization of the eye. Our analysis showed higher infiltration of endothelial cells correlate with relapse. The main function of endothelial cells is blood vessels formation, so they are directly related to angiogenesis. In a previous study, we reported the strong association of angiogenesis with poor outcome in UM but not in CM (mV). Angiogenesis drives immunosuppression by inhibiting T cell function, suppressing antigen presentation, and promoting MDSCs and Tregs (jmV). In this regard, we have found a cluster of samples with additive inflammatory and angiogenic functions, which confers extremely poor prognosis.

Based on these results, we hypothesize that immune response could happen after cancer cells have broken the blood-retinal barrier and disseminated to secondary organs due to the peculiar immunosuppressive microenvironment in the eye. This would explain the association of a high infiltration of cytotoxic lymphocytes and high angiogenesis with worse prognosis and recurrence.

Witnessing the central role of angiogenesis in modulating the immune microenvironment, treatments based on a combination of anti-angiogenic drugs with immunotherapy seem a promising strategy in order to make *cold* tumors more susceptible to respond to immunotherapies (jmp). Combinatory approaches for

targeting include the combination of bevacizumab (IgG antibody targeting VEGF-A) with ICIs which have been tested in clinical trials with promising results in some tumor types like renal cell carcinoma, hepatocellular carcinoma, colorectal cancer and others (VV). In uveal melanoma, however, results from clinical trials have been disappointing thus far (mV). In this regard, and based on the evidences from this and other studies on UM, a new clinical trial has been approved for metastatic UM patients from Bellvitge University Hospital that will be led by Dr. Josep Maria Piulats and will start to enroll patients shortly.

In summary, we have performed a pool analysis of uveal melanoma patients and have identified a subset of patients with high values of inflammation and angiogenesis that could be responders to combination immunotherapy targeting both functions.

1.2. Driver mutations in GNAQ and GNA11 genes are likely to be antigenic in uveal melanoma patients

Driver mutations have historically been described to generate low antigenic neoantigens compared to passenger mutations (rq,jmr). Nevertheless, in the last years, neoantigens from driver mutations have been proposed for immunotherapy-based treatments such as neoantigen vaccines. The rationale for studying the immunogenicity of recurrent mutations for cancer treatment is clear: these mutations are shared across patients. This is an opportunity to develop off-the-shelf vaccines for large subsets of patients rather than patient-specific vaccines. These vaccines would also reduce the likelihood of escape since driver mutations are shared by most clones within the tumor (jmq).

In this regard, a seminal work by Steven Rosenberg (VXjn), they effectively treated a colorectal cancer metastatic patient with adoptive TILs targeting KRAS GjVD mutation expressed by HLA-C*XW:XV (jmn). The same neoantigen has been recently used to treat metastatic pancreatic cancer with autologous T cells genetically engineered to clonally express HLA-C*XW:XV restricted TCRs (jmm). In the same trend, Yardena Samuels et al. (VXVj) have reported the combination RAS QnjK/HLA-A*Xj:Xj to be highly immunogenic in melanoma and to elicit reactivity of patients' TILs against this mutation (jmW). Other studies have been performed identifying and targeting driver mutations at BRAF, EGFR, NRAS and TPqp, among others (jmq).

GNAQ/jj QVXkL and GNAjj QVXkP genetic alterations have been identified as early driver mutations in up to Wq% of UM patients, driving activation of MAPK pathway (nn). Most research interest has been focused in understanding its functionality and trying to find actionable targets against the downstream signaling of GNAQ/jj activating mutations (ERKj/V and MEK inhibitors), with disappointing results (jmk,jWX). So far, little is known about the immunogenicity of GNAQ and GNAjj mutations. As it was explained in previous sections, UM grows in an immune privileged milieu and driver mutations GNAQ and GNAjj do not go through the immunosurveillance process. Thus, we hypothesize that these mutations could be immunogenic in UM patients.

(jWj)Comparing the clinical and histopathological differences between QVXkL vs QVXkP mutations, we found no differences with most clinical variables, in agreement with previous studies. Interestingly, we found differences for total mutational count, being QVXkL patients associated with higher number of mutations. This observation suggest that the two mutations have different consequences at the genomic level. To our knowledge, it the first time this observation is described; thus, it should be validated in other datasets

The binding affinity analyses of seven different predictive tools showed that QVXkL peptide has greater probability of being presented by HLA superfamily haplotypes than QVXkP peptide, with higher affinity and stability. Moreover, QVXkL mutations were shown to have higher likelihood to be presented by HLA molecules than most driver mutations across cancer types. This analysis was based on a recent study by Marco Punta and Stefano Lise et al. (VXVX), where they calculated the antigenic potential of several driver and resistance mutations across cancers (jWV). We identified HLA-C*Xm:XV as a candidate for presenting QVXkL with high affinity. In total, jj patients (jp,mq%) have the combination GNAQ/jj QVXkL and HLA-C*Xm:XV.

HLA alleles with high affinity are thought to be hidden by cancer cells, since they are the main mediators of immune surveillance during early stages of tumor development. In our results, UM did not show lower frequency of high affinity haplotypes, unless we found higher frequency of k low affinity haplotypes, suggesting a possible genetic selection towards low affinity haplotypes in order to hidden QVXkL neoantigen. In this regard, the immune pressure against high antigenic neoepitopes can also drive loss of heterozygosity (LOH) of specific HLA haplotypes by cancer cells(qV). Assessing the

LOH in uveal melanoma patients would be an interesting analysis to elucidate whether there is a differential LOH between QVXkL and QVXkP mutated patients.

The association of the different GNAQ and GNAJ mutations with prognosis is a controversial issue so far. In a dataset from the Bellvitge University Hospital we found that patients carrying QVXkL mutation to have better prognosis compared to QVXkP patients. This result is inconsistent with results from TCGA, where we found QVXkL patients slightly associated with worse prognosis. The same trend was observed by Terai et al. (VXVj), where they found that QVXkP patients showed longer time to death compared with QVXkL patients (jnj). In another study by Van Weeghel et al. (VXjk) they did not find any effect of the type of change in prognosis (jWj). The survival association should be assessed in extended data for clarifying this issue.

The recognition of immunogenic antigens might trigger the activation and infiltration of cytotoxic lymphocytes. The deconvolution analysis showed higher infiltration of CDW+ T cells and NK cells in patients harboring QVXkL. Additionally, results from gene expression analysis showed higher HLA class I expression in QVXkL mutated patients. The functional analysis showed enrichment of hypoxia, mTOR signaling, oxidative phosphorylation and fatty acid metabolism for QVXkP mutated patients. These results suggest different strategies of tumor growth, being tumors with QVXkP mutation more metabolic, whereas tumors with QVXkL mutations are more immunogenic.

This project has some limitations that are worth noting. One of them is the small sample size, which can affect the frequencies estimation and bias the results. The GNAQ/jj status is still missing in many datasets, since the information about these mutations is not useful for either targeted therapies selection nor for association with clinical outcomes. Another limitation is that the binding affinity analyses have been performed only for HLA class I, since the prediction power for HLA class II binding affinity tools do not get enough robustness for being reliable. Finally, this is an *in-silico* approach and results should be validated experimentally in order to demonstrate the immunogenicity of the mutation in patients.

As a proof of concept of our results, a recent study for patent request for a GNAQ-QVXkL DNA therapeutic vaccine demonstrate that QVXkL mutation is presented by HLA-A*XV:Xj molecules and it is able to trigger specific T cell activation (jWr). HLA-A*XV:Xj is the most common haplotype, representing up to qX% of UM patients. This

suggests that not only HLA-C**Xm:XV*, but also other frequent alleles with stronger binding affinity than HLA-A**XV:Xj* (like HLA-A**Xj:Xj*, HLA-A**Xp:Xj* and HLA-C**Xm:Xj*) could be good candidates for screening. This patent for vaccine is the evidence that QVXkL mutation generates T cell reactivities and that further efforts are necessary for elucidating the possibilities of targeting GNAQ and GNAJ1 mutations.

The generation of neoantigen vaccines from recurrent mutations can bring the development of personalized immunotherapies in a time and cost-effective manner and make it feasible for the clinical setting (jWq),jrq). We have demonstrated that QVXkL mutation shows strong binding prediction to HLA class I molecules and samples carrying QVXkL mutations have a higher immune phenotype. Based on this, we have proposed that this neoantigen could be a good candidate for off-the-shelf neoantigen vaccine therapies in UM.

2. Role of the immune microenvironment in metastatic homing

Metastasis represents the principal cancer-related cause of death and one of the major challenges in cancer research, since current treatments remain ineffective in most cases (jWn). Organ-specificity of metastatic spread is partially explained by the ‘seed and soil’ hypothesis, which postulates that molecular interactions between the host and neoplastic cells favor metastasis to certain organs (jWm). Nevertheless, the mechanisms that regulate these patterns of metastatic spread remain poorly understood.

The contribution of both the innate and the adaptive immune system in metastatic seeding to distant organs is already well-known, and increasing evidences are emerging pointing to the importance of the immune component in this process (rm,jWW). We have dissected the organ-specificity of metastasis from an immune point of view, to provide a comprehensive characterization of the tumor microenvironment among different tumor niches, compressing brain, bone, liver and lung. We used transcriptomics data to infer the immune state of pmr metastatic samples by quantification algorithms and statistical methods to generate a novel clustering of the samples based on their immune profiles.

2.1. Lung metastases share common immune features regardless of primary tumor origin

As mentioned before, each primary tumor shows an specific pattern of metastatic colonization to certain organs (mX,jnn). In our dataset, the metastatic frequencies for each cancer type in the collected data agrees with the frequencies defined by the literature. This indicates that data collection was performed properly and that the database was not biased by tissue location.

We have found that lung metastases share a high immunogenic microenvironment, regardless of their primary tumor of origin. Specifically, we found higher infiltration of adaptive immune components (T cells and B cells) and dendritic cells in lung metastases compared to bone, brain and liver metastasis. In the current clinical

setting, the decision of treatment strategies for most metastatic patients is based in their primary cancer type, but it has already been demonstrated that metastases differ significantly from their primary tumors (jkX). These results show evidence for considering the selection of treatments based on the immune context of the metastatic location rather than in the primary tumor type.

A clustering of samples based on immune profiles were performed generating three novel clusters (High -HIC-, Medium -MIC- and Low -LIC- Immune Clusters), with differences at the inflammatory and infiltration levels. As expected, the High Immune Cluster (HIC) was enriched in lung metastases. This cluster showed high immune infiltration, suggesting a possible target by immunotherapeutic drugs. Indeed, we interrogated the TIS score and found that all samples belonging to the HIC scored significantly higher for this signature. In a recent publication, TIS signature was shown to be highly associated with clinical response to anti-PD-1 treatment across a wide variety of tumor types, and demonstrated the utility of this signature as an independent predictive biomarker for pan-cancer studies (jkj).

Our results on the immune clusters were validated in an external dataset of different metastatic locations from skin melanoma tumors treated with anti-PD-1 (jkV). Patients belonging to the HIC had better overall survival compared to those from MIC or LIC. Recent studies on clinical trials have been published that confirm our hypothesis. In metastatic castration-resistant prostate cancer, Powles et al. showed that patients with high PD-L1 expression and CD8+ T cell infiltration were associated with better survival to ICIs (jkp). In the same line, Yang et al. (VXVj) performed a pan-cancer immunogenomics study on multiple metastatic patients across different primary tumors and showed high signatures of T cell activation and B cell receptor signaling associated with clinical benefit to pembrolizumab (jkr).

Regarding the markers of High Immune Metastases, different immune-related genes emerged as potential candidates after a differential expression analysis. Among them, CDmr was selected by a decision tree algorithm as the best candidate biomarker to differentiate between HIC and LIC samples. CDmr is an essential chaperon for regulation of the antigen presentation to the immune system. It associates to MHC class II, forming a complex that directs the transport of the neoantigens. During last years, CDmr has been associated to metastasis in certain cancer types. CDmr and HLA-DR expression have recently been shown to contribute to anti-cancer immune microenvironment in renal cancer (jkq). In brain metastatic patients, CDmr has been

found in circulating tumor cells and was suggested as a biomarker for metastatic events (jkn).

significantly enriched in HIC samples is C-C chemokine ligand q (CCLq). This pro-inflammatory cytokine is involved in cancer progression in many solid tumors (jkm). CCLq can be secreted by cancer cells or by components of the TME, and has been associated with ECM remodeling, angiogenesis and promotion of an immunosuppressive environment via MV macrophages polarization. In a recent study by Litchfield K et al. (VXVj) in more than m different cancer types, the CCLq receptor, CCRq, and CXCLjp (a T cell exhaustion marker) were found to be highly expressed in neoantigens-reactive T cells, and strongly associated with better response to ICIs (jjk).

It is important to mention Granzyme A (GZMA), since it is a direct marker of T cells cytotoxic activity and is highly expressed in the HIC group. Besides the main function of target cell lyses by CTLs and NKs; the role of GZMA in the modulation of inflammation is controversial, since it has been shown to contribute to immune evasion (jkW). For instance, Santiago L et al. (VXVX) showed that GZMA enhance gut inflammation in a CRC mouse model, consequently promoting CRC development (jkk).

The functional analysis reported interesting results of enrichment of molecular pathways in HIC patients, specifically for KRAS signaling. This result suggests a crosstalk between KRAS activation in tumor cells and the immune modulation in the niche microenvironment. This connection has been already supported by several studies, and current preclinical studies are trying to modulate KRAS induced inflammation in order to overcome KRAS mediated resistance (VXX).

2.2. Distinctive immune microenvironment across metastatic locations

In our study, lung metastases (accounting for the $V_p\%$ of the samples) come from kidney, breast, colorectal and melanoma. Lung pre-metastatic niche is characterized by high inflammatory microenvironment (VX_j). When lungs are infected, a mechanism driven by endotoxins induces vascular permeability, activating a flux of inflammatory cytokines that leads to an increase infiltration of lymphocytes, macrophage, neutrophils and monocytes (VX_V). These innate cells can be hijacked by the primary tumor towards promotion of the pre-metastatic niche, and this could explain the inflammatory phenotype observed in lung metastases in our study.

On the other hand, liver was the coldest metastatic location. Liver metastases represent the $V_m\%$ of the patients in our cohort and they come largely from colorectal cancer, followed by breast cancer and melanoma. Liver metastatic niche have been previously described to be highly immunosuppressed and tolerogenic milieu (W_r). This immunosuppressive landscape can be partially explained by the co-option pattern of metastatic growth in the liver, which consists in the replacement of normal liver cells by cancer cells, and does not generate an immune reaction. Accordingly, various clinical trials from different primary tumors have shown poorer responses to ICIs of liver metastases compared to extrahepatic metastases (WX, jkW).

Bone (accounting for the $VV\%$ of metastases) is a recurrent site of metastasis from prostate, and in lower proportion from breast cancer. Bone metastases were the only metastatic location that showed high differences in the immune landscape between the distinct primary tumors. Bone metastases can be osteoblastic (preferentially coming from prostate cancer) osteoclastic (coming from other cancer types) or, which have different molecular interactions with their host tissue (VX_r). In our clustering, more than $WX\%$ of bone metastases coming from breast, CRC or kidney belonged to HIC, whereas bone metastases from prostate were mainly belonging to the MIC and LIC, in agreement with previous results that show that osteoclastic metastases are more immunogenic than osteoblastic metastases (W_p). Thus, osteoclastic metastases could be susceptible to be treated with immunotherapy.

Finally, brain metastases represent the higher number of samples in the cohort ($V_k\%$ of the samples), and are a common metastatic site from lung cancer, breast cancer and

melanomas. Brain metastases are the deadliest metastatic location and current treatments fail to improve survival, representing an unmet clinical need. Due to blood-brain barrier, brain is considered an immune privileged organ, with a distinctive TME composition and low inflammatory infiltration (VXq). In our clustering, most brain metastases belong to LIC or MIC subgroup, and show the lowest values of immune activation. In the same line as our results, Biermann et al. (VXVV) compared melanoma brain *versus* extracranial metastases by single cell and showed that brain metastases express higher levels of metabolic factors and higher infiltration of macrophages and dysfunctional T cells, reinforcing the evasive features of brain metastasis (VXn).

On the other side, we found a small group of brain metastasis belonging to the HIC that could potentially respond to immunotherapy. In a study led by Manuel Valiente (VXjW), they found an immune escape mechanism in brain metastases that involves CDmr, the gene marker proposed by our analysis as best biomarker of high immunogenic metastases. They described a mechanism by which brain metastasis induce a pro-metastatic niche through the activation of STATp in a subpopulation of reactive astrocytes. These astrocytes have a direct effect on the TME by decreasing CDW+ T cells infiltration and increasing macrophages through CDmr (VXm). This study provided a proof-of-concept of a novel treatment targeting the microenvironment of brain metastases through CDmr.

In metastases from breast cancer, we assessed whether differences existed between the different molecular subtypes, but found no differences (data not found). This observation was recently replicated in a study leaded by Dr. Aleix Prat (VXVV), where they analyzed the immune profiles of jWr breast cancer metastatic samples across jj different metastatic sites (VXW). They found no differences in the molecular subtypes across organs. Similar to our results, they found TIS score, CDW+ T cells, B cells and macrophages over-expressed in lung and pleural metastases, while they were under-expressed in brain, bone and liver metastasis. Thus, suggesting that the immune modulation of metastatic cells is more dependent on secondary tumor tissue than in the intrinsic molecular features of the cancer cells.

3. Future perspectives of personalized oncology

Molecular profiling of tumors has brought an unprecedented change in the understanding of tumor biology and the mechanisms of tumor growth. It has been a turning point in treatment of cancer, which is changing to a more personalized selection of treatments with the focus in the profiling of patients and the classification into different subgroups based on their molecular characteristics (**Figure RN**) (VXk). Massive volumes of molecular data have been generated during the last years. Terabytes of data are stored at big supercomputing centers and institutional servers. The availability of these omics datasets and open databases will be a key resource for deciphering the underlying causes of resistance to therapy and for identification of response biomarkers (VjX).

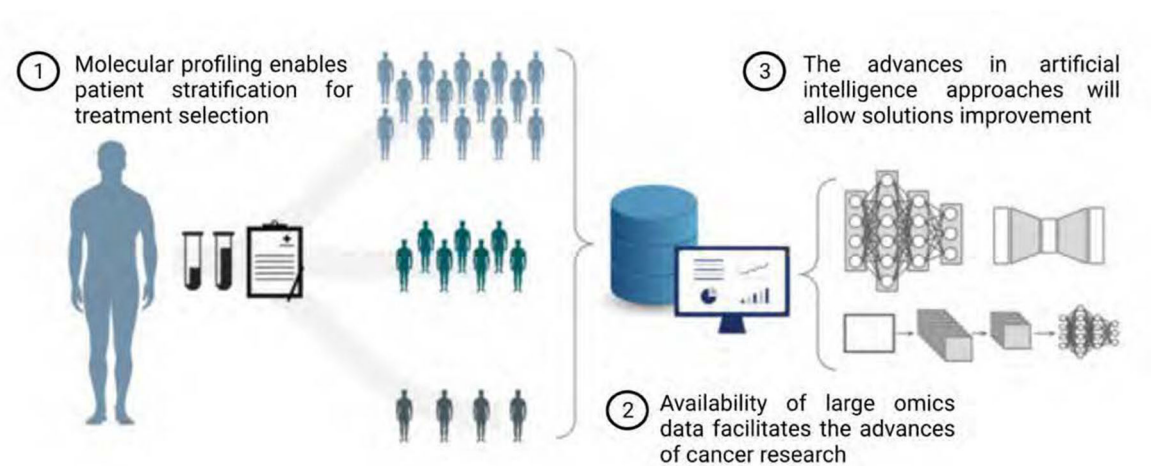


Figure 5@. Graphical overview of the different factors influencing the advances in precision oncology. Adapted from Cirillo D et al., Mol Oncol, ;:L.

Witnessing the high heterogeneity of tumors, forthcoming studies on immunology will focus in the understanding of tumor biology from a pan-cancer perspective, regardless of tumor location. Many evidences demonstrate that there can be higher similarities between molecular subtypes of different tumor locations than between tumors from the same tissue location. As a proof of concept, the studies on the singularities of MSI-high tumors across several tumor types have resulted in the identification of the first pan-cancer biomarker for immunotherapy (jXr).

The breakthrough in the generation of large omics datasets has led to an exponential increase in the use of bioinformatics and AI. This change needs of large computational resources and interdisciplinary teams to analyze large amounts of data, including scientists with a background in bioinformatics, computational programming and

machine learning. Moreover, the multi-omics integration (like genomics, proteomics, immunomics and transcriptomics) will optimize the molecular profiling of tumors (Vjj). We live in the era of big data, and the efficient and proper use of the data is a challenge at the same time than an opportunity for the future of research.

On the other side, the integration of precision oncology into the clinical routine seems more challenging to achieve. The inclusion of molecular profiling into the clinical practice requires accessibility to sequencing platforms, standardized protocols with expert's consensus, bioinformaticians to carry out the analyses, and an infrastructure that is difficult to establish in most hospitals at the moment. Furthermore, specific training programs for clinicians and collaborative efforts between researchers, agencies and oncologists are needed for implementation of precision oncology (jqp).

V. CONCLUSIONS

- H. Immunogenomics studies are a suitable approach for deciphering the role of the microenvironment in tumor progression and metastasis. The use of public omics databases can contribute to the advances towards precision immuno-oncology.
- R. In uveal melanoma, high infiltration of immune and stromal cell-types is associated with disease progression.
- U. Gene expression of HLA class I and II are associated with poor prognosis, suggesting a mechanism of evasion from NK cells attack in uveal melanoma.
- N. Overexpression of genes in antigen presentation and angiogenesis pathways confers an extremely bad prognosis in uveal melanoma tumors. Combination of immunotherapies with antiangiogenic factors could improve therapeutic responses in this group of patients.
- P. In uveal melanoma, driver mutations in GNAQ and GNAJ1 genes at QVXk hotspot generate two peptides (QVXkP and QVXkL) located in homologous amino acid sequences.
- V. Prediction tools show that GNAQ/J1 QVXkL neoantigen binds with stronger affinity to HLA class I molecules and can generate higher immunogenicity than GNAQ QVXkP neoantigen.
- O. Uveal melanoma patients carrying GNAQ/J1 QVXkL mutation show higher infiltration of CD4+ T cells and NK cells, and higher HLA class I expression than to patients harboring GNAQ QVXkP neoantigen, suggesting a role of this mutation in microenvironment remodeling.
- W. GNAQ/J1 QVXkL neoantigen is a potential candidate for neoantigen vaccine therapy in uveal melanoma.
- S. Lung metastases show a high immunogenic phenotype compared to brain, bone and liver metastases regardless of primary tumor origin.
- HQ. A clustering analysis classified metastatic samples into three subgroups of metastases: High, Medium and Low Immune Clusters. The High Immune Cluster mainly includes lung metastases, whereas in the Low Immune Cluster liver metastases are the predominant ones, followed by brain and bone.

- HH.** Metastatic samples classified as High Immune could be susceptible to be treated with immunotherapy.
- HR.** CDmr expression was identified as a candidate biomarker for selection of high immunogenic metastases.

VI. BIBLIOGRAPHY

- j. Hanahan D, Weinberg RA. Hallmarks of cancer: the next generation. *Cell*. VXjj Mar r;jrr(q):nrn-mr.
- V. Hanahan D. Hallmarks of Cancer: New Dimensions. *Cancer Discov*. VXVV Jan;jV(j):pj-rn.
- p. Topalian SL, Hom SS, Kawakami Y, Mancini M, Schwartzentruber DJ, Zakut R, et al. Recognition of shared melanoma antigens by human tumor-infiltrating lymphocytes. *J Immunother Off J Soc Biol Ther*. jkkV Oct;jV(p):VXp-n.
- r. Fridman WH, Pagès F, Sautès-Fridman C, Galon J. The immune contexture in human tumours: impact on clinical outcome. *Nat Rev Cancer*. VXjV Mar jq;jV(r):VkW-pXn.
- q. Anderson NM, Simon MC. The tumor microenvironment. *Curr Biol CB*. VXVX Aug jm;pX(jn):RkVj-q.
- n. Dranoff G. Cytokines in cancer pathogenesis and cancer therapy. *Nat Rev Cancer*. VXXr Jan;r(j):jj-VV.
- m. Nicholson LB. The immune system. *Essays Biochem*. VXjn Oct pj;nX(p):Vmq-pXj.
- W. Beutler B. Innate immunity: an overview. *Mol Immunol*. VXXr Feb;rX(jV):Wrq-qk.
- k. Bonilla FA, Oettgen HC. Adaptive immunity. *J Allergy Clin Immunol*. VXjX Feb;jVq(V Suppl V):Spp-rX.
- jX. Zagorulya M, Duong E, Spranger S. Impact of anatomic site on antigen-presenting cells in cancer. *J Immunother Cancer*. VXVX Oct;W(V):eXXjVXr.
- jj. Gajewski TF, Schreiber H, Fu YX. Innate and adaptive immune cells in the tumor microenvironment. *Nat Immunol*. VXjp Oct;jr(jX):jXjr-VV.
- jV. Galluzzi L, Chan TA, Kroemer G, Wolchok JD, López-Soto A. The hallmarks of successful anticancer immunotherapy. *Sci Transl Med*. VXjW Sep jk;jX(rqk):eaatmWXm.
- jp. Lei X, Lei Y, Li JK, Du WX, Li RG, Yang J, et al. Immune cells within the tumor microenvironment: Biological functions and roles in cancer immunotherapy. *Cancer Lett*. VXVX Feb j;rmX:jVn-pp.
- jr. Togashi Y, Shitara K, Nishikawa H. Regulatory T cells in cancer immunosuppression - implications for anticancer therapy. *Nat Rev Clin Oncol*. VXjk Jun;jn(n):pqn-mj.
- jq. Abel AM, Yang C, Thakar MS, Malarkannan S. Natural Killer Cells: Development, Maturation, and Clinical Utilization. *Front Immunol*. VXjW;k;jWnk.
- jn. Guillerey C, Huntington ND, Smyth MJ. Targeting natural killer cells in cancer immunotherapy. *Nat Immunol*. VXjn Aug jk;jm(k):jXVq-pn.

- jm. Cabrita R, Lauss M, Sanna A, Donia M, Skaarup Larsen M, Mitra S, et al. Tertiary lymphoid structures improve immunotherapy and survival in melanoma. *Nature*. VXX Jan;qmm(mmkj):qnj-q.
- jW. Mantovani A, Marchesi F, Malesci A, Laghi L, Allavena P. Tumour-associated macrophages as treatment targets in oncology. *Nat Rev Clin Oncol*. VXjm Jul;jr(m):pkk-rjn.
- jk. Quail DF, Amulic B, Aziz M, Barnes BJ, Eruslanov E, Fridlender ZG, et al. Neutrophil phenotypes and functions in cancer: A consensus statement. *J Exp Med*. VXVV Jun n;Vjk(n):eVXVVXXjj.
- VX. Talmadge JE, Gabrilovich DI. History of myeloid-derived suppressor cells. *Nat Rev Cancer*. VXjp Oct;jp(jX):mpk-qV.
- Vj. Turley SJ, Cremasco V, Astarita JL. Immunological hallmarks of stromal cells in the tumour microenvironment. *Nat Rev Immunol*. VXjq Nov;jq(jj):nnk-WV.
- X. Rahma OE, Hodi FS. The Intersection between Tumor Angiogenesis and Immune Suppression. *Clin Cancer Res Off J Am Assoc Cancer Res*. VXjk Sep jq;Vq(jW):qrrk-qm.
- Vp. Truffi M, Sorrentino L, Corsi F. Fibroblasts in the Tumor Microenvironment. *Adv Exp Med Biol*. VXXV;jVpr;jq-Vk.
- Vr. Liu Y, Cao X. Immunosuppressive cells in tumor immune escape and metastasis. *J Mol Med Berl Ger*. VXjn May;kr(q):qXk-VV.
- Vq. Whiteside TL. The tumor microenvironment and its role in promoting tumor growth. *Oncogene*. VXXW Oct n;Vm(rq):qkXr-jV.
- Vn. Bejarano L, Jordão MJC, Joyce JA. Therapeutic Targeting of the Tumor Microenvironment. *Cancer Discov*. VXVj Apr;jj(r):kpp-qk.
- Vm. Quail DF, Joyce JA. Microenvironmental regulation of tumor progression and metastasis. *Nat Med*. VXjp Nov;jk(jj):jrVp-pm.
- VW. Miao D, Margolis CA, Vokes NI, Liu D, Taylor-Weiner A, Wankowicz SM, et al. Genomic correlates of response to immune checkpoint blockade in microsatellite-stable solid tumors. *Nat Genet*. VXjW Sep;qX(k):jVmj-Wj.
- Vk. Hegde PS, Karanikas V, Evers S. The Where, the When, and the How of Immune Monitoring for Cancer Immunotherapies in the Era of Checkpoint Inhibition. *Clin Cancer Res Off J Am Assoc Cancer Res*. VXjn Apr jq;VV(W):jWnq-mr.
- pX. Rahma OE, Hodi FS. The Intersection Between Tumor Angiogenesis and Immune Suppression. *Clin Cancer Res Off J Am Assoc Cancer Res*. VXjk Apr p;
- pj. Jhunjhunwala S, Hammer C, Delamarre L. Antigen presentation in cancer: insights into tumour immunogenicity and immune evasion. *Nat Rev Cancer*. VXVj May;Vj(q):VkW-pjV.

- pV. Schreiber RD, Old LJ, Smyth MJ. Cancer immunoediting: integrating immunity's roles in cancer suppression and promotion. *Science*. VXjj Mar Vq;ppj(nXVr):jqnq-mX.
- pp. Syn NL, Teng MWL, Mok TSK, Soo RA. De-novo and acquired resistance to immune checkpoint targeting. *Lancet Oncol*. VXjm Dec;jW(jV):empj-rj.
- pr. Chen DS, Mellman I. Oncology meets immunology: the cancer-immunity cycle. *Immunity*. VXjp Jul Vq;pk(j):j-jX.
- pq. Garner H, de Visser KE. Immune crosstalk in cancer progression and metastatic spread: a complex conversation. *Nat Rev Immunol*. VXVX Aug;VX(W):rWp-km.
- pn. Nagel R, Pataskar A, Champagne J, Agami R. Boosting anti-tumor immunity with an expanded neoepitope landscape. *Cancer Res*. VXVV Jul Vk;CAN-VV-jqVq.
- pm. Alexandrov LB, Nik-Zainal S, Wedge DC, Aparicio SAJR, Behjati S, Biankin AV, et al. Signatures of mutational processes in human cancer. *Nature*. VXjp Aug VV;qXX(mrnp):rjq-Vj.
- pW. Lee CH, Yelensky R, Jooss K, Chan TA. Update on Tumor Neoantigens and Their Utility: Why It Is Good to Be Different. *Trends Immunol*. VXjW;pk(m):qpn-rW.
- pk. Bräunlein E, Krackhardt AM. Identification and Characterization of Neoantigens As Well As Respective Immune Responses in Cancer Patients. *Front Immunol*. VXjm;W;jmXV.
- rX. Neefjes J, Jongsma MLM, Paul P, Bakke O. Towards a systems understanding of MHC class I and MHC class II antigen presentation. *Nat Rev Immunol*. VXjj Nov jj;jj(jV):WVp-pn.
- rj. Robinson J, Barker DJ, Georgiou X, Cooper MA, Flicek P, Marsh SGE. IPD-IMGT/HLA Database. *Nucleic Acids Res [Internet]*. VXjk Oct pj [cited VXVV Aug p];gkzkqX. Available from: <https://academic.oup.com/nar/advance-article/doi/10.1093/nar/gkzkqX/qnjXprn>
- rV. Shankaran V, Ikeda H, Bruce AT, White JM, Swanson PE, Old LJ, et al. IFN γ and lymphocytes prevent primary tumour development and shape tumour immunogenicity. *Nature*. VXXj Apr Vn;rjX(nWpV):jjXm-jj.
- rp. Rodig SJ, Gusenleitner D, Jackson DG, Gjini E, Giobbie-Hurder A, Jin C, et al. MHC proteins confer differential sensitivity to CTLA- α and PD- α blockade in untreated metastatic melanoma. *Sci Transl Med*. VXjW Jul jW;jX(rqX):eaarpprV.
- rr. Chowell D, Morris LGT, Grigg CM, Weber JK, Samstein RM, Makarov V, et al. Patient HLA class I genotype influences cancer response to checkpoint blockade immunotherapy. *Science*. VXjW Feb V;pqk(npmq):qWV-m.
- rq. Marty R, Kaabinejadian S, Rossell D, Slifker MJ, van de Haar J, Engin HB, et al. MHC-I Genotype Restricts the Oncogenic Mutational Landscape. *Cell*. VXjm Nov pX;jmj(n):jVmV-jVWp.ejq.

- rn. Reinherz EL. $\alpha\beta$ TCR-mediated recognition: relevance to tumor-antigen discovery and cancer immunotherapy. *Cancer Immunol Res.* VXjq Apr;p(r):pXq-jV.
- rm. Garner H, de Visser KE. Immune crosstalk in cancer progression and metastatic spread: a complex conversation. *Nat Rev Immunol.* VXVX Aug;VX(W):rWp-km.
- rW. O'Donnell JS, Teng MWL, Smyth MJ. Cancer immunoediting and resistance to T cell-based immunotherapy. *Nat Rev Clin Oncol.* VXjk Mar;jn(p):jqj-nm.
- rk. Vitale I, Sistigu A, Manic G, Rudqvist NP, Trajanoski Z, Galluzzi L. Mutational and Antigenic Landscape in Tumor Progression and Cancer Immunotherapy. *Trends Cell Biol.* VXjk May;Vk(q):pkn-rjn.
- qX. Taylor BC, Balko JM. Mechanisms of MHC-I Downregulation and Role in Immunotherapy Response. *Front Immunol.* VXVV;jp:WrrWnn.
- qj. Zaretsky JM, Garcia-Diaz A, Shin DS, Escuin-Ordinas H, Hugo W, Hu-Lieskovan S, et al. Mutations Associated with Acquired Resistance to PD-j Blockade in Melanoma. *N Engl J Med.* VXjn Sep j;pmq(k):Wjk-Vk.
- qV. McGranahan N, Rosenthal R, Hiley CT, Rowan AJ, Watkins TBK, Wilson GA, et al. Allele-Specific HLA Loss and Immune Escape in Lung Cancer Evolution. *Cell.* VXjm Nov pX;jmj(n);jVqk-jVmj.ej.
- qp. Anagnostou V, Smith KN, Forde PM, Niknafs N, Bhattacharya R, White J, et al. Evolution of Neoantigen Landscape during Immune Checkpoint Blockade in Non-Small Cell Lung Cancer. *Cancer Discov.* VXjm Mar;m(p):Vnr-mn.
- qr. Gao J, Shi LZ, Zhao H, Chen J, Xiong L, He Q, et al. Loss of IFN- γ Pathway Genes in Tumor Cells as a Mechanism of Resistance to Anti-CTLA-r Therapy. *Cell.* VXjn Oct n;jnm(V):pkm-rXr.ek.
- qq. Shin DS, Zaretsky JM, Escuin-Ordinas H, Garcia-Diaz A, Hu-Lieskovan S, Kalbasi A, et al. Primary Resistance to PD-j Blockade Mediated by JAKj/V Mutations. *Cancer Discov.* VXjm Feb;m(V):jWW-VXj.
- qn. Freeman AJ, Vervoort SJ, Ramsbottom KM, Kelly MJ, Michie J, Pijpers L, et al. Natural Killer Cells Suppress T Cell-Associated Tumor Immune Evasion. *Cell Rep.* VXjk Sep jX;VW(jj):VmWr-Vmkr.eq.
- qm. Lanuza PM, Alonso MH, Hidalgo S, Uranga-Murillo I, García-Mulero S, Arnau R, et al. Adoptive NK Cell Transfer as a Treatment in Colorectal Cancer Patients: Analyses of Tumour Cell Determinants Correlating With Efficacy In Vitro and In Vivo. *Front Immunol.* VXVV;jp:WkXWpn.
- qW. Spranger S, Gajewski TF. Impact of oncogenic pathways on evasion of antitumour immune responses. *Nat Rev Cancer.* VXjW Mar;jW(p):jpk-rm.

- qk. Jhunjhunwala S, Hammer C, Delamarre L. Antigen presentation in cancer: insights into tumour immunogenicity and immune evasion. *Nat Rev Cancer*. V XVj May;Vj(q):VkW-pjV.
- nX. Burrell RA, McGranahan N, Bartek J, Swanton C. The causes and consequences of genetic heterogeneity in cancer evolution. *Nature*. VXjp Sep jk;qXj(mrn):ppW-rq.
- nj. Chen DS, Mellman I. Elements of cancer immunity and the cancer-immune set point. *Nature*. VXjm Jan jW;qrj(mn):pVj-pX.
- nV. Camus M, Tosolini M, Mlecnik B, Pagès F, Kirilovsky A, Berger A, et al. Coordination of intratumoral immune reaction and human colorectal cancer recurrence. *Cancer Res*. VXXk Mar jq;nk(n):VnWq-kp.
- np. Galon J, Bruni D. Approaches to treat immune hot, altered and cold tumours with combination immunotherapies. *Nat Rev Drug Discov*. VXjk Mar;jW(p):jkm-VjW.
- nr. Duan Q, Zhang H, Zheng J, Zhang L. Turning Cold into Hot: Firing up the Tumor Microenvironment. *Trends Cancer*. V XVX Jul;n(m):nXq-jW.
- nq. Mallone S, De Vries E, Guzzo M, Midena E, Verne J, Coebergh JW, et al. Descriptive epidemiology of malignant mucosal and uveal melanomas and adnexal skin carcinomas in Europe. *Eur J Cancer Oxf Engl jkkX*. V XVj May;rW(W):jnm-mq.
- nn. Jager MJ, Shields CL, Cebulla CM, Abdel-Rahman MH, Grossniklaus HE, Stern MH, et al. Uveal melanoma. *Nat Rev Dis Primer*. V XVX Apr k;n(j):Vr.
- nm. Algazi AP, Tsai KK, Shoushtari AN, Munhoz RR, Eroglu Z, Piulats JM, et al. Clinical outcomes in metastatic uveal melanoma treated with PD-j and PD-Lj antibodies. *Cancer*. V Xjn Nov jq;jVV(Vj):pprr-qp.
- nW. Lamas NJ, Martel A, Nahon-Estève S, Goffinet S, Macocco A, Bertolotto C, et al. Prognostic Biomarkers in Uveal Melanoma: The Status Quo, Recent Advances and Future Directions. *Cancers*. V XVj Dec Vq;jr(j):kn.
- nk. de Lange MJ, Nell RJ, van der Velden PA. Scientific and clinical implications of genetic and cellular heterogeneity in uveal melanoma. *Mol Biomed*. V XVj Aug VX;V(j):Vq.
- mX. Harbour JW. The genetics of uveal melanoma: an emerging framework for targeted therapy. *Pigment Cell Melanoma Res*. V XjV Mar;Vq(V):jmj-Wj.
- mj. Bailey MH, Tokheim C, Porta-Pardo E, Sengupta S, Bertrand D, Weerasinghe A, et al. Comprehensive Characterization of Cancer Driver Genes and Mutations. *Cell*. V XjW Apr q;jmp(V):pmj-pWq.ejW.
- mV. Castet F, Garcia-Mulero S, Sanz-Pamplona R, Cuellar A, Casanovas O, Caminal JM, et al. Uveal Melanoma, Angiogenesis and Immunotherapy, Is There Any Hope? *Cancers*. V Xjk Jun jm;jj(n):EWpr.

- mp. Notting IC, Missotten GSOA, Sijmons B, Boonman ZFHM, Keunen JEE, van der Pluijm G. Angiogenic profile of uveal melanoma. *Curr Eye Res.* VXXn Sep;pj(k):mmq-Wq.
- mr. Taylor AW. Ocular immune privilege. *Eye Lond Engl.* VXXk Oct;Vp(jX);jWWq-k.
- mq. Taylor AW, Alard P, Yee DG, Streilein JW. Aqueous humor induces transforming growth factor-beta (TGF-beta)-producing regulatory T-cells. *Curr Eye Res.* jkkm Sep;jn(k):kXX-W.
- mn. Basile MS, Mazzon E, Fagone P, Longo A, Russo A, Fallico M, et al. Immunobiology of Uveal Melanoma: State of the Art and Therapeutic Targets. *Front Oncol.* VXjk;k:jjrj.
- mm. Kim YJ, Park SJ, Maeng KJ, Lee SC, Lee CS. Multi-Platform Omics Analysis for Identification of Molecular Characteristics and Therapeutic Targets of Uveal Melanoma. *Sci Rep.* VXjk Dec jm;k(j):jkVpq.
- mW. Lambert AW, Pattabiraman DR, Weinberg RA. Emerging Biological Principles of Metastasis. *Cell.* VXjm Feb k;jnW(r):nmX-kj.
- mk. Ganesh K, Massagué J. Targeting metastatic cancer. *Nat Med.* VXXj Jan;Vm(j):pr-rr.
- WX. Nguyen DX, Bos PD, Massagué J. Metastasis: from dissemination to organ-specific colonization. *Nat Rev Cancer.* VXXk Apr;k(r):Vmr-Wr.
- Wj. Fidler IJ. The pathogenesis of cancer metastasis: the “seed and soil” hypothesis revisited. *Nat Rev Cancer.* VXXp Jun;p(n):rqp-W.
- WV. Budczies J, von Winterfeld M, Klauschen F, Bockmayr M, Lennerz JK, Denkert C, et al. The landscape of metastatic progression patterns across major human cancers. *Oncotarget.* VXjq Jan j;n(j):qmX-Wp.
- Wp. Obenauf AC, Massagué J. Surviving at a Distance: Organ-Specific Metastasis. *Trends Cancer.* VXjq Sep;j(j):mn-kj.
- Wr. Lee JC, Green MD, Huppert LA, Chow C, Pierce RH, Daud AI. The Liver-Immunity Nexus and Cancer Immunotherapy. *Clin Cancer Res Off J Am Assoc Cancer Res.* VXXV Jan j;VW(j):q-jV.
- Wq. Peinado H, Zhang H, Matei IR, Costa-Silva B, Hoshino A, Rodrigues G, et al. Pre-metastatic niches: organ-specific homes for metastases. *Nat Rev Cancer.* VXjm May;jm(q):pXV-jm.
- Wn. Liu Y, Cao X. Characteristics and Significance of the Pre-metastatic Niche. *Cancer Cell.* VXjn Nov jr;pX(q):nnW-Wj.
- Wm. Quail DF, Joyce JA. Microenvironmental regulation of tumor progression and metastasis. *Nat Med.* VXjp Nov;jk(jj):jrVp-pm.

- WW. Gao Y, Bado I, Wang H, Zhang W, Rosen JM, Zhang XHF. Metastasis Organotropism: Redefining the Congenial Soil. *Dev Cell*. VXiK May n;rk(p):pmq-kj.
- Wk. de Miguel M, Calvo E. Clinical Challenges of Immune Checkpoint Inhibitors. *Cancer Cell*. VXiX Sep jr;pW(p):pVn-pp.
- kX. Emens LA, Ascierto PA, Darcy PK, Demaria S, Eggermont AMM, Redmond WL, et al. Cancer immunotherapy: Opportunities and challenges in the rapidly evolving clinical landscape. *Eur J Cancer Oxf Engl jkkX*. VXiM Aug;Wj;jn-Vk.
- kj. Hodi FS, O'Day SJ, McDermott DF, Weber RW, Sosman JA, Haanen JB, et al. Improved survival with ipilimumab in patients with metastatic melanoma. *N Engl J Med*. VXiX Aug jk;pnp(W):mjj-Vp.
- kV. Robert C, Schachter J, Long GV, Arance A, Grob JJ, Mortier L, et al. Pembrolizumab versus Ipilimumab in Advanced Melanoma. *N Engl J Med*. VXiQ Jun Vq;pmV(Vn):VqVj-pV.
- kp. Osipov A, Murphy A, Zheng L. From immune checkpoints to vaccines: The past, present and future of cancer immunotherapy. *Adv Cancer Res*. VXiK;jrp:np-jrr.
- kr. Cercek A, Lumish M, Sinopoli J, Weiss J, Shia J, Lamendola-Essel M, et al. PD-j Blockade in Mismatch Repair-Deficient, Locally Advanced Rectal Cancer. *N Engl J Med*. VXiV Jun Vp;pWn(Vq):Vpnp-mn.
- kq. Neoadjuvant immunotherapy leads to pathological responses in MMR-proficient and MMR-deficient early-stage colon cancers - PubMed [Internet]. [cited VXiV Sep Vn]. Available from: <https://pubmed.ncbi.nlm.nih.gov/pVVqjrXX/>
- kn. June CH, O'Connor RS, Kawalekar OU, Ghassemi S, Milone MC. CAR T cell immunotherapy for human cancer. *Science*. VXiW Mar Vp;pqk(npWV):jpnj-q.
- km. Liu S, Galat V, Galat Y, Lee YKA, Wainwright D, Wu J. NK cell-based cancer immunotherapy: from basic biology to clinical development. *J Hematol Oncol J Hematol Oncol*. VXiV Jan n;jr(j):m.
- kW. Blass E, Ott PA. Advances in the development of personalized neoantigen-based therapeutic cancer vaccines. *Nat Rev Clin Oncol*. VXiV Apr;jW(r):Vjq-Vk.
- kk. Zhao B, Zhao H, Zhao J. Efficacy of PD-j/PD-Lj blockade monotherapy in clinical trials. *Ther Adv Med Oncol*. VXiX;jV:jmqWWpqkVXiKpmnjV.
- jXX. Liu D, Jenkins RW, Sullivan RJ. Mechanisms of Resistance to Immune Checkpoint Blockade. *Am J Clin Dermatol*. VXiK Feb;VXi(j):rj-qr.
- jXj. Keilson JM, Knochelmann HM, Paulos CM, Kudchadkar RR, Lowe MC. The evolving landscape of immunotherapy in solid tumors. *J Surg Oncol*. VXiV Mar;jVp(p):mkW-WXn.

- jXV. Upadhaya S, Neftelinov ST, Hodge J, Campbell J. Challenges and opportunities in the PDj/PDLj inhibitor clinical trial landscape. *Nat Rev Drug Discov.* VXVV Jul;Vj(m):rWV–p.
- jXp. Franklin MR, Platero S, Saini KS, Curigliano G, Anderson S. Immuno-oncology trends: preclinical models, biomarkers, and clinical development. *J Immunother Cancer.* VXVV Jan;jX(j):eXXpVpj.
- jXr. Cesano A, Warren S. Bringing the next Generation of Immuno-Oncology Biomarkers to the Clinic. *Biomedicines.* VXjW Feb V;n(j):Ejr.
- jXq. Sorensen SF, Zhou W, Dolled-Filhart M, Georgsen JB, Wang Z, Emancipator K, et al. PD-Lj Expression and Survival among Patients with Advanced Non-Small Cell Lung Cancer Treated with Chemotherapy. *Transl Oncol.* VXjn Feb;k(j):nr–k.
- jXn. Fridman WH, Pagès F, Sautès-Fridman C, Galon J. The immune contexture in human tumours: impact on clinical outcome. *Nat Rev Cancer.* VXjV Mar jq;jV(r):VkW–pXn.
- jXm. Galon J, Mlecnik B, Bindea G, Angell HK, Berger A, Lagorce C, et al. Towards the introduction of the “Immunoscore” in the classification of malignant tumours. *J Pathol.* VXjr Jan;VpV(V):jkk–VXk.
- jXW. Pagès F, Mlecnik B, Marliot F, Bindea G, Ou FS, Bifulco C, et al. International validation of the consensus Immunoscore for the classification of colon cancer: a prognostic and accuracy study. *Lancet Lond Engl.* VXjW May Vn;pkj(jXjpp):VjVW–pk.
- jXk. Nishino M, Ramaiya NH, Hatabu H, Hodi FS. Monitoring immune-checkpoint blockade: response evaluation and biomarker development. *Nat Rev Clin Oncol.* VXjm Nov;jr(jj):nqq–nW.
- jjX. Yarchoan M, Hopkins A, Jaffee EM. Tumor Mutational Burden and Response Rate to PD-j Inhibition. *N Engl J Med.* VXjm Vj;pmm(Vq):VqXX–j.
- jjj. Duffy MJ, Crown J. Biomarkers for Predicting Response to Immunotherapy with Immune Checkpoint Inhibitors in Cancer Patients. *Clin Chem.* VXjk Oct;nq(jX):jVW–pW.
- jjV. Hong M, Tao S, Zhang L, Diao LT, Huang X, Huang S, et al. RNA sequencing: new technologies and applications in cancer research. *J Hematol Oncol| Hematol Oncol.* VXVX Dec r;jp(j):jnn.
- jjp. Lau D, Bobe AM, Khan AA. RNA Sequencing of the Tumor Microenvironment in Precision Cancer Immunotherapy. *Trends Cancer.* VXjk Mar;q(p):jrk–qn.
- jjr. Bindea G, Mlecnik B, Tosolini M, Kirilovsky A, Waldner M, Obenauf AC, et al. Spatiotemporal dynamics of intratumoral immune cells reveal the immune landscape in human cancer. *Immunity.* VXjp Oct jm;pk(r):mWV–kq.

- jjq. Ayers M, Lunceford J, Nebozhyn M, Murphy E, Loboda A, Kaufman DR, et al. IFN- γ -related mRNA profile predicts clinical response to PD-1 blockade. *J Clin Invest*. 2014 Aug 13;124(8):1745-52.
- jjn. Hugo W, Zaretsky JM, Sun L, Song C, Moreno BH, Hu-Lieskovan S, et al. Genomic and Transcriptomic Features of Response to Anti-PD-1 Therapy in Metastatic Melanoma. *Cell*. 2014 Mar 27;156(3):914-27.
- jjm. Jiang P, Gu S, Pan D, Fu J, Sahu A, Hu X, et al. Signatures of T cell dysfunction and exclusion predict cancer immunotherapy response. *Nat Med*. 2013 Oct 3;19(10):1130-40.
- jjw. Kamal Y, Dwan D, Hoehn HJ, Sanz-Pamplona R, Alonso MH, Moreno V, et al. Tumor immune infiltration estimated from gene expression profiles predicts colorectal cancer relapse. *Oncoimmunology*. 2014 Mar 1;3(3):e92211.
- jjk. Litchfield K, Reading JL, Puttick C, Thakkar K, Abbosh C, Bentham R, et al. Meta-analysis of tumor- and T cell-intrinsic mechanisms of sensitization to checkpoint inhibition. *Cell*. 2014 Feb 27;156(5):1135-48.
- jvX. DiNatale RG, Hakimi AA, Chan TA. Genomics-based immuno-oncology: bridging the gap between immunology and tumor biology. *Hum Mol Genet*. 2014 Oct 1;23(20):4303-12.
- jVj. Cortés-Ciriano I, Gulhan DC, Lee JJK, Melloni GEM, Park PJ. Computational analysis of cancer genome sequencing data. *Nat Rev Genet*. 2014 May;15(5):321-34.
- jVV. Zewde M, Kiyotani K, Park JH, Fang H, Yap KL, Yew PY, et al. The era of immunogenomics/immunopharmacogenomics. *J Hum Genet*. 2014 Jul;95(7):1293-303.
- jVp. Finotello F, Rieder D, Hackl H, Trajanoski Z. Next-generation computational tools for interrogating cancer immunity. *Nat Rev Genet*. 2014 Dec;15(12):753-64.
- jVr. Hackl H, Charoentong P, Finotello F, Trajanoski Z. Computational genomics tools for dissecting tumour-immune cell interactions. *Nat Rev Genet*. 2014 Jul 1;15(7):445-57.
- jVq. Pavlopoulou A, Spandidos DA, Michalopoulos I. Human cancer databases (review). *Oncol Rep*. 2014 Jan;31(1):1-10.
- jVn. Cancer Genome Atlas Research Network, Weinstein JN, Collisson EA, Mills GB, Shaw KRM, Ozenberger BA, et al. The Cancer Genome Atlas Pan-Cancer analysis project. *Nat Genet*. 2014 Oct;46(10):1133-41.
- jVm. Hutter C, Zenklusen JC. The Cancer Genome Atlas: Creating Lasting Value beyond Its Data. *Cell*. 2014 Apr 24;157(2):284-91.
- jVW. Barrett T, Edgar R. Gene expression omnibus: microarray data storage, submission, retrieval, and analysis. *Methods Enzymol*. 2003;360:1-25.

- jVk. Zheng G, Ma Y, Zou Y, Yin A, Li W, Dong D. HCMDB: the human cancer metastasis database. *Nucleic Acids Res.* VXjW Jan r;rn(Dj):DkqX–q.
- jpX. Sturm G, Finotello F, Petitprez F, Zhang JD, Baumbach J, Fridman WH, et al. Comprehensive evaluation of transcriptome-based cell-type quantification methods for immuno-oncology. *Bioinforma Oxf Engl.* VXjk Jul jq;pq(jr):irpn–rq.
- npj. Sturm G, Finotello F, List M. Immunedeconv: An R Package for Unified Access to Computational Methods for Estimating Immune Cell Fractions from Bulk RNA-Sequencing Data. *Methods Mol Biol Clifton NJ.* VXVX;VjVX:VVp–pV.
- jpV. Sturm G, Finotello F, Petitprez F, Zhang JD, Baumbach J, Fridman WH, et al. Comprehensive evaluation of transcriptome-based cell-type quantification methods for immuno-oncology. *Bioinforma Oxf Engl.* VXjk Jul jq;pq(jr):irpn–rq.
- jpp. Hackl H, Charoentong P, Finotello F, Trajanoski Z. Computational genomics tools for dissecting tumour–immune cell interactions. *Nat Rev Genet [Internet].* VXjn Aug [cited VXjk Apr pX];jm(W):rrj–qW. Available from: <https://www.nature.com/articles/nrg.VXjn.nm>
- jpR. Yoshihara K, Shahmoradgoli M, Martínez E, Vegesna R, Kim H, Torres-Garcia W, et al. Inferring tumour purity and stromal and immune cell admixture from expression data. *Nat Commun.* VXjp;r:VnjV.
- jpq. Charoentong P, Finotello F, Angelova M, Mayer C, Efremova M, Rieder D, et al. Pan-cancer Immunogenomic Analyses Reveal Genotype-Immunophenotype Relationships and Predictors of Response to Checkpoint Blockade. *Cell Rep.* VXjm Jan p;jW(j):VrW–nV.
- jpn. Kiyotani K, Toyoshima Y, Nakamura Y. Immunogenomics in personalized cancer treatments. *J Hum Genet.* VXVj Sep;nn(k):kXj–m.
- jpm. Garcia-Garijo A, Fajardo CA, Gros A. Determinants for Neoantigen Identification. *Front Immunol.* VXjk;jX:jpkV.
- jpW. Marsh SGE, Albert ED, Bodmer WF, Bontrop RE, Dupont B, Erlich HA, et al. Nomenclature for factors of the HLA system, VXjX. *Tissue Antigens.* VXjX Apr;mq(r):Vkj–rqq.
- jpk. Szolek A, Schubert B, Mohr C, Sturm M, Feldhahn M, Kohlbacher O. OptiType: precision HLA typing from next-generation sequencing data. *Bioinforma Oxf Engl.* VXjr Dec j;pX(Vp):ppjX–n.
- jrX. Borden ES, Buetow KH, Wilson MA, Hastings KT. Cancer Neoantigens: Challenges and Future Directions for Prediction, Prioritization, and Validation. *Front Oncol.* VXVV;jV:WpnWVj.
- jrj. Karosiene E, Lundegaard C, Lund O, Nielsen M. NetMHCcons: a consensus method for the major histocompatibility complex class I predictions. *Immunogenetics.* VXjV Mar;nr(p):jmm–Wn.

- jrV. Garcia-Garijo A, Fajardo CA, Gros A. Determinants for Neoantigen Identification. *Front Immunol.* VXjk;jX:jpkV.
- jrP. Erfanian N, Derakhshani A, Nasser S, Fereidouni M, Baradaran B, Jalili Tabrizi N, et al. Immunotherapy of cancer in single-cell RNA sequencing era: A precision medicine perspective. *Biomed Pharmacother Biomedecine Pharmacother.* VXVV Feb;jrn;jjVqqW.
- jrR. Jia Q, Chu H, Jin Z, Long H, Zhu B. High-throughput single-cell sequencing in cancer research. *Signal Transduct Target Ther.* VXVV May p;m(j):jrQ.
- jrQ. Liu B, Li Y, Zhang L. Analysis and Visualization of Spatial Transcriptomic Data. *Front Genet.* VXVj;jV:mWqVkX.
- jrN. Dries R, Chen J, Del Rossi N, Khan MM, Sistig A, Yuan GC. Advances in spatial transcriptomic data analysis. *Genome Res.* VXVj Oct;pj(jX):jmXn-jW.
- jrM. Lewis SM, Asselin-Labat ML, Nguyen Q, Berthelet J, Tan X, Wimmer VC, et al. Spatial omics and multiplexed imaging to explore cancer biology. *Nat Methods.* VXVj Sep;jW(k):kkm-jXjV.
- jrW. Liu CC, Steen CB, Newman AM. Computational approaches for characterizing the tumor immune microenvironment. *Immunology.* VXjk Oct;jqW(V):mX-Wr.
- jrK. Sanz-Pamplona R, Melas M, Maoz A, Schmit SL, Rennert H, Lejbkowitz F, et al. Lymphocytic infiltration in stage II microsatellite stable colorectal tumors: A retrospective prognosis biomarker analysis. *PLoS Med.* VXVX Sep;jm(k):ejXXpVkV.
- jqX. Bhinder B, Gilvary C, Madhukar NS, Elemento O. Artificial Intelligence in Cancer Research and Precision Medicine. *Cancer Discov.* VXVj Apr;jj(r):kXX-jq.
- jqJ. Del Giudice M, Peirone S, Perrone S, Priante F, Varese F, Tirtei E, et al. Artificial Intelligence in Bulk and Single-Cell RNA-Sequencing Data to Foster Precision Oncology. *Int J Mol Sci.* VXVj Apr Vm;VV(k):rqnp.
- jqV. Johannet P, Coudray N, Donnelly DM, Jour G, Illa-Bochaca I, Xia Y, et al. Using Machine Learning Algorithms to Predict Immunotherapy Response in Patients with Advanced Melanoma. *Clin Cancer Res Off J Am Assoc Cancer Res.* VXVj Jan j;Vm(j):jPj-rX.
- jqP. Pich O, Bailey C, Watkins TBK, Zaccaria S, Jamal-Hanjani M, Swanton C. The translational challenges of precision oncology. *Cancer Cell.* VXVV May k;rX(q):rqW-mW.
- jqR. Tamborero D, Rubio-Perez C, Muiños F, Sabarinathan R, Piulats JM, Muntasell A, et al. A Pan-cancer Landscape of Interactions between Solid Tumors and Infiltrating Immune Cell Populations. *Clin Cancer Res Off J Am Assoc Cancer Res.* VXjW Aug j;Vr(jq):pmjm-VW.

- jqq. Banchereau R, Leng N, Zill O, Sokol E, Liu G, Pavlick D, et al. Molecular determinants of response to PD-L1 blockade across tumor types. *Nat Commun.* VXXV Jun Vq;jV(j):pknk.
- jqn. Liu D, Schilling B, Liu D, Sucker A, Livingstone E, Jerby-Arnon L, et al. Integrative molecular and clinical modeling of clinical outcomes to PD1 blockade in patients with metastatic melanoma. *Nat Med.* VXjk;Vq(jV):jkjn-Vm.
- jqm. Rubio-Perez C, Planas-Rigol E, Trincado JL, Bonfill-Teixidor E, Arias A, Marchese D, et al. Immune cell profiling of the cerebrospinal fluid enables the characterization of the brain metastasis microenvironment. *Nat Commun.* VXXV Mar W;jV(j):jqXp.
- jqW. Su J, Song Q, Qasem S, O'Neill S, Lee J, Furdulj CM, et al. Multi-Omics Analysis of Brain Metastasis Outcomes Following Craniotomy. *Front Oncol.* VXXV;jX:njqrmV.
- jqk. Finotello F, Rieder D, Hackl H, Trajanoski Z. Next-generation computational tools for interrogating cancer immunity. *Nat Rev Genet.* VXjk Dec;VX(jV):mVr-rn.
- jnX. Leek JT, Johnson WE, Parker HS, Jaffe AE, Storey JD. The sva package for removing batch effects and other unwanted variation in high-throughput experiments. *Bioinforma Oxf Engl.* VXjV Mar jq;VW(n):WWV-p.
- jnJ. Sturm G, Finotello F, Petitprez F, Zhang JD, Baumbach J, Fridman WH, et al. Comprehensive evaluation of transcriptome-based cell-type quantification methods for immuno-oncology. *Bioinforma Oxf Engl.* VXjk Jul jq;pq(jr):irpn-rq.
- jnV. Hänzelmann S, Castelo R, Guinney J. GSEA: gene set variation analysis for microarray and RNA-Seq data. *BMC Bioinformatics.* VXjp Jan jn;jr:m.
- jnP. Byrd JB, Greene AC, Prasad DV, Jiang X, Greene CS. Responsible, practical genomic data sharing that accelerates research. *Nat Rev Genet.* VXXV Oct;Vj(jX):njq-Vk.
- jnR. Tsimberidou AM, Fountzilas E, Bleris L, Kurzrock R. Transcriptomics and solid tumors: The next frontier in precision cancer medicine. *Semin Cancer Biol.* VXXV Sep;Wr;qX-k.
- jnQ. Robertson AG, Shih J, Yau C, Gibb EA, Oba J, Mungall KL, et al. Integrative Analysis Identifies Four Molecular and Clinical Subsets in Uveal Melanoma. *Cancer Cell.* VXjm Aug jr;pV(V):VXr-VVX.ejq.
- jnN. Thorsson V, Gibbs DL, Brown SD, Wolf D, Bortone DS, Ou Yang TH, et al. The Immune Landscape of Cancer. *Immunity.* VXjW Apr jm;rW(r):WjV-WpX.ejr.
- jnM. Bronkhorst IHG, Vu THK, Jordanova ES, Luyten GPM, Burg SH van der, Jager MJ. Different Subsets of Tumor-Infiltrating Lymphocytes Correlate with Macrophage Influx and Monosomy p in Uveal Melanoma. *Investig Ophthalmology Vis Sci* [Internet]. VXjV Aug k [cited VXXV Nov V];qp(k):qpmX. Available from: <http://iovs.arvojournals.org/article.aspx?doi=jX.jjnm/iovs.jj-kVWX>

- jnW. Helmink BA, Reddy SM, Gao J, Zhang S, Basar R, Thakur R, et al. B cells and tertiary lymphoid structures promote immunotherapy response. *Nature*. VXXV Jan;qmm(mmkj):qrk–qq.
- jnk. Dithmar SA, Rusciano DA, Armstrong CA, Lynn MJ, Grossniklaus HE. Depletion of NK cell activity results in growth of hepatic micrometastases in a murine ocular melanoma model. *Curr Eye Res*. jkkk Nov;jk(q):rVn–pj.
- jmX. Ericsson C, Seregard S, Bartolazzi A, Levitskaya E, Ferrone S, Kiessling R, et al. Association of HLA class I and class II antigen expression and mortality in uveal melanoma. *Invest Ophthalmol Vis Sci*. VXXj Sep;rV(jX):Vjqp–n.
- jmj. Ma D, Luyten GP, Luider TM, Niederhorn JY. Relationship between natural killer cell susceptibility and metastasis of human uveal melanoma cells in a murine model. *Invest Ophthalmol Vis Sci*. jkkq Feb;pn(V):rpq–rj.
- jmV. Ott PA, Hodi FS, Buchbinder EI. Inhibition of Immune Checkpoints and Vascular Endothelial Growth Factor as Combination Therapy for Metastatic Melanoma: An Overview of Rationale, Preclinical Evidence, and Initial Clinical Data. *Front Oncol*. VXjq;q:VXV.
- jmp. Fukumura D, Kloepper J, Amoozgar Z, Duda DG, Jain RK. Enhancing cancer immunotherapy using antiangiogenics: opportunities and challenges. *Nat Rev Clin Oncol*. VXjW May;jq(q):pVq–rX.
- jmr. Schumacher TN, Schreiber RD. Neoantigens in cancer immunotherapy. *Science*. VXjq Apr p;prW(nVpX):nk–mr.
- jmQ. Pearlman AH, Hwang MS, Konig MF, Hsiue EHC, Douglass J, DiNapoli SR, et al. Targeting public neoantigens for cancer immunotherapy. *Nat Cancer*. VXVj May;V(q):rWm–km.
- jmN. Tran E, Robbins PF, Lu YC, Prickett TD, Gartner JJ, Jia L, et al. T-Cell Transfer Therapy Targeting Mutant KRAS in Cancer. *N Engl J Med*. VXjn Dec W;pmq(Vp):VVqq–nV.
- jmm. Leidner R, Sanjuan Silva N, Huang H, Sprott D, Zheng C, Shih YP, et al. Neoantigen T-Cell Receptor Gene Therapy in Pancreatic Cancer. *N Engl J Med*. VXVV Jun V;pWn(VV):VjjV–k.
- jmW. Peri A, Greenstein E, Alon M, Pai JA, Dingjan T, Reich-Zeliger S, et al. Combined presentation and immunogenicity analysis reveals a recurrent RAS.QnjK neoantigen in melanoma. *J Clin Invest*. VXXVj Oct jq;jpj(VX):ejVkrnn.
- jmK. Akin-Bali DF. Bioinformatics analysis of GNAQ, GNAJ1, BAP1, SF3B1, SRSF11, EIF1AX, PLCB1, and CYSLTR1 genes and their role in the pathogenesis of Uveal Melanoma. *Ophthalmic Genet*. VXXVj Dec;rV(n):mpV–rp.
- jWX. Wei AZ, Maniar AB, Carvajal RD. New targeted and epigenetic therapeutic strategies for the treatment of uveal melanoma. *Cancer Gene Ther*. VXVV Mar V;

- jWj. van Weeghel C, Wierenga APA, Versluis M, van Hall T, van der Velden PA, Kroes WGM, et al. Do GNAQ and GNAJ1 Differentially Affect Inflammation and HLA Expression in Uveal Melanoma? *Cancers*. 2023 Aug 15;15(16):4553.
- jWV. Punta M, Jennings VA, Melcher AA, Lise S. The Immunogenic Potential of Recurrent Cancer Drug Resistance Mutations: An In Silico Study. *Front Immunol*. 2023;14:1187231.
- jWp. Terai M, Shimada A, Chervoneva I, Hulse L, Danielson M, Swensen J, et al. Prognostic Values of G-Protein Mutations in Metastatic Uveal Melanoma. *Cancers*. 2023 Nov 15;15(22):4383.
- jWr. Alexeev V, Sato T. Vaccine Vector Encoding Mutated Gnaq to Treat Uveal Melanoma and Cancers Having Mutated Gnaq and Gnaj1 Proteins [Internet]. 2023 [cited 2023 Jul 15]. Available from: <https://patentscope.wipo.int/search/en/detail.jsf?docId=W0VXjkVrjnnn#detailMainForm:MyTabViewId:PCTBIBLIO>
- jWq. Aldous AR, Dong JZ. Personalized neoantigen vaccines: A new approach to cancer immunotherapy. *Bioorg Med Chem*. 2023;35:117033.
- jWn. Lambert AW, Pattabiraman DR, Weinberg RA. Emerging Biological Principles of Metastasis. *Cell*. 2023 Feb 2;185(3):565–82.
- jWm. Ganesh K, Massagué J. Targeting metastatic cancer. *Nat Med*. 2023 Jan;19(1):10–20.
- jWW. Gajewski TF, Meng Y, Blank C, Brown I, Kacha A, Kline J, et al. Immune resistance orchestrated by the tumor microenvironment. *Immunol Rev*. 2023 Oct;403(1):1–15.
- jWk. Chen LL, Blumm N, Christakis NA, Barabási AL, Deisboeck TS. Cancer metastasis networks and the prediction of progression patterns. *Br J Cancer*. 2023 Sep 11;129(5):801–12.
- jkX. Giraldo NA, Becht E, Remark R, Damotte D, Sautès-Fridman C, Fridman WH. The immune contexture of primary and metastatic human tumours. *Curr Opin Immunol*. 2023 Apr;80:102004.
- jkj. Damotte D, Warren S, Arrondeau J, Boudou-Rouquette P, Mansuet-Lupo A, Biton J, et al. The tumor inflammation signature (TIS) is associated with anti-PD-1 treatment benefit in the CERTIM pan-cancer cohort. *J Transl Med*. 2023 Nov 15;15(22):4383.
- jkV. Liu D, Schilling B, Liu D, Sucker A, Livingstone E, Jerby-Arnon L, et al. Integrative molecular and clinical modeling of clinical outcomes to PD-1 blockade in patients with metastatic melanoma. *Nat Med*. 2023 Dec;29(12):1953–63.
- jkp. Powles T, Yuen KC, Gillessen S, Kadel EE, Rathkopf D, Matsubara N, et al. Atezolizumab with enzalutamide versus enzalutamide alone in metastatic

- castration-resistant prostate cancer: a randomized phase p trial. *Nat Med.* VXVV Jan;VW(j):jrr–qp.
- jkr. Cindy Yang SY, Lien SC, Wang BX, Clouthier DL, Hanna Y, Cirlan I, et al. Pan-cancer analysis of longitudinal metastatic tumors reveals genomic alterations and immune landscape dynamics associated with pembrolizumab sensitivity. *Nat Commun.* VXVj Aug Vn;jV(j):qjpm.
- jkq. Miura Y, Anami T, Yatsuda J, Motoshima T, Oka S, Suyama K, et al. HLA-DR and CDmr Expression and the Immune Microenvironment in Renal Cell Carcinoma. *Anticancer Res.* VXVj Jun;rj(n):VWrj–W.
- jkn. Loreth D, Schuette M, Zinke J, Mohme M, Piffko A, Schneegans S, et al. CDmr and CDrr Expression on CTCs in Cancer Patients with Brain Metastasis. *Int J Mol Sci.* VXVj Jun Vk;VV(jp):nkkp.
- jkm. Aldinucci D, Borghese C, Casagrande N. The CCLq/CCRq Axis in Cancer Progression. *Cancers.* VXVX Jul V;jV(m):Ejmnq.
- jkW. van Daalen KR, Reijneveld JF, Bovenschen N. Modulation of Inflammation by Extracellular Granzyme A. *Front Immunol.* VXVX;jj:kpj.
- jkk. Santiago L, Castro M, Sanz-Pamplona R, Garzón M, Ramirez-Labrada A, Tapia E, et al. Extracellular Granzyme A Promotes Colorectal Cancer Development by Enhancing Gut Inflammation. *Cell Rep.* VXVX Jul m;pV(j);jXmWrm.
- VXX. Pereira F, Ferreira A, Reis CA, Sousa MJ, Oliveira MJ, Preto A. KRAS as a Modulator of the Inflammatory Tumor Microenvironment: Therapeutic Implications. *Cells.* VXVV Jan Vr;jj(p):pkW.
- VXj. Maru Y. The lung metastatic niche. *J Mol Med Berl Ger.* VXjq Nov;kp(jj):jjWq–kV.
- VXV. Tomita T, Sakurai Y, Ishibashi S, Maru Y. Imbalance of Clara cell-mediated homeostatic inflammation is involved in lung metastasis. *Oncogene.* VXjj Aug r;pX(p):prVk–pk.
- VXp. Tumeh PC, Hellmann MD, Hamid O, Tsai KK, Loo KL, Gubens MA, et al. Liver Metastasis and Treatment Outcome with Anti-PD-j Monoclonal Antibody in Patients with Melanoma and NSCLC. *Cancer Immunol Res.* VXjm May;q(q):rjm–Vr.
- VXr. Yin JJ, Pollock CB, Kelly K. Mechanisms of cancer metastasis to the bone. *Cell Res.* VXXq Jan;jq(j):qm–nV.
- VXq. Quail DF, Joyce JA. The Microenvironmental Landscape of Brain Tumors. *Cancer Cell.* VXjm Mar jp;pj(p):pVn–rj.
- VXn. Biermann J, Melms JC, Amin AD, Wang Y, Caprio LA, Karz A, et al. Dissecting the treatment-naive ecosystem of human melanoma brain metastasis. *Cell.* VXVV Jul m;jWq(jr):Vqkj–VnXW.epX.

- VXm. Priego N, Zhu L, Monteiro C, Mulders M, Wasilewski D, Bindeman W, et al. STATp labels a subpopulation of reactive astrocytes required for brain metastasis. *Nat Med.* VXjW Jul;Vr(m):jXVr-pq.
- VXW. Brasó-Maristany F, Paré L, Chic N, Martínez-Sáez O, Pascual T, Mallafré-Larrosa M, et al. Gene expression profiles of breast cancer metastasis according to organ site. *Mol Oncol.* VXVV Jan;jn(j):nk-Wm.
- VXk. Tsimberidou AM, Fountzilas E, Bleris L, Kurzrock R. Transcriptomics and solid tumors: The next frontier in precision cancer medicine. *Semin Cancer Biol* [Internet]. VXVV Sep j [cited VXVV Jul Vn];Wr:qX-k. Available from: <https://www.sciencedirect.com/science/article/pii/SjXrrqmKXVXpXjknn>
- VjX. Pavlopoulou A, Spandidos DA, Michalopoulos I. Human cancer databases (review). *Oncol Rep.* VXjq Jan;pp(j):p-jW.
- Vjj. Cirillo D, Núñez-Carpintero I, Valencia A. Artificial intelligence in cancer research: learning at different levels of data granularity. *Mol Oncol.* VXVj Apr;jq(r):Wjm-Vk.